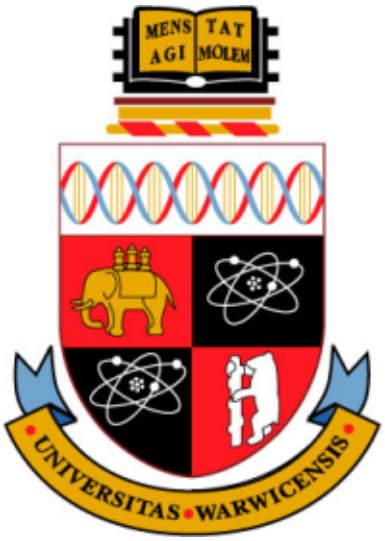

Interplay between Network Topology and Synchrony-breaking Bifurcation: Homogeneous Four-cell Coupled Cell Networks

by

Hiroko Kamei

Thesis

Submitted to the University of Warwick

for the degree of

Doctor of Philosophy

MOAC Doctoral Training Centre

July 2008

THE UNIVERSITY OF
WARWICK

Contents

Declarations

The author declares that, to the best of her knowledge, the work contained within this thesis is original and her own work under the supervision of her supervisor, Prof. Ian Stewart.

The material in this thesis is submitted for the degree of PhD. to the University of Warwick only and has not been submitted to any other university.

Acknowledgments

I want to express my sincere gratitude to my supervisor Prof. Ian Stewart. Without knowing him, I might not be in the U.K. now. He made a big change in my life. I still remember how exciting and impressive it was when I first met him, especially how he sees mathematics. I am grateful to Dr. Dave Wood who arranged this first chance to talk with Ian. I also appreciate Prof. Hugh Woodland, Dr. Robert Old and Prof. Nigel Burroughs for their advice.

I would like to thank Prof. Alison Rodger, director of MOAC, who is like a mother for the MOAC students and gave me comfort. I also thank all my MOAC friends – my PhD life would have been isolated without them.

I would like to acknowledge academic stimulation from all the researchers who I met in conferences or workshops, especially Uri Alon whose network motifs idea is motivating.

I also thank all those students whom I met through my teaching experience in the Maths Institute and Economics Department. I really felt teaching is learning. I appreciate both the university which gave me such an opportunity and all the students who gave me encouragement and joy.

I thank all those friends, from several parts of the world, I met since I came to the U.K. Even though I was away from my home country, they made me feel at home. I wish them all happiness wherever they are now in the world.

I am exceptionally grateful to Peter. He has provided assistance in numerous ways, including computer problems, proof-reading and listening to me talk about my work. I appreciate his unconditional support for always being on my side and I have a great respect for my best friend.

Finally, I am deeply grateful to my parents who supported my study financially and mentally. Since I was little, they have been open minded about whatever I wanted to do. Studying abroad must have been my most selfish request ever, but they still let me go. When I was struggling to justify my choice, I realised that to be happy is the only and best thing that I can do for them. Thanks to all the people I mentioned, and of course many other people I didn't name here, I am happy now. I delicate my thesis to my parents.

Abstract

Complex networks are studied across many fields of science. Much progress has been made on static and statistical features of networks, such as small world and scale-free networks. However, general studies of network dynamics are comparatively rare. Synchrony is one commonly observed dynamical behaviour in complex networks. Synchrony breaking is where a fully synchronised network loses coherence, and breaks up into multiple clusters of self-synchronised sub-networks. Mathematically this can be described as a bifurcation from a fully synchronous state, and in this thesis we investigate the effect of network topology on synchrony-breaking bifurcations.

Coupled cell networks represent a collection of individual dynamical systems (termed cells) that interact with each other. Each cell is described by an ordinary differential equation (ODE) or a system of ODEs. Schematically, the architecture of a coupled cell network can be represented by a directed graph with a node for each cell, and edges indicating cell couplings. Regular homogeneous networks are a special case where all the nodes/cells and edges are of the same type, and every node has the same number of input edges, which we call the valency of the network. Classes of homogeneous regular networks can be counted using an existing group theoretic enumeration formula, and this formula is extended here to enumerate networks with more generalised structures. However, this does not generate the networks themselves. We therefore develop a computer algorithm to display all connected regular homogeneous networks with less than six cells and analysed synchrony-breaking bifurcations for four-cell regular homogeneous networks.

Robust patterns of synchrony (invariant synchronised subspaces under all admissible vector fields) describe how cells are divided into multiple synchronised clusters, and their existence is solely determined by the network topology. These robust patterns of synchrony have a hierarchical relationship, and can be treated as a partially ordered set, and expressed as a lattice. For each robust pattern of synchrony (or lattice point) we can reduce the original network to a smaller network, called a quotient network, by representing each cluster as a single combined node.

Therefore, the lattice for a given regular homogeneous network provides robust patterns of synchrony and corresponding quotient networks. Some lattice structures allow a synchrony-breaking bifurcation analysis based solely on the dynamics of the quotient networks, which are *lifted* to the original network using the robust patterns of synchrony. However, in other cases the lattice structure also tells us of the existence and location of additional synchrony-breaking bifurcating branches not seen in the quotient networks.

In conclusion the work undertaken here shows that the invariant synchronised subspaces that arise from a network topology facilitate the classification of synchrony-breaking bifurcations of networks.

Chapter 1

Introduction

1.1 Networks Everywhere

A network consists of a number of individual systems, which are coupled together, meaning that they influence each other. The architecture or topology of the network is a diagram showing these influences, with nodes representing the systems and edges representing couplings. The following examples show networks from different areas of science. Nodes and edges carry different meanings in each network. How networks are represented is different depending on what we want to know from the networks and the nature of the problems under consideration. We discuss some examples to set the thesis in context.

1.1.1 Social Networks

Newman (2006) analysed the structure of collaboration networks of scientists from biology and medicine, various sub-disciplines of physics and computer science. They considered two scientists (nodes) to be connected via an edge if they had coauthored a paper together, and constructed explicit networks of such connections using the author attributions from papers or preprints appearing in scientific areas over a five year period. They found that scientific communities seemed to constitute a **small world** in which typically only about five or six steps are necessary to get from one randomly chosen scientist in a community to another. They also found that the networks are highly clustered. They speculated that this might indicate that the process of scientists introducing their collaborators to one another was important in the development of scientific communities. They highlighted a number of apparent differences in the patterns of collaboration between the fields of science studied.

Small world networks were identified as a class of random graphs by Watts and Strogatz (1998). A **scale-free network**, in which some nodes are more highly connected than other nodes, and the degree distribution follows a power law regardless the system's size, is another common type of complex network defined by a statistical feature. A large number of studies

have looked at these static and statistical features of complex networks. For a review see Albert and Barabási (2002).

1.1.2 Networks in Microbiology

A gene regulatory network can be described as a directed graph whose nodes are the genes. A directed edge from node A to node B indicates that the transcription factor produced by gene A regulates the activity of gene B. There is another representation for this gene regulatory network as a bipartite graph with two sets of nodes. One set represents transcription factors and the other represents genes. Each edge represents binding of a transcription factor to a gene; however, there are no edges between nodes in the same set (either the set of transcription factors or the set of genes). Methods for analysing complex cellular networks using the characteristics of network topology, such as bipartite graphs, are reviewed in Aittokallio and Schwikowski (2006). Graph-theoretic methods for the analysis of chemical reactions is also discussed in Mincheva and Roussel (2007).

Even in the simplest bacteria, few complete network structures are known. Reverse engineering methods aim to infer gene regulatory network topology using the growing sets of gene (protein and metabolite) expression data. In the opposite direction, starting with a known partial network, its theoretical behaviour can be compared to known data, and the model can be adjusted to match the desired outcome – for example by postulating additional nodes or edges.

One example of this is from the cyanobacterial circadian clock, which under transcriptionless conditions can be controlled by the protein KaiC. This protein exists in a number of states of phosphorylation, in isolation or in complex with other proteins (represented as protein interaction network with the states as nodes, and state-transitions as edges). The postulation of a further state (insertion of a new node) was required for the model to generate the *in vivo* observed oscillations (Takigawa-Imamura and Mochizuki, 2006).

1.1.3 Food Webs

Food webs show the flow of energy through an ecosystem, in which individual systems correspond to species and couplings describe which species eat which. For example, consider the predation links between the prey animals rabbits and pheasants, and their predators, foxes and hawks. Both foxes and hawks eat rabbits and pheasants (but not each other). The rabbits and pheasants do not eat other animals. Prey-predator models were initially studied by Lotka (1920), Lotka (1925) and Volterra (1926).

Mathematically, this food web is described using a directed graph. An arrow from,

say, rabbits to foxes means that foxes eat rabbits. Foxes also eat pheasants, giving rise to another arrow from pheasants to foxes, but pheasants do not eat rabbits and rabbits do not eat pheasants, so no arrows connect these two species. The second predator hawks also eat rabbits and pheasants, but not foxes.

Furthermore, we can distinguish prey (rabbits and pheasants) and predators (foxes and hawks) using two different node shapes: squares and ellipses, respectively. Figure 1.1 shows this food web as a directed graph.

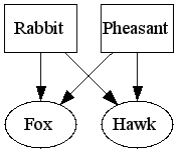

Figure 1.1: Two different node shapes represent prey and predators.

We can associate a dynamical system to the graph, which tells us how populations of species change over time as a result of predation. The equations reflect which species eat which, and of course the species' own dynamics. The representation in Figure 1.1 would help in simplifying the four species network into a more general associated dynamical system of just prey and predators (square and ellipse nodes).

1.2 Network Formalism: Coupled Cell Systems

Networks varying from small scale to large scale appear in nature and society, including the brain, the immune system, biological cells, metabolic networks, ant colonies, flocking behaviour in birds and fish, the Internet and World Wide Web, economic markets, and human social networks (Strogatz, 2001). So the above examples in Section 1.1 are just a few of the current research areas.

We consider a very general network formalism which can be applied to any branch of science. What we can observe first about complex networks is their linkage; which node is connected to which. However, what we are interested in is the network dynamics, which is constrained by the network architecture, rather than statistical features of the network.

We use the term "cell" to indicate an autonomous system of ODEs. A coupled cell system is a collection of individual, but interacting, dynamical systems (reviewed in Golubitsky and Stewart (2006)). A coupled cell system inherits the structure of the associated coupled cell network and the output of each cell in a coupled cell system is determined by the controlling

cells and itself.

Coupled cell systems take the view that the output from each cell is important – not just the dynamics considered as a whole. In these systems the signals from two or more cells can be compared, and this observation leads to various notions of "synchrony". A solution $(x_1(t), x_2(t), \ldots, x_n(t))$ for an n-cell coupled system has **synchrony** if there are (at least) two cells i and j that have identical outputs, that is $x_i(t) = x_j(t)$ for all t. The time evolution of each state can be of any form, such as steady states or oscillations. We are particularly interested in coupled cell systems that exhibit *robust synchrony* – whenever a solution has synchronous initial conditions, it exhibits synchrony for all time. Note that the term 'robust' does not directly imply any dynamical stability.

In complex networks, it is difficult to determine a specific dynamical law which describes how individuals behave and how they interact with each other. For example, in gene regulatory networks it is quite hard to determine regulatory functions fully. However, it is more approachable to determine links between individuals. We ask how much of the qualitative dynamics, especially robust synchrony, observed in coupled cell systems, is the product of network architecture.

One of the characteristic properties of a network architecture is symmetry. Networks with symmetry have been well studied, and the common qualitative dynamical behaviours among many different systems with the same symmetry have been categorised. See Golubitsky *et al.* (1998), Golubitsky and Stewart. (2002). However, it is beginning to appear that the global symmetry of a network, which is described in Section 1.3, is not the only property to generate robust synchrony.

In this thesis, we firstly aim to answer how robust patterns of synchrony are determined just by the network architecture. Secondly, we aim to answer how the synchrony pattern of a solution changes if a parameter of the system is varied and how this is related to robust patterns of synchrony of the network. Finally, we classify synchrony-breaking bifurcation behaviour of four-cell networks using robust patterns of synchrony.

1.3 Networks with Group Symmetry

A symmetry of a network is a permutation of its cell (node) labels that preserves directions (which labelled cell has arrows from which labelled cell) and the network topology. These permutations form a group: the permutations can be inverted; and if any two are performed in turn, the result is equivalent to performing another permutation that is a member of the group. For example, consider the following unidirectional ring $\mathcal{G}_1$:

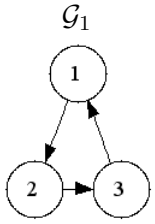

In $\mathcal{G}_1$, cell 1 has one input arrow from cell 3, cell 2 has one input arrow from cell 1 and cell 3 has one input arrow from cell 2. These directions are preserved by all cyclic permutations of cell labels; namely (123) and (132). For each cyclic permutation, the network topology is preserved. These permutations form a group. Hence this network has Z_3 symmetry.

Suppose each cell in a network determines a system of differential equation. For a given network there is a class of differential equations *compatible* with the network topology, describing the behaviour of each cell over time. The differential equations for each cell include dependence on other cells only if these cells are coupled in the network.

The symmetries of a network induce symmetry on any corresponding compatible dynamical system, and this has a very strong influence on the dynamical behaviour. The symmetries of a system can be used to work out a *catalogue* of typical forms of behaviour, which is largely independent of the specific differential equation's functional form.

Much can be deduced by knowing only the symmetries of the model. In a sense, all models with a given symmetry explore the same range of dynamical behaviour, and that range of behaviour can be studied in its own right without reference to many details of the model. However, Stewart *et al.* (2003) found that there exist networks which although not symmetric in the group-theoretic sense, behave in a similar manner to symmetric networks. This behaviour appears to be a consequence of hidden local symmetries among special subsets of the network.

1.4 Networks without Group Symmetry

Local symmetries can be identified from input sets – the set of all arrows that point to a given cell. For example, consider the following network which has two different cell types (described by circles and diamonds) and four different arrow types (black, red, green, and blue):

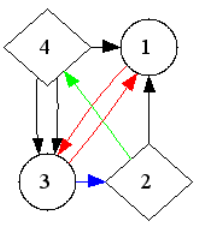

For each cell, we can list all its input arrows (and their head cells):

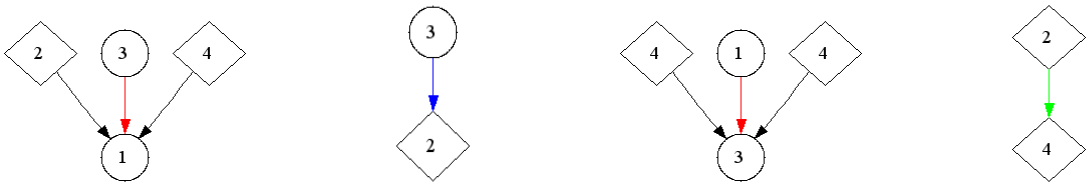

There is an arrow-type preserving bijection β between input sets of cell 1 and cell 3:

$$\beta(\overrightarrow{21}) = \overrightarrow{43}, \quad \beta(\overrightarrow{31}) = \overrightarrow{13}, \quad \beta(\overrightarrow{41}) = \overrightarrow{43}$$

Such a bijection β is called an input isomorphism from cell 1 to cell 3, and this shows there is a local symmetry between cell 1 and cell 3.

The above network has two different cell types and four different arrow types. In contrast, let us consider a network which has only one type of cell and one type of arrow.

This network is a 7 cell chain with feedback from cell 3 to cell 1: A motivating biological

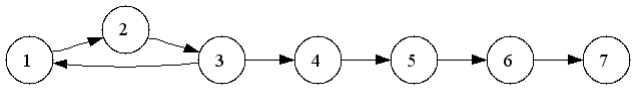

Figure 1.2: Seven cell chain with a feedback loop.

example for this network was given in Stewart (2004).

Compatible differential equations for this network topology can be constructed such that the state of any cell i is determined by the state of itself, x_i, and the states x_j of all cells j which have input arrow(s) to the cell i. Therefore, the equations compatible with the chain network (Figure 1.2) can be defined using some function f as follows:

$$\begin{aligned}
\dot{x}_1 &= f(x_1, x_3) \\
\dot{x}_2 &= f(x_2, x_1) \\
\dot{x}_3 &= f(x_3, x_2) \\
\dot{x}_4 &= f(x_4, x_3) \\
\dot{x}_5 &= f(x_5, x_4) \\
\dot{x}_6 &= f(x_6, x_5) \\
\dot{x}_7 &= f(x_7, x_6)
\end{aligned}$$

The same function f is used for all the cells because we are assuming all the cells and arrows are equivalent.

This network has no group-theoretic symmetry and neither do its associated equations. However, it supports periodic oscillations which are commonly seen in symmetric networks. Actually this seven cell chain network with feedback has hidden local symmetries.

In this network, every cell receives an input arrow from exactly one other cell. All cells are identical and all arrows are identical, so the input sets are all isomorphic.

Even if there is only one type of cells, we can consider a grouping of cells (equivalence relation) by colouring cells. Now consider the following colouring of the cells:

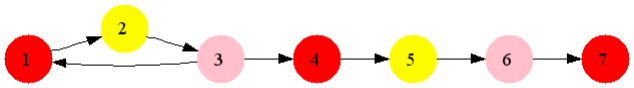

The input sets for all seven cells are shown below:

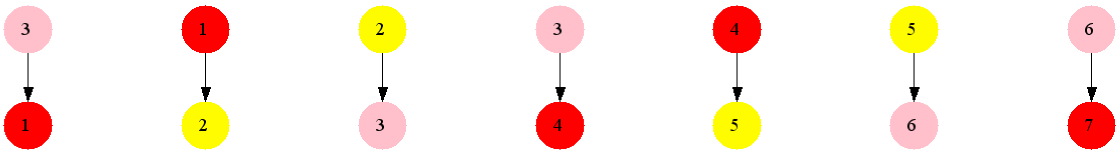

A network colouring is called **balanced** if any two cells with the same colour have input sets which are isomorphic via a permutation that keeps all colours of head cells fixed. The above colouring is balanced since every red cell has one input from a pink cell, every yellow cell has one input from a red cell, and every pink cell has one input from a yellow cell (no permutation is needed).

Note that the balanced colouring is solely determined by the network topology. However, this balanced colouring has a striking link to the network dynamics.

1.5 From Network Topology to Network Dynamics

Given a balanced colouring for the network, we define a **quotient network** where cells with the same colour in the original network are identified as one single cell in the quotient network. For example, the quotient network of the seven cell chain with feedback is shown in Figure 1.3.

We relabel the cell “147” by “1”, the cell “25” by “2”, and the node “36” by “3”. Then

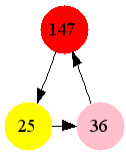

Figure 1.3: Quotient network of the seven cell chain with feedback (Figure 1.2). Three cells 1, 4 and 7 in the original network are clumped together as a single cell labelled by "147". Similarly cells 2 and 5 are clumped into a cell labelled by "25" and cells 3 and 6 are clumped into a cell labelled by "36".

the compatible differential equations are given by:

$$\begin{aligned} \dot{y}_1 &= g(y_1, y_3) \\ \dot{y}_2 &= g(y_2, y_1) \\ \dot{y}_3 &= g(y_3, y_2) \end{aligned}$$

This quotient network has the same topology as unidirectional ring $\mathcal{G}_1$ and the network is symmetric under cyclic permutations of cell labels, and so are the equations. One common dynamical behaviour of a network with this symmetry is a rotating wave: a periodic oscillation in which successive cells differ by a phase shift of one-third of a period; that is cell 2 is one-third of a period out of phase with cell 1 and cell 3 is two-thirds of a period out of phase with cell 1.

What is the connection between a quotient network and the original network?

We say the colouring is **robustly polysynchronous** if, for every admissible (compatible with network topology) dynamical system, whenever two cells of the same colour begin in the same state, then they stay in the same state for all time (this means two cells of the same colour are synchronous). Stewart *et al.* (2003) Theorem 6.5 states that a colouring is robustly polysynchronous if and only if it is balanced.

Hence, the above balanced colouring (cells 1, 4, 7 have red colour, cells 2 and 5 have yellow colour, and cells 3 and 6 have pink colour) tells us that the following subspace

$$(x_1, x_2, x_3, x_4, x_5, x_6, x_7) = (y_1, y_2, y_3, y_1, y_2, y_3, y_1)$$

is a *synchronous subspace* and the dynamics restricted to this subspace has the form determined by the quotient network.

Using what we know from this quotient network, in the original chain network with feedback, there exists a periodic state in which cells 1, 4 and 7 are in synchrony, and cells 2 and 5 are in synchrony. The synchronous state of cells 2 and 5 is one-third of a period out of phase with the synchronous state of cells 1, 4 and 7. Similarly, cells 3 and 6 are in synchrony with each

other but their synchronous state is two-thirds of a period out of phase with the synchronous state of cells 1, 4 and 7. That is, there are travelling-wave states in which successive cells along the chain differing only by a phase shift of one-third of a period. A sample simulation of the 7 cell chain with feedback network is shown in Stewart *et al.* (2003).

All patterns of robust synchrony in a network, which occur (stably or unstably) for all differential equations compatible with the network topology, can be obtained from balanced colourings (balanced equivalence relations). These balanced colourings are determined just by the network architecture (topology). But how exactly can we determine the balanced colourings from the network architecture?

The topological structure of the network is determined by the **adjacency matrix** $A = (a_{ij})$, where a_{ij} is the number of arrows whose tail is at cell j and whose head is at cell i. For simplicity, assume that networks have one cell type and one arrow type for the rest of this discussion. Consider the following four-cell coupled cell network $\mathcal{G}$ with the associated 4×4 adjacency matrix A in Table 1.1.

Network $\mathcal{G}$	Adjacency matrix A	Eigenvalues	Eigenvectors
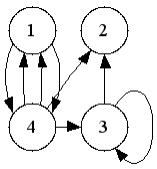	$A = \begin{pmatrix} 0 & 0 & 0 & 2 \\ 0 & 0 & 1 & 1 \\ 0 & 0 & 1 & 1 \\ 2 & 0 & 0 & 0 \end{pmatrix}$	$\lambda_0 = 2$ $\lambda_1 = 1$ $\lambda_2 = 0$ $\lambda_3 = -2$	$\mathbf{v}_0 = (1,1,1,1)$ $\mathbf{v}_1 = (0,1,1,0)$ $\mathbf{v}_2 = (0,1,0,0)$ $\mathbf{v}_3 = (3,1,1,-3)$

Table 1.1: Four-cell network (#61 in Figure 3.3) with the associated adjacency matrix and its eigenvalues and the corresponding eigenvectors.

Just using the adjacency matrix A, all balanced colourings (balanced equivalence relations) are determined. There are four balanced colourings in total. Two of them are coloured by two colours and the other two balanced colourings have three colours. Let $\mathcal{G}/_{\bowtie}$ be a quotient network determined by a balanced colouring $\bowtie$. The corresponding quotient networks for these four balanced colourings are shown in Figure 1.4.

Note that each balanced colouring (and the corresponding quotient network) denoted by $\bowtie_i$ ($\mathcal{G}/_{\bowtie_i}$) is related to the eigenvector structure of $\mathbf{v}_i$. For example, the balanced colouring $\bowtie_2$ corresponds to the partition of four cells such as (134)(2). If we observe the entries of eigenvector $\mathbf{v}_2$, they satisfy $v_1 = v_3 = v_4$, but v_2 is distinct. Similar properties are satisfied for $\bowtie_1$ and $\bowtie_3$.

Now we see that there is a relation between a balanced colouring and an eigenvector of the adjacency matrix that describes the network architecture. *Can this relation tell us about the bifurcation behaviour of the network?*

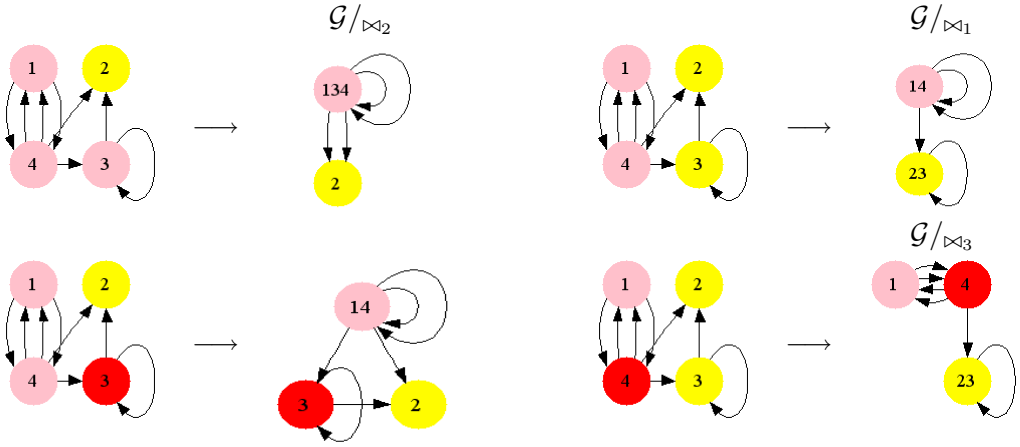

Figure 1.4: Four quotient networks from four balanced colourings.

1.6 Synchrony-Breaking Bifurcation in Coupled Cell Networks

So far we have discussed synchronous solutions for a coupled cell system and what kind of synchronous solutions the system has. Namely, a solution has synchrony if there are at least two states whose dynamical behaviours are identical for all times. Moreover, all possible robust synchronous solutions are determined by the network topology (adjacency matrix).

Coupled cell systems may have several parameters which describe certain characteristics of the system, and these parameters can be varied. When we change parameter values, this may cause a qualitative change in the dynamical behaviour of the system, such as the number of steady states, or the stability of solutions. Such parameters are called **bifurcation parameters**. We consider a coupled cell system which has only one parameter and ask: *How does the synchrony of solutions change as this parameter is varied?* We only consider steady state solutions, not periodic solutions.

All possible forms of robust synchronous solutions are listed just from the network topology, and now bifurcation theory can be used to decide which of these forms are likely to be seen first.

We use the same network $\mathcal{G}$ in Table 1.1. The compatible system of differential equations with the network topology along with a bifurcation parameter $\mu \in \mathbb{R}$ is given by the same function $f(u, \overline{v, w}, \mu)$ such as:

$$\begin{aligned}
\dot{x}_1 &= f(x_1, \overline{x_4, x_4}, \mu) \\
\dot{x}_2 &= f(x_2, \overline{x_3, x_4}, \mu) \\
\dot{x}_3 &= f(x_3, \overline{x_3, x_4}, \mu) \\
\dot{x}_4 &= f(x_4, \overline{x_1, x_1}, \mu)
\end{aligned}$$

where $f(x_i, \overline{x_j, x_k}, \mu)$ means that influences from cells j and k to cell i are identical (i.e., $f(u, v, w, \mu) = f(u, w, v, \mu)$).

Assume that all four cells are in the fully synchronous state for any bifurcation parameter μ; that is $(x_1, x_2, x_3, x_4, \mu) = (u, u, u, u, \mu)$, where $u \in \mathbb{R}$ for all $\mu \in \mathbb{R}$. Without loss of generality, we can shift this fully synchronous state to the origin $(0, 0, 0, 0)$. Now we are interested in how this fully synchronous solution loses coherence and breaks into less synchronous solutions.

Recall that all possible robust synchronous subspaces are defined by balanced colourings $\bowtie$ and we denote these subspaces by $\triangle_{\bowtie}$. We also denote the fully synchronous subspace by $\triangle$.

The Jacobian of the system, evaluated at $(0, 0, 0, 0, \mu)$ and its eigenvalues and the corresponding eigenvectors are given by:

Jacobian J				e.vals	e.vecs
$f_u(\mathbf{0},\mu)$	0	0	$2f_v(\mathbf{0},\mu)$	$f_u(\mathbf{0},\mu) + 2f_v(\mathbf{0},\mu)$	$\mathbf{v}_0 \in \triangle$
0	$f_u(\mathbf{0},\mu)$	$f_v(\mathbf{0},\mu)$	$f_v(\mathbf{0},\mu)$	$f_u(\mathbf{0},\mu) + f_v(\mathbf{0},\mu)$	$\mathbf{v}_1 \in \triangle_{\bowtie_1}$
0	0	$f_u(\mathbf{0},\mu) + f_v(\mathbf{0},\mu)$	$f_v(\mathbf{0},\mu)$	$f_u(\mathbf{0},\mu) + 0 \cdot f_v(\mathbf{0},\mu)$	$\mathbf{v}_2 \in \triangle_{\bowtie_2}$
$2f_v(\mathbf{0},\mu)$	0	0	$f_u(\mathbf{0},\mu)$	$f_u(\mathbf{0},\mu) - 2f_v(\mathbf{0},\mu)$	$\mathbf{v}_3 \in \triangle_{\bowtie_3}$

where f_u is the first derivative with respect to the internal variable and $f_v (= f_w)$ is the first derivative with respect to the coupling variables.

By local bifurcation theory, when each distinct real critical eigenvalue passes zero with nonzero speed, the fully synchronous state bifurcates, stably or unstably, towards the corresponding eigenvector direction (that is, less synchrony). Since each eigenvector belongs to a synchronous subspace, which is determined by a balanced colouring, the dynamical behaviour in this subspace is determined by the corresponding quotient network.

What kind of bifurcation we have in this subspace can be determined by the geometry of the equilibrium solution curve near a bifurcation point. In some cases, the network topology forces one bifurcation type. For example, if a network has Z_2 symmetry, the generic bifurcation from a trivial branch is a pitchfork. Conditions for a solution curve geometry then provide nondegeneracy conditions of functions. Dynamical behaviour occurring in the quotient network can then describe a synchronous solution in the original network.

So far, we have discussed bifurcation at distinct eigenvalues (simple eigenvalues). From simple eigenvalues, we expect to have a unique synchrony-breaking bifurcating branch if it exists. However, when the adjacency matrix of the network (equivalently the Jacobian of the system) has repeated eigenvalues, the existence of bifurcating branches at each bifurcation point is not unique, and we expect multiple bifurcating branches as there might be more than one

polysynchronous subspaces at a single bifurcation point. Often they are symmetrically related synchronous solutions. *How can we systematically predict the existence of bifurcating branches at which bifurcating point, and how many branches occur?*

1.7 Ordered Structure of Balanced Colourings

Remember that there are four balanced colourings on the network $\mathcal{G}$ in Table 1.1 and three of them correspond to the eigenvector structures of $\mathbf{v}_1$, $\mathbf{v}_2$, and $\mathbf{v}_3$ of the adjacency matrix A. If we know all of the eigenvector structures for a given network, these tell us possible bifurcating branch directions (if they determine balanced colourings). Some eigenvector structures do not give balanced colourings. For simple eigenvalues associated with networks, this approach gives all possible (nontrivial) bifurcating directions. However, for a repeated eigenvalue, the corresponding eigenspace is not one-dimensional, and therefore there is no one-to-one relationship between the representative eigenvectors and the bifurcating branch directions.

What about the converse? How can we tell which balanced colourings correspond to the eigenvectors? We can determine all possible balanced colourings for the network, and order them hierarchically. From this ordered structure we can determine which balanced colourings correspond to eigenvector structures. In this approach we identify in which synchronous subspace bifurcating branches exist, and how many branches there are, regardless of the eigenvalue structure (simple or non-simple).

Finally, ordered structures of balanced colourings are used for a broad classification of the existence of synchrony-breaking bifurcating branches. If two networks belong to the same ordered structure of balanced colourings, they are candidates to have equivalent bifurcation behaviour. To determine if their bifurcation is equivalent, meaning that their bifurcation types are the same (in the same synchronous subspace or not) at each bifurcation point, we compare which quotient networks for each balanced colouring these networks have. This kind of detailed classification enables us to tell which networks show a desired bifurcation.

1.8 Thesis overview

Existing results and definitions are summarised in preliminary (sub)sections, or clearly cited in the main content of the thesis (which is otherwise new work).

In the following chapter we enumerate inhomogeneous regular networks where each node can have at most six input arrows by extending an existing group theoretic formula developed by Aldosray and Stewart (2005). Additionally, multiple cell types are considered (represented

by different cell colours), and how many of these coloured networks are invariant under a permutation of the cell colour.

In Chapter 3 we visualise connected graphs with two, three or four cells, with exactly two input arrows each (homogeneous regular networks). Then in Chapter 4, we compute all possible balanced equivalence relations (balanced colourings) for regular homogeneous networks with n cells (where all the cells have the same fixed number of input arrows). We show that finding balanced equivalence relations is equivalent to finding invariant polydiagonals of an adjacency matrix which describes a given network structure. These invariant polydiagonals are determined by considering projection maps onto polydiagonals. We next show that an adjacency matrix which leaves a given polydiagonal invariant has a block structure. This matrix property leads to a computer algorithm which searches all balanced equivalence relations of a network. Stewart (2007) proved that all balanced equivalence relations form a lattice. Using balanced equivalence relations computed by this algorithm, and the refinement relation, we construct explicit forms for lattices of 3 and 4 cell regular homogeneous networks. These lattices are illustrated in Appendix A.

Chapter 5 firstly reviews basic local bifurcation theory, including how Liapunov-Schmidt reduction is used to compute nondegeneracy conditions. Previous work on codimension-one synchrony breaking bifurcations of regular homogeneous networks is introduced. In new work, we show the spectrum of eigenvalues of an adjacency matrix of any regular homogeneous network is linked to the number of input arrows, where this result is equivalent to a well known property of stochastic matrices. We finally show that symmetric coupling constrains the form of the Taylor expansion of admissible vector fields.

Chapter 6 looks at the synchrony-breaking bifurcations in two cell regular homogeneous networks. The nondegeneracy conditions for the existence for generic bifurcations (transcritical and pitchfork) are computed using Liapunov-Schmidt reduction or the Implicit Function Theorem using the Taylor expansion form from Chapter 5.

Chapter 7 constructs all possible lattice structures for simple eigenvalue regular homogenous networks with three or four cells of any valency. In Stewart (2007), it is shown that there exists a bijection between a lattice of balanced equivalence relations and a lattice of balanced polydiagonals. Here, we further prove that there exists a third form of lattice constructed from the eigenvalues of the quotient networks, order-isomorphic to the other two lattices. Each lattice node p can be assigned an integer $\eta(p)$, whose properties allow the construction of all possible lattice structures. Some lattice nodes are linked to the adjacency matrix's eigenvector structures, and we show these important nodes can generate the full lattice, and also give rise to synchrony-

breaking bifurcating branches. The existence of synchrony-breaking bifurcating branches and their directions (although not their type of bifurcations and their stability) are determined for all possible lattice structures of three and four cell regular networks. One four-cell regular network of valency 2 is chosen as an example, and the lattice based predictions are verified against a Liapunov-Schmidt reduction and a numerical analysis using xppaut. This analysis using lattices is extended to non-simple eigenvalue three and four cell networks of valency 2 in Chapter 8, where all possible lattice structures are classified, and each lattice can be reduced to a simple eigenvalue lattice. The existence and direction of synchrony-breaking bifurcating branches is analysed in a similar manner to the simple eigenvalue case, and the number of multiple branches is determined from the original lattice.

Finally, conclusions and possible future work are given in Chapter 9.

Chapter 2

Enumeration of Inhomogeneous Coupled Cell Networks

This chapter is an extension of the work of Aldosray and Stewart (2005) to enumerate homogeneous coupled cell networks using group-theoretic formulas. Their work is summarised in preliminary sub-sections, interleaved with new results, followed by the enumeration of inhomogeneous networks. The results in this Chapter are not used in the rest of thesis, but they would be useful for future work.

2.1 Introduction to Coupled Cell Networks

We briefly introduce the notions of a coupled cell network. This formalism will be made precise in Chapter 4.

A coupled cell network can be thought of as a directed graph whose cells (nodes) represent dynamical systems and whose arrows (edges) represent couplings. The network is **homogeneous of valency** r if there is one type of cell and every cell has r input arrows. Moreover, a homogeneous network that has one type of arrow is said to be **regular**.

For more complex applied networks, such as gene regulatory networks or social networks, we often want to allow different types of cells and arrows in the system with different valencies for each cell. We call these generalised regular coupled cell networks **inhomogeneous** coupled cell networks.

The enumeration of n-cell regular homogeneous networks of valency r when $n, r \leq 6$, up to graph-isomorphism was done by Aldosray and Stewart (2005). In this Chapter, we consider two different kinds of inhomogeneous coupled cell networks. Firstly, we generalise their method for the enumeration of n-cell networks where each cell has any valency less than or equal to r for one type of cell and one type of arrow as shown in Figure 2.1.

Secondly, we allow different types of cells for n-cell networks with one type of arrow and

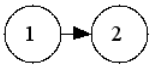

Figure 2.1: Regular inhomogeneous two-cell network of valency less than or equal to 1. There is only one cell type and one arrow type. Cell 1 has valency zero and cell 2 has valency 1.

fixed valency for all cells and enumerate networks up to graph-isomorphism, further allowing cell types permutations.

2.2 Enumeration of All Possible Adjacency Matrices

2.2.1 Preliminaries

Let $\mathcal{G}$ be a regular coupled cell network (that is, all arrows are identical.) with one type of cell. Instead of all cells having the same number of input arrows, assume that each cell of $\mathcal{G}$ has at most $r \in \mathbb{N}_0$ input arrows. We permit multiple arrows and internal arrows (self-couplings). The n cells in $\mathcal{G}$ are labelled $1, 2, \ldots, n$.

The topological structure of $\mathcal{G}$ is determined by the **adjacency matrix**, which is the $n \times n$ matrix $A = (a_{ij})$ over $\mathbb{N}_0$, where a_{ij} is the number of arrows whose tail is at node j and whose head is at node i. Throughout, we denote the set of the square matrices of order n and non-negative integer entries by $M_{n\times n}(\mathbb{N}_0)$ and the identity matrix in this set by I_n.

In the case of regular homogeneous networks, all row-sums of A are equal to r, the valency of $\mathcal{G}$. For example, a homogeneous three-cell network ($n = 3$) of valency $r = 2$, there are six possible rows in A, namely:

$$011 \quad 101 \quad 110 \quad 200 \quad 020 \quad 002 \tag{2.1}$$

Let

$$V_{n_r} = \{v \in \mathbb{N}_0^n : \sum_{i=1}^{n} v_i = r\}$$

be the set of all possible row-vectors for the adjacency matrix of a regular homogeneous n-cell network of valency r. Let

$$X_{n_r} = (V_{n_r})^n$$

be the set of all possible adjacency matrices. We calculate the cardinalities of these sets for regular homogeneous networks as follows:

Lemma 2.1. *(Regular Homogeneous Networks)*

$$|V_{n_r}| = \begin{pmatrix} n+r-1 \\ r \end{pmatrix} \quad \textit{and} \quad |X_{n_r}| = \begin{pmatrix} n+r-1 \\ r \end{pmatrix}^n$$

Proof. See Aldosray and Stewart (2005). □

This result shows that there are six possible row vectors for regular homogeneous three-cell networks of valency 2, as we showed in Equation (2.1), and hence, there are precisely $6^3 = 198$ possible distinct adjacency matrices to express these networks.

2.2.2 Regular Inhomogeneous Network Case

Now we generalise Lemma 2.1 for inhomogeneous regular networks.

In regular inhomogeneous networks where each cell has at most r input arrows, all row-sums of A are less than or equal to r. For example, when $r \leq 2$, $n = 3$, there are ten possible rows in A, namely:

$$000 \quad 001 \quad 010 \quad 100 \quad 011 \quad 101 \quad 110 \quad 200 \quad 020 \quad 002 \tag{2.2}$$

Note that these possible rows in A are the union of the cases of valency r equal to 0, 1 and 2 in regular homogeneous three-cell networks.

For the case of regular inhomogeneous networks, we define $V_{n_{\leq r}}$ as follows:

$$V_{n_{\leq r}} = \{v \in \mathbb{N}_0^n : \sum_{i=1}^{n} v_i \leq r\}$$

Lemma 2.2. *(Inhomogeneous Regular Networks)*

$$|V_{n_{\leq r}}| = \begin{pmatrix} n+r \\ r \end{pmatrix} \quad \textit{and} \quad |X_{n_{\leq r}}| = \begin{pmatrix} n+r \\ r \end{pmatrix}^n$$

Proof. The set of all possible row-vectors of valency less than or equal to r is the result of combining all possible row vectors of valency 0, 1, ... and r. Therefore, using the identity from Lemma 2.1

$$\begin{aligned} |V_{n_{\leq r}}| &= \sum_{k=0}^{r} \begin{pmatrix} n+k-1 \\ k \end{pmatrix} \\ &= \begin{pmatrix} n-1 \\ 0 \end{pmatrix} + \begin{pmatrix} n \\ 1 \end{pmatrix} + \begin{pmatrix} n+1 \\ 2 \end{pmatrix} + \begin{pmatrix} n+2 \\ 3 \end{pmatrix} + \cdots + \begin{pmatrix} n+r-1 \\ r \end{pmatrix} \\ &= \begin{pmatrix} n+r \\ r \end{pmatrix} \end{aligned}$$

Since there are $|V_{n_{\leq r}}|$ possibilities for each n row, the cardinality of all possible adjacency matrices is:

$$|X_{n_{\leq r}}| = \left\{ \sum_{k=0}^{r} \begin{pmatrix} n+k-1 \\ k \end{pmatrix} \right\}^n = \begin{pmatrix} n+r \\ r \end{pmatrix}^n$$

□

$\mathcal{G}_1$	A_1	$\mathcal{G}_2$	A_2
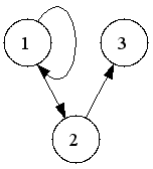	$\begin{pmatrix} 1 & 0 & 0 \\ 1 & 0 & 0 \\ 0 & 1 & 0 \end{pmatrix}$	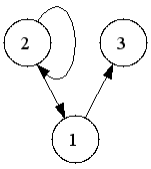	$\begin{pmatrix} 0 & 1 & 0 \\ 0 & 1 & 0 \\ 1 & 0 & 0 \end{pmatrix}$

Table 2.1: Two isomorphic regular homogeneous three-cell coupled cell networks $\mathcal{G}_1$ and $\mathcal{G}_2$ and their adjacency matrices A_1 and A_2, respectively.

The cardinality of all possible row vectors in (2.2) is easily verified using the above result. Hence, there are $10^3 = 1000$ distinct adjacency matrices for regular inhomogeneous three-cell networks of valency at most 2.

2.3 Isomorphic Networks

2.3.1 Preliminaries

Some adjacency matrices obtained in the previous section 2.2 may express the same network topology.

Example 2.1. Table 2.1 shows two three-cell regular homogeneous networks of valency 1 and their adjacency matrices.

Since the adjacency matrix of network $\mathcal{G}_i$ for $i = 1, 2$ is determined using a fixed numbering of the cells, A_1 and A_2 are different. The labellings of these two networks are different, however, $\mathcal{G}_1$ and $\mathcal{G}_2$ are topologically the same (isomorphic). We can obtain network $\mathcal{G}_1$ from network $\mathcal{G}_2$ by swapping the labels "1" and "2".

$\diamond$

This example poses a question: how can we show that $\mathcal{G}_1$ and $\mathcal{G}_2$ are isomorphic under permutation of labellings of cell 1 and cell 2 solely from their adjacency matrices A_1 and A_2?

To deal with isomorphic networks of labelled by n numbers in general, we consider the action of the permutation group S_n on the set of all possible adjacency matrices X_{n_r} by conjugation:

$$P \cdot A = PAP^{-1}$$

where $\cdot$ means group action, and P is an $n \times n$ permutation matrix.

Let $\pi \in S_n$. The corresponding permutation matrix $P = (p_{ij})$ is defined by

$$p_{i,\pi(i)} = 1$$

with all other entries being 0.

If $A = (a_{ij})$ is any $n \times n$ matrix, it follows that

$$(PAP^{-1})_{ij} = a_{\pi(i),\pi(j)}$$

The action of P has the effect of permuting the node labels by permuting the rows (input arrows to the nodes) and columns (output arrows from the nodes) of A according to π.

In Example 2.1, let $\pi = (12) \in S_3$. Then the corresponding permutation matrix P is defined by:

$$P = \begin{pmatrix} 0 & 1 & 0 \\ 1 & 0 & 0 \\ 0 & 0 & 1 \end{pmatrix} \quad \text{and} \quad P^{-1} = \begin{pmatrix} 0 & 1 & 0 \\ 1 & 0 & 0 \\ 0 & 0 & 1 \end{pmatrix}$$

Therefore, two networks $\mathcal{G}_1$ and $\mathcal{G}_2$ are isomorphic under permutation (12) because

$$PA_1P^{-1} = \begin{pmatrix} 0 & 1 & 0 \\ 1 & 0 & 0 \\ 0 & 0 & 1 \end{pmatrix} \begin{pmatrix} 1 & 0 & 0 \\ 1 & 0 & 0 \\ 0 & 1 & 0 \end{pmatrix} \begin{pmatrix} 0 & 1 & 0 \\ 1 & 0 & 0 \\ 0 & 0 & 1 \end{pmatrix} = \begin{pmatrix} 0 & 1 & 0 \\ 0 & 1 & 0 \\ 1 & 0 & 0 \end{pmatrix} = A_2$$

Now we can define when two networks are essentially the same (isomorphic): namely, the action of one of these permutations on one network produces the other.

Definition 2.1. *Suppose G is a group which acts on the set X. We define a relation $\sim_G$ on X as follows:*

$$\textit{For all} \quad x, y \in X, \quad x \sim_G y \Leftrightarrow \textit{for some} \quad g \in G, \quad g \cdot x = y.$$

Clearly $\sim_G$ is an equivalence relation on X.

In general, the equivalence classes of the relation $\sim_G$ are called the **orbits** of the group action. Thus, in our example, two networks $\mathcal{G}_1$ and $\mathcal{G}_2$ lie in the same S_n-orbit for the action on X_{n_r} for $n = 3$ and $r = 1$. The orbit to which the element $x \in X$ belongs is written as Orb_x. Thus for $x, y \in X$,

$$\mathrm{Orb}_x = \mathrm{Orb}_y \Leftrightarrow x \sim_G y$$

Since $x \sim_G y$ if and only if $y = g \cdot x$ for some $g \in G$, it follows that

$$\mathrm{Orb}_x = \{g \cdot x : g \in G\}$$

Lemma 2.3. *The orbits partition X into disjoint sets.*

Proof. The orbits are equivalence classes. See Slomson (1991) for more details. □

2.4 Orbit Counting Theorem

The number of distinct isomorphism classes of networks is the number of distinct orbits of S_n on the set of all possible adjacency matrices X_{n_r} (and $X_{n_{\leq r}}$ for inhomogeneous regular networks). If we write $\mathrm{Orb}_{X_{n_r}}(S_n)$ (or $\mathrm{Orb}_{X_{n_{\leq r}}}(S_n)$) for the set of orbits, we want to compute $|\mathrm{Orb}_{X_{n_r}}(S_n)|$ (or $|\mathrm{Orb}_{X_{n_{\leq r}}}(S_n)|$).

2.4.1 Preliminaries

Let G be a group and H be a subgroup of G. For each $g \in G$, the **coset** gH is defined to be the set

$$\{gx : x \in H\}$$

Thus gH is the set of all those elements of G obtained by combining the fixed element g with the elements of H in turn.

The number of distinct cosets of H in G is called the **index** of H in G, written $|G : H|$. The distinct cosets of H partition G into $|G : H|$ sets each containing $|H|$ elements. Therefore, we have

$$|G : H| \times |H| = |G| \tag{2.3}$$

Lemma 2.4. *If H is a subgroup of the group G, and $g_1, g_2 \in G$, then*

$$g_1H = g_2H \Leftrightarrow g_2^{-1}g_1 \in H$$

Proof. See Slomson (1991). □

We call the set of group elements of G which fix a particular $x \in X$, the **stabilizer** of x, and we denote it by S_x. Thus

$$S_x = \{g \in G : g \cdot x = x\}$$

Lemma 2.5. *If a group G acts on a set X, then for each $x \in X$, the set S_x is a subgroup of G.*

Proof. See Slomson (1991). □

There is a very close relationship between the size of the orbit and the size of the stabilizer:

Theorem 2.1 (Orbit-Stabilizer Theorem). *Let G be a group which acts on a set X. Then for each $x \in X$,*

$$|Orb_x| \times |S_x| = |G| \tag{2.4}$$

Proof. We can show that there is a one-to-one correspondence between the elements of Orb_x and the cosets of S_x in G using Lemma 2.4. See Slomson (1991) for more details. □

The Orbit-Stabilizer Theorem relates the number of elements in each orbit to the number of elements in each stabilizer, but as the next theorem shows, it can easily be rearranged to give a formula for the number of distinct orbits of the set X (not for each element of X).

Theorem 2.2. *Let G be a finite group which acts on a set X. Then the number of distinct orbits k is given by*

$$k = \frac{1}{|G|} \sum_{x \in X} |S_x|$$

Proof. This is well known but we include it for completeness.

Suppose that there are k distinct orbits $\mathrm{Orb}_{x_1}, \ldots, \mathrm{Orb}_{x_k}$. For any t such that $1 \leq t \leq k$,

$$\begin{aligned} \sum_{x \in \mathrm{Orb}_{x_t}} |S_x| &= \sum_{x \in \mathrm{Orb}_{x_t}} \frac{|G|}{|\mathrm{Orb}_x|} \\ &= \frac{|G|}{|\mathrm{Orb}_{x_t}|} \times |\mathrm{Orb}_{x_t}|, \quad \text{since} \quad \mathrm{Orb}_x = \mathrm{Orb}_{x_t} \quad \text{for each} \quad x \in \mathrm{Orb}_{x_t} \\ &= |G| \end{aligned}$$

Since the sum of the numbers $|S_x|$ taken over the elements of just one orbit comes to $|G|$ in each case, when we take the sum over all the elements of X we get a total of $|G|$ for each orbit and hence $k|G|$ in total. That is,

$$\begin{aligned} \sum_{x \in X} |S_x| &= \sum_{t=1}^{k} \sum_{x \in \mathrm{Orb}_{x_t}} |S_x| \\ &= \sum_{t=1}^{k} |G| \\ &= k|G| \end{aligned}$$

Therefore,

$$k = \frac{1}{|G|} \sum_{x \in X} |S_x|$$

□

This theorem enable us to calculate the number of distinct orbits easily if $|X|$ is not too large. For example, assume that we want to calculate the number of topologically distinct three-cell homogeneous regular networks of valency 1. There are $|X_{3_1}| = 3^3 = 27$ elements in the set of all possible adjacency matrices for three-cell homogeneous networks of valency 1 and the group acts on this set is S_3. We count group elements which fix each element $x \in X_{3_1}$; however, this calculation is not practical if $|X|$ is too large.

Notice that what we are counting is the same as counting the number of elements $x \in X_{3_1}$ which are fixed by each group element $g \in S_3$. In general the set X can become very large

depending on the problem, while the group G acting on the set X remains the same. Thus the problem of evaluating the sum becomes much easier by replacing the sum over X by a sum over G. Therefore, instead of the number of elements

$$\{g \in G : g \cdot x_i = x_i\}$$

we use the number of elements in the set

$$\{x \in X : g_i \cdot x = x\}$$

This is the set of those elements of X which are fixed by the group element g_i. We call it the **fixed-point set** of g_i, written $\mathrm{Fix}(g_i)$. The sum over G is thus $\sum_{g\in G} |\mathrm{Fix}(g)|$. Thus we can replace the sum $\sum_{x\in X} |S_x|$ by $\sum_{g\in G} |\mathrm{Fix}(g)|$ and deduce the following theorem called the **Orbit Counting Theorem** by Aldosray and Stewart (2005).

Theorem 2.3 (Orbit Counting Theorem). *Let a finite group G act on a finite set Ω. Then*

$$|Orb_\Omega(G)| = \frac{1}{|G|} \sum_{g\in G} |Fix_\Omega(g)|$$

where

$$Fix_\Omega(g) = \{x \in \Omega : g \cdot x = x\}$$

is the fixed-point set of g.

Proof. If $g, h \in G$ are conjugate then $g = khk^{-1}$ for some $k \in G$. Hence, for $x \in \mathrm{Fix}_\Omega(g)$

$$\begin{aligned} g \cdot x = x &\Leftrightarrow (khk^{-1}) \cdot x = x \\ &\Leftrightarrow k \cdot h \cdot (k^{-1} \cdot x) = x \\ &\Leftrightarrow h \cdot (k^{-1} \cdot x) = k^{-1} \cdot x \end{aligned}$$

Therefore, $k^{-1} \cdot x$ is fixed by h. Thus,

$$\begin{aligned} \mathrm{Fix}_\Omega(h) = k^{-1} \cdot x &\Leftrightarrow k\mathrm{Fix}_\Omega(h) = x \\ &\Leftrightarrow k\mathrm{Fix}_\Omega(h) = \mathrm{Fix}_\Omega(g) \end{aligned}$$

Since the fixed-point set of g is equal to the fixed-point set of h multiplied by some $k \in G$, we have $|Fix_\Omega(g)| = |Fix_\Omega(h)|$. Therefore, we may compute one fixed-point space per conjugacy class and weight the sum by the size of the conjugacy class. That is, if the conjugacy classes are $C_1, C_2, \ldots, C_t$ and we pick a unique element $g_i \in C_i$ for each i, then

$$|Org_\Omega(G)| = \frac{1}{|G|} \sum_{i=1}^{t} |C_i||\mathrm{Fix}_\Omega(g_i)| \tag{2.5}$$

□

2.5 Enumeration of Four-Cell Inhomogeneous Regular Networks

In this section, we give an example showing how the number of topologically distinct regular inhomogeneous four-cell networks of valency at most 2 is computed.

2.5.1 Preliminaries

Let $\pi \in S_n$ with the corresponding permutation matrix P. Let $\mathrm{Fix}(P)$ be the set of adjacency matrices which are fixed by the permutation matrix P. Then $A \in \mathrm{Fix}(P)$ if and only if $PA = AP$, since if $A \in \mathrm{Fix}(P)$, then

$$P \cdot A = A \Leftrightarrow PAP^{-1} = A \Leftrightarrow PA = AP$$

2.5.2 Example

We compute the number of all possible row-vectors and adjacency matrices for four-cell (i.e. $n = 4$) inhomogeneous regular networks of valency at most 2 (i.e. $r \leq 2$). By Lemma 2.2, $|V_{4_{\leq 2}}| = \begin{pmatrix} 4+2 \\ 2 \end{pmatrix} = 15$. Therefore, there are fifteen possibilities for each row in the adjacency matrix A, namely:

$$\begin{array}{cccccccc} 0000 & 0001 & 0010 & 0100 & 1000 & 0011 & 0101 & 1001 \\ 0110 & 1010 & 1100 & 2000 & 0200 & 0020 & 0002 & \end{array}$$

The number of all possible adjacency matrices for these row-vectors is: $|X_{4_{\leq 2}}| = \begin{pmatrix} 4+2 \\ 2 \end{pmatrix}^4$. Therefore in this case there are precisely 15^4 distinct adjacency matrices with all rows-sums less than or equal to 2.

The elements of S_4 split into five conjugacy classes: the class consisting of the identity i, the class consisting of six two-cycles, conjugate to $\alpha = (12)$, the class consisting of eight three-cycles, conjugate to $\beta = (123)$, the class consisting of six four-cycles, conjugate to $\gamma = (1234)$, and the class consisting of three double two-cycles, conjugate to $\delta = (12)(34)$.

Now we count the number of fixed-point set $\mathrm{Fix}(P)$, where P corresponds to the permutation matrix for each representative permutation in each conjugacy class.

Clearly $\mathrm{Fix}(i) = X_{4_{\leq 2}}$ so $|\mathrm{Fix}(i)| = 15^4$.

To compute $\mathrm{Fix}(\alpha)$ we take

$$\mathbf{P} = \begin{pmatrix} 0 & 1 & 0 & 0 \\ 1 & 0 & 0 & 0 \\ 0 & 0 & 1 & 0 \\ 0 & 0 & 0 & 1 \end{pmatrix} \qquad \mathbf{A} = \begin{pmatrix} a & b & c & d \\ e & f & g & h \\ i & j & k & l \\ m & n & o & p \end{pmatrix}$$

Then

$$\mathbf{PA} = \begin{pmatrix} e & f & g & h \\ a & b & c & d \\ i & j & k & l \\ m & n & o & p \end{pmatrix} \qquad \mathbf{AP} = \begin{pmatrix} b & a & c & d \\ e & f & g & h \\ j & i & k & l \\ n & m & o & p \end{pmatrix}$$

so $PA = AP$ if and only if

$$\mathbf{A} = \begin{pmatrix} a & b & c & d \\ b & a & c & d \\ i & i & k & l \\ m & m & o & p \end{pmatrix}$$

for suitable $a, b, c, d, i, k, l, m, o, p \in \mathbb{N}_0$. We count the matrices of this form that have all row-sums less than or equal to 2. The top row can be any of the fifteen possibilities. The second row is uniquely determined by the top row. The third row must be any of the following:

$$0000 \quad 0001 \quad 0010 \quad 0011 \quad 1100 \quad 0020 \quad 0002$$

The fourth row can be any of the seven possibilities as above. So $|\mathrm{Fix}(\alpha)| = 15 \cdot 1 \cdot 7 \cdot 7 = 735$.

Similarly, we compute $|\mathrm{Fix}(\beta)|$ where $\beta = (123)$. Now we take

$$\mathbf{P} = \begin{pmatrix} 0 & 1 & 0 & 0 \\ 0 & 0 & 1 & 0 \\ 1 & 0 & 0 & 0 \\ 0 & 0 & 0 & 1 \end{pmatrix}$$

Then

$$\mathbf{PA} = \begin{pmatrix} e & f & g & h \\ i & j & k & l \\ a & b & c & d \\ m & n & o & p \end{pmatrix} \qquad \mathbf{AP} = \begin{pmatrix} c & a & b & d \\ g & e & f & h \\ h & i & j & l \\ o & m & n & p \end{pmatrix}$$

so $PA = AP$ if and only if

$$\mathbf{A} = \begin{pmatrix} a & b & c & d \\ c & a & b & d \\ b & c & a & d \\ m & m & m & p \end{pmatrix}$$

for suitable $a, b, c, d, m, p \in \mathbb{N}_0$. The top row can be any of the fifteen possibilities. The second and third rows are uniquely determined by the top row. The fourth row must be any of:

$$0000 \quad 0001 \quad 0002$$

So $|\mathrm{Fix}(\beta)| = 15 \cdot 1 \cdot 1 \cdot 3 = 45$.

For $\gamma = (1234)$, we take

$$\mathbf{P} = \begin{pmatrix} 0 & 1 & 0 & 0 \\ 0 & 0 & 1 & 0 \\ 0 & 0 & 0 & 1 \\ 1 & 0 & 0 & 0 \end{pmatrix}$$

Then

$$\mathbf{PA} = \begin{pmatrix} e & f & g & h \\ i & j & k & l \\ m & n & o & p \\ a & b & c & d \end{pmatrix} \qquad \mathbf{AP} = \begin{pmatrix} d & a & b & c \\ h & e & f & g \\ l & i & j & k \\ p & m & n & o \end{pmatrix}$$

so $PA = AP$ if and only if

$$\mathbf{A} = \begin{pmatrix} a & b & c & d \\ d & a & b & c \\ c & d & a & b \\ b & c & d & a \end{pmatrix}$$

for suitable $a, b, c, d \in \mathbb{N}_0$. The top row can be any of the fifteen possibilities. The other rows are uniquely determined by the top row. So $|\mathrm{Fix}(\gamma)| = 15 \cdot 1 \cdot 1 \cdot 1 = 15$.

Finally, for $\delta = (12)(34)$, we take

$$\mathbf{P} = \begin{pmatrix} 0 & 1 & 0 & 0 \\ 1 & 0 & 0 & 0 \\ 0 & 0 & 0 & 1 \\ 0 & 0 & 1 & 0 \end{pmatrix}$$

Then

$$\mathbf{PA} = \begin{pmatrix} e & f & g & h \\ a & b & c & d \\ m & n & o & p \\ i & j & k & l \end{pmatrix} \qquad \mathbf{AP} = \begin{pmatrix} b & a & d & c \\ f & e & h & g \\ j & i & l & k \\ n & m & p & o \end{pmatrix}$$

so $PA = AP$ if and only if

$$\mathbf{A} = \begin{pmatrix} a & b & c & d \\ b & a & d & c \\ i & j & k & l \\ j & i & l & k \end{pmatrix}$$

for suitable $a, b, c, d, i, j, k, l \in \mathbb{N}_0$. The top row can be any of the fifteen possibilities. The second row is uniquely determined by the top row. The third row can by any of the fifteen possibilities. And the fourth row is uniquely determined by the third row. So $|\mathrm{Fix}(\delta)| = 15 \cdot 1 \cdot 1 \cdot 15 = 225$.

Finally, we apply Equation (2.5) from the Orbit Counting Theorem to obtain

$$|\mathrm{Orb}_X(S_4)| = \frac{1}{24}[1 \cdot 15^4 + 6 \cdot 735 + 8 \cdot 45 + 6 \cdot 15 + 3 \cdot 225] = 2340$$

and conclude that the number of topologically distinct inhomogeneous four-cell networks of valency at most 2 is 2340.

2.6 Periodic Banded Matrices

2.6.1 Preliminaries

A **partition** of an integer n is a representation of n in the form

$$n = \alpha_1 \cdot 1 + \alpha_2 \cdot 2 + \cdots + \alpha_n \cdot n$$

where all $\alpha_j \in \mathbb{N}_0$. The coefficient α_j is the **multiplicity** of the **part** j. We denote this partition by

$$[1^{\alpha_1} 2^{\alpha_2} \cdots n^{\alpha_n}] \tag{2.6}$$

When it is convenient, we omit terms j^{α_j} with $\alpha_j = 0$. For example, if $n = 4$ then there are five partitions and these partitions are denoted by symbols as in (2.6):

$4 \cdot 1$	$[1^4]$
$2 \cdot 1 + 1 \cdot 2$	$[1^2 2^1]$
$1 \cdot 1 + 1 \cdot 3$	$[1^1 3^1]$
$1 \cdot 4$	$[4^1]$
$2 \cdot 2$	$[2^2]$

The set of all partitions of n is denoted Π_n. If $\rho \in \Pi_n$ we define the multiplicities α_j^ρ by $\rho = [1^{\alpha_1^\rho} 2^{\alpha_2^\rho} \cdots n^{\alpha_n^\rho}]$.

Every element of S_n can be written as a product of disjoint cycles. This decomposition is unique except for the order in which the cycles occur. Disjoint cycles commute. The **cycle**

type of an element $\pi \in S_n$ is the partition of n determined by the lengths of the component cycles of π. Two permutations in S_n are conjugate if and only if they have the same cycle type. When π has cycle type $[1^{\alpha_1}2^{\alpha_2}\cdots n^{\alpha_n}]$, the size of the corresponding conjugacy class is

$$\frac{n!}{1^{\alpha_1}2^{\alpha_2}\cdots n^{\alpha_n}\alpha_1!\alpha_2!\cdots\alpha_n!}$$

Within each conjugacy class we distinguish a canonical element, which we say is written in **normal form**. This element is obtained by writing the numbers $1, 2, \ldots, n$ in order into the product of cycles, starting with the 1-cycles, then the 2-cycles, and so on in increasing order of length. For example, the permutation

$$(1)(2)(3)(45)(678) \in S_8$$

is in normal form for the (conjugacy class determined by the) partition $[1^3 2^1 3^1]$.

As motivation, suppose that

$$\pi = (1)(23)(456) \in S_6$$

which is the normal form for the partition $[1^1 2^1 3^1]$. Let A be a 6×6 matrix, and write A as a block matrix where the blocks correspond to pairs of cycles from π, with one cycle determining a set of rows and the other a set of columns. That is,

$$A = \left(\begin{array}{c|cc|ccc} a_{11} & a_{12} & a_{13} & a_{14} & a_{15} & a_{16} \\ \hline a_{21} & a_{22} & a_{23} & a_{24} & a_{25} & a_{26} \\ a_{31} & a_{32} & a_{33} & a_{34} & a_{35} & a_{36} \\ \hline a_{41} & a_{42} & a_{43} & a_{44} & a_{45} & a_{46} \\ a_{51} & a_{52} & a_{53} & a_{54} & a_{55} & a_{56} \\ a_{61} & a_{62} & a_{63} & a_{64} & a_{65} & a_{66} \end{array}\right)$$

There are nine blocks in the matrix A; A_{ij} where $1 \leq i, j \leq 3$ and $|A_{ij}| = i \times j$. A block is uniquely determined by a pair of cycles (ρ, γ), where ρ is the permutation for rows and γ is the permutation for columns. Thus, the length of $\rho = i$ and the length of $\gamma = j$. For example, the pair $((23), (456))$ determines a 2×3 block in rows $2, 3$ and columns $4, 5, 6$, namely

$$A_{23} = \begin{pmatrix} a_{24} & a_{25} & a_{26} \\ a_{34} & a_{35} & a_{36} \end{pmatrix}$$

Let P be the permutation matrix of π. Then conjugation of A by P permutes both the rows and columns according to π, however, this operation preserves the block structure. Actually, in

this case

$$P = \begin{pmatrix} 1 & 0 & 0 & 0 & 0 & 0 \\ 0 & 0 & 1 & 0 & 0 & 0 \\ 0 & 1 & 0 & 0 & 0 & 0 \\ 0 & 0 & 0 & 0 & 1 & 0 \\ 0 & 0 & 0 & 0 & 0 & 1 \\ 0 & 0 & 0 & 1 & 0 & 0 \end{pmatrix} \quad \text{and} \quad P^{-1} = \begin{pmatrix} 1 & 0 & 0 & 0 & 0 & 0 \\ 0 & 0 & 1 & 0 & 0 & 0 \\ 0 & 1 & 0 & 0 & 0 & 0 \\ 0 & 0 & 0 & 0 & 0 & 1 \\ 0 & 0 & 0 & 1 & 0 & 0 \\ 0 & 0 & 0 & 0 & 1 & 0 \end{pmatrix}$$

Therefore,

$$\begin{aligned} & PAP^{-1} \\ = & \begin{pmatrix} 1 & 0 & 0 & 0 & 0 & 0 \\ 0 & 0 & 1 & 0 & 0 & 0 \\ 0 & 1 & 0 & 0 & 0 & 0 \\ 0 & 0 & 0 & 0 & 1 & 0 \\ 0 & 0 & 0 & 0 & 0 & 1 \\ 0 & 0 & 0 & 1 & 0 & 0 \end{pmatrix} \left(\begin{array}{c|cc|ccc} a_{11} & a_{12} & a_{13} & a_{14} & a_{15} & a_{16} \\ \hline a_{21} & a_{22} & a_{23} & a_{24} & a_{25} & a_{26} \\ a_{31} & a_{32} & a_{33} & a_{34} & a_{35} & a_{36} \\ \hline a_{41} & a_{42} & a_{43} & a_{44} & a_{45} & a_{46} \\ a_{51} & a_{52} & a_{53} & a_{54} & a_{55} & a_{56} \\ a_{61} & a_{62} & a_{63} & a_{64} & a_{65} & a_{66} \end{array}\right) \begin{pmatrix} 1 & 0 & 0 & 0 & 0 & 0 \\ 0 & 0 & 1 & 0 & 0 & 0 \\ 0 & 1 & 0 & 0 & 0 & 0 \\ 0 & 0 & 0 & 0 & 0 & 1 \\ 0 & 0 & 0 & 1 & 0 & 0 \\ 0 & 0 & 0 & 0 & 1 & 0 \end{pmatrix} \\ = & \left(\begin{array}{c|cc|ccc} a_{11} & a_{13} & a_{12} & a_{15} & a_{16} & a_{14} \\ \hline a_{31} & a_{33} & a_{32} & a_{35} & a_{36} & a_{34} \\ a_{21} & a_{23} & a_{22} & a_{25} & a_{26} & a_{24} \\ \hline a_{51} & a_{53} & a_{52} & a_{55} & a_{56} & a_{54} \\ a_{61} & a_{63} & a_{62} & a_{65} & a_{66} & a_{64} \\ a_{41} & a_{43} & a_{42} & a_{45} & a_{46} & a_{44} \end{array}\right) \end{aligned}$$

The matrix A is fixed by P if and only if each block is fixed. For example, since $PA_{23}P^{-1} = \begin{pmatrix} a_{35} & a_{36} & a_{34} \\ a_{25} & a_{26} & a_{24} \end{pmatrix}$, A_{23} is fixed by the action of P if and only if all

$$\begin{pmatrix} a_{24} & a_{25} & a_{26} \\ a_{34} & a_{35} & a_{36} \end{pmatrix} = \begin{pmatrix} a_{35} & a_{36} & a_{34} \\ a_{25} & a_{26} & a_{24} \end{pmatrix}$$

$$\Rightarrow a_{24} = a_{35} = a_{26} = a_{34} = a_{25} = a_{36}$$

Therefore, the entries of A_{23} must have the following form:

$$A_{23} = \begin{pmatrix} a & a & a \\ a & a & a \end{pmatrix}$$

where $a \in \mathbb{N}_0$.

The following Lemma 2.6 in Aldosray and Stewart (2005) gives a general method to find the matrix form which is fixed by the permutation group action.

Lemma 2.6. *Let R be the $s \times s$ permutation matrix of the cycle $(1 \dots s)$, let C be the $t \times t$ permutation matrix of the cycle $(1 \dots t)$, and let B be an arbitrary $s \times t$ matrix. Define $h = hcf(s,t)$ to be the highest common factor of s and t. Then $RBC = B$ if and only if the first row of B is periodic with period h, and each successive row is shifted one place to the right. That is,*

$$b_{1i} = b_{1j} \quad \text{if} \quad i \equiv j \pmod{h}$$

$$b_{1i} = b_{k,i+k-1}$$

where $i + k - 1$ is taken modulo t.

Proof. See Aldosray and Stewart (2005). □

A fixed block of the above form is called an **h-periodic banded matrix**. It now follows that:

Proposition 2.1. *A matrix A is fixed under conjugation by a permutation matrix P in normal form if and only if each block of A is an h-periodic banded matrix, where $h = hcf(s,t)$ for an $s \times t$ block.*

Proof. See Aldosray and Stewart (2005). □

For example, in the 6×6 case above, the matrix A is fixed by P if and only if it has the form

$$A = \left(\begin{array}{c|cc|ccc} a & b & b & c & c & c \\ \hline d & e & f & g & g & g \\ d & f & e & g & g & g \\ \hline h & i & i & j & k & l \\ h & i & i & l & j & k \\ h & i & i & k & l & j \end{array}\right) \tag{2.7}$$

for suitable $a, b, c, d, e, f, g, h, i, j, k, l \in \mathbb{N}_0$.

2.7 Fixed-Point Sets

2.7.1 Preliminaries

For regular homogeneous networks, we enumerate matrices of the type described in Proposition 2.1, subject to the condition that the entries are natural numbers (including zero) and every row-sum is r. Notice that the matrix form in (2.7) is determined uniquely by the first row of each row cycle. The first row is determined by the three arbitrary numbers a , b and

c, corresponding to the row cycle (1). Once we define the second row using the four arbitrary numbers d, e, f and g, then the third row is uniquely determined by the second row. These two rows correspond to the row cycle (23). Finally, the fourth row is defined by the five arbitrary numbers h, i, j, k, and l. The fifth and sixth rows are uniquely determined by the fourth row. These three rows correspond to the row cycle (456).

Next, we require the sum of the entries in the first row of each cycle to be equal to r. The form of such a row depends on the lengths of the cycles concerned, and on the type ρ of the permutation π. Specifically, it must be h-periodic in each $s \times t$ block, where $h = \mathrm{hfc}(s, t)$. Such a vector is called (s, ρ)-**compatible**.

For example, the row 4 of the matrix A ($(3, \rho)$-compatible vector), associated with a six-cell regular homogeneous network of valency r, in (2.7) satisfies the following condition

$$h + (i + i) + (j + k + l) = r$$

As a more complicated example, suppose that

$$\pi = (1)(23)(456)(7 \quad 8 \quad 9 \quad 10) \in S_{10}$$

which is the normal form for partition $\rho = [1^1 2^1 3^1 4^1]$ of the integer 10. When $s = 3$, an (s, ρ)-compatible vector (the row 4 of a 10×10 matrix) has the form

$$[a \quad b \quad b \quad c \quad d \quad e \quad f \quad f \quad f \quad f] \tag{2.8}$$

For a ten-cell regular homogeneous network of valency r, $(3, \rho)$-compatible vector (2.8) satisfies the following row-sum condition:

$$a + (b + b) + (c + d + e) + (f + f + f + f) = r$$

The same method applies in full generality. For each partition $\rho = [1^{\alpha_1} 2^{\alpha_2} \dots n^{\alpha_n}]$ of n, each cycle-length s, and each natural number r, we define $V_{n_r}(s, \rho)$ to be the set of all (s, ρ)-compatible vectors in V_{n_r}.

Let

$$\phi_{n_r}(s, \rho) = |V_{n_r}(s, \rho)|$$

and consider the generating function

$$\Phi_{s\rho}(z) = \sum_{r=0}^{\infty} \phi_r(s, \rho) z^r$$

This leads to the following result:

Proposition 2.2. *The number of (s,ρ)-compatible vector which satisfy the sum of all coordinates is equal to r is obtained as the coefficient of z^r in the following form:*

$$\Phi_{s\rho}(z) = \prod_{k=1}^{n}(1 - z^{\frac{k}{h}})^{-\alpha_k^\rho h}$$

where $h = hcf(s,k)$.

Proof. See Aldosray and Stewart (2005). □

Hence, the cardinality of the fixed-point set is computed such as:

Proposition 2.3 (Regular Homogeneous Networks). *If $\pi \in S_n$ has type $\rho = [1^{\alpha_1}2^{\alpha_2}\dots n^{\alpha_n}]$, then its fixed-point set in X_{n_r} has cardinality*

$$\prod_{k=1}^{n}\phi_{n_r}(k,\rho)^{\alpha_k^\rho}$$

Proof. Since there are $\phi_{n_r}(k,\rho)$ all possible (k,ρ)-compatible vectors in a cycle which have the length k and there are α_k^ρ such cycles. See Aldosray and Stewart (2005) for more details. □

2.7.2 Inhomogeneous Network Case

We start this subsection with new work. Firstly, we give the form of (s,ρ)-compatible vectors for each partition of n in Table 2.2.

We now generalise the formula for the computation of fixed-point set for regular inhomogeneous networks of valency at most r.

Let

$$\phi_{n_{\leq r}}(s,\rho) = |V_{n_{\leq r}}(s,\rho)|$$

Then we have:

Proposition 2.4 (Regular Inhomogeneous Networks). *If $\pi \in S_n$ has type $\rho = [1^{\alpha_1^\rho}2^{\alpha_2^\rho}\dots n^{\alpha_n^\rho}]$, then its fixed-point set in $X_{n_{\leq r}}$ for regular inhomogeneous networks has cardinality*

$$\prod_{k=1}^{n}\left(\sum_{i=0}^{r}\phi_{n_i}(k,\rho)\right)^{\alpha_k^\rho}$$

where $\phi_{n_0}(k,\rho)) := 1$.

Proof. $V_{n_{\leq r}}(k,\rho)$ is expressed as a sum of compatible vectors for each valency as follows:

$$V_{n_{\leq r}}(k,\rho) = V_{n_0}(k,\rho) \cup V_{n_1}(k,\rho) \cup \dots \cup V_{n_r}(k,\rho)$$

n	Partition ρ	s=1	s=2	s=3	s=4	s=5	s=6
1	$[1^1]$	$[a]$					
2	$[1^2]$	$[a\|b]$					
	$[2^1]$		$[ab]$				
3	$[1^3]$	$[a\|b\|c]$					
	$[1^1 \cdot 2^1]$	$[a\|bb]$	$[a\|bc]$				
	$[3^1]$			$[abc]$			
4	$[1^4]$	$[a\|b\|c\|d]$					
	$[1^2 \cdot 2^1]$	$[a\|b\|cc]$	$[a\|b\|cd]$				
	$[1^1 \cdot 3^1]$	$[a\|bbb]$		$[a\|bcd]$			
	$[4^1]$				$[abcd]$		
	$[2^2]$		$[ab\|cd]$				
5	$[1^5]$	$[a\|b\|c\|d\|e]$					
	$[1^3 \cdot 2^1]$	$[a\|b\|c\|dd]$	$[a\|b\|c\|de]$				
	$[1^2 \cdot 3^1]$	$[a\|b\|ccc]$		$[a\|b\|cde]$			
	$[1^1 \cdot 4^1]$	$[a\|bbbb]$			$[a\|bcde]$		
	$[5^1]$					$[abcde]$	
	$[1^1 \cdot 2^2]$	$[a\|bb\|cc]$	$[a\|bc\|de]$				
	$[2^1 \cdot 3^1]$		$[ab\|ccc]$	$[aa\|bcd]$			
6	$[1^6]$	$[a\|b\|c\|d\|e\|f]$					
	$[1^4 \cdot 2^1]$	$[a\|b\|c\|d\|ee]$	$[a\|b\|c\|d\|ef]$				
	$[1^3 \cdot 3^1]$	$[a\|b\|c\|ddd]$		$[a\|b\|c\|def]$			
	$[1^2 \cdot 4^1]$	$[a\|b\|cccc]$			$[a\|b\|cdef]$		
	$[1^1 \cdot 5^1]$	$[a\|bbbbb]$				$[a\|bcdef]$	
	$[6^1]$						$[abcdef]$
	$[2^1 \cdot 4^1]$		$[ab\|cdcd]$		$[ab\|cdef]$		
	$[1^1 \cdot 2^1 \cdot 3^1]$	$[a\|bb\|ccc]$	$[a\|bc\|ddd]$	$[a\|bb\|cde]$			
	$[3^2]$			$[abc\|def]$			
	$[2^3]$		$[ab\|cd\|ef]$				
	$[1^2 \cdot 2^2]$	$[a\|b\|cc\|dd]$	$[a\|b\|cd\|ef]$				

Table 2.2: (s, ρ)-compatible vector for partitions of n and $a, b, \ldots, f \in \mathbb{N}_0$. Symbols $a, \ldots, f$ are used to show periodic patterns in a (s, ρ)-compatible vector.

By Lemma 2.2, the cardinality of $V_{n_{\leq r}}(k, \rho)$ is a sum of the cardinalities of $V_{n_i}(k, \rho)$, where $i = 0, 1, \ldots, r$. Hence, the cardinality of (k, ρ)-compatible vectors which satisfy the condition that the row-sum is less than or equal to r is:

$$\phi_{n_{\leq r}}(k, \rho) = \sum_{i=0}^{r} \phi_{n_i}(k, \rho)$$

We take a power α_k^ρ for each cardinality since there are α_k^ρ rows which have (k, ρ)-compatible vector with $\phi_{n_{\leq r}}(k, \rho)$ possible forms. (Note that we can omit terms with $\alpha_k^\rho = 0$ since these contribute a factor 1.)

Hence, the set of regular inhomogeneous networks of valency at most r has cardinality

$$\prod_{k=1}^{n} \left(\sum_{i=0}^{r} \phi_{n_i}(k, \rho) \right)^{\alpha_k^\rho}$$

□

We show how to compute the cardinality of the fixed-point set of a three-cell regular inhomogeneous network of valency at most 3 for a given partition in the following example.

Example 2.2. Let $\rho = [1^1 2^1]$ be the partition of $n = 3$. Using (s, ρ)-compatible vector forms in Table 2.2, the periodic banded matrix A has the following form:

$$A = \left(\begin{array}{c|cc} a & b & b \\ \hline a' & b' & c' \\ a' & c' & b' \end{array}\right)$$

To compute $\phi_{3_{\leq 3}}(1, \rho)$, we enumerate all possible cases which satisfy:

$$\begin{aligned} \{(a,b) \in \mathbb{N}^2 : a + b + b \leq 3\} &= \{(a,b) : a + 2b = 0\} \cup \\ &\quad \{(a,b) : a + 2b = 1\} \cup \\ &\quad \{(a,b) : a + 2b = 2\} \cup \\ &\quad \{(a,b) : a + 2b = 3\} \end{aligned}$$

where $0 \leq a, b \leq 3$.

Therefore, there are six combinations for a and b, namely:

$$(a,b) = (0,0), (1,0), (2,0), (0,1), (1,1), (3,0)$$

Next, we find $\phi_{3_{\leq 3}}(2, \rho)$ for arbitrary numbers $0 \leq a', b', c' \leq 3$ which satisfy:

$$a' + b' + c' \leq 3$$

Then,

$$|(a', b', c')| = \left(\begin{array}{c} 3+3 \\ 3 \end{array}\right) = 20$$

Since $6 = 1 + 1 + 2 + 2$ and $20 = 1 + 3 + 6 + 10$, this agrees with Lemma 2.2.

Hence, by Proposition 2.4, $6^1 \cdot 20^1 = 120$ adjacency matrices are fixed by the permutation of label of two cells.

◇

Proposition 2.4 implied that we can compute the cardinalities of regular inhomogeneous networks using the same data set as regular homogeneous networks, however, we take the sum of data from different valencies. For this reason, we modify data table 1 in Aldosray and Stewart (2005) as the following Table 2.3 which shows the cardinalities of each compatible vector.

n	Partition	$r=0$	$r=1$	$r=2$	$r=3$	$r=4$	$r=5$	$r=6$
1	$[1^1]$	1	1	1	1	1	1	1
2	$[1^2]$	1^2	2^2	3^2	4^2	5^2	6^2	7^2
	$[2^1]$	1^1	2^1	3^1	4^1	5^1	6^1	7^1
3	$[1^3]$	1^3	3^3	6^3	10^3	15^3	21^3	28^3
	$[1^1 \cdot 2^1]$	$1^1 \cdot 1^1$	$1^1 \cdot 3^1$	$2^1 \cdot 6^1$	$2^1 \cdot 10^1$	$3^1 \cdot 15^1$	$3^1 \cdot 21^1$	$4^1 \cdot 28^1$
	$[3^1]$	1^1	3^1	6^1	10^1	15^1	21^1	28^1
4	$[1^4]$	1^4	4^4	10^4	20^4	35^4	56^4	84^4
	$[1^2 \cdot 2^1]$	$1^2 \cdot 1^1$	$2^2 \cdot 4^1$	$4^2 \cdot 10^1$	$6^2 \cdot 20^1$	$9^2 \cdot 35^1$	$12^2 \cdot 56^1$	$16^2 \cdot 84^1$
	$[1^1 \cdot 3^1]$	$1^1 \cdot 1^1$	$1^1 \cdot 4^1$	$1^1 \cdot 10^1$	$2^1 \cdot 20^1$	$2^1 \cdot 35^1$	$2^1 \cdot 56^1$	$3^1 \cdot 84^1$
	$[4^1]$	1^1	4^1	10^1	20^1	35^1	56^1	84^1
	$[2^2]$	1^2	4^2	10^2	20^2	35^2	56^2	84^2
5	$[1^5]$	1^5	5^5	15^5	35^5	70^5	126^5	210^5
	$[1^3 \cdot 2^1]$	$1^3 \cdot 1^1$	$3^3 \cdot 5^1$	$7^3 \cdot 15^1$	$13^3 \cdot 35^1$	$22^3 \cdot 70^1$	$34^3 \cdot 126^1$	$50^3 \cdot 210^1$
	$[1^2 \cdot 3^1]$	$1^2 \cdot 1^1$	$2^2 \cdot 5^1$	$3^2 \cdot 15^1$	$5^2 \cdot 35^1$	$7^2 \cdot 70^1$	$9^2 \cdot 126^1$	$12^2 \cdot 210^1$
	$[1^1 \cdot 4^1]$	$1^1 \cdot 1^1$	$1^1 \cdot 5^1$	$1^1 \cdot 15^1$	$1^1 \cdot 35^1$	$2^1 \cdot 70^1$	$2^1 \cdot 126^1$	$2^1 \cdot 210^1$
	$[5^1]$	1^1	5^1	15^1	35^1	70^1	126^1	210^1
	$[1^1 \cdot 2^2]$	$1^1 \cdot 1^2$	$1^1 \cdot 5^2$	$3^1 \cdot 15^2$	$3^1 \cdot 35^2$	$6^1 \cdot 70^2$	$6^1 \cdot 126^2$	$10^1 \cdot 210^2$
	$[2^1 \cdot 3^1]$	$1^1 \cdot 1^1$	$2^1 \cdot 3^1$	$3^1 \cdot 7^1$	$5^1 \cdot 13^1$	$7^1 \cdot 22^1$	$9^1 \cdot 34^1$	$12^1 \cdot 50^1$
6	$[1^6]$	1^6	6^6	21^6	56^6	126^6	252^6	462^6
	$[1^4 \cdot 2^1]$	$1^4 \cdot 1^1$	$4^4 \cdot 6^1$	$11^4 \cdot 21^1$	$24^4 \cdot 56^1$	$46^4 \cdot 126^1$	$80^4 \cdot 252^1$	$130^4 \cdot 462^1$
	$[1^3 \cdot 3^1]$	$1^3 \cdot 1^1$	$3^3 \cdot 6^1$	$6^3 \cdot 21^1$	$11^3 \cdot 56^1$	$18^3 \cdot 126^1$	$27^3 \cdot 252^1$	$39^3 \cdot 462^1$
	$[1^2 \cdot 4^1]$	$1^2 \cdot 1^1$	$2^2 \cdot 6^1$	$3^2 \cdot 21^1$	$4^2 \cdot 56^1$	$6^2 \cdot 126^1$	$8^2 \cdot 252^1$	$10^2 \cdot 462^1$
	$[1^1 \cdot 5^1]$	$1^1 \cdot 1^1$	$1^1 \cdot 6^1$	$1^1 \cdot 21^1$	$1^1 \cdot 56^1$	$1^1 \cdot 126^1$	$2^1 \cdot 252^1$	$2^2 \cdot 462^1$
	$[6^1]$	1^1	6^1	21^1	56^1	126^1	252^1	462^1
	$[2^1 \cdot 4^1]$	$1^1 \cdot 1^1$	$2^1 \cdot 6^1$	$5^1 \cdot 21^1$	$8^1 \cdot 56^1$	$14^1 \cdot 126^1$	$20^1 \cdot 252^1$	$30^2 \cdot 462^1$
	$[1^1 \cdot 2^1 \cdot 3^1]$	$1^1 \cdot 1^1 \cdot 1^1$	$1^1 \cdot 3^1 \cdot 4^1$	$2^1 \cdot 6^1 \cdot 11^1$	$3^1 \cdot 11^1 \cdot 24^1$	$4^1 \cdot 18^1 \cdot 46^1$	$5^1 \cdot 27^1 \cdot 80^1$	$7^1 \cdot 39^1 \cdot 130^1$
	$[3^2]$	1^2	6^2	21^2	56^2	126^2	252^2	462^2
	$[2^3]$	1^3	6^3	21^3	56^3	126^3	252^3	462^3
	$[1^2 \cdot 2^2]$	$1^2 \cdot 1^2$	$2^2 \cdot 6^2$	$5^2 \cdot 21^2$	$8^2 \cdot 56^2$	$14^2 \cdot 126^2$	$20^2 \cdot 252^2$	$30^2 \cdot 462^2$

Table 2.3: Cardinality of fixed-point sets in $X_{n_r}, 0 \leq r \leq 6$ under symmetric groups $S_n, 1 \leq n \leq 6$.

2.8 Enumeration Formulas

Note that the networks enumerated by the following formulas will include disconnected networks. Enumeration for connected networks will be discussed in a later section.

2.8.1 Preliminaries

By substituting the cardinality of the fixed-point set in (2.5) as $|\mathrm{Fix}_\Omega(g_i)|$ for the corresponding partition, the enumeration formula is:

Theorem 2.4. *Let $n, r \in \mathbb{N}$. Then the number of n-cell regular homogeneous networks of valency r is*

$$H_{n_r} = \frac{1}{n!} \sum_{\rho \in \Pi_n} \frac{n!}{1^{\alpha_1^\rho} 2^{\alpha_2^\rho} \cdots n^{\alpha_n^\rho} \alpha_1^\rho! \alpha_2^\rho! \cdots \alpha_n^\rho!} \times \prod_{k=1}^{n} \phi_{n_r}(k, \rho)^{\alpha_k^\rho}$$

Proof. See Aldosray and Stewart (2005). □

2.8.2 Regular Inhomogeneous Network Case

The enumeration formula for regular inhomogeneous networks is given by:

Theorem 2.5. *Let $n \in \mathbb{N}$, $r \in \mathbb{N}_0$. Then the number of n-cell regular inhomogeneous networks of valency at most r is*

$$I_{n_{\leq r}} = \frac{1}{n!} \sum_{\rho \in \Pi_n} \frac{n!}{1^{\alpha_1^\rho} 2^{\alpha_2^\rho} \cdots n^{\alpha_n^\rho} \alpha_1^\rho! \alpha_2^\rho! \cdots \alpha_n^\rho!} \times \prod_{k=1}^{n} \left(\sum_{i=0}^{r} \phi_{n_i}(k, \rho) \right)^{\alpha_k^\rho}$$

Proof. This follows directly from Theorem 2.4. □

2.9 Manipulation of Network Structure

2.9.1 Homogeneous Networks without Self-Coupling

In some applications, we wish to consider networks which do not have self-coupling. We enumerate regular homogeneous networks without self-coupling.

Lemma 2.7. *Let $\tilde{A}$ be the adjacency matrix associated with an n-cell regular homogeneous network $\tilde{\mathcal{G}}$, which does not have self-coupling. Let $\tilde{V}_{n_r}$ be the set of all possible row vectors of $\tilde{A}$ and $\tilde{\phi}_{n_r}(s, \rho) = |\tilde{V}_{n_r}(s, \rho)|$ be the cardinality of the set of all (s, ρ)-compatible vectors in $\tilde{V}_{n_r}$. Then*

$$\tilde{\phi}_{n_r}(s, \rho) = \phi_{n_r}(s, \rho) - \phi_{n_{r-1}}(s, \rho)$$

where $\phi_{n_i}(s, \rho)$ is the set of all (s, ρ)-compatible vectors for regular homogeneous networks of valency i.

Proof. Suppose that

$$\phi_{n_r}(s,\rho) = \begin{pmatrix} p \\ q \end{pmatrix}$$

for arbitrary positive integers p and q.

If $\tilde{\mathcal{G}}$ has no self-couplings, one of the coordinates in $\mathbf{v} \in V_{n_r}(s,\rho)$ is always zero. Hence

$$\tilde{\phi}_{n_r}(s,\rho) = \begin{pmatrix} p-1 \\ q \end{pmatrix}$$

Now

$$\begin{aligned} \begin{pmatrix} p-1 \\ q \end{pmatrix} &= \begin{pmatrix} p \\ q \end{pmatrix} - \begin{pmatrix} p-1 \\ q-1 \end{pmatrix} \\ &= \phi_{n_r}(s,\rho) - \phi_{n_{r-1}}(s,\rho) \end{aligned}$$

□

Theorem 2.6. *The number of n-cell regular homogeneous networks of valency r without self-coupling is*

$$\tilde{H}_{n_r} = \frac{1}{n!} \sum_{\rho \in \Pi_n} \frac{n!}{1^{\alpha_1^\rho} 2^{\alpha_2^\rho} \cdots n^{\alpha_n^\rho} \alpha_1^\rho! \alpha_2^\rho! \cdots \alpha_n^\rho!} \times \prod_{k=1}^{n} \tilde{\phi}_{n_r}(k,\rho)^{\alpha_k^\rho}$$

Proof. This immediately follows from Lemma 2.7 and Theorem 2.4. □

The following example illustrates the computation of the cardinality of the fixed-point sets for a 4-cell regular homogeneous network without self-coupling.

Example 2.3. Let $\rho = [1^2 2^1]$ be the cycle type of the partition of integer $n = 4$. We compute the fixed-point set of $\rho = [1^2 2^1]$ in the set of adjacency matrices of regular homogeneous networks of valency $r = 3$ without self-coupling. Using Table 2.2, the matrix form which is fixed by a given partition is:

$$\left(\begin{array}{c|c|cc} a & b & c & c \\ \hline d & e & f & f \\ \hline g & h & i & j \\ g & h & j & i \end{array}\right)$$

To obtain $\tilde{\phi}_{4_3}(1,\rho)$, we enumerate all possible cases which satisfy:

$$a + b + c + c = 3 \Leftrightarrow a + b + 2c = 3$$

where $a = 0$ (since no self-couplings) and $0 \leq b, c \leq 3$.

Therefore, all combinations of a b and c are the following two cases:

$$(a,b,c) = (0,1,1), (0,3,0)$$

Next, for $\tilde{\phi}_{4_3}(2,\rho)$, we consider all possible cases of :

$$g+h+i+j=3$$

where $0 \leq g,h,i,j \leq 3$.

Since $i=0$ (no self-couplings), $g+h+i+j=3 \Leftrightarrow g+h+j=3$, therefore

$$|(g,h,i,j)| = \begin{pmatrix} 3+3-1 \\ 3 \end{pmatrix} = 10$$

Thus, the cardinality of the set of adjacency matrices which is fixed by a given partition is:

$$2^2 \cdot 10^1 = 40$$

Using Table 2.3, we can verify the result in Theorem 2.6 since

$$\begin{aligned} 2 &= 6-4 = \phi_{4_3}(1,\rho) - \phi_{4_2}(1,\rho) \\ 10 &= 20-10 = \phi_{4_3}(2,\rho) - \phi_{4_2}(2,\rho) \end{aligned}$$

◇

The relevant data for fixed-point sets for regular homogeneous networks without self-coupling are obtained using Lemma 2.7 and shown in Table 2.4.

2.9.2 Regular Inhomogeneous Networks without Self-Coupling

Theorem 2.7. *Let $N \in \mathbb{N}$ and $r \in \mathbb{N}_0$. Then the number of n-cell regular inhomogeneous networks of valency at most r is*

$$I_{n_{\leq r}} = \frac{1}{n!} \sum_{\rho \in \Pi_n} \frac{n!}{1^{\alpha_1^\rho} 2^{\alpha_2^\rho} \cdots n^{\alpha_n^\rho} \alpha_1^\rho! \alpha_2^\rho! \cdots \alpha_n^\rho!} \times \prod_{k=1}^{n} \left(\sum_{i=0}^{r} \tilde{\phi}_{n_i}(k,\rho) \right)^{\alpha_k^\rho}$$

Proof. This follows directly from Proposition 2.4 and Theorem 2.4. □

2.9.3 Computational Results

Table 2.5 shows the enumeration results. n is the number of cells and r is the valency of networks. Although trivial, the enumeration results of networks with valency 0 are shown for completeness.

2.9.4 Bijection Between Homogeneous and Inhomogeneous Networks

Note that the enumeration results of "regular homogeneous networks" (the first data set) and "regular inhomogeneous networks without self-coupling" (the fourth data set) in Table 2.5 are identical. The reason is:

n	Partition	$r=0$	$r=1$	$r=2$	$r=3$	$r=4$	$r=5$	$r=6$
1	$[1^1]$	1	0	0	0	0	0	0
2	$[1^2]$	1^2	1^2	1^2	1^2	1^2	1^2	1^2
	$[1^1]$	1^1	1^1	1^1	1^1	1^1	1^1	1^1
3	$[1^3]$	1^3	2^3	3^3	4^3	5^3	6^3	7^3
	$[1^1 \cdot 2^1]$	$1^1 \cdot 1^1$	$0^1 \cdot 2^1$	$1^1 \cdot 3^1$	$0^1 \cdot 4^1$	$1^1 \cdot 5^1$	$0^1 \cdot 6^1$	$1^1 \cdot 7^1$
	$[3^1]$	1^1	2^1	3^1	4^1	5^1	6^1	7^1
4	$[1^4]$	1^4	3^4	6^4	10^4	15^4	21^4	28^4
	$[1^2 \cdot 2^1]$	$1^2 \cdot 1^1$	$1^2 \cdot 3^1$	$2^2 \cdot 6^1$	$2^2 \cdot 10^1$	$3^2 \cdot 15^1$	$3^2 \cdot 21^1$	$4^2 \cdot 28^1$
	$[1^1 \cdot 3^1]$	$1^1 \cdot 1^1$	$0^1 \cdot 3^1$	$0^1 \cdot 6^1$	$1^1 \cdot 10^1$	$0^1 \cdot 15^1$	$0^1 \cdot 21^1$	$1^1 \cdot 28^1$
	$[4^1]$	1^1	3^1	6^1	10^1	15^1	21^1	28^1
	$[2^2]$	1^2	3^2	6^2	10^2	15^2	21^2	28^2
5	$[1^5]$	1^5	4^5	10^5	20^5	35^5	56^5	84^5
	$[1^3 \cdot 2^1]$	$1^3 \cdot 1^1$	$2^3 \cdot 4^1$	$4^3 \cdot 10^1$	$6^3 \cdot 20^1$	$9^3 \cdot 35^1$	$12^3 \cdot 56^1$	$16^3 \cdot 84^1$
	$[1^2 \cdot 3^1]$	$1^2 \cdot 1^1$	$1^2 \cdot 4^1$	$1^2 \cdot 10^1$	$2^2 \cdot 20^1$	$2^2 \cdot 35^1$	$2^2 \cdot 56^1$	$3^2 \cdot 84^1$
	$[1^1 \cdot 4^1]$	$1^1 \cdot 1^1$	$0^1 \cdot 4^1$	$0^1 \cdot 10^1$	$0^1 \cdot 20^1$	$1^1 \cdot 35^1$	$0^1 \cdot 56^1$	$0^1 \cdot 84^1$
	$[5^1]$	1^1	4^1	10^1	20^1	35^1	56^1	84^1
	$[1^1 \cdot 2^2]$	$1^1 \cdot 1^2$	$0^1 \cdot 4^2$	$2^1 \cdot 10^2$	$0^1 \cdot 20^2$	$3^1 \cdot 35^2$	$0^1 \cdot 56^2$	$4^1 \cdot 84^2$
	$[2^1 \cdot 3^1]$	$1^1 \cdot 1^1$	$1^1 \cdot 2^1$	$1^1 \cdot 4^1$	$2^1 \cdot 6^1$	$2^1 \cdot 9^1$	$2^1 \cdot 12^1$	$3^1 \cdot 16^1$
6	$[1^6]$	1^6	5^6	15^6	35^6	70^6	126^6	210^6
	$[1^4 \cdot 2^1]$	$1^4 \cdot 1^1$	$3^4 \cdot 5^1$	$7^4 \cdot 15^1$	$13^4 \cdot 35^1$	$22^4 \cdot 70^1$	$34^4 \cdot 126^1$	$50^4 \cdot 210^1$
	$[1^3 \cdot 3^1]$	$1^3 \cdot 1^1$	$2^3 \cdot 5^1$	$3^3 \cdot 15^1$	$5^3 \cdot 35^1$	$7^3 \cdot 70^1$	$9^3 \cdot 126^1$	$12^3 \cdot 210^1$
	$[1^2 \cdot 4^1]$	$1^2 \cdot 1^1$	$1^2 \cdot 5^1$	$1^2 \cdot 15^1$	$1^2 \cdot 35^1$	$2^2 \cdot 70^1$	$2^2 \cdot 126^1$	$2^2 \cdot 210^1$
	$[1^1 \cdot 5^1]$	$1^1 \cdot 1^1$	$0^1 \cdot 5^1$	$0^1 \cdot 15^1$	$0^1 \cdot 35^1$	$0^1 \cdot 70^1$	$1^1 \cdot 126^1$	$0^2 \cdot 210^1$
	$[6^1]$	1^1	5^1	15^1	35^1	70^1	126^1	210^1
	$[2^1 \cdot 4^1]$	$1^1 \cdot 1^1$	$1^1 \cdot 5^1$	$3^1 \cdot 15^1$	$3^1 \cdot 35^1$	$6^1 \cdot 70^1$	$6^1 \cdot 126^1$	$10^2 \cdot 210^1$
	$[1^1 \cdot 2^1 \cdot 3^1]$	$1^1 \cdot 1^1 \cdot 1^1$	$0^1 \cdot 2^1 \cdot 3^1$	$1^1 \cdot 3^1 \cdot 7^1$	$1^1 \cdot 5^1 \cdot 13^1$	$1^1 \cdot 7^1 \cdot 22^1$	$1^1 \cdot 9^1 \cdot 34^1$	$2^1 \cdot 12^1 \cdot 50^1$
	$[3^2]$	1^2	5^2	15^2	35^2	70^2	126^2	210^2
	$[2^3]$	1^3	5^3	15^3	35^3	70^3	126^3	210^3
	$[1^2 \cdot 2^2]$	$1^2 \cdot 1^2$	$1^2 \cdot 5^2$	$3^2 \cdot 15^2$	$3^2 \cdot 35^2$	$6^2 \cdot 70^2$	$6^2 \cdot 126^2$	$10^2 \cdot 210^2$

Table 2.4: Cardinality of fixed-point sets in the set of all possible adjacency matrices of regular homogeneous networks without self-coupling under symmetric groups $S_n, 1 \leq n \leq 6$.

Enumeration of regular homogeneous networks

n	$r=0$	$r=1$	$r=2$	$r=3$	$r=4$	$r=5$	$r=6$
1	1	1	1	1	1	1	1
2	1	3	6	10	15	21	28
3	1	7	44	180	590	1582	3724
4	1	19	475	6915	63420	412230	2080827
5	1	47	6874	444722	14072268	265076184	3405665412
6	1	130	126750	43242604	5569677210	355906501686	13508534834704

Enumeration of regular inhomogeneous networks

n	$r=0$	$r\leq 1$	$r\leq 2$	$r\leq 3$	$r\leq 4$	$r\leq 5$	$r\leq 6$
1	1	2	3	4	5	6	7
2	1	6	21	55	120	231	406
3	1	16	190	1400	7315	29624	99484
4	1	45	2340	64225	1009680	10540782	81171405
5	1	121	36796	4658320	265706712	8479734126	175485117498
6	1	338	712996	492565066	119362310539	13513121673238	864517486233114

Enumeration of regular homogeneous networks without self-coupling

n	$r=0$	$r=1$	$r=2$	$r=3$	$r=4$	$r=5$	$r=6$
1	1	0	0	0	0	0	0
2	1	1	1	1	1	1	1
3	1	2	7	12	25	38	63
4	1	6	66	445	2175	8211	25837
5	1	13	916	27046	440310	4597548	34883346
6	1	40	16816	2575900	163762914	5561236158	119147448025

Enumeration of regular inhomogeneous networks without self-coupling

n	$r=0$	$r\leq 1$	$r\leq 2$	$r\leq 3$	$r\leq 4$	$r\leq 5$	$r\leq 6$
1	1	1	1	1	1	1	1
2	1	3	6	10	15	21	28
3	1	7	44	180	590	1582	3724
4	1	19	475	6915	63420	412230	2080827
5	1	47	6874	444722	14072268	265076184	3405665412
6	1	130	126750	43242604	5569677210	355906501686	13508534834704

Table 2.5: Computational results for four different network types.

Proposition 2.5. *Let M_{n_r} be the set of adjacency matrices of n-cell regular homogeneous networks of valency r and let $\tilde{M}_{n_{\leq r}}$ be the set of adjacency matrices of n-cell regular inhomogeneous networks of valency up to r without self-coupling. Then, the cardinalities of these sets are equal; that is*

$$|M_{n_r}| = |\tilde{M}_{n_{\leq r}}|$$

Proof. We show that there is a bijection between M_{n_r} and $\tilde{M}_{n_{\leq r}}$. Firstly we show there is a one-to-one map f such that

$$f : \tilde{M}_{n_{\leq r}} \to M_{n_r}$$

Since there exist some elements $\tilde{A} \in \tilde{M}_{n_r}$ such that $\tilde{A} \in \tilde{M}_{n_r} \cap M_{n_r}$, we only need to consider the case when $\tilde{A} \in \tilde{M}_{n_{\leq r}} \setminus M_{n_r}$. $\tilde{A} \in \tilde{M}_{n_{\leq r}} \setminus M_{n_r}$ has the following form:

$$\tilde{A} = \begin{pmatrix} 0 & \tilde{a}_{12} & \cdots & \cdots & \tilde{a}_{1n} \\ \tilde{a}_{21} & 0 & \tilde{a}_{13} & \cdots & \tilde{a}_{2n} \\ \vdots & \cdots & \cdots & \cdots & \vdots \\ \tilde{a}_{n1} & \cdots & \cdots & \cdots & 0 \end{pmatrix}$$

where $0 \leq \tilde{a}_{ij} \leq r$ for $i, j = 1, \ldots, n$ with $i \neq j$.

Construct a diagonal matrix $\tilde{D} = (\tilde{d}_{ij})$ such that $\tilde{d}_{ii} + \sum_{j=1}^{n} \tilde{a}_{ij} = r$ with $0 \leq \tilde{d}_{ii} \leq r$ for all $i = 1, \ldots, n$. Adding this diagonal matrix $\tilde{D}$ to $\tilde{A}$ gives the following form:

$$\tilde{A} + \tilde{D} = \begin{pmatrix} \tilde{d}_{11} & \tilde{a}_{12} & \cdots & \cdots & \tilde{a}_{1n} \\ \tilde{a}_{21} & \tilde{d}_{22} & \tilde{a}_{13} & \cdots & \tilde{a}_{2n} \\ \vdots & \cdots & \cdots & \cdots & \vdots \\ \tilde{a}_{n1} & \cdots & \cdots & \cdots & \tilde{d}_{nn} \end{pmatrix} \tag{2.9}$$

The matrix form in (2.9) corresponds to a unique homogeneous regular network. Therefore, f is one-to-one.

Similarly, we define a map f^{-1} (which we will show is the inverse of f) such that

$$f^{-1} : M_{n_r} \to \tilde{M}_{n_{\leq r}}$$

If $A \in M_{n_r}$ does not have any self-loop, there is a unique element in $\tilde{M}_{n_{\leq r}}$ which corresponds to A. Hence, we only consider the case when $A \in M_{n_r}$ has self-loops. Suppose A has the following form:

$$A = \begin{pmatrix} a_{11} & a_{12} & \cdots & \cdots & a_{1n} \\ a_{21} & a_{22} & a_{13} & \cdots & a_{2n} \\ \vdots & \cdots & \cdots & \cdots & \vdots \\ a_{n1} & \cdots & \cdots & \cdots & a_{nn} \end{pmatrix}$$

where $0 \leq a_{ij} \leq r$ for $i, j = 1, \ldots, n$ with $i \neq j$ and $a_{ii} \neq 0$ for some i. By subtracting a diagonal matrix D, whose diagonal elements consists of $a_{11}, \ldots, a_{nn}$, from $\tilde{A}$ gives the following form:

$$A - D = \begin{pmatrix} 0 & a_{12} & \cdots & \cdots & a_{1n} \\ a_{21} & 0 & a_{13} & \cdots & a_{2n} \\ \vdots & \cdots & \cdots & \cdots & \vdots \\ a_{n1} & \cdots & \cdots & \cdots & 0 \end{pmatrix}$$

This corresponds to a unique inhomogeneous regular network in $\tilde{M}_{n_{\leq r}}$. Hence f^{-1} is also one-to-one and provides an inverse for f. As a result, $|M_{n_r}| = |\tilde{M}_{n_{\leq r}}|$. □

Example 2.4. The following figures show how one network is constructed from the other.

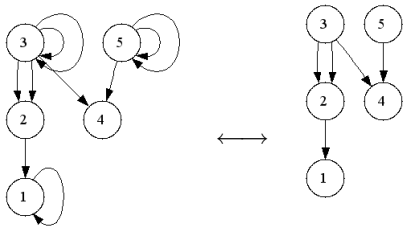

In one direction all self-couplings are removed, in the other sufficient self-couplings are added so that each cell has the desired valency (here 2).

◇

2.10 Connected Graphs

2.10.1 Preliminaries

The enumeration of networks in Theorem 2.4 and 2.5 includes some disconnected networks. If a network is disconnected, it decomposes into more than one connected subnetwork. For example, a five-cell disconnected network can be decomposed into

Case 1: four-cell connected subnetwork and one isolated cell,

Case 2: three-cell connected subnetwork and two-cell connected subnetwork,

Case 3: three-cell connected subnetwork and two isolated cells,

Case 4: two two-cell connected subnetworks and one isolated cell,

Case 5: two-cell connected subnetwork and three isolated cells,

Case 6: five isolated cells.

Therefore, the enumeration of connected networks can be done recursively by removing all possible disconnected subnetworks from the total number of networks as described in the following.

Let K_{n_r} be the number of isomorphism classes of connected n-cell regular homogeneous networks of valency r. For the case $n = 5$, $r = 2$, we computed the number of regular homogeneous networks (including disconnected networks) $H_{5_2} = 6874$. Since there is only one network with one cell (corresponding to isolated cell for each case above), K_{5_2} is computed such as

$$K_{5_2} = H_{5_2} - \left\{ K_{4_2} + K_{3_2}K_{2_2} + K_{3_2} + \frac{K_{2_2}(K_{2_2}+1)}{2} + K_{2_2} + K_{1_2} \right\}$$

where the term $\frac{K_{2_2}(K_{2_2}+1)}{2}$ corresponds to the case 4. In this case we have to remember interchanging the two subnetworks is a possible isomorphism.

Therefore, K_{5_2} is expressed recursively in terms of H_{5_2} and K_{n_2} for $1 \leq n < 5$. In general, we have

Theorem 2.8. *Let $n, r \in \mathbb{N}$. Then the number of isomorphism classes of connected regular homogeneous n-cell networks of valency r is*

$$K_{n_r} = H_{n_r} - \sum_{[n^1] \neq \rho \in \Pi_n} \prod_{k=1}^{n} \begin{pmatrix} K_{k_r} + \alpha_k^\rho - 1 \\ \alpha_k^\rho \end{pmatrix}$$

Proof. See Aldosray and Stewart (2005). □

2.10.2 Regular Inhomogeneous Network Case

Theorem 2.9. *Let $n \in \mathbb{N}$ and $r \in \mathbb{N}_0$. Then the number of isomorphism classes of connected regular inhomogeneous n-cell networks of valency up to r is*

$$IK_{n_{\leq r}} = I_{n_{\leq r}} - \sum_{[n^1] \neq \rho \in \Pi_n} \prod_{k=1}^{n} \begin{pmatrix} IK_{k_{\leq r}} + \alpha_k^\rho - 1 \\ \alpha_k^\rho \end{pmatrix}$$

where $I_{n_{\leq r}}$ is the number of isomorphism classes of n-cell regular inhomogeneous networks of valency at most r.

Proof. Since the structures of disconnected networks are the same as regular homogeneous networks case, the same method enable us to enumerate connected networks for inhomogeneous case. □

2.11 Computational Results

The enumeration results for connected regular homogeneous networks and connected regular inhomogeneous networks are listed in the following Table 2.6.

Enumeration of connected regular homogeneous networks

n	$r=0$	$r=1$	$r=2$	$r=3$	$r=4$	$r=5$	$r=6$
1	1	1	1	1	1	1	1
2	0	2	5	9	14	20	27
3	0	4	38	170	575	1561	3696
4	0	9	416	6690	62725	410438	2076725
5	0	20	6209	436277	14000798	264632734	3403484793
6	0	51	117020	42722972	5554560632	355631996061	13505066262007

Enumeration of connected regular inhomogeneous networks

n	$r=0$	$r\leq 1$	$r\leq 2$	$r\leq 3$	$r\leq 4$	$r\leq 5$	$r\leq 6$
1	1	2	3	4	5	6	7
2	0	3	15	45	105	210	378
3	0	6	135	1200	6755	28308	96754
4	0	13	1710	57905	968695	10344243	80411702
5	0	29	28300	4355604	260021011	8410984578	174882419829
6	0	71	573928	470969051	117919071374	13459826248926	863255706129012

Enumeration of connected regular homogeneous networks without self-coupling

n	$r=0$	$r=1$	$r=2$	$r=3$	$r=4$	$r=5$	$r=6$
1	1	0	0	0	0	0	0
2	0	1	1	1	1	1	1
3	0	2	7	12	25	38	63
4	0	6	66	445	2175	8211	25837
5	0	13	916	27046	440310	4597548	34883346
6	0	40	16816	2575900	163762914	5561236158	119147448025

Enumeration of connected regular inhomogeneous networks without self-coupling

n	$r=0$	$r\leq 1$	$r\leq 2$	$r\leq 3$	$r\leq 4$	$r\leq 5$	$r\leq 6$
1	1	1	1	1	1	1	1
2	0	2	5	9	14	20	27
3	0	4	38	170	575	1561	3696
4	0	9	416	6690	62725	410438	2076725
5	0	20	6209	436277	14000798	264632734	3403484793
6	0	51	117020	42722972	5554560632	355631996061	13505066262007

Table 2.6: Enumeration results of connected networks.

2.12 Regular Networks with Different Cell Types

In the preceding sections, we discussed enumeration of inhomogeneous regular networks, meaning that they have one cell type and one arrow type and different valencies for each cell. Often complex networks consist of several different types of cells (nodes). For example, in gene regulatory network, genes and proteins might be represented with two different cell types (node types). We express different roles of cells in the network by colouring cells.

We assume that arrows with same head/tail types are same types (this follows from property 6 in Definition 4.1 in Chapter 4). Under this assumption, it suffices to vary only cell types for the consideration of regular networks with different cell types as well as different arrow types.

In this section, we consider how many networks are possible if we allow more than one cell type (colour). Every cell has the same valency. Moreover, we explore how many networks preserve their colour-dependent topology after permuting the cell colours (although it is difficult to see a real-world application of this type of symmetry). This work is new and we motivate our discussion by showing a simple example.

Example 2.5. Consider two-cell regular homogeneous networks of valency 1. There are three topologically distinct such networks (including disconnected networks) as shown in Figure 2.2.

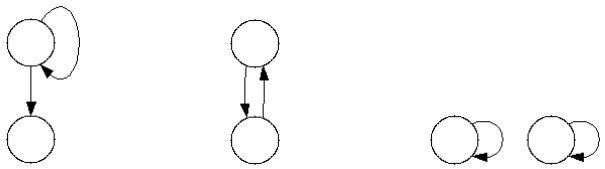

Figure 2.2: Three topologically distinct two-cell regular homogeneous networks of valency 1.

There are 10 possible colourings using up to two colours as shown in Figure 2.3. Trivially all ten networks are preserved if both two colours are fixed; that is black stays as black and white stays as white. This trivial colour permutation is expressed as $(b)(w)$ where "b" means black and "w" means white.

Which coloured networks preserve colour-dependent network topology after swapping black and white colours? We observe that only two networks 5 and 8 are not changed after this colour permutation, in symbol (bw).

$\diamond$

We consider a systematic method to enumerate the number networks which are fixed by a given colour permutation in the following subsections.

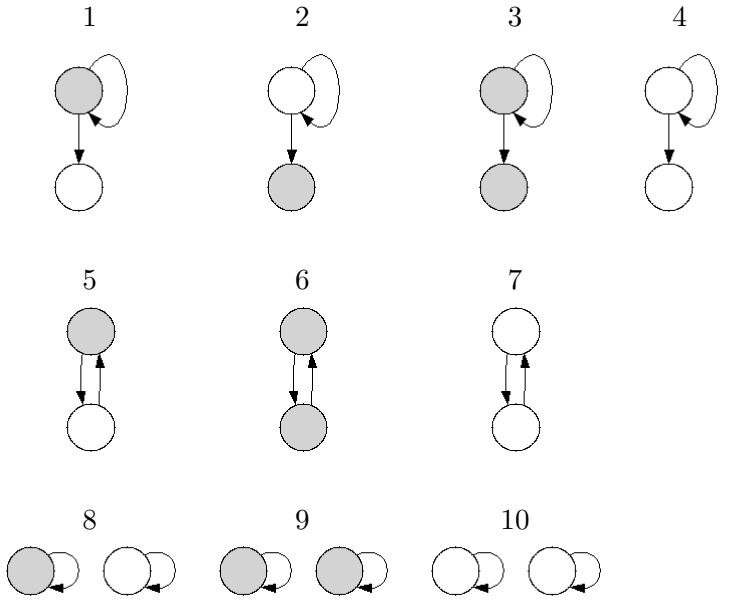

Figure 2.3: Ten possible colourings of two-cell networks using up to two colours.

2.12.1 Vector Notation of Coloured Cells

Define different cell types by colouring cells. An n-cell network is expressed by $n \times n$ adjacency matrix A. If we colour cells, how can we put this information into the adjacency matrix A?

Let σ be a partition of n cells and let P be the corresponding permutation matrix to σ. Note that a permutation group action on the adjacency matrix A, that is PAP^{-1}, preserves diagonal positions such as:

$$a_{ii} \rightarrow a_{\sigma(i)\sigma(i)}$$

where these diagonal elements correspond to each of n cells.

It tells us that we can put colour information into the diagonal element vector, $\mathbf{v} = [a_{11}, a_{22}, \ldots, a_{nn}]$. Specifically, when A is fixed by a permutation σ with associated cycle type $\sigma = [1^1 2^1 3^1]$, it maps a vector $\mathbf{v} \in \mathbb{R}^6$ such that:

$$\begin{aligned} \mathbf{v} &= [a_{11}|a_{22}a_{33}|a_{44}a_{55}a_{66}] \\ &\rightarrow [a_{\sigma(1)\sigma(1)}|a_{\sigma(2)\sigma(2)}a_{\sigma(3)\sigma(3)}|a_{\sigma(4)\sigma(4)}a_{\sigma(5)\sigma(5)}a_{\sigma(6)\sigma(6)}] \\ &= [a_{11}|a_{33}a_{22}|a_{55}a_{66}a_{44}] \end{aligned}$$

Note that a mapped vector has the same cycle type as σ since the block structure of A is fixed.

We next assign algebraic symbols, which express colours, to each element of $\mathbf{v}$. Let $V \subset \mathbb{N}^n$,$C \subset \mathbb{N}^k$ be two different sets. Let f be the set of all mappings from V to C. Here $V = \{v_1, v_2, \ldots, v_n\}$ stands for the set of cells and $C = \{c_1, c_2, \ldots, c_k\}$ stands for the set of

colourings which are assigned to elements of V. We let V_C be the image of V by the map f. Therefore, each $v_i \in V_C, 1 \leq i \leq n$ is an element in $\{c_1, c_2, \ldots, c_k\}$, which are algebraic symbols, corresponding to each cell's colour at the i-th element in the vector.

2.12.2 Fixed-Point Set under a Group Action (P, Q)

We motivate our discussion by the following simple example.

Example 2.6. Three cells in a unidirectional ring are coloured red, green, and blue. In the following figure, the three colours are permuted so that red $\rightarrow$ green $\rightarrow$ blue $\rightarrow$ red:

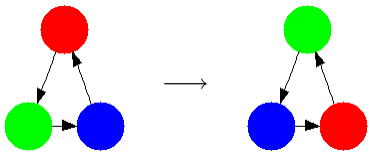

We observe that the colour-dependent network topology is preserved by the permutation of the three colours, in symbols (rgb). The green cell has an arrow from the red cell, the blue cell has an arrow from the green cell, and the red cell has an arrow from the blue cell.

However, if we swap green and blue, but red is fixed, then we have

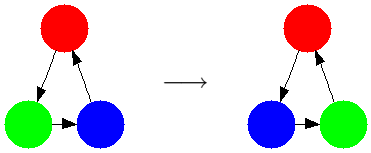

Now, the blue cell has an arrow from the red (not from the green cell), and the green cell has an arrow from the blue cell (not from the red cell), and the red cell has an arrow from the green cell (not from the blue cell). Here the colour-dependent network structure changes after the colour permutation $(r)(gb)$.

$\diamond$

Example 2.6 shows that a unidirectional three-cell ring network is fixed by the colour permutation (rgb), but not by the colour permutation $(r)(gb)$.

We firstly allow cells in a network to have up to $k \in \mathbb{N}$ colours. For example, if we colour a three-cell network with three colours, we allow all three cells have the same colour (one colour in total), two cells have the same colour and the third cell has the different colour (two colours in total), or all three cells have different colours (three colours in total). Then we consider which network structures are preserved (fixed) after changing colours by a given colour permutation.

Suppose that $P \in S_n$ is some group of permutation of an adjacency matrix $A \in M_{n\times n}(\mathbb{N}_0)$ and $Q \in S_k$ is some group of permutation of $\mathbf{v}$, which is the vector of cells with colour information. We define an action of (P, Q) on $(A, \mathbf{v})$ by

$$(P, Q) \cdot (A, \mathbf{v}) = (PAP^{-1}, (P, Q) \cdot \mathbf{v}) \tag{2.10}$$

Specifically, the group action on $\mathbf{v}$ is given by

$$(P, Q) \cdot (v_1, v_2, \ldots, v_n) = (Q(v_{P^{-1}(1)}), Q(v_{P^{-1}(2)}), \ldots, Q(v_{P^{-1}(n)})) \tag{2.11}$$

Lemma 2.8. *Formula (2.11) defines a group action.*

Proof. Let i_P and i_Q be the identity elements of P and Q, respectively. Then i_P is the identity map $i_P : A \to A$ and i_Q is the identity map $i_Q : C \to C$ and for each $v_c \in V_C$,

$$\begin{aligned}(i_P, i_Q) \cdot (v_1, v_2, \ldots, v_N) &= (i_Q(v_1), i_Q(v_2), \ldots, i_Q(v_N)) \\ &= (v_1, v_2, \ldots, v_N)\end{aligned}$$

and thus the identity element exists.

Now let P_1, P_2 be two permutations from P and Q_1, Q_2 be two permutations from Q. Then

$$\begin{aligned}(P_1P_2, Q_1Q_2) \cdot (v_1, v_2, \ldots, v_N) &= (Q_1Q_2) \cdot (v_{P_2P_1(1)}, v_{P_2P_1(2)}, \ldots, v_{P_2P_1(n)}) \\ &= (Q_1Q_2(v_{P_2P_1(1)}), Q_1Q_2(v_{P_2P_1(2)}), \ldots, Q_1Q_2(v_{P_2P_1(n)})) \\ &= (P_1, Q_1) \cdot (Q_2(v_{P_2(1)}), Q_2(v_{P_2(2)}), \ldots, Q_2(v_{P_2(n)})) \\ &= (P_1, Q_1) \cdot \{(P_2, Q_2) \cdot (v_1, v_2, \ldots, v_n)\}\end{aligned}$$

Hence the second axiom of a group action also holds, thus completing the proof. □

To find networks which are preserved by colour permutation as well as cell label permutation by P, we want to calculate fixed-point sets for group action $S_n \times S_k$ such that

$$(P, Q) \cdot (A, \mathbf{v}) = (PAP^{-1}, (P, Q) \cdot \mathbf{v})$$

where $P \in S_n, Q \in S_k$, A is an adjacency matrix and $\mathbf{v}$ is a vector of colours. Therefore, orbits of $S_n \times S_k$ on a set $\Omega(A, \mathbf{v})$ enumerate graphs up to topological changes and colour permutations. The fixed-point set $\mathrm{Fix}_{(A,\mathbf{v})}(P, Q)$ is defined by

$$(A, \mathbf{v}) \in \mathrm{Fix}_{(A,\mathbf{v})}(P, Q) \iff (PAP^{-1}, (P, Q) \cdot \mathbf{v}) = (A, \mathbf{v})$$

Therefore, we must have

1. $PAP^{-1} = A \Leftrightarrow PA = AP$
2. $(P, Q) \cdot \mathbf{v} = \mathbf{v}$

The cardinality of $\mathrm{Fix}_{(A,\mathbf{v})}(P,Q)$ is

$$|\mathrm{Fix}_{(A,\mathbf{v})}(P,Q)| = |\mathrm{Fix}_A P| \times |\mathrm{Fix}_{\mathbf{v}}(P,Q)|$$

We have already found the cardinality of $\mathrm{Fix}_A P$ in Proposition 2.3. The cardinality of $\mathrm{Fix}_{\mathbf{v}}(P,Q)$ is obtained from the lemmas below. Note that for the rest of arguments, we denote cycle types in the normal form only when the multiplicities are not zero.

Lemma 2.9. *Let P be a permutation with cycle type $[l_1^{\alpha_1} l_2^{\alpha_2} \cdots l_s^{\alpha_s}]$ on an $n \times n$ adjacency matrix, and let Q be a permutation of cycle type $[m_1^{\beta_1} m_2^{\beta_2} \ldots m_t^{\beta_t}]$ on k colours, where $\sum_{i=1}^{s} l_i \alpha_i = n$, $\alpha_i \neq 0$ for all i and $\sum_{j=1}^{t} m_j \beta_j = k$, $\beta_j \neq 0$ for all j. Let $\mathbf{v} = (v_1, \ldots, v_n)$ be an arbitrary vector with each $v_i \in \{c_1, \ldots, c_k\}$. Then $(P,Q) \cdot \mathbf{v} = \mathbf{v}$ if and only if $\forall l_i, i = 1, \ldots, s$ $\exists m_j, j = 1, \ldots, t$ such that $m_j \mid l_i$.*

Proof. If $(P,Q) \cdot \mathbf{v} = \mathbf{v}$, then

$$\begin{aligned} (P,Q) \cdot \mathbf{v} &= (P,Q) \cdot (v_1, v_2, \ldots, v_n) \\ &= (Q(v_{P^{-1}(1)}), Q(v_{P^{-1}(2)}), Q(v_{P^{-1}(n)})) \\ &= (v_1, v_2, \ldots, v_n) \end{aligned}$$

Let an element $v_x \in \mathbf{v}$ is in cycle l_i of P. Therefore, for each cycle l_i of P, we must have

$$v_x = Q^{l_i}(v_x), \forall i = 1, \ldots, s$$

This is true if and only if there is a cycle length m_j of Q which divides the cycle length of l_i. □

We now show that for each cycle l_i of P, the corresponding vector elements of $\mathbf{v}$ to this cycle; that is $(v_x, v_{x+1}, \ldots, v_{x+l_i-1})$, have a periodic property.

Lemma 2.10. *Let $M(l_i)$ be the set of cycles m_j of a permutation ρ of Q such that $m_j \mid l_i$ and let $H(l_i)$ be the set of highest common factors $h = hcf(l_i, m_j)$ for all $m_j \in M(l_i)$. Let elements $(v_{x_i}, v_{x_i+1}, \ldots, v_{x_i+l_i-1})$ of $\mathbf{v}$ be in a given cycle l_i of P. Then $\mathbf{v}$ is fixed if and only if for all $i = 1, \ldots, s$,*

$$v_{x_i} = v_{y_i} \quad \textit{if} \quad x_i \equiv y_i \pmod{h} \quad \textit{for any} \quad h \in H(l_i)$$

Proof. If $(P,Q) \cdot \mathbf{v} = \mathbf{v}$, then we must have $v_{x_i} = Q^{l_i}(v_{x_i})$ for all $i = 1, \ldots, s$. We can express $Q^{l_i}(v_{x_i})$ such as $Q^{l_i}(v_{x_i}) = Q^{h \cdot p}(v_{x_i})$ for any $h \in H(l_i)$ and $p \in \mathbb{Z}^+$. Hence if $v_{x_i} = v_{x_i+h}$, then $Q^h(v_{x_i}) = v_{x_i}$ and moreover, $Q^{l_i}(v_{x_i}) = Q^{h \cdot p}(v_{x_i}) = v_{x_i}$. The converse follows similarly. □

Let ρ be the cycle type of P and κ be the cycle type of Q. We call a vector which has the periodic property of Lemma 2.10 an h-**periodic** (κ, ρ)-**compatible coloured** vector. Let $|\mathrm{Fix}_v(P,Q)|$ be the number of fixed vector under an action (P,Q). Then we have the following:

Theorem 2.10. *Let n be the number of cells and k be the number of colours. Let P have cycle type $\rho = [l_1^{\alpha_1} l_2^{\alpha_2} \cdots l_s^{\alpha_s}]$ and Q have cycle type $\kappa = [m_1^{\beta_1} m_2^{\beta_2} \cdots m_t^{\beta_t}]$, where $\sum_{i=1}^{s} l_i \alpha_i = n$ and $\sum_{j=1}^{t} m_j \beta_j = k$. The cardinality of the fixed-point set under the action (P, Q) is*

$$|Fix_{A,\mathbf{v}}(P,Q)| = \prod_{j=1}^{s} \left\{ \sum_{i=1,\ m_i | l_j}^{t} (m_i \times \beta_i) \right\}^{\alpha_j} \tag{2.12}$$

Proof. Using Lemma 2.10, we consider how many colourings are possible in the (κ, ρ)-compatible coloured vector which corresponds to each cycle l_i of P.

The (κ, ρ)-compatible coloured vector is h-periodic for any h, where $h = \mathrm{hcf}(m_j, l_i)$ for all possible m_j such that $m_j \mid l_i$. Hence the number of colours which satisfy h-periodic property is $\sum_{i=1,\ m_i | l_j}^{t} (m_i \times \beta_i)$. There are α_j such cycles. Therefore we take the power α_j over this sum. Repeating this computation for the rest of cycles give the result required. □

Corollary 2.1. *If $\exists l_i$ such that $m_j \nmid l_i$ for all m_j, then $|Fix_{A,\mathbf{v}}(P,Q)| = 0$.*

Proof. This is the contrapositive of Lemma 2.9 and it implies there is no fixed-point set. Also, this case gives $\sum_{i=1, m_i | l_j}^{t} (m_i \times \beta_i) = 0$ in Equation (2.12). Hence, $|\mathrm{Fix}_{A,\mathbf{v}}(P,Q)| = 0$. □

Example 2.7. Let $\rho = [2^1 3^1]$ by the cycle type of P and let $\kappa = [1^1 2^1]$ be the cycle type of Q. Then (P, Q) acts on $\mathbf{v} = (v_1, v_2, v_3, v_4, v_5)$ such as

$$(v_1, v_2, v_3, v_4, v_5) \xrightarrow{P} (v_2, v_1, v_5, v_3, v_4) \xrightarrow{Q} (Q(v_2), Q(v_1), Q(v_5), Q(v_3), Q(v_4))$$

Hence $(P, Q) \cdot \mathbf{v} = \mathbf{v}$ implies

$$\begin{aligned} v_1 &= Q(v_2) \\ v_2 &= Q(v_1) \\ v_3 &= Q(v_5) \\ v_4 &= Q(v_3) \\ v_5 &= Q(v_4) \end{aligned}$$

This means

$$v_i = Q^2(v_i) \quad \text{for} \quad i = 1, 2 \quad \text{and} \quad v_i = Q^3(v_i) \quad \text{for} \quad i = 3, 4, 5. \tag{2.13}$$

Let $(a)(bc)$ be a representative permutation of colours for the conjugacy class determined by the cycle type $\kappa = [1^1 2^1]$. Algebraic symbols “a”, “b”, and “c” represent three colours.

Since both cycle lengths of "(a)" and "(bc)"in Q divide the first cycle "2^1" of P, there are three possible colouring for this first cycle "2^1" of P. However, only the cycle length of "(a)" in Q divides the second cycle "3^1" of P, so there is only one possible colouring for the second cycle "3^1" of P. Therefore, the cardinality of the fixed-point set is

$$|\mathrm{Fix}_{\mathbf{v}}(P,Q)| = (1\times 1 + 2\times 1)^1 \times (1\times 1)^1 = 3$$

Namely, all possible colourings which satisfy Equation (2.13) are

$$\begin{aligned}(v_1v_2v_3v_4v_5) &= (aa|aaa)\\ (v_1v_2v_3v_4v_5) &= (bc|aaa)\\ (v_1v_2v_3v_4v_5) &= (cb|aaa)\end{aligned}$$

◇

In the following tables 2.7 and 2.8 show examples of a (κ,ρ)-compatible coloured vector for each colour permutation. Algebraic symbols, e.g., "a", "b",... express colours for each vector element. For example, $[a|bc]$ means that the first element of $\mathbf{v}$ has colour "a", the second has colour "b" and the third has colour "c".

2.12.3 Enumeration Formulas

By substituting the cardinality of the fixed-point set obtained in Theorem 2.10 as $|\mathrm{Fix}_\Omega(g_i)|$ for the corresponding partition, the enumeration formula is given by:

Theorem 2.11. *Let $n,r\in\mathbb{N}$. Let $\rho=[l_1^{\alpha_1^\rho}l_2^{\alpha_2^\rho}\cdots l_s^{\alpha_s^\rho}]$ be a cycle type of permutation of n labels on cells and let $\kappa=[m_1^{\beta_1^\kappa}m_2^{\beta_2^\kappa}\cdots m_t^{\beta_t^\kappa}]$ be a cycle type of a permutation of k colours. Let $\mathbf{v}$ be a vector which contains cells' colour information. Then the number of n-cell homogeneous networks of valency r with k different cell types, which are fixed by a colour permutation κ is*

$$\begin{aligned}CH_{n_r} &= \frac{1}{n!}\frac{k!}{m_1^{\beta_1^\kappa}m_2^{\beta_2^\kappa}\cdots m_t^{\beta_t^\kappa}\beta_1^\kappa!\beta_2^\kappa!\cdots\beta_t^\kappa!}\sum_{\rho\in\Pi_n}\left\{\frac{n!}{l_1^{\alpha_1^\rho}l_2^{\alpha_2^\rho}\cdots l_s^{\alpha_s^\rho}\alpha_1^\rho!\alpha_2^\rho!\cdots\alpha_s^\rho!}\right.\\ &\left.\times\prod_{k=1}^{n}\phi_{n_r}(k,\rho)^{\alpha_k^\rho}\times|Fix_{\mathbf{v}}(\rho,\kappa)|\right\}\end{aligned}$$

Proof. W multiply by the size of the corresponding conjugacy class of the colour permutation given by:

$$\frac{k!}{m_1^{\beta_1^\kappa}m_2^{\beta_2^\kappa}\cdots m_t^{\beta_t^\kappa}\beta_1^\kappa!\beta_2^\kappa!\cdots\beta_t^\kappa!}$$

The rest of part follows directly from Theorem 2.4. □

n	Partition ρ	$\kappa = (a)(b)$	$\lvert\mathrm{Fix}_{\mathbf{v}}\rvert$	$\kappa = (ab)$	$\lvert\mathrm{Fix}_{\mathbf{v}}\rvert$
1	$[1^1]$	$[*]$	2^1	$\emptyset$	0
2	$[1^2]$	$[*\lvert*]$	2^2	$\emptyset$	0
	$[2^1]$	$[aa], [bb]$	2^1	$[ab]$	2^1
3	$[1^3]$	$[*\lvert *\lvert *]$	2^3	$\emptyset$	0
	$[1^1 \cdot 2^1]$	$[a\lvert aa], [a\lvert bb], [b\lvert aa], [b\lvert bb]$	2^2	$\emptyset$	0
	$[3^1]$	$[aaa], [bbb]$	2^1	$\emptyset$	0
4	$[1^4]$	$[*\lvert *\lvert *\lvert *]$	2^4	$\emptyset$	0
	$[1^2 \cdot 2^1]$	$[*\lvert *\lvert aa], [*\lvert *\lvert bb]$	2^3	$\emptyset$	0
	$[1^1 \cdot 3^1]$	$[*\lvert aaa], [*\lvert bbb]$	2^2	$\emptyset$	0
	$[4^1]$	$[aaaa], [bbbb]$	2^1	$[abab], [baba]$	2^1
	$[2^2]$	$[aa\lvert aa], [aa\lvert bb], [bb\lvert aa], [bb\lvert aa]$	2^2	$[ab\lvert ab], [ab\lvert ba], [ba\lvert ab], [ba\lvert ba]$	2^2
5	$[1^5]$	$[*\lvert *\lvert *\lvert *\lvert *]$	2^5	$\emptyset$	0
	$[1^3 \cdot 2^1]$	$[*\lvert *\lvert *\lvert aa], [*\lvert *\lvert *\lvert bb]$	2^4	$\emptyset$	0
	$[1^2 \cdot 3^1]$	$[*\lvert *\lvert aaa], [*\lvert *\lvert bbb]$	2^3	$\emptyset$	0
	$[1^1 \cdot 4^1]$	$[*\lvert aaaa], [*\lvert bbbb]$	2^2	$\emptyset$	0
	$[5^1]$	$[aaaaa], [bbbbb]$	2^1	$\emptyset$	0
	$[1^1 \cdot 2^2]$	$[*\lvert aa\lvert aa], [*\lvert aa\lvert bb], [*\lvert bb\lvert aa], [*\lvert bb\lvert bb]$	2^3	$\emptyset$	0
	$[2^1 \cdot 3^1]$	$[aa\lvert aaa], [aa\lvert bbb], [bb\lvert aaa], [bb\lvert bbb]$	2^2	$\emptyset$	0
6	$[1^6]$	$[*\lvert *\lvert *\lvert *\lvert *\lvert *]$	2^6	$\emptyset$	0
	$[1^4 \cdot 2^1]$	$[*\lvert *\lvert *\lvert *\lvert aa], [*\lvert *\lvert *\lvert *\lvert bb]$	2^5	$\emptyset$	0
	$[1^3 \cdot 3^1]$	$[*\lvert *\lvert *\lvert aaa], [*\lvert *\lvert *\lvert bbb]$	2^4	$\emptyset$	0
	$[1^2 \cdot 4^1]$	$[*\lvert *\lvert aaaa], [*\lvert *\lvert bbbb]$	2^3	$\emptyset$	0
	$[1^1 \cdot 5^1]$	$[*\lvert aaaa], [*\lvert bbbbb]$	2^2	$\emptyset$	0
	$[6^1]$	$[aaaaaa], [bbbbbb]$	2^1	$[ababab], [bababa]$	2^1
	$[2^1 \cdot 4^1]$	$[aa\lvert aaaa], [aa\lvert bbbb], [bb\lvert aaaa], [bb\lvert bbbb]$	2^2	$[ab\lvert abab], [ab\lvert baba], [ba\lvert abab], [ba\lvert baba]$	2^2
	$[1^1 \cdot 2^1 \cdot 3^1]$	$[*\lvert aa\lvert aaa], [*\lvert aa\lvert bbb], [*\lvert bb\lvert aaa], [*\lvert bb\lvert bbb]$	2^3	$\emptyset$	0
	$[3^2]$	$[aaa\lvert aaa], [aaa\lvert bbb], [bbb\lvert aaa], [bbb\lvert bbb]$	2^2	$\emptyset$	0
	$[2^3]$	$[aa\lvert aa\lvert aa], [aa\lvert aa\lvert bb], \ldots$	2^3	$[ab\lvert ab\lvert ab], [ab\lvert ab\lvert ba], \ldots$	2^3
	$[1^2 \cdot 2^2]$	$[*\lvert *\lvert aa\lvert aa], [*\lvert *\lvert aa\lvert bb], [*\lvert *\lvert bb\lvert aa], [*\lvert *\lvert bb\lvert bb]$	2^4	$\emptyset$	0

Table 2.7: (κ, ρ)-compatible coloured vector for two colours. "*" means it can take either "a" or "b".

n	Partition ρ	$\kappa = (a)(b)(c)$	$\lvert\mathrm{Fix}_{\mathbf{v}}\rvert$	$\kappa = (a)(bc)$	$\lvert\mathrm{Fix}_{\mathbf{v}}\rvert$	$\kappa = (abc)$	$\lvert\mathrm{Fix}_{\mathbf{v}}\rvert$
1	$[1^1]$	$[*]$	3^1	$[a]$	1^1	$\emptyset$	0
2	$[1^2]$	$[*\|*]$	3^2	$[a\|a]$	1^2	$\emptyset$	0
	$[2^1]$	$[aa], [bb], [cc]$	3^1	$[aa], [bc], [cb]$	3^1	$\emptyset$	0
3	$[1^3]$	$[*\|*\|*]$	3^3	$[a\|a\|a]$	1^3	$\emptyset$	0
	$[1^1 \cdot 2^1]$	$[*\|aa], [*\|bb], [*\|cc]$	3^2	$[a\|aa], [a\|bc], [a\|cb]$	$1^1 \cdot 3^1$	$\emptyset$	0
	$[3^1]$	$[aaa], [bbb], [ccc]$	3^1	$[aaa]$	1^1	$[abc]$	3^1
4	$[1^4]$	$[*\|*\|*\|*]$	3^4	$[a\|a\|a\|a]$	1^4	$\emptyset$	0
	$[1^2 \cdot 2^1]$	$[*\|*\|aa], [*\|*\|bb], [*\|*\|cc]$	3^3	$[a\|a\|aa], [a\|a\|bc], [a\|a\|cb]$	$1^2 \cdot 3^1$	$\emptyset$	0
	$[1^1 \cdot 3^1]$	$[*\|aaa], [*\|bbb], [*\|ccc]$	3^2	$[a\|aaa]$	$1^1 \cdot 1^1$	$\emptyset$	0
	$[4^1]$	$[aaaa], [bbbb], [cccc]$	3^1	$[aaaa], [bcbc], [cbcb]$	3^1	$\emptyset$	0
	$[2^2]$	$[aa\|aa], [aa\|bb], [aa\|cc], \ldots$	3^2	$[2] : [aa], [bc], [cb]$	3^2	$\emptyset$	0
5	$[1^5]$	$[*\|*\|*\|*\|*]$	3^5	$[a\|a\|a\|a\|a]$	1^5	$\emptyset$	0
	$[1^3 \cdot 2^1]$	$[*\|*\|*\|aa], [*\|*\|*\|bb], [*\|*\|*\|cc]$	3^4	$[a\|a\|a\|aa], [a\|a\|a\|bc], [a\|a\|a\|cb]$	$1^1 \cdot 3^1$	$\emptyset$	0
	$[1^2 \cdot 3^1]$	$[*\|*\|aaa], [*\|*\|bbb], [*\|*\|ccc]$	3^3	$[a\|a\|aaa]$	$1^2 \cdot 1^1$	$\emptyset$	0
	$[1^1 \cdot 4^1]$	$[*\|aaaa], [*\|bbbb], [*\|cccc]$	3^2	$[a\|aaaa], [a\|bcbc], [a\|cbcb]$	$1^1 \cdot 3^1$	$\emptyset$	0
	$[5^1]$	$[aaaaa], [bbbbb], [ccccc]$	3^1	$[aaaaa]$	1^1	$\emptyset$	0
	$[1^1 \cdot 2^2]$	$[*\|aa\|aa], [*\|aa\|bb], [*\|aa\|cc], \ldots$	3^3	$[2] : [aa], [bc], [cb]$	3^2	$\emptyset$	0
	$[2^1 \cdot 3^1]$	$[aa\|aaa], [aa\|bbb], [aa\|ccc]$	3^2	$[aa\|aaa], [bc\|aaa], [cb\|aaa]$	$3^1 \cdot 1^1$	$\emptyset$	0
6	$[1^6]$	$[*\|*\|*\|*\|*\|*]$	3^6	$[a\|a\|a\|a\|a\|a]$	1^6	$\emptyset$	0
	$[1^4 \cdot 2^1]$	$[*\|*\|*\|*\|aa], [*\|*\|*\|*\|bb], [*\|*\|*\|*\|cc]$	3^5	$[a\|a\|a\|a\|aa], [a\|a\|a\|a\|bc], [a\|a\|a\|a\|cb]$	$1^4 \cdot 3^1$	$\emptyset$	0
	$[1^3 \cdot 3^1]$	$[*\|*\|*\|aaa], [*\|*\|*\|bbb], [*\|*\|*\|ccc]$	3^4	$[a\|a\|a\|aaa]$	$1^3 \cdot 1^1$	$\emptyset$	0
	$[1^2 \cdot 4^1]$	$[*\|*\|aaaa], [*\|*\|bbbb], [*\|*\|cccc]$	3^3	$[a\|a\|aaaa], [a\|a\|bcbc], [a\|a\|cbcb]$	$1^2 \cdot 3^1$	$\emptyset$	0
	$[1^1 \cdot 5^1]$	$[*\|aaaaa], [*\|bbbbb], [*\|ccccc]$	3^2	$[a\|aaaaa]$	$1^1 \cdot 1^1$	$\emptyset$	0
	$[6^1]$	$[aaaaaa], [bbbbbb], [cccccc]$	3^1	$[aaaaaa], [bcbcbc], [cbcbcb]$	3^1	$[abcabc]$	3^1
	$[2^1 \cdot 4^1]$	$[aa\|aaaa], [aa\|bbbb], [aa\|cccc], \ldots$	3^2	$[2^1] : [aa], [bc], [cb]$ $[4^1] : [aaaa], [bcbc], [cbcb], \ldots$	3^2	$\emptyset$	0
	$[1^1 \cdot 2^1 \cdot 3^1]$	$[*\|aa\|aaa], [*\|aa\|bbb], [*\|aa\|ccc], \ldots$	3^3	$[a\|aa\|aaa], [a\|bc\|aaa], [a\|cb\|aaa]$	$1^1 \cdot 3^1 \cdot 1^1$	$\emptyset$	0
	$[3^2]$	$[aaa\|aaa], [aaa\|bbb], [aaa\|ccc], \ldots$	3^2	$[aaa\|aaa]$	1^2	$[abc\|abc]$	3^2
	$[2^3]$	$[aa\|aa\|aa], [aa\|aa\|bb], [aa\|aa\|cc], \ldots$	3^3	$[2] : [aa], [bc], [cb]$	3^3	$\emptyset$	0
	$[1^2 \cdot 2^2]$	$[*\|*\|aa\|aa], [*\|*\|aa\|bb], [*\|*\|aa\|cc], \ldots$	3^4	$[2] : [aa], [bc], [cb]$	3^2	$\emptyset$	0

Table 2.8: (κ, ρ)-compatible coloured vector for three colours. "*" means it can take either "a", "b" or "c" and [2] : means the possible periodic patterns in the cycle [2].

2.12.4 Computational Results

In Tables 2.9 and 2.10, we show the computational results for the number of n-cell networks of valency r with $2 \leq k \leq n$ different cell types (colours) which are fixed by a given colour permutation. Colours are expressed using algebraic symbols "a", "b", "c", and "d" in the table.

Using more colours than cells ($k > n$) is a simple combinatorial extension to the results for n colours. Note that the following enumeration results in Tables 2.9 and 2.10 include disconnected networks.

2.13 Conclusions

All possible networks, for a given number of cells and valency constraint, are expressed as a set of adjacency matrices. Two different adjacency matrices may express topologically identical networks. In such cases, we can obtain one adjacency matrix from the other by applying a permutation matrix P to the cell labels. Therefore, the number of topologically distinct networks is equivalent to the number of distinct orbits of the symmetric group S_n for n-cell networks.

In the Orbit Counting Theorem, the number of distinct orbits of S_n is enumerated by considering the cardinality of fixed-point sets of a group element for each conjugacy class. The cardinalities of the fixed-point sets are computed by using the periodic property of row vectors in an adjacency matrix.

Firstly, we considered the enumeration of more generalised regular networks, where each equivalent cell can have a different number of input arrows (valency), unlike regular homogeneous networks have the fixed valency for every cell. To compute the cardinalities of fixed-point sets for regular inhomogeneous networks, we decomposed the number of fixed-points sets of regular homogeneous networks into the product of the number of fixed-point sets for each permutation cycle.

We next considered another generalisation of regular networks by allowing different cell types with the fixed valency for every cell and enumerated how many networks are preserved by a colour permutation Q. Different cell types are expressed by assigning colours to cells.

Since a permutation P preserves diagonal positions in an adjacency matrix, colour information of cells are given to the diagonal elements vector $\mathbf{v}$. Therefore, the number of networks which are fixed by cell label permutation and colour permutation is given by the product of the fixed-point set of P on the set of adjacency matrices and the fixed-point set of Q on $\mathbf{v}$. $|\mathrm{Fix}_{\mathbf{v}}(P, Q)|$ is computed as a combination of permutation cycles of P and Q.

Which networks are fixed after colour permutation relates to symmetry of networks.

Two Colour permutation $\kappa = (a)(b)$						
n	$r = 1$	$r = 2$	$r = 3$	$r = 4$	$r = 5$	$r = 6$
2	10	21	36	55	78	105
3	44	316	1380	4600	12488	29512
4	218	7055	108370	1006810	6574204	33238338
5	1076	210250	14113294	449214724	8475504276	108944842224
6	5556	7845769	2754105864	356069475096	22771026254124	864457495629000
Two Colour permutation $\kappa = (ab)$						
n	$r = 1$	$r = 2$	$r = 3$	$r = 4$	$r = 5$	$r = 6$
2	2	3	4	5	6	7
3	0	0	0	0	0	0
4	10	55	210	630	1596	3570
5	0	0	0	0	0	0
6	44	1603	29512	334320	2669772	16442272
Three Colour permutation $\kappa = (a)(b)(c)$						
n	$r = 1$	$r = 2$	$r = 3$	$r = 4$	$r = 5$	$r = 6$
3	138	1032	46000	15405	41979	99316
4	1005	34980	545445	5085360	33249762	168185493
5	7437	1575423	106892376	3408563928	64343684556	827209266426
6	56775	88477773	31322009244	4054399225731	259349883140466	9846375655326063
Three Colour permutation $\kappa = (a)(bc)$						
n	$r = 1$	$r = 2$	$r = 3$	$r = 4$	$r = 5$	$r = 6$
3	30	168	600	1905	4935	11508
4	135	1980	23055	198240	1258278	6296031
5	297	25263	1383756	42678048	797991156	10231445466
6	1221	450879	132639540	16787481849	1069073890614	40542546986277
Three Colour permutation $\kappa = (abc)$						
n	$r = 1$	$r = 2$	$r = 3$	$r = 4$	$r = 5$	$r = 6$
3	6	12	20	30	42	56
4	0	0	0	0	0	0
5	0	0	0	0	0	0
6	42	462	3192	16002	63756	213906

Table 2.9: Enumeration results for networks with two and three different cell types.

Four colour permutations:

Colour permutation $\kappa = (a)(b)(c)(d)$

n	$r=1$	$r=2$	$r=3$	$r=4$	$r=5$	$r=6$
4	3044	109490	1719220	16054885	105037240	531422388
5	30000	6596728	449866168	14358147160	271107860664	3485663374008
6	303484	494729964	175851792080	22776210845436	1457123896297224	4081497668791493

Colour permutation $\kappa = (a)(b)(cd)$

n	$r=1$	$r=2$	$r=3$	$r=4$	$r=5$	$r=6$
4	1656	45180	662520	6086010	39570384	199751832
5	8040	1314984	85361544	2701781880	50894361432	653886996264
6	43944	48570912	16603810848	2138743571400	136668014683632	5187276929811480

Colour permutation $\kappa = (a)(bcd)$

n	$r=1$	$r=2$	$r=3$	$r=4$	$r=5$	$r=6$
4	184	3880	55640	507920	3298736	16648632
5	480	55616	3561536	112592480	2120651520	27245446656
6	1568	1023600	346064512	44558517048	2847259094544	108068316784904

Colour permutation $\kappa = (abcd)$

n	$r=1$	$r=2$	$r=3$	$r=4$	$r=5$	$r=6$
4	24	60	120	210	336	504
5	0	0	0	0	0	0
6	0	0	0	0	0	0

Colour permutation $\kappa = (ab)(cd)$

n	$r=1$	$r=2$	$r=3$	$r=4$	$r=5$	$r=6$
4	108	630	2460	7455	18984	42588
5	0	0	0	0	0	0
6	948	37716	705264	8012340	64042776	394528596

Table 2.10: Enumeration results for networks with four different cell types.

Chapter 3

Enumeration and Visualisation of Homogeneous Networks

3.1 Introduction

In the previous chapter, we enumerated networks (graphs) under certain restrictions. However, for dynamical analysis, we need to consider the topology of the network. In this chapter, we explain a computer algorithm in Python which displays all connected and strongly connected (that is path-connected) regular homogeneous networks of a given valency. There are 416 connected four-cell regular homogeneous networks of valency 2. We will use these four-cell regular homogeneous networks for bifurcation analysis. The list of 416 networks is shown as well as the lists of 38 three-cell and 5 two-cell regular homogeneous networks of valency 2.

3.2 Preliminaries

3.2.1 Connected Networks

In graph theory, a **path** in a graph (network) is a sequence of vertices (cells) such that from each of its vertices there is an edge (arrow) to the next vertex in the sequence. The length of a path is the number of edges that the path uses.

In an **undirected graph** $\mathcal{G}$, two vertices u and v are called **connected** if $\mathcal{G}$ contains a path from u to v. A graph is called **connected** if every pair of distinct vertices in the graph is connected (directly or indirectly).

A **directed graph** is called **connected** if replacing all of its directed edges with undirected edges produces a connected (undirected) graph.

The following Theorem 3.1 is useful to check the connectedness of a given network.

Theorem 3.1. *If A is the adjacency matrix of a connected directed graph with n nodes, the*

number of paths of length k from a vertex v_j to v_i is given by the (i,j)-th entry of A^k, where $1 \leq k \leq n-1$.

Proof. See Koshy (2003). □

In general, the total number of paths from v_j to v_i within k length is given by:

$$\sum_{l=1}^{k} A^l.$$

If a network is connected, any vertex can be reached from any other arbitrary vertex with at most $n-1$ edges. Hence, we considered the following two steps to determine if a n-cell network (directed graph) $\mathcal{G}$ with the associated $n \times n$ adjacency matrix is connected:

- Form a symmetric matrix $\hat{A} = (\hat{a}_{ij})$ from an asymmetric adjacency matrix $A = (a_{ij})$ defined in the following way: $\hat{a}_{ij} = \hat{a}_{ji} = 1$ if there exist at least one directed edge between cell j to cell i (in either direction).
- If all entries of $\sum_{l=1}^{k} \hat{A}^l$ are nonzero for some $1 \leq k \leq n-1$, then $\mathcal{G}$ is connected.

3.2.2 Path-Connected Networks

A directed graph is called **strongly connected** (or **path-connected**) if it contains a directed path from u to v for every pair of vertices u, v.

Theorem 3.2. *A directed graph with n vertices is strongly connected if and only if its adjacency matrix A has the property that*

$$\sum_{l=1}^{n-1} A^l$$

has no zero entries.

Proof. See Bernard and Hill (2005). □

An algorithm to determine if a given network is strongly connected uses Theorem 3.2 directly. However as in the algorithm to determine the connectedness of a network, we do not need to compute the whole summation. It is sufficient to check if all entries of $\sum_{l=1}^{k} A^l$ are nonzero for some $1 \leq k \leq n-1$.

3.3 Computer Algorithms

Step 1: All possible $n \times n$ adjacency matrices with valency r are considered in turn. These are generated by first computing all possible row vectors with sum equal to the valency r, and then taking all possible combinations of n row vectors.

Step 2: Loop over each adjacency matrix generated in Step 1.

Step 3: For the current adjacency matrix, determine if the associated regular homogeneous network is connected or not. If not, further analysis is skipped, returning to Step 2 to consider the next matrix.

Step 4: For the current adjacency matrix, check if the associated network is isomorphic to any previously considered network by comparing it with previously recorded adjacency matrices. If a permutation of the current adjacency matrix has been observed, further analysis is skipped, returning to Step 2 to consider the next matrix.

Step 5: Increment the count of isomorphic connected networks[1].

Step 6: For the current adjacency matrix, check if the associated network is strongly connected using Theorem 3.2. It is strongly connected, then increment the number of isomorphic strongly connected networks.

Step 7: Record the current adjacency matrix and all permutations of it (for use in Step 4).

Step 8: Using the current adjacency matrix, draw a figure of the associated network.

For graph visualisation, in general GraphViz (www.graphviz.org) was used. However, for the listings in the following figures compact PDF figures were created using bespoke code with the ReportLab python library (www.reportlab.org).

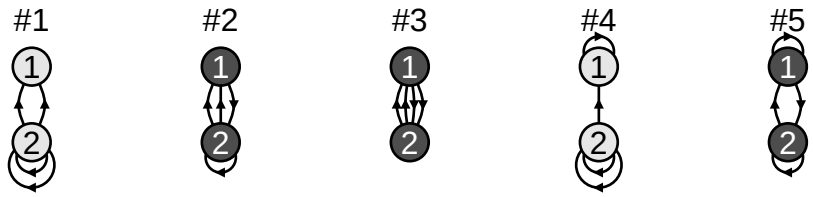

Figure 3.1: All 5 connected regular homogeneous two-cell networks of valency two ($n = 2, r = 2$). The 3 strongly connected networks are shown with dark grey cells, the rest have pale grey cells.

[1]The current count is used as a unique reference number for the associated network within the set of n-cell homogeneous networks of valency r.

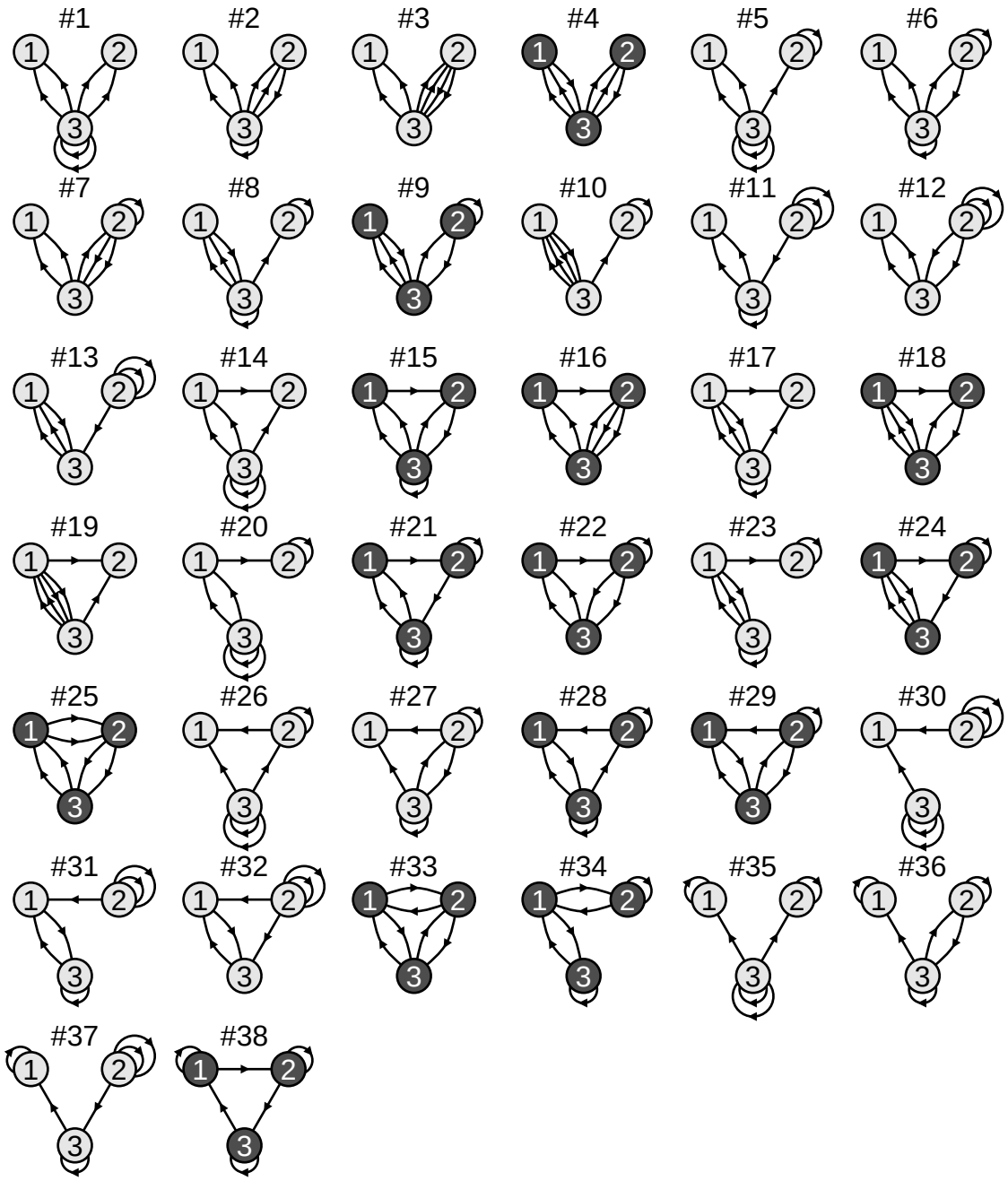

Figure 3.2: All 38 connected regular homogeneous three-cell networks of valency two ($n = 3$, $r = 2$). The 14 strongly connected networks are shown with dark grey cells, the rest have pale grey cells.

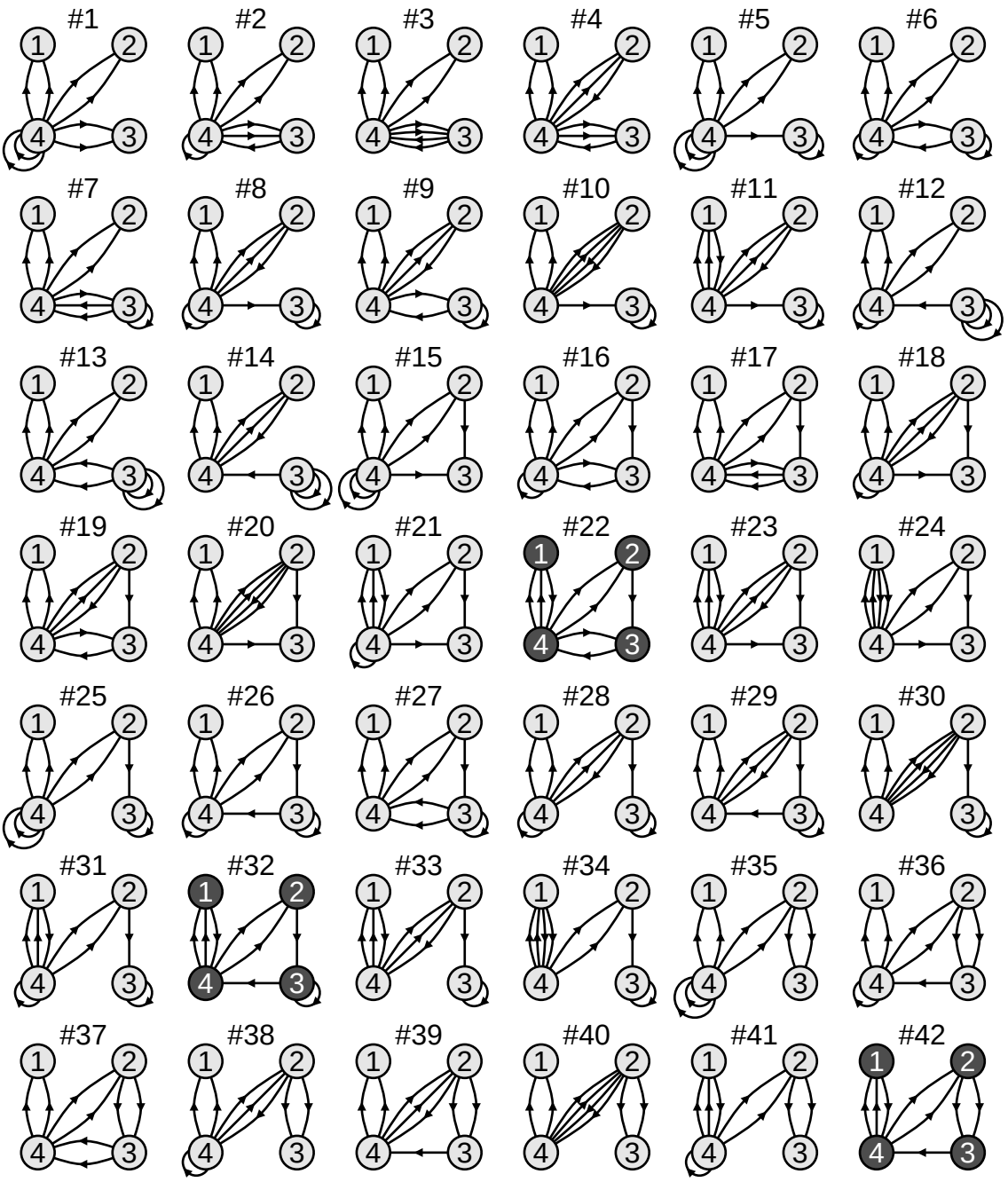

Figure 3.3: All 416 connected regular homogeneous four-cell networks of valency two ($n = 4$, $r = 2$), split over eight pages. The 108 strongly connected networks are shown with dark grey cells, the rest have pale grey cells. In some cases the cells have been rearranged to allow the graph to be drawn with the minimum of crossing edges.

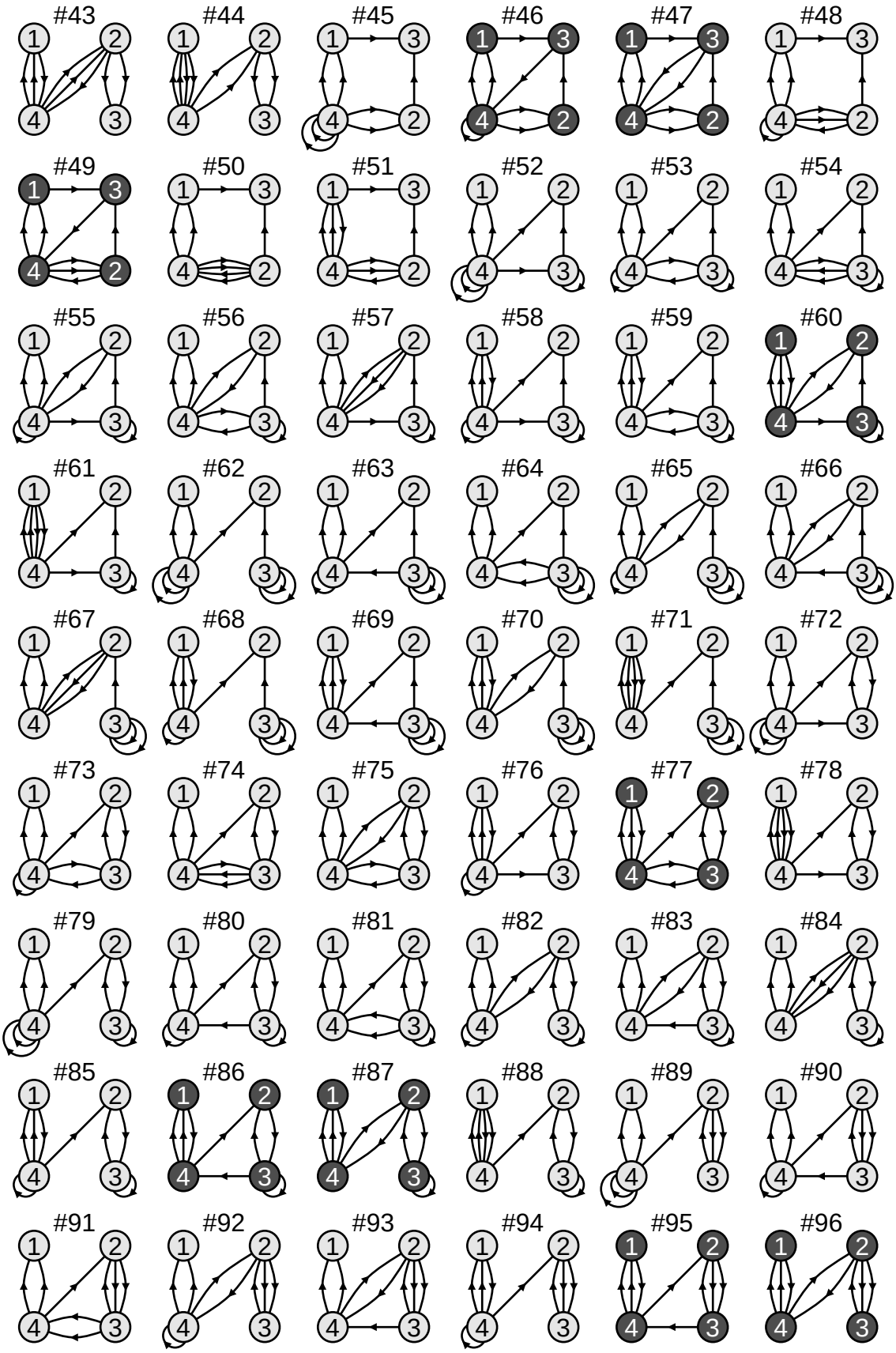
#43
#44
#45
#46
#47
#48
#49
#50
#51
#52
#53
#54
#55
#56
#57
#58
#59
#60
#61
#62
#63
#64
#65
#66
#67
#68
#69
#70
#71
#72
#73
#74
#75
#76
#77
#78
#79
#80
#81
#82
#83
#84
#85
#86
#87
#88
#89
#90
#91
#92
#93
#94
#95
#96

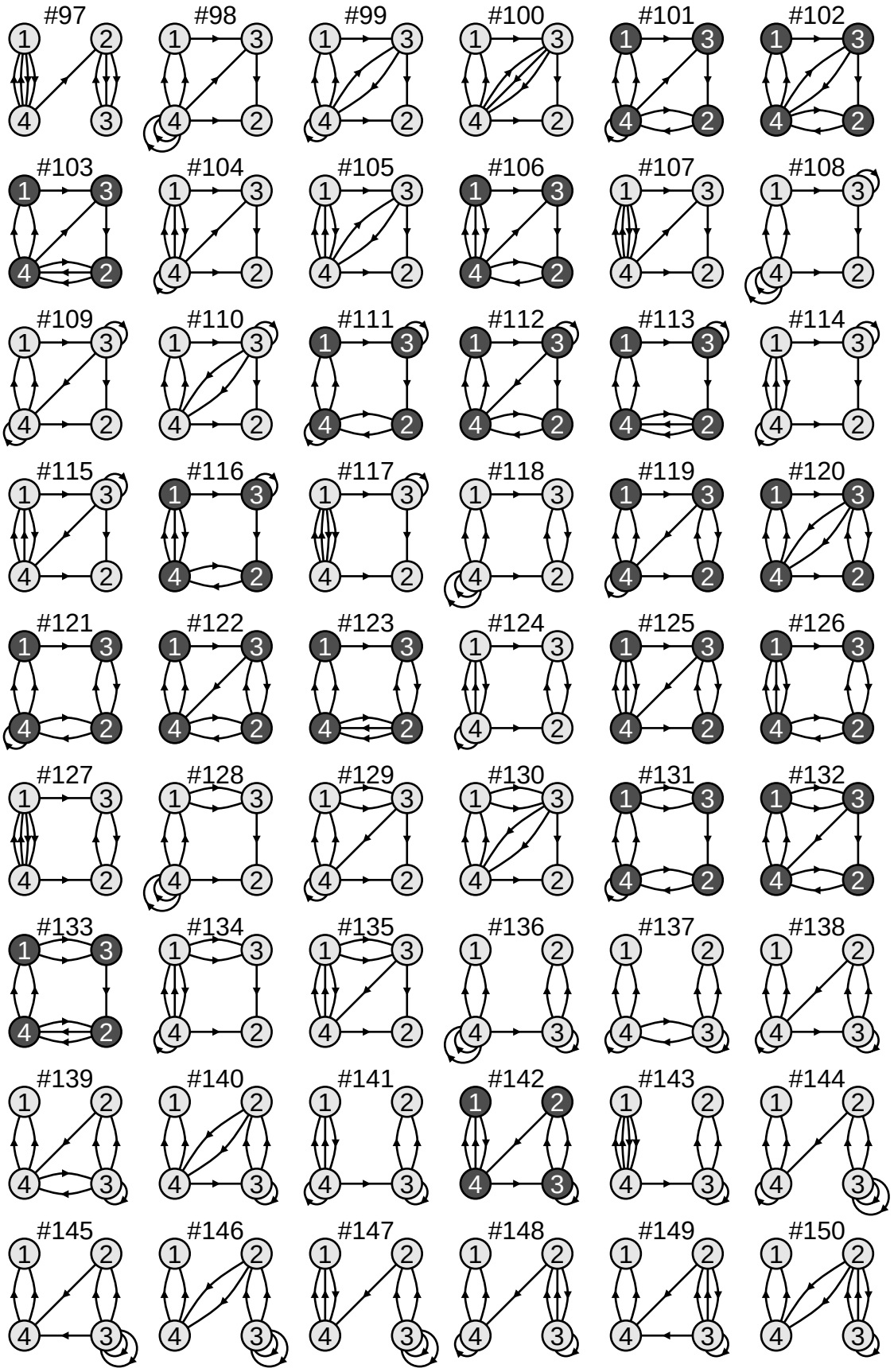
#97
#98
#99
#100
#101
#102
#103
#104
#105
#106
#107
#108
#109
#110
#111
#112
#113
#114
#115
#116
#117
#118
#119
#120
#121
#122
#123
#124
#125
#126
#127
#128
#129
#130
#131
#132
#133
#134
#135
#136
#137
#138
#139
#140
#141
#142
#143
#144
#145
#146
#147
#148
#149
#150

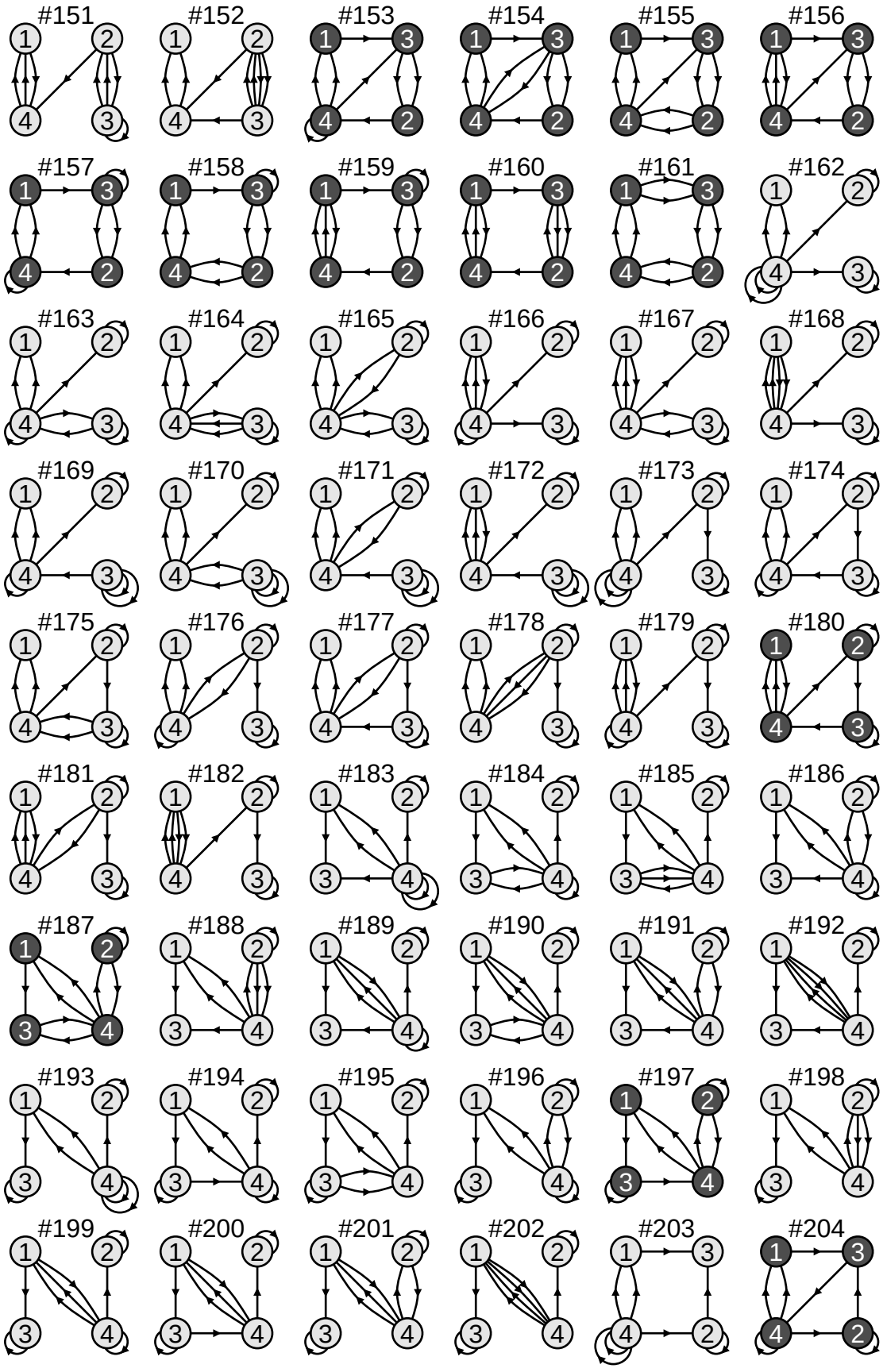
#151
#152
#153
#154
#155
#156
#157
#158
#159
#160
#161
#162
#163
#164
#165
#166
#167
#168
#169
#170
#171
#172
#173
#174
#175
#176
#177
#178
#179
#180
#181
#182
#183
#184
#185
#186
#187
#188
#189
#190
#191
#192
#193
#194
#195
#196
#197
#198
#199
#200
#201
#202
#203
#204

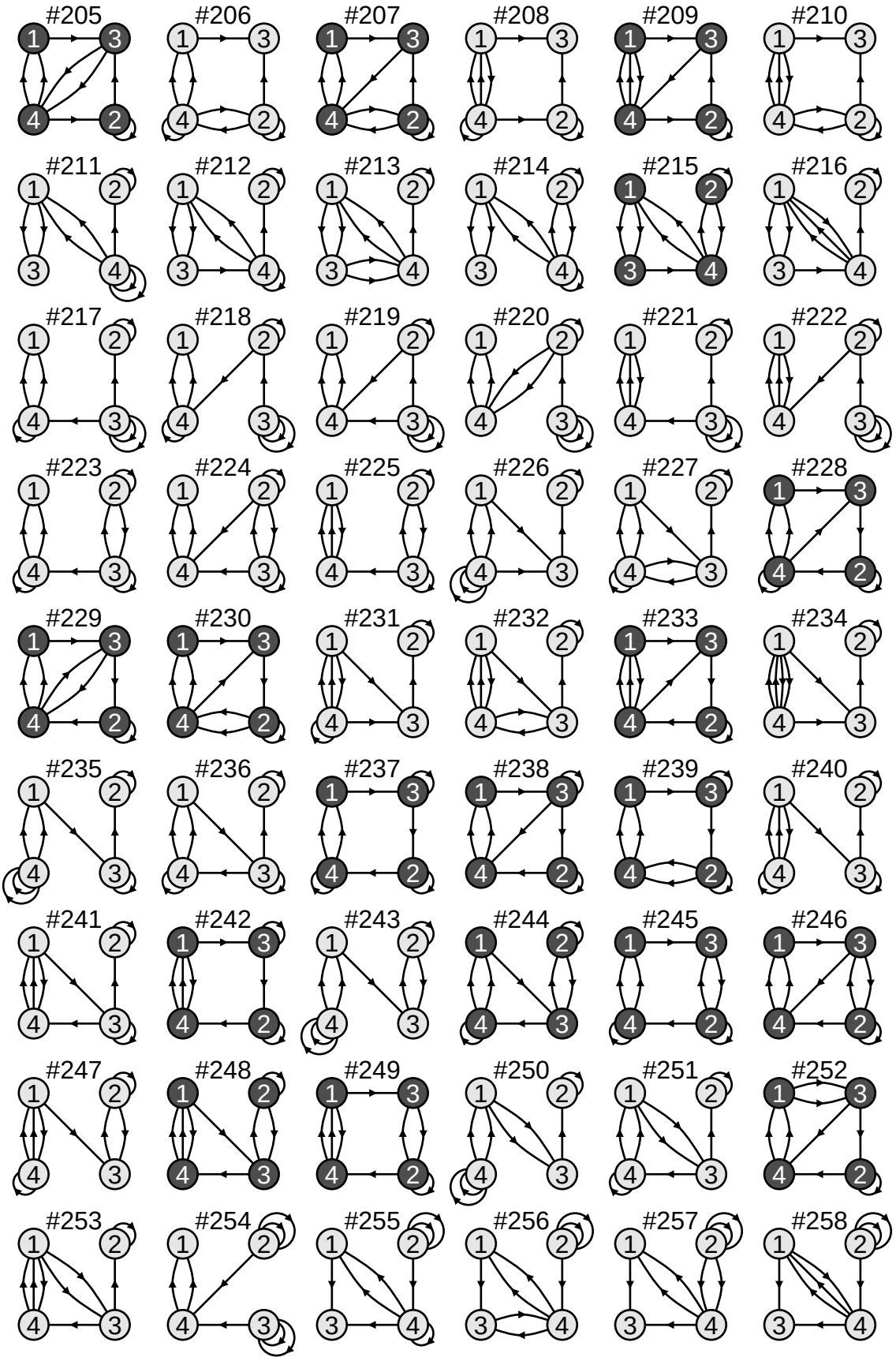
#205
#206
#207
#208
#209
#210
#211
#212
#213
#214
#215
#216
#217
#218
#219
#220
#221
#222
#223
#224
#225
#226
#227
#228
#229
#230
#231
#232
#233
#234
#235
#236
#237
#238
#239
#240
#241
#242
#243
#244
#245
#246
#247
#248
#249
#250
#251
#252
#253
#254
#255
#256
#257
#258

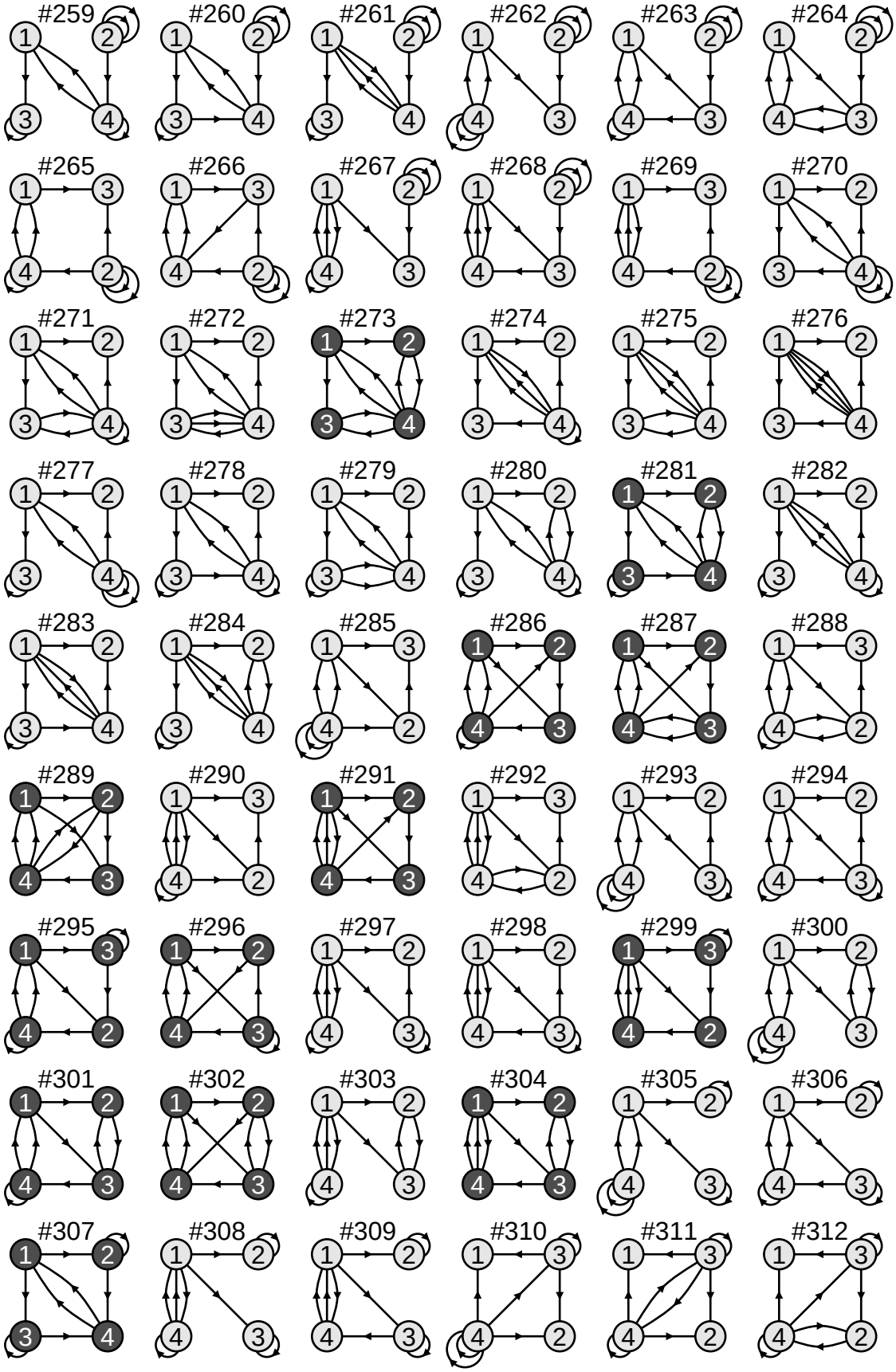
#259
#260
#261
#262
#263
#264
#265
#266
#267
#268
#269
#270
#271
#272
#273
#274
#275
#276
#277
#278
#279
#280
#281
#282
#283
#284
#285
#286
#287
#288
#289
#290
#291
#292
#293
#294
#295
#296
#297
#298
#299
#300
#301
#302
#303
#304
#305
#306
#307
#308
#309
#310
#311
#312

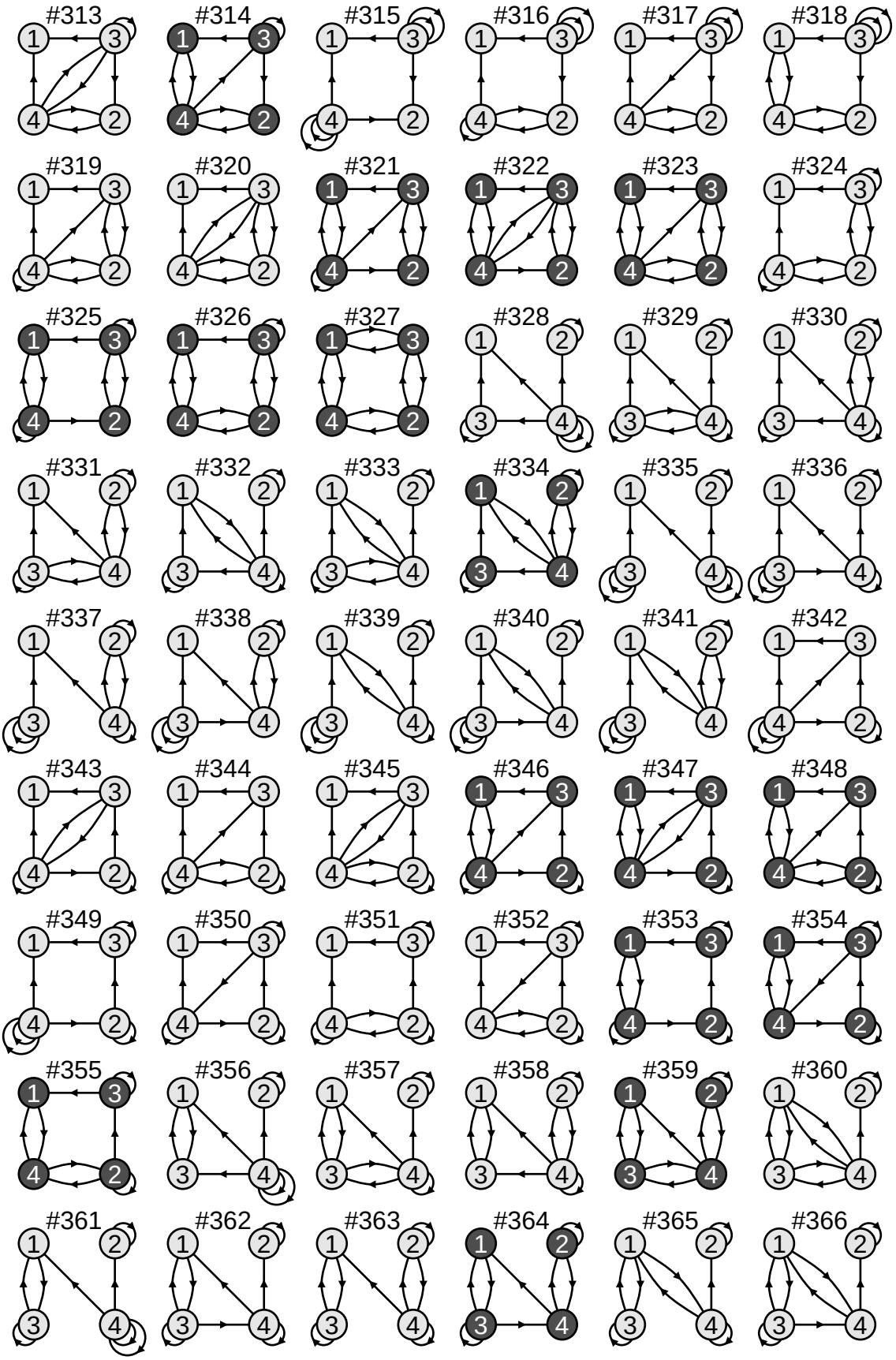
#313
#314
#315
#316
#317
#318
#319
#320
#321
#322
#323
#324
#325
#326
#327
#328
#329
#330
#331
#332
#333
#334
#335
#336
#337
#338
#339
#340
#341
#342
#343
#344
#345
#346
#347
#348
#349
#350
#351
#352
#353
#354
#355
#356
#357
#358
#359
#360
#361
#362
#363
#364
#365
#366

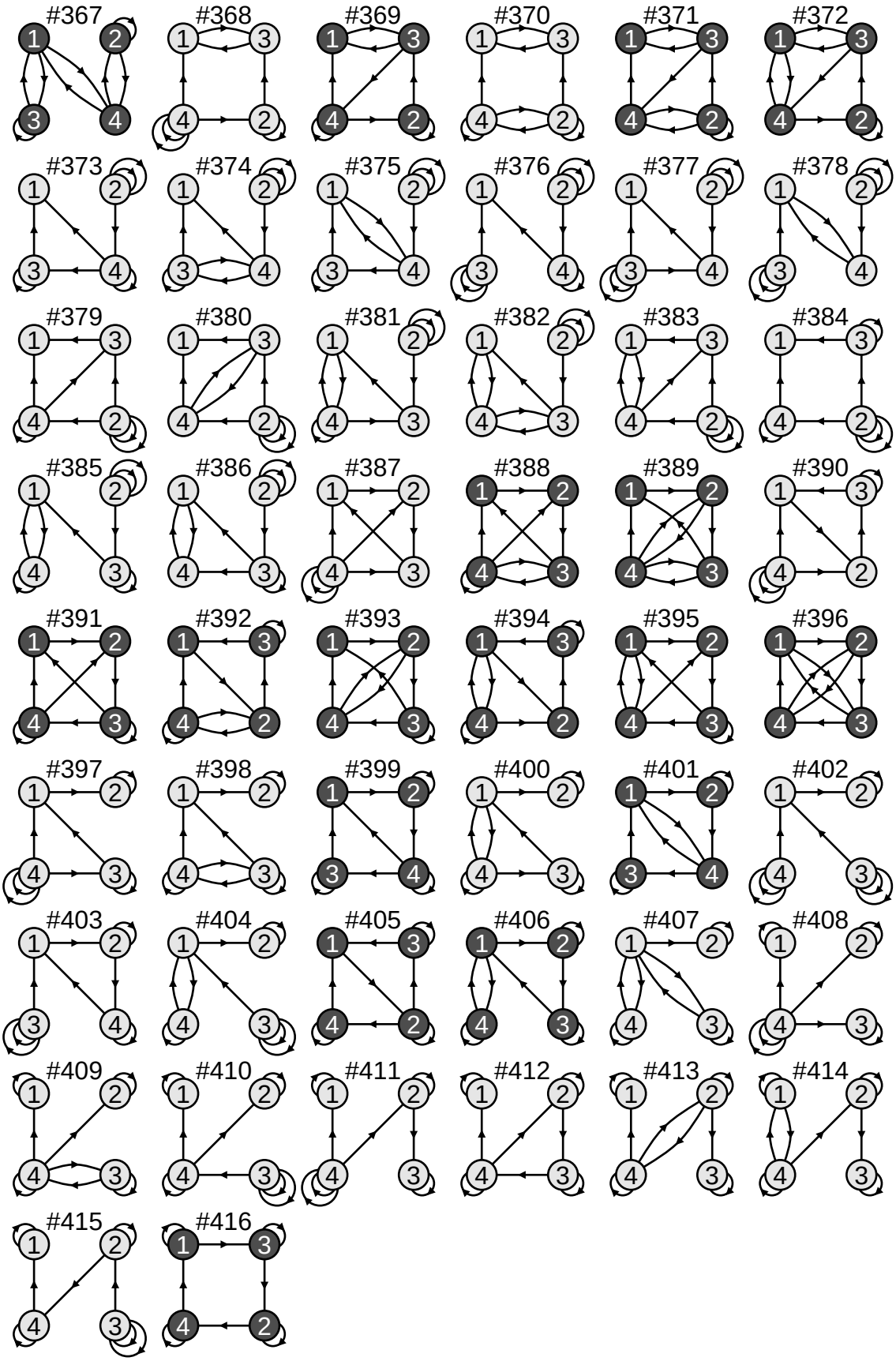
#367
#368
#369
#370
#371
#372
#373
#374
#375
#376
#377
#378
#379
#380
#381
#382
#383
#384
#385
#386
#387
#388
#389
#390
#391
#392
#393
#394
#395
#396
#397
#398
#399
#400
#401
#402
#403
#404
#405
#406
#407
#408
#409
#410
#411
#412
#413
#414
#415
#416

3.4 Conclusions

The network reference numbers in the preceding figures will be used in later chapters[2].

For each adjacency matrix, the corresponding eigenvalues and eigenvectors can easily be computed. It can happen for some four-cell networks that the four eigenvalues consist of the valency, a real value, and a complex conjugate pair where the these last three all have the same real part (e.g. $r, 0, i, -i$ where r is the valency). Indeed there are 9 such four-cell networks of valency 2. These are networks #26, #109, #138, #175, #238, #278, #294 #295 and #391.

Although we only consider steady-state bifurcations of regular homogeneous networks in later chapters, such networks are interesting as we expect to see Steady-state/Hopf synchrony-breaking bifurcations when the critical eigenvalue crosses the imaginary axis with nonzero speed, and is therefore associated with all of these three eigenvalues. This phenomenon cannot occur in three-cell networks.

[2]Note that Leite and Golubitsky (2006) uses a different set of reference numbers for three-cell networks of valency 2.

Chapter 4

Computation of All Balanced Equivalence Relations

4.1 Introduction

An important feature of networks is the possibility of synchrony, which occurs when distinct nodes exhibit identical dynamics at all instants of time. When a fully synchronised network loses coherence, it breaks up into multiple clusters of synchronised sub-networks. We use the term **pattern of synchrony** to describe which nodes in a given network are synchronised. Some patterns of synchrony are more robust than others. Theorem 4.2 (Stewart *et al.*, 2003, Theorem 6.5) states that all *robust* patterns of synchrony — those determined by the network architecture rather than any specific choice of dynamic — correspond to **balanced equivalence relations** (balanced colourings) on the set of cells. Associated with each balanced equivalence relation is a **polysynchronous subspace** (**balanced polydiagonal**). A coupled cell network restricted to a balanced polydiagonal defines a **quotient network** which describes multiple clusters of synchronised sub-networks.

In this chapter, we describe a method to determine all possible balanced equivalence relations on a given regular homogeneous coupled cell network. To determine which equivalence relations are balanced is equivalent to finding which corresponding polydiagonals are flow-invariant for every coupled cell system with the given network architecture. We show that balanced polydiagonals are determined solely by the adjacency matrix which describes the network architecture, by considering projection maps onto polydiagonals. An adjacency matrix which leaves a given polydiagonal invariant has a block structure, and this matrix property leads to a computer algorithm which determines all balanced equivalence relations and adjacency matrices of the corresponding quotient networks using matrix computations.

It has been shown that balanced equivalence relations form a complete lattice in a general

context in Stewart (2007). We construct the lattice of balanced equivalence relations using a refinement relation as an order for the lattice. Lattices of balanced equivalence relations for all 38 three-cell regular homogeneous networks of valency 2 and 416 four-cell regular homogeneous networks of valency 2 are listed in Appendix A.

4.2 Preliminaries

4.2.1 Coupled cell network formalism

The state of cell c at time t is determined by a list of state variables for that cell. Each cell c must be assigned a **cell phase space** P_c, and its state $x_c(t)$ at time t is an element of P_c. In general, P_c should be a manifold, and for simplicity we take it to be a finite-dimensional real vector space, which is sufficient for local bifurcation theory.

Each cell typically has an internal dynamic, an ODE that determines its behaviour in isolation. In a network, the internal dynamic of a given cell is modified by coupling effects from other cells. The direction of coupling is important since it determines which cell is affected by which. Therefore the cells are represented as the nodes of a directed graph, and the couplings as directed edges, drawn as arrows.

In many applications the cells occur in a variety of different types, and cells of the same type have the same phase space. There are two ways to formalise this requirement. One is to attach *labels* to cells, symbols drawn from some finite set such as circle, square, triangle. Cells with identical labels are required to have the same type. Alternatively, we can introduce an equivalence relation *same type* on cells.

Similarly, coupling among cells also occurs in various distinguishable types. We can *label* arrows graphically by using different kinds of lines (solid, dashed, dotted). Alternatively, we can introduce an equivalence relation *same type* on arrows as we introduced on cells.

Finally, we represent the topology of the network by two *incidence relations*, $\mathcal{H}$ and $\mathcal{T}$, which determine the cells that lie at the head and tail of a given arrow. Now we can state a formal definition of a coupled cell network as a directed graph.

4.2.2 Definition of a coupled cell network

Definition 4.1. *A coupled cell network $\mathcal{G}$ comprises:*

1. *A finite set $\mathcal{C} = \{1, \ldots, N\}$ of nodes or cells.*

2. *An equivalence relation $\sim_C$ on cells in $\mathcal{C}$.*

3. *A finite set $\mathcal{E}$ of edges or arrows.*

4. *An equivalence relation $\sim_E$ on edges in $\mathcal{E}$.*

5. *Two maps $\mathcal{H} : \mathcal{E} \to \mathcal{C}$ and $\mathcal{T} : \mathcal{E} \to \mathcal{C}$.*
   For $e \in \mathcal{E}$ we call $\mathcal{H}(e)$ the head of e and $\mathcal{T}(e)$ the tail of e.
   The following compatibility condition is required:

6. *Equivalent arrows have equivalent tails and heads. That is, if $e_1, e_2 \in \mathcal{E}$ and $e_1 \sim_E e_2$, then*

$$\mathcal{H}(e_1) \sim_C \mathcal{H}(e_2) \qquad \mathcal{T}(e_1) \sim_C \mathcal{T}(e_2)$$

Two noteworthy features of this definition are:

- Self-coupling is permitted: we allow $\mathcal{H}(e) = \mathcal{T}(e)$ for an edge e.
- Multiple arrows are permitted: we allow $\mathcal{H}(e_1) = \mathcal{H}(e_2)$ and $\mathcal{T}(e_1) = \mathcal{T}(e_2)$ for $e_1 \neq e_2$.

The reasons for these conditions are explained in Golubitsky *et al.* (2005).

4.2.3 Input sets and Groupoid of a network

Associated with each cell $c \in \mathcal{C}$ is a canonical set of edges, namely, those that represent couplings into cell c.

Definition 4.2. *If $c \in \mathcal{C}$, then the **input set** of c is*

$$I(c) = \{e \in \mathcal{E} : \mathcal{H}(e) = c\}$$

*An element of $I(c)$ is called an **input edge** or **input arrow** of c.*

Input edges determine the form of the ODEs associated with $\mathcal{G}$. For a given cell $c \in \mathcal{C}$, the form of $\dot{x}_c$ should depend only on the cells coupled to cell c, that is, on x_c and on those x_i for which there exists an arrow with head c and tail i. If two cells have a common input structure, it reflects that the occurrence of the same function in the ODEs for both cells. We now state these ideas formally.

Definition 4.3. *The relation $\sim_I$ of **input equivalence** on $\mathcal{C}$ is defined by $c \sim_I d$ if and only if there exists an arrow-type preserving bijection*

$$\beta : I(c) \to I(d)$$

That is, for every input arrow $i \in I(c)$

$$i \sim_E \beta(i)$$

*Any such bijection β is called an **input isomorphism** from cell c to cell d. The set $B(c,d)$ denotes the collection of all input isomorphisms from cell c to cell d. The set*

$$\mathcal{B}_{\mathcal{G}} = \bigcup_{c,d \in \mathcal{C}} B(c,d)$$

*is the **(symmetry) groupoid of the network**. The set $B(c,c)$ is a permutation group acting on the input set $I(c)$, which we call the **vertex group** of cell c.*

Note that with a suitable interpretation the union above is disjoint. Suppose there exists $\beta \in B(c,d) \cap B(c',d')$, where $B(c,d) \neq B(c',d')$ and $c \neq c'$ and $d \neq d'$. Then $\beta : I(c) \to I(d)$ such that $i \to \sim_E \beta(i)$ for all $i \in I(c)$. Also $\beta : I(c') \to I(d')$ such that $i \to \sim_E \beta(i)$ for all $i \in I(c')$. Therefore we must have $I(c) = I(c')$ and $I(d) = I(d')$. This contradict to $c \neq c'$ and $d \neq d'$. Hence the union $\mathcal{B}_{\mathcal{G}} = \bigcup_{c,d \in \mathcal{C}} B(c,d)$ is disjoint. See Stewart *et al.* (2003) for more details.

Clearly

$$c \sim_I d \quad \Rightarrow \quad c \sim_C d$$

The proof is easy. If $c \sim_I d$, $\exists \beta : I(c) \to I(d)$ such that $i \sim_E \beta(i)$ for all $i \in I(c)$. By the consistency condition (6) of Definition 4.1, $\mathcal{H}(i) \sim_C \mathcal{H}(\beta(i))$. Therefore, $c \sim_C d$ since $\mathcal{H}(i) = c$ and $\mathcal{H}(\beta(i)) = d$.

However, the converse

$$c \sim_C d \quad \Rightarrow \quad c \sim_I d$$

fails in general. For example, consider the following network in which all three cells are equivalent:

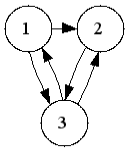

Although the only $\sim_C$-equivalence class is $\{1,2,3\}$, there is no input isomorphism between cell 1 and cell 2, or between cell 1 and cell 3.

Definition 4.4. *A **homogeneous** network is a coupled cell network such that $B(c,d) \neq \emptyset$ for every pair of cells c,d. That is, all cells are input isomorphic. A homogeneous network that has one equivalence class of edges is said to be **regular**. The **valency** of a regular network is the number of arrows in any (hence every) input set.*

4.2.4 Admissible vector fields

We now define the class $\mathcal{F}_{\mathcal{G}}^{P}$ of **admissible vector fields** corresponding to a given coupled cell network $\mathcal{G}$. This class consists of all vector fields that are compatible with the labelled graph structure, or equivalently are symmetric under the groupoid $\mathcal{B}_{\mathcal{G}}$. The class $\mathcal{F}_{\mathcal{G}}^{P}$ also depends on a choice of **total phase space** P, which we assume is fixed throughout the subsequent discussion. We construct P as follows.

For each cell in $\mathcal{C}$ define a **cell phase space** P_c. We assume P_c to be a nonzero finite-dimensional real vector space. We require

$$c \sim_c d \quad \Rightarrow \quad P_c = P_d$$

and we assign the same coordinate systems on P_c and P_d.

Define the corresponding **total phase space** to be

$$P = \prod_{c_i \in \mathcal{C}} P_{c_i}, \quad i = 1, \ldots, N$$

and employ the coordinate system

$$x = (x_{c_1}, \ldots, x_{c_N})$$

on the total phase space P, where $x_{c_i} \in P_{c_i}$.

More generally, suppose that $\mathcal{D} = (d_1, \ldots, d_s)$ is any finite ordered set of s cells in $\mathcal{C}$. In particular, the same cell can appear more than once in $\mathcal{D}$, in order to accommodate multiple arrows. Define

$$P_{\mathcal{D}} = P_{d_1} \times \cdots \times P_{d_s}$$

and employ the coordinate system

$$x_{\mathcal{D}} = (x_{d_1}, \ldots, x_{d_s})$$

on $\mathcal{D}$, where $x_{d_i} \in P_{d_i}$.

Suppose that $\mathcal{D}_1$, $\mathcal{D}_2$ are ordered sets of $\mathcal{C}$, and that there is a bijection $\gamma : \mathcal{D}_1 \to \mathcal{D}_2$ such that $\gamma(d) \sim_C d$ for all $d \in \mathcal{D}_1$. Define the **pullback map**

$$\gamma^* : P_{\mathcal{D}_2} \to P_{\mathcal{D}_1}$$

by

$$(\gamma^*(z))_j = z_{\gamma(j)}$$

for all $j \in \mathcal{D}_1$ and $z \in P_{\mathcal{D}_2}$.

Now we use pullback maps on isomorphic input sets.

Suppose $c, d \in \mathcal{C}$ and $c \sim_I d$. $\mathcal{T}(I(c))$ and $\mathcal{T}(I(d))$ are subsets of $\mathcal{C}$. For a given cell c the **internal phase space** is P_c and the **coupling phase space** is

$$P_{\mathcal{T}(I(c))} = P_{\mathcal{T}(i_1)} \times \cdots \times P_{\mathcal{T}(i_s)}$$

where $\mathcal{T}(I(c))$ denotes the ordered set of cells $(\mathcal{T}(i_1), \ldots, \mathcal{T}(i_s))$ as the arrows i_k run through $I(c)$.

For any $\beta \in B(c, d)$, define the pullback map $\beta^* : P_{\mathcal{T}(I(d))} \to P_{\mathcal{T}(I(c))}$ as follows. Write $x_{\mathcal{T}(I(c))} = (x_{\mathcal{T}(i_1)}, \ldots, x_{\mathcal{T}(i_s)})$. Then

$$\beta^* x_{\mathcal{T}(I(d))} = (x_{\mathcal{T}(\beta(i_1))}, \ldots, x_{\mathcal{T}(\beta(i_s))})$$

We use pullback maps to relate different components of a vector field associated with a given coupled cell network. Specifically, the class of vector fields that is encoded by a coupled cell network is given by:

Definition 4.5. *A vector field $f : P \to P$ is $\mathcal{G}$-**admissible** if:*

(a) *(domain condition) For all $c \in \mathcal{C}$ the component $f_c(x)$ depends only on the internal phase space variable x_c and the coupling phase space variables $x_{\mathcal{T}(I(c))}$; that is, there exists $\hat{f}_c : P_c \times P_{\mathcal{T}(I(c))} \to P_c$ such that*

$$f_c(x) = \hat{f}_c(x_c, x_{\mathcal{T}(I(c))}) \tag{4.1}$$

(b) *(pullback condition) For $c, d \in \mathcal{C}$ and $\beta \in B(c, d)$*

$$\hat{f}_d(x_d, x_{\mathcal{T}(I(d))}) = \hat{f}_c(x_d, \beta^* x_{\mathcal{T}(I(d))}) \quad \textit{for all} \quad x \in P \tag{4.2}$$

Remark: If β belongs to the vertex group $B(c, c)$, then (4.2) implies that

$$\hat{f}_c(x_c, x_{\mathcal{T}(I(c))}) = \hat{f}_c(x_c, \beta^*(x_{\mathcal{T}(I(c))})) \quad \text{for all} \quad x \in P$$

That is, $\hat{f}_c$ is $B(c, c)$-invariant.

Definition 4.6. *For a given choice of the P_c we define the class $\mathcal{F}_{\mathcal{G}}^P$ to consist of all $\mathcal{G}$-admissible vector fields on P.*

These are the most general vector fields on P that are consistent with the structure of the coupled cell network. The following theorem states that f is determined if we specify one mapping (on the appropriate spaces) for each input equivalence class of cells.

Theorem 4.1. *Let $\overline{\mathcal{C}} \subseteq \mathcal{C}$ be an $\sim_I$-equivalence class. Let $\hat{f}_c : P_c \times P_{\mathcal{T}(I(c))} \to P_c$ be $B(c,c)$-invariant for $c \in \overline{\mathcal{C}}$. Then $\hat{f}_c$ extends uniquely to a vector field in $\mathcal{F}^P_{\mathcal{G}}(\overline{\mathcal{C}})$.*

Proof. Extend to input-equivalent cells using the pullback condition, for details, see Stewart *et al.* (2003). □

In particular, each admissible vector field on a regular homogeneous cell system is uniquely determined by a single mapping $\hat{f}_c$ at some (indeed, any) node c. The following example shows how to determine f for a given homogeneous coupled cell network with valency 2.

Example 4.1. Consider the following three-cell regular homogeneous network

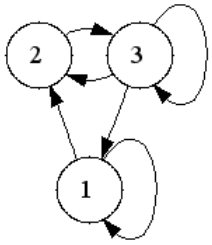

We describe $\mathcal{F}^P_{\mathcal{G}}$ for this network. There is only one cell type labelled by a symbol ◯. We choose P_1 as the cell phase space of cell 1. Then the state variable is $x = (x_1, x_2, x_3)$, where $x_i \in P_1$ for all $i = 1, 2, 3$ and the total phase space is $P = (P_1)^3$. We claim that the $\mathcal{G}$-admissible vector fields f are those of the form

$$\begin{aligned} f_1(x) &= A(x_1, \overline{x_1, x_3}) \\ f_2(x) &= A(x_2, \overline{x_1, x_3}) \\ f_3(x) &= A(x_3, \overline{x_2, x_3}) \end{aligned}$$

where $A(x_i, \overline{x_j, x_k})$ means $A(x_i, x_j, x_k) = A(x_i, x_k, x_j)$ (i.e., inputs have symmetric effects)

Input sets are

$$I(1) = \{\overrightarrow{11}, \overrightarrow{31}\}, \quad I(2) = \{\overrightarrow{12}, \overrightarrow{32}\}, \quad I(3) = \{\overrightarrow{23}, \overrightarrow{33}\}$$

The non-empty sets $B(c,d)$ are given by

$$\begin{aligned}
B(1,1) &= \{\{\beta_1(\overrightarrow{11}) = \overrightarrow{11}, \beta_1(\overrightarrow{31}) = \overrightarrow{31}\}, \{\beta_2(\overrightarrow{11}) = \overrightarrow{31}, \beta_2(\overrightarrow{31}) = \overrightarrow{11}\}\} \\
B(2,2) &= \{\{\beta_1(\overrightarrow{12}) = \overrightarrow{12}, \beta_1(\overrightarrow{32}) = \overrightarrow{32}\}, \{\beta_2(\overrightarrow{12}) = \overrightarrow{32}, \beta_2(\overrightarrow{32}) = \overrightarrow{12}\}\} \\
B(3,3) &= \{\{\beta_1(\overrightarrow{23}) = \overrightarrow{23}, \beta_1(\overrightarrow{33}) = \overrightarrow{33}\}, \{\beta_2(\overrightarrow{23}) = \overrightarrow{33}, \beta_2(\overrightarrow{33}) = \overrightarrow{23}\}\} \\
B(1,2) &= \{\{\beta_1(\overrightarrow{11}) = \overrightarrow{12}, \beta_1(\overrightarrow{31}) = \overrightarrow{32}\}, \{\beta_2(\overrightarrow{11}) = \overrightarrow{32}, \beta_2(\overrightarrow{31}) = \overrightarrow{12}\}\} \\
B(2,1) &= \{\{\beta_1(\overrightarrow{12}) = \overrightarrow{11}, \beta_1(\overrightarrow{32}) = \overrightarrow{31}\}, \{\beta_2(\overrightarrow{12}) = \overrightarrow{31}, \beta_2(\overrightarrow{32}) = \overrightarrow{11}\}\} \\
B(1,3) &= \{\{\beta_1(\overrightarrow{11}) = \overrightarrow{23}, \beta_1(\overrightarrow{31}) = \overrightarrow{33}\}, \{\beta_2(\overrightarrow{11}) = \overrightarrow{33}, \beta_2(\overrightarrow{31}) = \overrightarrow{23}\}\} \\
B(3,1) &= \{\{\beta_1(\overrightarrow{23}) = \overrightarrow{11}, \beta_1(\overrightarrow{33}) = \overrightarrow{31}\}, \{\beta_2(\overrightarrow{23}) = \overrightarrow{31}, \beta_2(\overrightarrow{33}) = \overrightarrow{11}\}\} \\
B(2,3) &= \{\{\beta_1(\overrightarrow{12}) = \overrightarrow{23}, \beta_1(\overrightarrow{32}) = \overrightarrow{33}\}, \{\beta_2(\overrightarrow{12}) = \overrightarrow{33}, \beta_2(\overrightarrow{32}) = \overrightarrow{23}\}\} \\
B(3,2) &= \{\{\beta_1(\overrightarrow{23}) = \overrightarrow{12}, \beta_1(\overrightarrow{33}) = \overrightarrow{32}\}, \{\beta_2(\overrightarrow{23}) = \overrightarrow{32}, \beta_2(\overrightarrow{33}) = \overrightarrow{12}\}\}
\end{aligned}$$

Now all cells are input-isomorphic. By Theorem 4.1 any $f \in \mathcal{F}_{\mathcal{G}}^P$ can be expressed in terms of a single $B(c,c)$-invariant map $\hat{f}_c : P_c \times P_{\mathcal{T}(I(c))} \to P_c$. Let $\hat{f}_1 : P_1 \times P_{\mathcal{T}(I(1)} \to P_1$ be $B(1,1)$-invariant. Suppose we define a function $A : P_1 \times P_{\mathcal{T}(I(1)} \to P_1$ by

$$A(x_1, x_1, x_3) = \hat{f}_1(x)$$

so that $A = \hat{f}_1$. Then the admissible vector field on this system is uniquely determined by this single mapping $\hat{f}_1$ as following:

$$\hat{f}_d(x_d, x_{\mathcal{T}(I(d))}) = \hat{f}_1(x_d, \beta^* x_{\mathcal{T}(I(d))}) \quad \forall \beta \in B(1,d)$$

The function f_1 is not arbitrary: there is a symmetry condition. We find this as follows.

Determination of $f_1(x)$: The non-trivial element of $B(1,1)$ is

$$\beta_2(\overrightarrow{11}) = \overrightarrow{31}, \quad \beta_2(\overrightarrow{31}) = \overrightarrow{11}$$

Since $x_{\mathcal{T}(I(1))} = (x_{\mathcal{T}(\overrightarrow{11})}, x_{\mathcal{T}(\overrightarrow{31})}) \equiv (x_1, x_3)$ so

$$\beta_2^*(x_{\mathcal{T}(I(1))}) = (x_{\mathcal{T}(\beta_2(\overrightarrow{11}))}, x_{\mathcal{T}(\beta_2(\overrightarrow{31}))}) \equiv (x_3, x_1)$$

Then the invariance condition demands that

$$\hat{f}_1(x_1, x_1, x_3) = \hat{f}_1(x_1, x_3, x_1)$$

Thus

$$A(x_1, x_1, x_3) = A(x_1, x_3, x_1)$$

Therefore

$$f_1(x) = A(x_1, \overline{x_1, x_3})$$

Determination of $f_2(x)$: The first element of $B(1,2)$ is

$$\beta_1(\overrightarrow{11}) = \overrightarrow{12}, \quad \beta_1(\overrightarrow{31}) = \overrightarrow{32}$$

The pullback condition demands that

$$\hat{f}_2(x_2, x_{\mathcal{T}(I(2))}) = \hat{f}_1(x_2, \beta_1^* x_{\mathcal{T}(I(2))})$$

Since $\mathcal{T}(I(2)) = (1,3)$, $\mathcal{T}(I(1)) = (1,3)$, we have $x_{\mathcal{T}(I(2))} \equiv (x_1, x_3)$. Therefore

$$\beta_1^* x_{\mathcal{T}(I(2))} = (x_{\mathcal{T}(\beta_1(\overrightarrow{11}))}, x_{\mathcal{T}(\beta_1(\overrightarrow{31}))}) \equiv (x_1, x_3)$$

Thus

$$\hat{f}_2(x_2, x_1, x_3) = \hat{f}_1(x_2, x_1, x_3) = A(x_2, x_1, x_3)$$

Similarly, we perform the computation for the second element of $B(1,2)$ is

$$\beta_2(\overrightarrow{11}) = \overrightarrow{32}, \quad \beta_2(\overrightarrow{31}) = \overrightarrow{12}$$

The pullback condition demands that

$$\hat{f}_2(x_2, x_{\mathcal{T}(I(2))}) = \hat{f}_1(x_2, \beta_2^* x_{\mathcal{T}(I(2))})$$

The pullback map β_2^* satisfies

$$\beta_2^* x_{\mathcal{T}(I(2))} = (x_{\mathcal{T}(\beta_2(\overrightarrow{11}))}, x_{\mathcal{T}(\beta_2(\overrightarrow{31}))}) \equiv (x_3, x_1)$$

Thus

$$\hat{f}_2(x_2, x_1, x_3) = \hat{f}_1(x_2, x_3, x_1) = A(x_2, x_3, x_1)$$

The domain condition implies that

$$f_2(x) = \hat{f}_2(x_2, x_{\mathcal{T}(I(2))}) = A(x_2, x_1, x_3) = A(x_2, x_3, x_1)$$

Therefore

$$f_2(x) = A(x_2, \overline{x_1, x_3})$$

Determination of $f_3(x)$: A similar method for the determination of $f_2(x)$ gives:

$$f_3(x) = A(x_3, \overline{x_2, x_3})$$

Hence

$$\begin{aligned} f_1(x) &= A(x_1, \overline{x_1, x_3}) \\ f_2(x) &= A(x_2, \overline{x_1, x_3}) \\ f_3(x) &= A(x_3, \overline{x_2, x_3}) \end{aligned}$$

as claimed.

◇

An ODE defined by an admissible vector field on a coupled cell network is called a **coupled cell system**.

4.2.5 Balanced Equivalence Relations

In the following two subsections, we introduce the concepts of balanced equivalence relations and quotient networks based on the formalism for coupled cell networks which permits multiple couplings between cells and self-coupling, as in Golubitsky *et al.* (2005).

Let $\mathcal{G} = (\mathcal{C}, \mathcal{E}, \sim_C, \sim_E)$ be a coupled cell network. Choose a total phase space P, and let $\bowtie$ be an equivalence relation on $\mathcal{C}$, partitioning the cells into equivalence classes. Abstractly, the relation "c and d are synchronous" is an equivalence relation on the set of cells, so we formalise pattern of synchrony in terms of an equivalence relation $\bowtie$ on $\mathcal{C}$. Since cells can be considered synchronous only when they have the same cell-type, $\bowtie$ must be refinement of $\sim_C$; that is, if $c \bowtie d$, then $c \sim_C d$.

For a given equivalence relation $\bowtie$ which determines a unique partition of $\mathcal{C}$, the corresponding **polysynchronous subspace** of P is defined by

$$\triangle_{\bowtie} = \{x \in P : c \bowtie d \Rightarrow x_c = x_d\}$$

A polysynchronous subspace is **robustly polysynchronous** if it is flow-invariant for every coupled cell system with the given network architecture. That is,

$$f(\triangle_{\bowtie}) \subseteq \triangle_{\bowtie} \quad \forall f \in \mathcal{F}_{\mathcal{G}}^{P}$$

and we say $\bowtie$ is **robustly polysynchronous**. Equivalently, if $x(t)$ is a trajectory of any $f \in \mathcal{F}_{\mathcal{G}}^{P}$, with initial condition $x(0) \in \triangle_{\bowtie}$, then $x(t) \in \triangle_{\bowtie}$ for all $t \in \mathbb{R}$. For example, the diagonal subspace $x_1 = \cdots = x_n$ in $\mathbb{R}^n$ is always robustly polysynchronous in a homogeneous coupled cell network.

Patterns of *robust* synchrony do not depend on the choice of P, because they are classified by a special type of equivalence relation:

Definition 4.7. *An equivalence relation on $\mathcal{C}$ is **balanced** if for every $c, d \in \mathcal{C}$ with $c \bowtie d$, there exists an input isomorphism $\beta \in B(c,d)$ such that $\mathcal{T}(i) \bowtie \mathcal{T}(\beta(i))$ for all $i \in I(c)$.*

In particular, $B(c,d) \neq \emptyset$ implies $c \sim_I d$. Hence, balanced equivalence relations refine input equivalence $\sim_I$. Now we state a necessary and sufficient condition for a polysynchronous subspace to be a robustly polysynchronous:

Theorem 4.2. *Let $\bowtie$ be an equivalence relation on a coupled cell network. Then $\bowtie$ is **robustly polysynchronous** if and only if $\bowtie$ is balanced.*

Proof. See (Stewart *et al.*, 2003, Theorem 6.5). □

4.2.6 Quotient networks

A balanced equivalence relation $\bowtie$ on a network $\mathcal{G}$ guarantees the existence of associated synchronised states in a robust manner. Now we ask: *what kinds of synchronous dynamics can occur for a given network and a given balanced equivalence relation?* The answer is: the dynamics are determined by a network whose nodes correspond to clusters of synchronous cells (that is, $\bowtie$-equivalence classes) and whose edges are defined to preserve the *isomorphic input sets* defined by $\bowtie$. We call this network the **quotient** of $\mathcal{G}$ by $\bowtie$.

We observe that each balanced equivalence relation $\bowtie$ of a coupled cell network $\mathcal{G}$ induces a unique canonical coupled cell network $\mathcal{G}/_{\bowtie}$ on $\triangle_{\bowtie}$, called the **quotient network**.

To define a network as in Definition 4.1, we must specify (1) the cells, (2) an equivalence relation on cells, (3) the arrows, (4) an equivalence relation on arrows, and (5) the head and tail incidence relations. We must also specify (6) to satisfy a consistency relation between arrows and cells.

1. Let $\overline{c}$ denote the $\bowtie$-equivalence class of $c \in \mathcal{C}$. The cells in $\mathcal{C}_{\bowtie}$ are the $\bowtie$-equivalence classes in $\mathcal{C}$, that is,

   $$\mathcal{C}_{\bowtie} = \{\overline{c} : c \in \mathcal{C}\}$$

   Thus we obtain $\mathcal{C}_{\bowtie}$ by forming the **quotient** of $\mathcal{C}$ by $\bowtie$, that is, $\mathcal{C}_{\bowtie} = \mathcal{C}/\bowtie$.

2. Define

   $$\overline{c} \sim_{C_{\bowtie}} \overline{d} \Leftrightarrow c \sim_C d$$

   The relation $\sim_{C_{\bowtie}}$ is well-defined since $\bowtie$ refines $\sim_C$.

3. Let $\mathcal{S} \subset \mathcal{C}$ be a set of cells consisting of precisely one cell c from each $\bowtie$-equivalence class. The input arrows for a quotient cell $\overline{c}$ are identified with the input arrows in cell c, where

$c \in \mathcal{S}$, that is $I(\overline{c}) = I(c)$.

When viewing the arrow $i \in I(c)$ as an arrow in $I(\overline{c})$, we denote that arrow by $\overline{i}$. Thus, the arrows in the quotient network are the projection of arrows in the original network formed by the disjoint union

$$\mathcal{E}_{\bowtie} = \dot{\bigcup}_{c \in \mathcal{S}} I(c) \tag{4.3}$$

The definition of the quotient network structure is independent of the choice of the representative cells $c \in \mathcal{S}$.

4. Two quotient arrows are equivalent when the original arrows are equivalent. That is,

$$\overline{i_1} \sim_{E_{\bowtie}} \overline{i_2} \Leftrightarrow i_1 \sim_E i_2 \tag{4.4}$$

where $i_1 \in I(c_1)$, $i_2 \in I(c_2)$, and $c_1, c_2 \in \mathcal{S}$.

5. Define the heads and tails of quotient arrows by

$$\mathcal{H}(\overline{i}) = \overline{\mathcal{H}(i)} \quad \mathcal{T}(\overline{i}) = \overline{\mathcal{T}(i)}$$

6. It is easy to verify that the quotient network satisfies the compatibility condition in Definition 4.1 (6). The quotient network is independent of the choice of cells in $\mathcal{S}$ because $\bowtie$ is balanced.

Any dynamics on the quotient *lifts* to a synchronous dynamic on the original network as the following Theorem states.

Theorem 4.3. *Let $\bowtie$ be a balanced equivalence relation on a coupled cell network $\mathcal{G}$.*

(a) *The restriction of a $\mathcal{G}$-admissible vector field to $\triangle_{\bowtie}$ is $\mathcal{G}/_{\bowtie}$-admissible.*

(b) *Every $\mathcal{G}$-admissible vector field on the quotient lifts to a $\mathcal{G}$-admissible vector field on the original network.*

Proof. See Golubitsky *et al.* (2005). □

4.2.7 Invariant Subspaces

We now restate concepts of invariant subspaces and projection mappings. For more details, see Hohn (1973).

Definition 4.8. *Let T be a linear transformation on a vector space V. A subspace W of V is said to be invariant under T (or T-invariant) if and only if $T(\mathbf{x}) \in W$ for every $\mathbf{x} \in W$, or equivalently $T(W) \in W$.*

The transformation T on V defines a transformation $T|_W$ on W, called T restricted to W.

4.2.8 Projection Mappings

A stronger form of invariance occurs in connection with familiar mappings called projections. A projection P is defined simply as any idempotent linear transformation:

$$P^2 = P$$

Suppose that a vector $\mathbf{v}$ belongs to the range of the projection. Then there exists a vector $\mathbf{u}$ such that $P(\mathbf{u}) = \mathbf{v}$. Since

$$P(\mathbf{v}) = P(P(\mathbf{u})) = P^2(\mathbf{u}) = P(\mathbf{u}) = \mathbf{v}$$

it follows that for every vector $\mathbf{v}$ of the range

$$P(\mathbf{v}) = \mathbf{v}$$

Hence not only is the range of P invariant under P as a subspace, but each point of the range of P is invariant. Furthermore, $\text{range}(P) \cap \text{kernel}(P) = \mathbf{0}$, so $V = \text{range}(P) \oplus \text{kernel}(P)$. Hence any projection P on V decomposes V into the direct sum of two subspaces; P is the identity mapping on one of these subspaces and the zero mapping on the other.

Conversely, if $V = M_1 \oplus M_2$, each $\mathbf{v} \in V$ has a unique expression $\mathbf{v} = \mu_\mathbf{1} + \mu_\mathbf{2}$ where $\mu_\mathbf{1} \in M_1$, $\mu_\mathbf{2} \in M_2$. The mapping P defined by

$$P(\mathbf{v}) = \mu_\mathbf{1}$$

is linear and idempotent, and hence a projection, called the projection of V on M_1 along M_2. Clearly, $M_1 = \text{range}(\mathbf{P})$ and $M_2 = \text{kernel}(\mathbf{P})$.

4.2.9 Lattice Theory: Part 1

We recall some basic facts about lattice theory. See Davey and Priestley (1990) for more details.
Orders: An *order* $L = \langle L, \leq \rangle$ consists of a nonempty set L and a binary relation $\leq$ on L (that is, a subset of L) — called an **ordering** — such that the relation $\leq$ is:

- reflexive ($a \leq a$ for all $a \in L$)
- antisymmetric ($a \leq b$ and $b \leq a$ imply that $a = b$ for all $a, b \in L$)
- transitive ($a \leq b$ and $b \leq c$ imply that $a \leq c$ for all $a, b, c \in L$)

An order that is *linear* ($a \leq b$ or $b \leq a$ for all $a, b \in L$) is called a **chain**.
Join and Meet: In an order L, the element u is an **upper bound** of $H \subseteq L$ if and only if $h \leq u$ for all $h \in H$. An upper bound u of H is the **least upper bound** of H if and only

if, for any upper bound v of H, we have $u \leq v$. We shall write $u = \bigvee H$. The concepts of **lower bound** and **greatest lower bound** (denoted by $\bigwedge H$) are similarly defined. We use the notation $a \wedge b = \bigwedge\{a, b\}$ and $a \vee b = \bigvee\{a, b\}$ and call $\wedge$ the **meet** and $\vee$ the **join** of the elements a and b.

Lattices and Complete lattices: An order L is a **lattice** if and only if $a \wedge b$ and $a \vee b$ always exist for all $a, b \in L$. An order L is a **complete lattice** if and only if $\bigwedge H$ and $\bigvee H$ exist for all $H \subseteq L$.

Let L be a lattice and $\emptyset \neq M \subseteq L$. Then M is a **sublattice** of L if

$$a, b \in M \quad \Rightarrow \quad a \wedge b \in M \quad \text{and} \quad a \vee b \in M$$

In lattices, the join and meet are both binary operations, which means that they can be applied to a pair of elements a, b of L to yield again an element of L. They are

- idempotent ($a \wedge a = a$, $a \vee a = a$ for all $a \in L$)
- commutative ($a \wedge b = b \wedge a$, $a \vee b = b \vee a$ for all $a, b \in L$)
- associative ($(a \wedge b) \wedge c = a \wedge (b \wedge c)$, $(a \vee b) \vee c = a \vee (b \vee c)$ for all $a, b, c \in L$)

and satisfy the:

- absorption identities ($a \wedge (a \vee b) = a$, $a \vee (a \wedge b) = a$ for all $a, b \in L$)

On the set Part(X) of all equivalence relations on X, we can introduce an ordering $\mathcal{R}_1 \prec \mathcal{R}_2$ if $\mathcal{R}_1$ is a refinement of $\mathcal{R}_2$; that is, $x\mathcal{R}_1 y$ implies that $x\mathcal{R}_2 y$, where $x\mathcal{R}y$ means that x and y are in relation $\mathcal{R}$. Consequently, the partition of X defined by $\mathcal{R}_1$ is *finer* than defined by $\mathcal{R}_2$ in the sense that for any $x \in X$

$$[x]_1 \subseteq [x]_2$$

where $[x]_j$ is the $\mathcal{R}_j$-equivalence class of x for $j = 1, 2$.
The refinement relation is a partial order on the set of partitions of X.

In fact, with this ordering, the corresponding Part(X) is a lattice, called the **partition lattice** of X with the meet and join operations are defined as follows.

$\langle x, y\rangle \in \mathcal{R}_1 \wedge \mathcal{R}_2$ if and only if $\langle x, y\rangle \in \mathcal{R}_1$ and $\langle x, y\rangle \in \mathcal{R}_2$.

The join, however, is more complicated to describe: $\langle x, y\rangle \in \mathcal{R}_1 \vee \mathcal{R}_2$ if and only if $\exists x_1, x_2, \ldots, x_n \in X$ such that $\langle x_i, x_{i+1}\rangle \in \mathcal{R}_1$ or $\langle x_i, x_{i+1}\rangle \in \mathcal{R}_2$, $i = 1, \ldots, n-1$ and $x = x_1$ and $y = x_n$.

Diagrams: In the order L, a is covered by b (written $a \prec b$) if and only if $a < b$ and $a < x < b$ holds for no x. The covering relation, $\prec$, determines the ordering in a finite order.

The diagram of an order L represents the elements with small circles. The circles representing two elements x, y are connected by a straight line if and only if one covers the other: if x is covered by y, then the circle representing y is higher than the circle representing x. For example, the following diagram represents a partition lattice of three elements $\{1, 2, 3\}$.

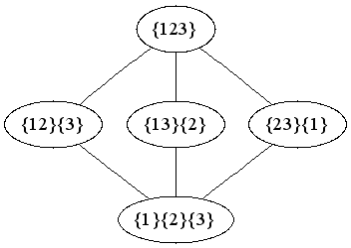

4.3 Computation of All Balanced Equivalence Relations

4.3.1 Balanced Polydiagonals are Invariant Subspaces of the Adjacency Matrix

When a fully synchronised network breaks its synchrony, we would like to determine how this network breaks into multiple clusters of synchronised sub-networks. We are interested in determining these patterns of synchrony not from a particular function form which describes the cells' dynamics, but from the network structure which describes how cells are interacting.

There are $T_n = \sum_{k=1}^{n} S(n,k)$ possible patterns of synchrony for a given n-cell homogeneous network, including two trivial patterns (fully synchronised state and all cells have different state), where $S(n,k)$ are Stirling numbers (of the second kind) Biggs (1989). Here however, some patterns of synchrony are more *robust* than others. We aim to determine these robust patterns of synchrony of a network solely from the network structure.

Assume that the dimension of the internal dynamics of a cell is one dimensional. For a given n-cell regular homogeneous network $\mathcal{G}$ with valency r, we define an associated admissible vector field F where i-th coordinate of the admissible vector field has the form:

$$f(x_i, \overline{x_{i_1}, \ldots, x_{i_r}}) : \mathbb{R} \times \underbrace{\mathbb{R} \times \cdots \times \mathbb{R}}_{r} \to \mathbb{R}$$

where $f_i(x_i, \overline{x_{i_1}, \ldots, x_{i_r}})$ distinguishes between the single internal variable x_i and the r external inputs $\overline{x_{i_1}, \ldots, x_{i_r}}$, with the bar indicating the coupling from these external cells is symmetric.

Proposition 4.1 relates robust polysynchronous subspaces to the adjacency matrix A which describes the network structure. This result is well known, but seems not to have been stated explicitly, so we provide a proof.

Proposition 4.1. *Let A be the adjacency matrix of a regular homogeneous coupled cell network $\mathcal{G}$. $\bowtie$ is robustly polysynchronous, that is $F(\triangle_{\bowtie}) \subseteq \triangle_{\bowtie}$, if and only if $A(\triangle_{\bowtie}) \subseteq \triangle_{\bowtie}$.*

Proof. $F(\triangle_{\bowtie}) \subseteq \triangle_{\bowtie} \Rightarrow A(\triangle_{\bowtie}) \subseteq \triangle_{\bowtie}$ is trivial. We show the converse. In Theorem 4.3 in Golubitsky *et al.* (2005), they proved that if $F(\triangle_{\bowtie}) \subseteq \triangle_{\bowtie}$, then $\bowtie$ is balanced by considering admissible linear vector fields.

For a regular homogeneous network $\mathcal{G}$, $\mathcal{G}$-admissible linear vector fields are expressed as:

$$\mathbb{R}\{I, A\}$$

where I is the identity matrix.

Since all vector spaces are invariant under the identity matrix I, $\triangle_{\bowtie}$ is invariant under any $\mathcal{G}$-admissible linear vector fields if $A(\triangle_{\bowtie}) \subseteq \triangle_{\bowtie}$. This implies the corresponding equivalence relation $\bowtie$ is balanced. Hence, if $A(\triangle_{\bowtie}) \subseteq \triangle_{\bowtie}$ then $\bowtie$ is robustly polysynchronous. □

Therefore, polydiagonal invariant subspaces of an adjacency matrix A are robust polysynchronous subspaces and corresponding equivalence relations are balanced. Now, we ask: *Which polysynchronous subspaces are invariant subspaces of the adjacency matrix A?*

4.3.2 Projection onto a Polysynchronous Subspace

Let $\triangle_{\bowtie} \subseteq V$ be a polysynchronous subspace, and $\triangle'_{\bowtie}$ denote its complement. Then,

$$V = \triangle_{\bowtie} \oplus \triangle'_{\bowtie}$$

where $\oplus$ is a direct sum.
Each $\mathbf{v} \in V$ is uniquely expressed as $\mathbf{v} = \boldsymbol{\mu_1} + \boldsymbol{\mu_2}$ where $\boldsymbol{\mu_1} \in \triangle_{\bowtie}$, $\boldsymbol{\mu_2} \in \triangle'_{\bowtie}$. The mapping $P_{\bowtie}$ defined by

$$P_{\bowtie}(\mathbf{v}) = \boldsymbol{\mu_1}$$

is the projection of V on $\triangle_{\bowtie}$ along $\triangle'_{\bowtie}$.

In general, we can construct a projection map on a given polysynchronous subspace as follows.

A polysynchronous subspace is defined by a given equivalence relation which determines a unique partition of cells. We consider this partition using a cycle notation. Every partition of cells can be written as a product of disjoint cycles. Especially, here we use normal form cycle notation which is obtained by writing the cell numbers $1, \ldots, n$ in increasing order in each cycle, starting with the 1-cycle, then the 2-cycles, and so on in increasing order of length. For example, the following polysynchronous subspace

$$\triangle_{\bowtie} = \{(x_1, x_2, x_3) | x_2 = x_3\}$$

is written as a product of disjoint cycles

$$(1)(23)$$

and this is in normal form for the partition $[1^1 2^1]$.

Now we define a map π which maps each element to the first element of the cycle that they belong to when written in normal form. For example, the elements in the above product of disjoint cycles are mapped to

$$1 \to 1$$

$$2 \to 2$$

$$3 \to 2$$

by a map π.

Now we can define a projection matrix $P_{\bowtie} = (p_{ij})$ on $\triangle_{\bowtie}$, which is written in normal form of a partition using the map π as following:

$$p_{i,\pi(i)} = 1$$

with all other entries being 0.

Now we can see a projection matrix which is defined from normal form as a block diagonal matrix having the form

$$P_{\bowtie} = \begin{pmatrix} P_1 & 0 & \cdots & 0 \\ 0 & P_2 & \cdots & 0 \\ \vdots & \vdots & \ddots & \vdots \\ 0 & 0 & \cdots & P_k \end{pmatrix}$$

where k is the number of disjoint cycles and P_i, $i = 1, \cdots, k$ is a $t_i \times t_i$ square projection matrix on $\triangle = \{(x_1, \ldots, x_{t_i}) | x_1 = \cdots = x_{t_i}\}$ and off-diagonal blocks are zero matrices. $P_{\bowtie}$ can also be indicated as

$$P_{\bowtie} = P_1 \oplus P_2 \oplus \cdots \oplus P_k$$

Proposition 4.2. *Let $P_{\bowtie}$ and A be linear mapping of V and let $V = \triangle_{\bowtie} \oplus \triangle'_{\bowtie}$. $\triangle_{\bowtie}$ is A-invariant if and only if $P_{\bowtie} A P_{\bowtie} = A P_{\bowtie}$, where $P_{\bowtie}$ is the projection on $\triangle_{\bowtie}$ along $\triangle'_{\bowtie}$ and A is the adjacency matrix of a given coupled cell network.*

Proof. Assume $\triangle_{\bowtie}$ is A-invariant and let $\mu_1 \in \triangle_{\bowtie}$, then

$$\begin{aligned} P_{\bowtie} A P_{\bowtie}(\mu_1) &= P_{\bowtie} A(\mu_1) \\ &= P_{\bowtie}(\mu'_1) \quad \text{where} \quad \mu'_1 \in \triangle_{\bowtie} \\ &= \mu'_1 \end{aligned}$$

Similarly,

$$\begin{aligned} AP_{\bowtie}(\mu_1) &= A(\mu_1) \\ &= \mu_1' \quad \text{where} \quad \mu_1' \in \triangle_{\bowtie} \end{aligned}$$

Above equalities hold for any $\mu_1' \in \triangle_{\bowtie}$. Therefore, $P_{\bowtie}AP_{\bowtie} = AP_{\bowtie}$.

Now, we show the converse. Let $v = \mu_1 + \mu_2$ where $\mu_1 \in \triangle_{\bowtie}$, $\mu_2 \in \triangle_{\bowtie}'$. If $P_{\bowtie}AP_{\bowtie} = AP_{\bowtie}$, then

$$\begin{aligned} AP_{\bowtie}(v) &= AP_{\bowtie}(\mu_1 + \mu_2) \\ &= A(\mu_1) \\ &= \mu_1' \quad \text{where} \quad \mu_1' \in V \end{aligned}$$

However, this should be the same as

$$\begin{aligned} P_{\bowtie}AP_{\bowtie}(v) &= P_{\bowtie}AP_{\bowtie}(\mu_1 + \mu_2) \\ &= P_{\bowtie}A(\mu_1) \\ &= P_{\bowtie}(\mu_1') \quad \text{where} \quad \mu_1' \in V \\ &= \mu_1'' \quad \text{where} \quad \mu_1'' \in \triangle_{\bowtie} \end{aligned}$$

for any $\mu_1 \in \triangle_{\bowtie}$. It means $\mu_1' = \mu_1'' \in \triangle_{\bowtie}$. Therefore,

$$A(\triangle_{\bowtie}) \subseteq \triangle_{\bowtie}$$

Hence $\triangle_{\bowtie}$ is A-invariant. □

Now, we state

Theorem 4.4. *$\triangle_{\bowtie}$ is a robust polysynchronous subspace if and only if $P_{\bowtie}AP_{\bowtie} = AP_{\bowtie}$, where $P_{\bowtie}$ is the projection on $\triangle_{\bowtie}$ along $\triangle_{\bowtie}'$.*

Proof. From Proposition 4.1, if $\triangle_{\bowtie}$ is a robust polysynchronous subspace, then $\triangle_{\bowtie}$ is A-invariant and from Proposition 4.2, the corresponding projection map $P_{\bowtie}$ to $\triangle_{\bowtie}$ satisfies $P_{\bowtie}AP_{\bowtie} = AP_{\bowtie}$. Conversely, if $P_{\bowtie}AP_{\bowtie} = AP_{\bowtie}$, then the corresponding subspace $\triangle_{\bowtie}$ is A-invariant by Proposition 4.2 and by Proposition 4.1, it is a robust polysynchronous subspace. □

4.3.3 Block Structure of an Adjacency Matrix

We show that if $\triangle_{\bowtie}$ is invariant under the adjacency matrix A, then A has a block matrix representation similar to a block matrix form of the corresponding projection matrix $P_{\bowtie}$.

Example 4.2. Suppose the projection mapping on $\triangle_{\bowtie} = \{(x_1, x_2, x_3) | x_2 = x_3\}$ is:

$$P_{\bowtie} = \left(\begin{array}{c|cc} 1 & 0 & 0 \\ \hline 0 & 1 & 0 \\ 0 & 1 & 0 \end{array}\right)$$

Now, we determine a matrix form of A which leaves $\triangle_{\bowtie}$ invariant. $\triangle_{\bowtie}$ is invariant under A if and only if $P_{\bowtie} A P_{\bowtie} = A P_{\bowtie}$. Let

$$A = \begin{pmatrix} a_{11} & a_{12} & a_{13} \\ a_{21} & a_{22} & a_{23} \\ a_{31} & a_{32} & a_{33} \end{pmatrix}$$

Then,

$$\begin{aligned} P_{\bowtie} A P_{\bowtie} &= \begin{pmatrix} 1 & 0 & 0 \\ 0 & 1 & 0 \\ 0 & 1 & 0 \end{pmatrix} \begin{pmatrix} a_{11} & a_{12} & a_{13} \\ a_{21} & a_{22} & a_{23} \\ a_{31} & a_{32} & a_{33} \end{pmatrix} \begin{pmatrix} 1 & 0 & 0 \\ 0 & 1 & 0 \\ 0 & 1 & 0 \end{pmatrix} \\ &= \begin{pmatrix} 1 & 0 & 0 \\ 0 & 1 & 0 \\ 0 & 1 & 0 \end{pmatrix} \left(\begin{array}{c|c|c} a_{11} & a_{12} + a_{13} & 0 \\ \hline a_{21} & a_{22} + a_{23} & 0 \\ \hline a_{31} & a_{32} + a_{33} & 0 \end{array}\right) \\ &= \left(\begin{array}{c|c|c} a_{11} & a_{12} + a_{13} & 0 \\ \hline a_{21} & a_{22} + a_{23} & 0 \\ \hline a_{21} & a_{22} + a_{23} & 0 \end{array}\right) \end{aligned}$$

Therefore,

$$P_{\bowtie} A P_{\bowtie} = A P_{\bowtie} \quad \Rightarrow \quad a_{21} = a_{31} \quad \text{and} \quad a_{22} + a_{23} = a_{32} + a_{33}$$

Hence, $\triangle_{\bowtie}$ is invariant under A if and only if A has the following block structure:

$$A = \left(\begin{array}{c|cc} a_{11} & a_{12} & a_{13} \\ \hline a_{21} & a_{22} & a_{23} \\ a_{21} & a_{32} & a_{33} \end{array}\right)$$

where the lower right 2×2 block matrix itself is an adjacency matrix associated with a regular homogeneous coupled cell network with valency either 0, 1 or 2 (i.e. $a_{22} + a_{23} = a_{32} + a_{33} = r$ where $r = 0, 1, 2$).

$\diamond$

Lemma 4.1. *Let A be the $n \times n$ adjacency matrix of a given coupled cell network $\mathcal{G}$. Suppose a polysynchronous subspace $\triangle_{\bowtie}$ is defined by a partition $[1^{\alpha_1} 2^{\alpha_2} \cdots n^{\alpha_n}]$ and the corresponding projection matrix $P_{\bowtie}$ is a block diagonal matrix whose diagonal blocks P_i, $i = 1, \ldots, k$, where*

$k = \sum_{i=1}^{n} \alpha_i$ *are projection matrices on diagonal subspaces* $\triangle$ *in the corresponding dimensions. Then* $P_{\bowtie} A P_{\bowtie} = A P_{\bowtie}$ *if and only if corresponding blocks of* A *to* $P_{\bowtie}$ *satisfy the following condition:*

- *Let* A_{ij}*, where* $i, j = 1, \ldots, k$ *be blocks of* A*. For all blocks* A_{ij}*, the sum of each row is the same.*

Proof. Let $P_{\bowtie} A P_{\bowtie} = A P_{\bowtie}$, where $P_{\bowtie} = \begin{pmatrix} P_1 & & 0 \\ & \ddots & \\ 0 & & P_k \end{pmatrix}$. Since

$$\text{RHS:} \quad AP_{\bowtie} = \begin{pmatrix} A_{11} & \cdots & A_{1k} \\ \vdots & \ddots & \vdots \\ A_{k1} & \cdots & A_{kk} \end{pmatrix} \begin{pmatrix} P_1 & & 0 \\ & \ddots & \\ 0 & & P_k \end{pmatrix}$$

$$= \begin{pmatrix} A_{11}P_1 & A_{12}P_2 & \cdots & A_{1k}P_k \\ A_{21}P_1 & A_{22}P_2 & \ddots & A_{2k}P_k \\ \vdots & \vdots & \ddots & \vdots \\ A_{k1}P_1 & A_{k2}P_2 & \ddots & A_{kk}P_k \end{pmatrix}$$

$$\text{LHS:} \quad P_{\bowtie} A P_{\bowtie} = \begin{pmatrix} P_1 & \cdots & 0 \\ & \ddots & \\ 0 & \cdots & P_k \end{pmatrix} \begin{pmatrix} A_{11}P_1 & A_{12}P_2 & \cdots & A_{1k}P_k \\ A_{21}P_1 & A_{22}P_2 & \ddots & A_{2k}P_k \\ \vdots & \vdots & \ddots & \vdots \\ A_{k1}P_1 & A_{k2}P_2 & \ddots & A_{kk}P_k \end{pmatrix}$$

$$= \begin{pmatrix} P_1A_{11}P_1 & P_1A_{12}P_2 & \cdots & P_1A_{1k}P_k \\ P_2A_{21}P_1 & P_2A_{22}P_2 & \ddots & P_2A_{2k}P_k \\ \vdots & \vdots & \ddots & \vdots \\ P_kA_{k1}P_1 & P_kA_{k2}P_2 & \ddots & P_kA_{kk}P_k \end{pmatrix}$$

$\iff \quad P_s A_{st} P_t = A_{st} P_t$, where $s, t = 1, \ldots, k$.

Let any arbitrary block $A_{st} = (a^{st})_{ij}$ be a $l \times m$ matrix. Then P_t is a $m \times m$ square matrix and P_s is a $l \times l$ square matrix. Since P_t and P_s are projection matrices onto m-dimensional and

l-dimensional diagonals, respectively,

$$
\begin{aligned}
A_{st}P_t &= \begin{pmatrix} a_{11}^{st} & \cdots & a_{1m}^{st} \\ \vdots & \ddots & \vdots \\ a_{l1}^{st} & \cdots & a_{lm}^{st} \end{pmatrix} \begin{pmatrix} 1 & 0 & \cdots & 0 \\ 1 & 0 & \cdots & 0 \\ \vdots & \vdots & \ddots & \vdots \\ 1 & 0 & \cdots & 0 \end{pmatrix} \\
&= \begin{pmatrix} a_{11}^{st} + \cdots + a_{1m}^{st} & 0 & \cdots & 0 \\ a_{21}^{st} + \cdots + a_{2m}^{st} & 0 & \ddots & 0 \\ \vdots & \vdots & \ddots & \vdots \\ a_{l1}^{st} + \cdots + a_{lm}^{st} & 0 & \ddots & 0 \end{pmatrix}
\end{aligned}
$$

$$
\begin{aligned}
P_sA_{st}P_t &= \begin{pmatrix} 1 & 0 & \cdots & 0 \\ 1 & 0 & \cdots & 0 \\ \vdots & \vdots & \ddots & \vdots \\ 1 & 0 & \cdots & 0 \end{pmatrix} \begin{pmatrix} a_{11}^{st} + \cdots + a_{1m}^{st} & 0 & \cdots & 0 \\ a_{21}^{st} + \cdots + a_{2m}^{st} & 0 & \ddots & 0 \\ \vdots & \vdots & \ddots & \vdots \\ a_{l1}^{st} + \cdots + a_{lm}^{st} & 0 & \ddots & 0 \end{pmatrix} \\
&= \begin{pmatrix} a_{11}^{st} + \cdots + a_{1m}^{st} & 0 & \cdots & 0 \\ a_{11}^{st} + \cdots + a_{1m}^{st} & 0 & \ddots & 0 \\ \vdots & \vdots & \ddots & \vdots \\ a_{11}^{st} + \cdots + a_{1m}^{st} & 0 & \ddots & 0 \end{pmatrix}
\end{aligned}
$$

$\iff$ $a_{11}^{st} + \cdots + a_{1m}^{st} = a_{21}^{st} + \cdots + a_{2m}^{st} = \cdots = a_{l1}^{st} + \cdots + a_{lm}^{st}$

$\iff$ $\sum_{j=1}^{m} a_{ij}^{st}$ is same for all $i = 1, \ldots, l$

$\iff$ For all blocks A_{ij}, sum of each row is same. □

We call a block of this form a **homogeneous block matrix**. It now follows immediately that:

Proposition 4.3. *A polysynchronous subspace $\triangle_{\bowtie}$ is a robust polysynchronous subspace if and only if each block of an adjacency matrix A, which corresponds to a block of $P_{\bowtie}$, is a homogeneous block matrix.*

Proof. Let each block of A is a homogeneous block matrix.

$\iff$ $P_{\bowtie}AP_{\bowtie} = AP_{\bowtie}$ (by Lemma 4.1)

$\iff$ $\triangle_{\bowtie}$ is a robust polysynchronous subspace (by Theorem 4.4) □

Table 4.1 shows polysynchronous subspaces $\triangle_{\bowtie}$ and corresponding projection mappings $P_{\bowtie}$ for three-cell and four-cell regular homogeneous networks. The last columns show the matrix which leaves $\triangle_{\bowtie}$ invariant with each block being a homogeneous block matrix.

Only representative projection mappings and invariant matrix forms from each equivalence class of partitions are shown in Table 4.1.

$\triangle_{\bowtie} \subseteq \mathbb{R}^3$	Partition	$P_{\bowtie}$	A
$(x_1, x_2, x_3) = (u, u, u)$	(123)	$\left(\begin{array}{ccc} 1 & 0 & 0 \\ 1 & 0 & 0 \\ 1 & 0 & 0 \end{array}\right)$	$\left(\begin{array}{ccc} a_{11} & a_{12} & a_{13} \\ a_{21} & a_{22} & a_{23} \\ a_{31} & a_{32} & a_{33} \end{array}\right)$
$(x_1, x_2, x_3) = (u, v, v)$	(1)(23)	$\left(\begin{array}{c\|cc} 1 & 0 & 0 \\ \hline 0 & 1 & 0 \\ 0 & 1 & 0 \end{array}\right)$	$\left(\begin{array}{c\|cc} a_{11} & a_{12} & a_{13} \\ \hline a_{21} & a_{22} & a_{23} \\ a_{21} & a_{32} & a_{33} \end{array}\right)$
$(x_1, x_2, x_3) = (u, v, w)$	(1)(2)(3)	$\left(\begin{array}{c\|c\|c} 1 & 0 & 0 \\ \hline 0 & 1 & 0 \\ \hline 0 & 0 & 1 \end{array}\right)$	$\left(\begin{array}{c\|c\|c} a_{11} & a_{12} & a_{13} \\ \hline a_{21} & a_{22} & a_{23} \\ \hline a_{31} & a_{32} & a_{33} \end{array}\right)$

$\triangle_{\bowtie} \subseteq \mathbb{R}^4$	Partition	$P_{\bowtie}$	A
$(x_1, x_2, x_3, x_4) = (u, u, u, u)$	(1234)	$\left(\begin{array}{cccc} 1 & 0 & 0 & 0 \\ 1 & 0 & 0 & 0 \\ 1 & 0 & 0 & 0 \\ 1 & 0 & 0 & 0 \end{array}\right)$	$\left(\begin{array}{cccc} a_{11} & a_{12} & a_{13} & a_{14} \\ a_{21} & a_{22} & a_{23} & a_{24} \\ a_{31} & a_{32} & a_{33} & a_{34} \\ a_{41} & a_{42} & a_{43} & a_{44} \end{array}\right)$
$(x_1, x_2, x_3, x_4) = (u, v, v, v)$	(1)(234)	$\left(\begin{array}{c\|ccc} 1 & 0 & 0 & 0 \\ \hline 0 & 1 & 0 & 0 \\ 0 & 1 & 0 & 0 \\ 0 & 1 & 0 & 0 \end{array}\right)$	$\left(\begin{array}{c\|ccc} a_{11} & a_{12} & a_{13} & a_{14} \\ \hline a_{21} & a_{22} & a_{23} & a_{24} \\ a_{21} & a_{32} & a_{33} & a_{34} \\ a_{21} & a_{42} & a_{43} & a_{44} \end{array}\right)$
$(x_1, x_2, x_3, x_4) = (u, u, w, w)$	(12)(34)	$\left(\begin{array}{cc\|cc} 1 & 0 & 0 & 0 \\ 1 & 0 & 0 & 0 \\ \hline 0 & 0 & 1 & 0 \\ 0 & 0 & 1 & 0 \end{array}\right)$	$\left(\begin{array}{cc\|cc} a_{11} & a_{12} & a_{13} & a_{14} \\ a_{21} & a_{22} & a_{23} & a_{24} \\ \hline a_{31} & a_{32} & a_{33} & a_{34} \\ a_{41} & a_{42} & a_{43} & a_{44} \end{array}\right)$
$(x_1, x_2, x_3, x_4) = (u, v, w, w)$	(1)(2)(34)	$\left(\begin{array}{c\|c\|cc} 1 & 0 & 0 & 0 \\ \hline 0 & 1 & 0 & 0 \\ \hline 0 & 0 & 1 & 0 \\ 0 & 0 & 1 & 0 \end{array}\right)$	$\left(\begin{array}{c\|c\|cc} a_{11} & a_{12} & a_{13} & a_{14} \\ \hline a_{21} & a_{22} & a_{23} & a_{24} \\ \hline a_{31} & a_{32} & a_{33} & a_{34} \\ a_{31} & a_{32} & a_{43} & a_{44} \end{array}\right)$
$(x_1, x_2, x_3, x_4) = (u, v, w, z)$	(1)(2)(3)(4)	$\left(\begin{array}{c\|c\|c\|c} 1 & 0 & 0 & 0 \\ \hline 0 & 1 & 0 & 0 \\ \hline 0 & 0 & 1 & 0 \\ \hline 0 & 0 & 0 & 1 \end{array}\right)$	$\left(\begin{array}{c\|c\|c\|c} a_{11} & a_{12} & a_{13} & a_{14} \\ \hline a_{21} & a_{22} & a_{23} & a_{24} \\ \hline a_{31} & a_{32} & a_{33} & a_{34} \\ \hline a_{41} & a_{42} & a_{43} & a_{44} \end{array}\right)$

Table 4.1: Block structures of invariant adjacency matrices for three-cell and four-cell regular homogeneous coupled cell networks.

Next we derive an adjacency matrix of a quotient network which is defined as the adjacency matrix A restricted on a robust polysynchronous subspace $\triangle_{\bowtie}$.

Proposition 4.4. *Let $\triangle_{\bowtie}$ be a robust polysynchronous subspace defined by a partition $[1^{\alpha_1}2^{\alpha_2}\cdots n^{\alpha_n}]$ with $k = \alpha_1 + \cdots + \alpha_n$ conjugacy classes, and $P_{\bowtie}$ be the corresponding block projection matrix. Let A_{st} for $s,t = 1,\ldots,k$ corresponding to the blocks of $P_{\bowtie}$ be blocks of an $n \times n$ adjacency matrix A. If blocks $A_{st} = (a^{st})_{ij}$ are homogeneous block matrices such that:*

$$A = \left(\begin{array}{c|c|c||c|c|c||c||c|c|c} A_{11} & \cdots & A_{1\alpha_1} & A_{1(\alpha_1+1)} & \cdots & A_{1(\alpha_1+\alpha_2)} & \cdots & A_{1(\alpha_1+\cdots+\alpha_{n-1}+1)} & \cdots & A_{1k} \\ \hline A_{21} & \cdots & A_{2\alpha_1} & A_{2(\alpha_1+1)} & \cdots & A_{2(\alpha_1+\alpha_2)} & \cdots & A_{2(\alpha_1+\cdots+\alpha_{n-1}+1)} & \cdots & A_{2k} \\ \hline \vdots & \ddots & \vdots & \vdots & \ddots & \vdots & \ddots & \vdots & \ddots & \vdots \\ \hline A_{k1} & \cdots & A_{k\alpha_1} & A_{k(\alpha_1+1)} & \cdots & A_{k(\alpha_1+\alpha_2)} & \cdots & A_{k(\alpha_1+\cdots+\alpha_{n-1}+1)} & \cdots & A_{kk} \end{array}\right)$$

then the quotient network corresponding to $\bowtie$ has a $k \times k$ adjacency matrix $A|_{\triangle_{\bowtie}}$, denoted by $A_{\bowtie}$, of the form:

$$A_{\bowtie} = \left(\begin{array}{c|c|c||c|c|c||c|c} \sum_{j=1}^{1} a_{1j}^{11} & \cdots & \sum_{j=1}^{1} a_{1j}^{1\alpha_1} & \cdots & \sum_{j=1}^{n} a_{1j}^{1(\alpha_1+\cdots+\alpha_{n-1}+1)} & \cdots & \sum_{j=1}^{n} a_{1j}^{1k} \\ \hline \sum_{j=1}^{1} a_{1j}^{21} & \cdots & \sum_{j=1}^{1} a_{1j}^{2\alpha_1} & \cdots & \sum_{j=1}^{n} a_{1j}^{2(\alpha_1+\cdots+\alpha_{n-1}+1)} & \cdots & \sum_{j=1}^{n} a_{1j}^{2k} \\ \hline \vdots & \ddots & \vdots & \ddots & \vdots & \ddots & \vdots \\ \hline \sum_{j=1}^{1} a_{1j}^{k1} & \cdots & \sum_{j=1}^{1} a_{1j}^{k\alpha_1} & \cdots & \sum_{j=1}^{n} a_{1j}^{k(\alpha_1+\cdots+\alpha_{n-1}+1)} & \cdots & \sum_{j=1}^{n} a_{1j}^{kk} \end{array}\right)$$

Proof. Let $\{v_1,\ldots,v_{\alpha_1},v_{\alpha_1+1},\ldots,v_k\}$ be a basis of a robust polysynchronous subspace. Each basis element corresponds to a conjugacy class of the partition $\bowtie$ and is an $n \times 1$ vector. Therefore, the basis elements have the following forms:

$$\begin{aligned} v_1 &= [1,0,\ldots,0]^t \\ &\vdots \\ v_{\alpha_1} &= [\underbrace{0,\ldots,0}_{\alpha_1-1},1,0,\ldots,0]^t \\ v_{\alpha_1+1} &= [\underbrace{0,\ldots,0}_{\alpha_1},\underbrace{1,1}_{2},0,\ldots,0]^t \\ &\vdots \\ v_k &= [\underbrace{0,\ldots,0}_{\sum_{i=1}^{n-1} i\alpha_i},\underbrace{1,\ldots,1}_{n}]^t \end{aligned}$$

Since each block A_{st} is a homogeneous block matrix, i.e., the sum of each row is the same, we can express the image of each basis element using a linear combination of a basis with

the sum of the first row of each A_{st} being used as a coefficient such as:

$$\begin{aligned}
Av_1 &= \begin{pmatrix} \sum_{j=1}^{1} a_{1j}^{11} \\ \sum_{j=1}^{1} a_{1j}^{21} \\ \vdots \\ \sum_{j=1}^{1} a_{1j}^{k1} \end{pmatrix} \\
&= \sum_{j=1}^{1} a_{1j}^{11} v_1 + \sum_{j=1}^{1} a_{1j}^{21} v_2 + \cdots + \sum_{j=1}^{1} a_{1j}^{k1} v_k \\
Av_2 &= \begin{pmatrix} \sum_{j=1}^{1} a_{1j}^{12} \\ \sum_{j=1}^{1} a_{1j}^{22} \\ \vdots \\ \sum_{j=1}^{1} a_{1j}^{k2} \end{pmatrix} \\
&= \sum_{j=1}^{1} a_{1j}^{12} v_1 + \sum_{j=1}^{1} a_{1j}^{22} v_2 + \cdots + \sum_{j=1}^{1} a_{1j}^{k2} v_k \\
&\vdots \\
Av_k &= \begin{pmatrix} \sum_{j=1}^{n} a_{1j}^{1k} \\ \sum_{j=1}^{n} a_{1j}^{2k} \\ \vdots \\ \sum_{j=1}^{n} a_{1j}^{kk} \end{pmatrix} \\
&= \sum_{j=1}^{n} a_{1j}^{1k} v_1 + \sum_{j=1}^{n} a_{1j}^{2k} v_2 + \cdots + \sum_{j=1}^{n} a_{1j}^{kk} v_k
\end{aligned}$$

Therefore a $k \times k$ matrix $A_{\bowtie}$, which is an adjacency matrix A restricted on $\triangle_{\bowtie}$, is written as

$$A_{\bowtie} = \left(\begin{array}{c|c|c||c|c|c} \sum_{j=1}^{1} a_{1j}^{11} & \cdots & \sum_{j=1}^{1} a_{1j}^{1\alpha_1} & \cdots & \sum_{j=1}^{n} a_{1j}^{1(\alpha_1+\cdots+\alpha_{n-1}+1)} & \cdots & \sum_{j=1}^{n} a_{1j}^{1k} \\ \hline \sum_{j=1}^{1} a_{1j}^{21} & \cdots & \sum_{j=1}^{1} a_{1j}^{2\alpha_1} & \cdots & \sum_{j=1}^{n} a_{1j}^{2(\alpha_1+\cdots+\alpha_{n-1}+1)} & \cdots & \sum_{j=1}^{n} a_{1j}^{2k} \\ \hline \vdots & \ddots & \vdots & \ddots & \vdots & \ddots & \vdots \\ \hline \sum_{j=1}^{1} a_{1j}^{k1} & \cdots & \sum_{j=1}^{1} a_{1j}^{k\alpha_1} & \cdots & \sum_{j=1}^{n} a_{1j}^{k(\alpha_1+\cdots+\alpha_{n-1}+1)} & \cdots & \sum_{j=1}^{n} a_{1j}^{kk} \end{array}\right)$$

and this is the adjacency matrix of the quotient network corresponding to $\bowtie$. □

The above adjacency matrix forms state the combinatorial properties of adjacency matrices that determine, for a given homogeneous coupled cell network, which polysynchronous subspaces are balanced, and what the corresponding quotient network is.

4.3.4 Enumeration Algorithm using Adjacency Matrix Combinatorics

The above combinatorial properties of adjacency matrices leads to a computer algorithm which determines all balanced equivalence relations and adjacency matrices $A_{\bowtie}$ of associated quotient networks $\mathcal{G}/_{\bowtie}$ for a given regular homogeneous network $\mathcal{G}$.

Firstly, for all possible equivalence relations $\bowtie$ of n-cells, we construct $n \times k$ matrices, where k is the number of equivalence classes of $\bowtie$, from a $n \times n$ adjacency matrix of $\mathcal{G}$. To determine which equivalence relations are balanced, we check if all rows in each equivalence class are the same. Finally, for balanced equivalence relations, we construct adjacency matrices $A_{\bowtie}$ of the corresponding quotient networks $\mathcal{G}/_{\bowtie}$.

Step 1: For a given n-cell regular homogeneous coupled cell network $\mathcal{G} = (\mathcal{C}, \mathcal{E}, \sim_C, \sim_E)$, we express the corresponding $n \times n$ adjacency matrix A as

$$A = [C_1 \cdots C_n]$$

where $C_i \in \mathbb{R}^{n\times 1}, i = 1, \ldots, n$ are column vectors. Let $\overline{C}_p$ denote the $\bowtie$-equivalence classes on $\mathcal{C}$ where $p = 1, \ldots, k$. For example, if $\mathcal{C} = \{\{1, 3, 5\}, \{2\}, \{4\}\}$ then $\overline{C}_1 = \{1, 3, 5\}$, $\overline{C}_2 = \{2\}$, and $\overline{C}_3 = \{4\}$. Note that $\sum_{p=1}^{k} |\overline{C}_p| = n$. Let $\overline{C}_{p1}$ be the first element of each equivalence class. We assume that $\overline{C}_{11} < \overline{C}_{21} < \cdots < \overline{C}_{k1}$, where these cell numbers are used as index for row vectors in Step 3.

We generate a new $n \times k$ matrix $\widetilde{A}_{\bowtie}$ with columns

$$\widetilde{C}_{\bowtie_p} = \sum_{j\in\overline{C}_p} C_j \quad \text{for} \quad p = 1, \ldots, k$$

for all possible equivalence relations $\bowtie$.

Let $\widetilde{R}_{\bowtie_i} \in \mathbb{R}^{1\times k}$, where $i = 1, \ldots, n$, denote the row vectors of this new $n \times k$ matrix $\widetilde{A}_{\bowtie}$. Therefore,

$$\widetilde{A}_{\bowtie} = \begin{pmatrix} \widetilde{R}_{\bowtie_1} \\ \vdots \\ \widetilde{R}_{\bowtie_n} \end{pmatrix} = [\widetilde{C}_{\bowtie_1} \cdots \widetilde{C}_{\bowtie_k}]$$

Step 2: Now we determine which balanced equivalence relations $\bowtie$ are balanced. An equivalence relation $\bowtie$ on $\mathcal{C}$ is balanced if and only if for all $p = 1, \ldots, k$, $\widetilde{R}_{\bowtie_l} = \widetilde{R}_{\bowtie_m}$ $\forall l, m \in \overline{C}_p$. Hence we check if

$$\widetilde{R}_{\bowtie_l} = \widetilde{R}_{\bowtie_m} \quad \forall l, m \in \overline{C}_p \tag{4.5}$$

Step 3: If the above condition (4.5) is satisfied, a $k \times k$ adjacency matrix of the quotient

network $A_{\bowtie}$ corresponding to a balanced equivalence relation $\bowtie$ is given by:

$$A_{\bowtie} = \begin{pmatrix} R_{\bowtie_1} \\ \vdots \\ R_{\bowtie_k} \end{pmatrix}$$

where $R_{\bowtie_i} \in \mathbb{R}^{1\times k}$, $i = 1, \ldots, k$ are representative row vectors in each equivalence class.

Table 4.2 shows forms of adjacency matrices $A_{\bowtie}$ of three and four-cell regular homogeneous networks. Note that all blocks in each adjacency matrix A are **homogeneous block matrices**, therefore, which satisfy the condition (4.5) in Step 2.

$\triangle_{\bowtie} \subseteq \mathbb{R}^3$	A	$A_{\bowtie}$
$(x_1, x_2, x_3) = (u, u, u)$	$\left(\begin{array}{ccc} a_{11} & a_{12} & a_{13} \\ a_{21} & a_{22} & a_{23} \\ a_{31} & a_{32} & a_{33} \end{array}\right)$	—
$(x_1, x_2, x_3) = (u, v, v)$	$\left(\begin{array}{c\|cc} a_{11} & a_{12} & a_{13} \\ \hline a_{21} & a_{22} & a_{23} \\ a_{21} & a_{32} & a_{33} \end{array}\right)$	$\left(\begin{array}{c\|c} a_{11} & a_{12}+a_{13} \\ \hline a_{21} & a_{22}+a_{23} \end{array}\right)$
$(x_1, x_2, x_3) = (u, v, w)$	$\left(\begin{array}{c\|c\|c} a_{11} & a_{12} & a_{13} \\ \hline a_{21} & a_{22} & a_{23} \\ \hline a_{31} & a_{32} & a_{33} \end{array}\right)$	—

$\triangle_{\bowtie} \subseteq \mathbb{R}^4$	A	$A_{\bowtie}$
$(x_1, x_2, x_3, x_4) = (u, u, u, u)$	$\left(\begin{array}{cccc} a_{11} & a_{12} & a_{13} & a_{14} \\ a_{21} & a_{22} & a_{23} & a_{24} \\ a_{31} & a_{32} & a_{33} & a_{34} \\ a_{41} & a_{42} & a_{43} & a_{44} \end{array}\right)$	—
$(x_1, x_2, x_3, x_4) = (u, v, v, v)$	$\left(\begin{array}{c\|ccc} a_{11} & a_{12} & a_{13} & a_{14} \\ \hline a_{21} & a_{22} & a_{23} & a_{24} \\ a_{21} & a_{32} & a_{33} & a_{34} \\ a_{21} & a_{42} & a_{43} & a_{44} \end{array}\right)$	$\left(\begin{array}{c\|c} a_{11} & a_{12}+a_{13}+a_{14} \\ \hline a_{21} & a_{22}+a_{23}+a_{24} \end{array}\right)$
$(x_1, x_2, x_3, x_4) = (u, u, w, w)$	$\left(\begin{array}{cc\|cc} a_{11} & a_{12} & a_{13} & a_{14} \\ a_{21} & a_{22} & a_{23} & a_{24} \\ \hline a_{31} & a_{32} & a_{33} & a_{34} \\ a_{41} & a_{42} & a_{43} & a_{44} \end{array}\right)$	$\left(\begin{array}{c\|c} a_{11}+a_{12} & a_{13}+a_{14} \\ \hline a_{31}+a_{32} & a_{33}+a_{34} \end{array}\right)$
$(x_1, x_2, x_3, x_4) = (u, v, w, w)$	$\left(\begin{array}{c\|c\|cc} a_{11} & a_{12} & a_{13} & a_{14} \\ \hline a_{21} & a_{22} & a_{23} & a_{24} \\ \hline a_{31} & a_{32} & a_{33} & a_{34} \\ a_{31} & a_{32} & a_{43} & a_{44} \end{array}\right)$	$\left(\begin{array}{c\|c\|c} a_{11} & a_{12} & a_{13}+a_{14} \\ \hline a_{21} & a_{22} & a_{23}+a_{24} \\ \hline a_{31} & a_{32} & a_{33}+a_{34} \end{array}\right)$
$(x_1, x_2, x_3, x_4) = (u, v, w, z)$	$\left(\begin{array}{c\|c\|c\|c} a_{11} & a_{12} & a_{13} & a_{14} \\ \hline a_{21} & a_{22} & a_{23} & a_{24} \\ \hline a_{31} & a_{32} & a_{33} & a_{34} \\ \hline a_{41} & a_{42} & a_{43} & a_{44} \end{array}\right)$	—

Table 4.2: Block structures of invariant adjacency matrices under given robust polysynchronous subspaces and adjacency matrices of the corresponding quotient networks.

4.3.5 Lattice of Balanced Equivalence Relations

Using the above computer algorithm, we can determine all balanced equivalence relations and corresponding quotient networks for a given regular homogeneous coupled cell network. Now, using the refinement relation of partitions, we construct a lattice of balanced equivalence relations for a given regular homogeneous coupled cell network.

Example 4.3. Consider the following four-cell regular homogeneous network of valency 2:

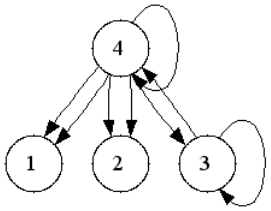

This network has 5 non-trivial balanced equivalence relations. The following table shows the robust polysynchronous subspaces and the corresponding partitions:

Polysynchronous subspace	Partition
$\triangle = \{(u,u,u,u)\}$	(1234)
$\triangle_{\bowtie_1} = \{(u,v,v,v)\}$	$(1)(234)$
$\triangle_{\bowtie_2} = \{(u,v,u,u)\}$	$(2)(134)$
$\triangle_{\bowtie_3} = \{(u,u,w,w)\}$	$(12)(34)$
$\triangle_{\bowtie_4} = \{(u,u,w,z)\}$	$(12)(3)(4)$
$\triangle_{\bowtie_5} = \{(u,v,w,w)\}$	$(1)(2)(34)$
$\triangle_{=} = \{(u,v,w,z)\}$	$(1)(2)(3)(4)$

The above seven partitions form a subset of the partition lattice of four elements. The partition lattice of four elements has the following structure:

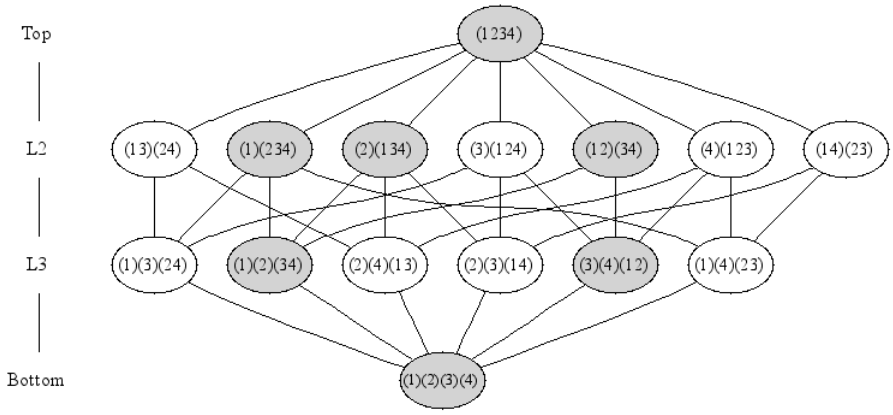

Balanced equivalence relations, which are found in the above network, are shaded in the following partition lattice of four elements.

At the top level, there is only one trivial partition (1234). The second level (L2) contains seven non-trivial partitions. There are six non-trivial partitions at the third level (L3). Finally the bottom level has only one trivial partition (1)(2)(3)(4).

Now, using a refinement relation, we order the balanced equivalence relations as follows:

Bottom — L3	L3 — L2	L2 — Top
		$(1)(234) \prec (1234)$
		$(2)(134) \prec (1234)$
		$(12)(34) \prec (1234)$
	$(1)(2)(34) \prec (1)(234)$	
	$(1)(2)(34) \prec (2)(134)$	
	$(1)(2)(34) \prec (12)(34)$	
	$(12)(3)(4) \prec (12)(34)$	
$(1)(2)(3)(4) \prec (12)(3)(4)$		
$(1)(2)(3)(4) \prec (1)(2)(34)$		

The following diagram shows the lattice of balanced equivalence relations of the given network using the above covering relations:

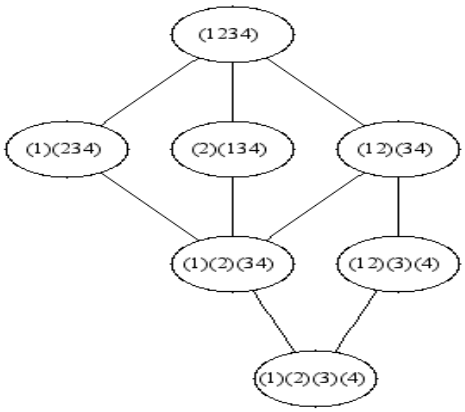

◇

Hence a lattice of balanced equivalence relations can be seen as an intersection of invariant subspaces with all possible balanced polydiagonals. In Appendix A, we show the lattice of balanced equivalence relations for all 38 three-cell regular homogeneous networks and 416 four-cell regular homogeneous networks.

4.4 Conclusions

When a fully synchronised network loses coherence, we expect it to break up into multiple clusters of synchronised sub-networks. All possible balanced equivalence relations for a given regular

homogeneous network, which describe clusters of synchronised sub-networks, were determined by using projection mappings $P_{\bowtie}$ along polysynchronous directions $\triangle_{\bowtie}$ using the relation:

$$P_{\bowtie} A P_{\bowtie} = A P_{\bowtie}$$

where A is the adjacency matrix of the given network.

We found that an adjacency matrix forms a block structure if it satisfies the above relation for each polysynchronous subspace. This block matrix form leads to a computer algorithm to search for all possible balanced equivalence relations and the corresponding quotient networks, solely from the adjacency matrix of the network. Some authors actually take this matrix property as their definition of the balanced equivalence relation (e.g. Aguiar *et al.* (2008)).

Using the refinement relation, we constructed a lattice of balanced equivalence relations for all three and four-cell regular homogeneous networks of valency 2. These lattices are used for a bifurcation analysis which will be discussed in Chapter 7 and 8.

Even though the number of networks increases with valency, the number of possible distinct lattice structures is the same. This raises a question: *How does it change if we allow different arrow types?* However, we leave it as future work.

Chapter 5

Codimension-one Bifurcation of Homogeneous Networks

5.1 Introduction

We study local bifurcation from a fully synchronous equilibrium of an admissible ODE for an n-cell regular homogeneous coupled cell network. Without loss of generality we may assume that this equilibrium is at the origin for all values of the bifurcation parameter in some interval. When the Jacobian of the system crosses the imaginary axis with nonzero speed, there are two types of codimension-one steady-state bifurcation. One is synchrony-preserving (i.e., the eigenspace is in the fully synchronous direction); the other is synchrony-breaking (i.e., the eigenspace is not in the fully synchronous direction). We consider how codimension-one steady-state synchrony-breaking bifurcations occur from the fully synchronous state. Generically, transcritical and pitchfork bifurcations may occur and conditions for their existence are derived by Liapunov-Schmidt reduction, including nonlinear terms.

We use the Liapunov-Schmidt reduction method to reduce the original system of n equations to a single *reduced* equation. We compute the derivatives of the reduced equation, expressing them in terms of the derivatives of the original system. Since these derivatives of the reduced system describe the geometry of steady states, we can determine generic conditions for existence, and the types of bifurcating branches.

We first review the basics of bifurcation theory and derive nondegeneracy conditions for generic codimension-one bifurcations. Then we compute these nondegeneracy conditions by Liapunov-Schmidt reduction.

5.2 Bifurcation Theory

5.2.1 Flows

We start with a system of ordinary differential equations

$$\frac{d\mathbf{x}}{dt} = F(\mathbf{x}, \mu), \quad \mathbf{x} \in \mathbb{R}^n, \mu \in \mathbb{R}^m \tag{5.1}$$

where $t \in \mathbb{R}$ is time, $\mathbf{x} \in \mathbb{R}^n$, and $\mu \in \mathbb{R}^m$ is a system of parameters.

Solutions of the system define a parameterised family of **flows** $\phi_\mu(\mathbf{x}, t)$ in phase space passing through $\mathbf{x}_\mu(0)$ such that $\mathbf{x}_\mu(t) = \phi_\mu(\mathbf{x}_\mu(0), t)$, where $\mathbf{x}_\mu(0)$ is the family of initial values at $t = 0$ depending on μ, i.e., $\phi_\mu(\mathbf{x}_\mu(0), 0) = \mathbf{x}_\mu(0)$.

The collective representation of these flows for all points in phase space comprises the **phase portrait**. This portrait provides a global qualitative picture of the dynamics.

There are some flows which play a central role in the qualitative study of differential equations, as well as in applications.

A **steady state** (or **fixed point** or **stationary point**) is a point $(\mathbf{x}, \mu) = (\mathbf{x}_*, \mu_*)$ such that

$$\frac{d\mathbf{x}}{dt} = F(\mathbf{x}_*, \mu_*) = \mathbf{0}$$

Note that given a steady state can always be moved to the origin $(\mathbf{0}, \mathbf{0})$ by a change of coordinates.

A point $(\mathbf{x}, \mu)$ is **periodic** with period T if and only if $\phi_\mu(\mathbf{x}, t + T) = \phi_\mu(\mathbf{x}, t)$ for all t and $\phi_\mu(\mathbf{x}, t + s) \neq \phi_\mu(\mathbf{x}, t)$ for all $0 < s < T$. The trajectory starting at $(\mathbf{x}, \mu)$ at time t first returns after an additional time T. The closed curve

$$\mathcal{C} = \{\mathbf{y} | \mathbf{y} = \phi_\mu(\mathbf{x}, t), 0 \leq t < T\}$$

is a **periodic orbit**, and consists of the trajectory joining the periodic point $(\mathbf{x}, \mu)$ back to itself in phase space.

5.2.2 Stability of Steady States

If a system of differential equations has steady states, we can consider the stability of those steady states. Roughly speaking, a steady state $\mathbf{x}_*$ is stable if all solutions near μ stay nearby. Stability of a steady state μ can be analysed by linearising the system around the steady state:
Linear Theory: Perturb a steady state $\mathbf{x}_*$ so that $\mathbf{x} = \mathbf{x}_* + \eta(t)$, with $0 < |\eta| \ll 1$:

$$\begin{aligned} \frac{d\eta}{dt} &= F(\mathbf{x}_* + \eta, \mu) \\ &= F(\mathbf{x}_*, \mu) + DF(\mathbf{x}_*, \mu) \cdot \eta + O(|\eta|^2) \end{aligned}$$

where DF represents the $n \times n$ square matrix with elements

$$(DF)_{ij} = \frac{\partial F_i}{\partial x_j} \quad i, j = 1, \ldots, n \tag{5.2}$$

and $O(|\eta|^2)$ indicates higher-order terms that are at least quadratic in the components of η. Since the constant term vanishes at $\mu = \mu_*$ and near $\mathbf{x}_*$ we study the linearised system

$$\frac{d\eta}{dt} = DF(\mathbf{x}_*, \mu_*) \cdot \eta \tag{5.3}$$

Since $(\mathbf{x}_*, \mu_*)$ is a steady state, $DF(\mathbf{x}_*, \mu_*)$ is a matrix with constant entries, and the solutions of Equation (5.3) through the point $\eta_0 \in \mathbb{R}^n$ of $t = 0$ can be written as

$$\eta(t) = e^{DF(\mathbf{x}_*, \mu_*)t}\eta_0 \tag{5.4}$$

Thus, $\eta(t)$ is asymptotically stable if all eigenvalues of $DF(\mathbf{x}_*, \mu_*)$ have negative real parts. Since this solution describes the evolution near $(\mathbf{x}_*, \mu_*)$, the following theorem shows the stability of a steady state $(\mathbf{x}_*, \mu_*)$.

Theorem 5.1. *Suppose all of the eigenvalues of $DF(\mathbf{x}_*, \mu_*)$ have negative real parts. the steady state $(\mathbf{x}, \mu) = (\mathbf{x}_*, \mu_*)$ of the nonlinear vector field (5.1) is asymptotically stable.*

Proof. See Wiggins (1990). □

5.2.3 Hyperbolic Steady States

There is a steady state of a nonlinear vector field which is stable in the linear approximation, but is actually unstable. Hence, linearly stable solutions may be nonlinearly unstable. However, if the eigenvalues of the associated linear vector field have nonzero real parts, then the flow structure near a steady state of the nonlinear vector field is essentially the same as that of the linear vector field. Such steady states are called **hyperbolic steady states**.

Definition 5.1. *Let $(\mathbf{x}, \mu) = (\mathbf{x}_*, \mu_*)$ be a steady state of $\frac{d\mathbf{x}}{dt} = F(\mathbf{x}, \mu) \quad \mathbf{x} \in \mathbb{R}^n, \mu \in \mathbb{R}^m$. Then $(\mathbf{x}_*, \mu_*)$ is called a hyperbolic steady state if no eigenvalue of $DF(\mathbf{x}_*, \mu_*)$ has zero real part.*

Some steady states have the following terminology:

- If all of the eigenvalues of $DF(\mathbf{x}_*, \mu_*)$ have negative real parts, then the hyperbolic steady state is called a **stable node** or **sink**, and if all of the eigenvalues have positive real parts, then the hyperbolic steady state is called an **unstable node** or **source**.
- If some, but not all, of the eigenvalues have positive real parts and the rest of the eigenvalues have negative real parts, then the hyperbolic steady state is called a **saddle**.

- If the eigenvalues are purely imaginary and nonzero, then the steady state is called a **centre**. It is not hyperbolic.

If the steady state $(\mathbf{x}_*, \mu_*)$ is hyperbolic, the stability of $(\mathbf{x}_*, \mu_*)$ is determined by the equation (5.3). Furthermore, a hyperbolic steady state persists under small perturbations of the governing differential equation. That is, if the governing equation is changed slightly to

$$\frac{d\mathbf{x}}{dt} = F(\mathbf{x}, \mu) + \epsilon P(\mathbf{x}, \mu), \quad \mathbf{x} \in \mathbb{R}^n, \mu \in \mathbb{R}^m$$

where $P(\mathbf{x}, \mu)$ is a smooth vector field and $0 < \epsilon \ll 1$ is sufficiently small, then for each hyperbolic steady state of the original equation, there is a hyperbolic steady state of the perturbed equation that lies very close to the unperturbed steady state in phase space and has the same stability type. However, the stability type of a nonhyperbolic, i.e., when $DF(\mathbf{x}_*, \mu_*)$ has an eigenvalue on the imaginary axis, steady state cannot be analysed in the same way as that of a hyperbolic steady state.

5.2.4 Nonhyperbolic Steady States

If some parameters of the system are varied, the phase portrait may deform slightly without altering its qualitative features. Alternatively, sometimes the dynamics may be modified significantly, producing a qualitative change in the phase portrait. Small changes to the parameter values are equivalent to making a small perturbation to the governing ordinary differential equation, and hyperbolic steady states persist under those circumstances. Therefore local changes in the number or stability-type of steady states can only happen when those steady states are not hyperbolic. In this case, for μ very close to μ_*, different behaviour can occur.

Bifurcation theory studies these qualitative changes in the phase portrait, which typically includes the appearance or disappearance of equilibria and periodic orbits, change of stability properties of equilibria and periodic orbits, or more complicated features such as strange attractors.

The parameters that lead to these changes are called **bifurcation parameters** and the point in parameter space at which the changes occur is called the **bifurcation point**. **Local bifurcation** theory is concerned with changes in the phase portrait in the neighbourhood of a single point. By contrast, on **global bifurcations**, qualitative changes in the phase portrait occur that are not captured by looking near a single point. Here we concentrate on local bifurcations.

The **codimension** of a bifurcation is the difference between the dimension of the bifurcation parameter space and the dimension of the object (e.g., surface, line or point) that gives

the location of the bifurcation in that space. Alternatively, we can regard the codimension as the number of bifurcation parameters that we need to vary in order for the bifurcation to arise typically. Bifurcations that are typical in systems depending on a single parameter are referred to as **codimension-one** bifurcations. More generally, a codimension-n bifurcation is one that can occur robustly in systems with n parameters, but not in systems with $n-1$ parameters.

5.2.5 Codimension-one Steady-state Bifurcations

For codimension-one bifurcations, we consider the following system of ODEs:

$$\frac{d\mathbf{x}}{dt} = F(\mathbf{x}, \mu), \quad \mathbf{x} \in \mathbb{R}^n, \mu \in \mathbb{R}.$$

A local bifurcation at $(\mathbf{x}, \mu) = (\mathbf{x}_*, \mu_*)$ will occur when an eigenvalue of the Jacobian matrix

$$J_{\mu_*} = DF(\mathbf{x}_*, \mu_*)$$

crosses the imaginary axis with nonzero speed as parameters are varied. When $J_{\mu_*} = DF(\mathbf{x}_*, \mu_*)$ has real coefficients, either real eigenvalues or complex conjugate pairs of eigenvalues cross this axis (often called **critical eigenvalues**). Hence, when a single parameter is involved, there are two cases:

- **Steady-state bifurcation:** J_{μ_*} has a zero eigenvalue.
- **Hopf bifurcation:** J_{μ_*} has a complex conjugate pair of eigenvalues $\pm i\omega$, where $0 \neq \omega \in \mathbb{R}$

We consider steady-state bifurcations that correspond to a real eigenvalue passing through zero, using the one-dimensional system

$$\dot{x} = f(x, \mu), \quad x \in \mathbb{R}, \quad \mu \in \mathbb{R} \tag{5.5}$$

We consider the case where the bifurcation occurs at $\mu = 0$. When there is a nonhyperbolic steady state at $\mu = 0$, Equation (5.5) must satisfy

$$f(0, 0) = 0 \tag{5.6}$$

$$\frac{\partial f}{\partial x}(0, 0) = 0 \tag{5.7}$$

Equation (5.6) is simply the steady state condition and Equation (5.7) is the zero eigenvalue condition. We remark that the system (5.5) is given by a smooth function.

There are three basic types of steady state orbit structures near the bifurcation point; Saddle-Node, Transcritical, and Pitchfork bifurcation.

Saddle-Node Bifurcation: Consider the vector field

$$\dot{x} = f(x, \mu) = \mu - x^2, \quad x \in \mathbb{R}, \quad \mu \in \mathbb{R} \tag{5.8}$$

It is easy to verify that

$$f(0, 0) = 0 \tag{5.9}$$

and

$$\frac{\partial f}{\partial x}(0, 0) = 0 \tag{5.10}$$

The set of all steady states of Equation (5.8) is given by

$$\mu - x^2 = 0 \quad \Rightarrow x = \pm\sqrt{\mu} \tag{5.11}$$

This represents a parabola in the $\mu - x$ plane as shown in Figure 5.1, which is referred to as a **bifurcation diagram**. For $\mu > 0$, Equation (5.8) has two steady states, and no steady states for $\mu < 0$. The Jacobian at the steady states $x = \pm\sqrt{\mu}$ is

$$Df|_{x=\pm\sqrt{\mu}} = -2x|_{x=\pm\sqrt{\mu}} = \mp 2\sqrt{\mu}$$

Therefore, the steady state $x = \sqrt{\mu}$ is stable and $x = -\sqrt{\mu}$ is unstable. This particular type of bifurcation (i.e., where on one side of a parameter value there are no fixed points and on the other there are two steady states) is referred to as a **saddle-node bifurcation**.

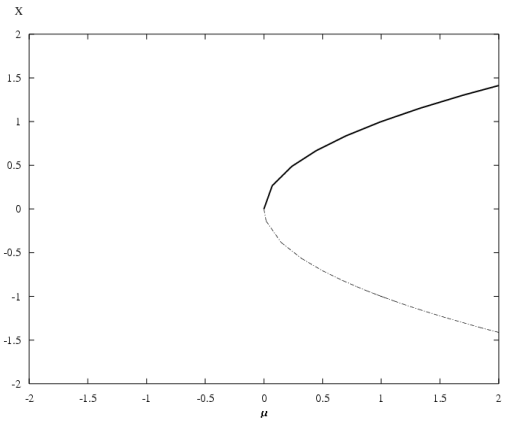

Figure 5.1: Saddle-node bifurcation diagram.

A Saddle-node is the **generic** codimension-one steady-state bifurcation. We would expect to find saddle-node bifurcation when no special conditions have been imposed on the system. The bifurcation problem

$$\dot{x} = f(x, \mu)$$

is generic for its class, if for sufficiently small $\epsilon > 0$ the perturbed problem

$$\dot{x} = f(x, \mu) + \epsilon v(x, \mu)$$

has the same type of bifurcation at a nearby value of μ for all perturbations $v(x, \mu)$.

Consider a smooth perturbation to the system (5.8)

$$\dot{x} = \mu - x^2 + \epsilon v(x, \mu)$$

Taylor expansion at $(x, \mu) = (0, 0)$ gives

$$\dot{x} = \mu(1 + \epsilon v_1 + \epsilon v_2 \mu) + \epsilon(v_3 + v_4\mu)x - (1 + \epsilon v_5)x^2 + \cdots$$

up to quadratic order in x and μ, for some constant v_i.

Steady states are

$$x = \frac{1}{2(1 + \epsilon v_5)} \left\{ \epsilon(v_3 + v_4\mu) \pm \sqrt{\epsilon^2(v_3 + v_4\mu)^2 + 4\mu(1 + \epsilon v_5)(1 + \epsilon v_1 + \epsilon v_2\mu)} \right\}$$

and exist only for

$$\mu > \mu_c \equiv -\frac{\epsilon^2 v_3^2}{4} + O(\epsilon^3)$$

There is a saddle-node bifurcation at $\mu = \mu_c \sim \epsilon^2$, close to $\mu = 0$. Thus a saddle-node is generic for one-dimensional steady-state bifurcation problems.

Transcritical Bifurcation: The simplest codimension-one steady-state bifurcation, under the condition that the steady state that persists for all values of the bifurcation parameter; that is

$$f(0, \mu) = 0, \quad \forall \mu \in \mathbb{R}$$

is the **transcritical bifurcation**.

Consider the vector field

$$\dot{x} = f(x, \mu) = \mu x - x^2, \quad x \in \mathbb{R}, \quad \mu \in \mathbb{R} \tag{5.12}$$

It is easy to verify that

$$f(0, 0) = 0 \tag{5.13}$$

and

$$\frac{\partial f}{\partial x}(0, 0) = 0 \tag{5.14}$$

Moreover, the steady states of (5.12) are given by

$$\mu x - x^2 = 0 \quad \Rightarrow x = 0 \quad \text{and} \quad x = \mu, \quad \forall \mu \in \mathbb{R} \tag{5.15}$$

and are plotted in Figure 5.2.

The Jacobian at $x = 0$ and $x = \mu$ is

$$Df|_{x=0} = \mu - 2x|_{x=0} = \mu$$

and

$$Df|_{x=\mu} = \mu - 2x|_{x=\mu} = -\mu$$

Therefore, $x = 0$ is stable for $\mu < 0$ and unstable for $\mu > 0$. However, $x = \mu$ is unstable for $\mu < 0$ and stable for $\mu > 0$. Hence at the bifurcation point $\mu = 0$, the stability of the two steady states is exchanged.

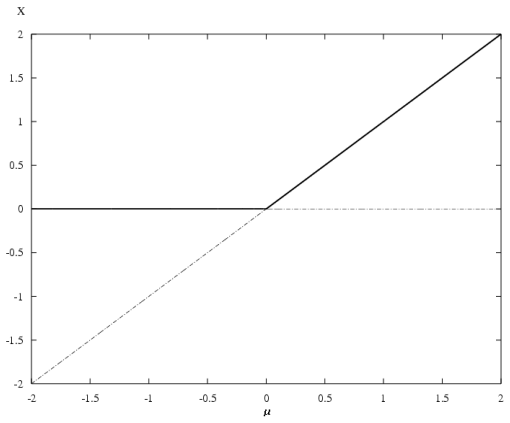

Figure 5.2: Transcritical bifurcation diagram.

The additional constraint on $f(x, \mu)$ for a transcritical bifurcation, beyond that for a saddle-node, is

$$f(0, \mu) = 0, \quad \forall \mu \in \mathbb{R} \tag{5.16}$$

which forces $x = 0$ to be a steady state of Equation (5.16) for all μ. In this case, transcritical bifurcations are generic. On the other hand, they are not generic within the wider class of steady-state bifurcation problems in one dimension. Consider the following perturbed equation in linear order that does not satisfy (5.16)

$$\dot{x} = \epsilon v_1 + \mu x - x^2 \tag{5.17}$$

Steady states are

$$x = \frac{1}{2}(\mu \pm \sqrt{\mu^2 + 4\epsilon v_1}) \tag{5.18}$$

as long as $\mu^2 + 4\epsilon v_1 > 0$. If $v_1 \geq 0$ there are steady states for all values of μ, and there is no bifurcation. On the other hand if $v_1 < 0$ steady states only exist in the regions $|\mu| > 2\sqrt{-\epsilon v_1}$, and the transcritical bifurcation breaks up into two saddle-nodes. It is no surprise that if we

see bifurcations in the perturbed case they are saddle-nodes, because these are generic when the constraint $f(0,\mu) = 0$ for all μ is broken.

Pitchfork Bifurcation: If we require both that $x = 0$ is a steady state for all values of the bifurcation parameter, and also that the system is symmetric under the transformation $x \to -x$, then we obtain a **pitchfork bifurcation**. There are two possible forms. The first case is known as **subcritical** pitchfork bifurcation shown in Figure 5.3:

$$\dot{x} = \mu x + x^3, \quad x \in \mathbb{R}, \quad \mu \in \mathbb{R} \tag{5.19}$$

The steady states are $x = 0$ for all μ and $x = \pm\sqrt{-\mu}$ for $\mu < 0$. The Jacobian at $x = 0$ is

$$Df|_{x=0} = \mu + 3x^2|_{x=0} = \mu$$

so $x = 0$ is stable for $\mu < 0$ and unstable for $\mu > 0$.

Similarly, the Jacobian at $x = \pm\sqrt{-\mu}$ is

$$Df|_{x=\pm\sqrt{-\mu}} = \mu + 3x^2|_{x=\pm\sqrt{-\mu}} = -2\mu$$

therefore, these steady states $x = \pm\sqrt{-\mu}$ are unstable for $\mu < 0$ (and does not exist for $\mu > 0$).

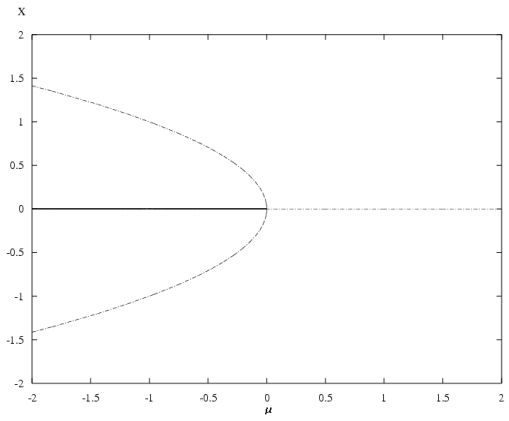

Figure 5.3: Subcritical bifurcation diagram.

The second case is known as **supercritical** pitchfork bifurcation shown in Figure 5.4;

$$\dot{x} = \mu x - x^3, \quad x \in \mathbb{R}, \quad \mu \in \mathbb{R} \tag{5.20}$$

The steady states are $x = 0$ for all μ and $x = \pm\sqrt{\mu}$ for $\mu > 0$. The Jacobian at $x = 0$ is

$$Df|_{x=0} = \mu - 3x^2|_{x=0} = \mu$$

so $x = 0$ is stable for $\mu < 0$ and unstable for $\mu > 0$.

Similarly, the Jacobian at $x = \pm\sqrt{\mu}$ is

$$Df|_{x=\pm\sqrt{\mu}} = \mu - 3x^2|_{x=\pm\sqrt{\mu}} = -2\mu$$

therefore, these steady states $x = \pm\sqrt{\mu}$ are stable for $\mu > 0$ (and does not exist for $\mu < 0$).

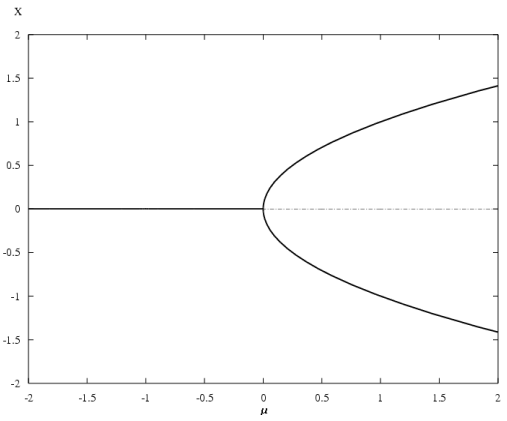

Figure 5.4: Supercritical bifurcation diagram.

In both cases there is a bifurcation at $\mu = 0$ where the zero steady state loses stability.

Pitchfork bifurcations are generic for the class of one-dimensional steady-state bifurcation problems satisfying

$$f(0, \mu) = 0 \tag{5.21}$$

$$f(-x, \mu) = -f(x, \mu) \tag{5.22}$$

in other words those that not only have a steady state $x = 0$ for all μ, but are also symmetric under the reflection symmetry $x \to -x$. The reflection symmetry requires f to be an odd function in x. Pitchforks are not generic in the wider class of one-dimensional steady state bifurcation problems that satisfy only $f(0, \mu) = 0$. Without loss of generality, we perturb a supercritical pitchfork bifurcation problem such as:

$$\dot{x} = \mu x + \epsilon v_1 x^2 - x^3 + \cdots \tag{5.23}$$

where v_1 is a constant. The steady states are:

$$x = 0, \quad \text{and} \quad x = \frac{1}{2}(\epsilon v_1 \pm \sqrt{(\epsilon v_1)^2 + 4\mu})$$

The nonzero steady states exist only for

$$\mu > -\frac{(\epsilon v_1)^2}{4}$$

and there is a saddle-node bifurcation at $\mu = \mu_c \equiv -\frac{(\epsilon v_1)^2}{4}$ where this pair of steady states is formed. There is also a transcritical bifurcation at $\mu = 0$. As a result of the perturbation, the bifurcation problem (5.23) breaks the $x \to -x$ symmetry, but it still lies in the class where $f(0, \mu) = 0$, for which transcritical bifurcations are generic. It is natural that there is a transcritical, rather than a pitchfork bifurcation at the origin in the perturbed case.

In all three bifurcation types,

$$f(0,0) = 0 \tag{5.24}$$

$$\frac{\partial f}{\partial x}(0,0) = 0 \tag{5.25}$$

However, the orbit structure of steady states near $\mu = 0$ is different in all three cases. Hence, knowing that a steady state has a zero eigenvalue for $\mu = 0$ is not sufficient to determine the orbit structure of steady states for μ near zero.

Now we want to derive conditions under which a general one-parameter family of one-dimensional vector fields will undergo the above three bifurcation types. These conditions involve derivatives of the vector field evaluated at the bifurcation point, and are obtained by consideration of the geometry of the curve of fixed points in the (μ, x)-plane in a neighbourhood of the bifurcation point. In the following, we consider a general one-parameter family of one-dimensional vector fields

$$\dot{x} = f(x, \mu) \quad x \in \mathbb{R}, \quad \mu \in \mathbb{R} \tag{5.26}$$

Suppose Equation (5.26) has a fixed point at $(x, \mu) = (0, 0)$, i.e.,

$$f(0,0) = 0 \tag{5.27}$$

Further, suppose that the fixed point is not hyperbolic, i.e.,

$$\frac{\partial f}{\partial x}(0,0) = 0 \tag{5.28}$$

We derive additional general conditions for Saddle-Node, Transcritical, and Pitchfork bifurcations followed by the technique of Liapunov-Schmidt reduction.

5.2.6 Nondegeneracy Conditions for Saddle-Node Bifurcation

In the saddle-node bifurcation, a unique curve of steady states, parameterised by x, passes through $(x, \mu) = (0, 0)$. We denote the curve of steady states by $\mu(x)$. The curve of steady states satisfies two properties.

1. It is tangent to the line $\mu = 0$ at $x = 0$, i.e.,

$$\frac{d\mu}{dx}(0) = 0$$

2. It lies entirely to one side of $\mu = 0$. Locally, this will be satisfied if

$$\frac{d^2\mu}{dx^2}(0) \neq 0$$

Now we want to derive conditions in terms of derivatives of f evaluated at $(x, \mu) = (0, 0)$ so that

$$\frac{d\mu}{dx}(0) = 0 \tag{5.29}$$

$$\frac{d^2\mu}{dx^2}(0) \neq 0 \tag{5.30}$$

We can derive expressions for (5.29) and (5.30) in terms of derivatives of f at the bifurcation point by implicitly differentiating f along the curve of fixed point (see Wiggins (1990) for the details). In order for (5.26) to undergo a saddle-node bifurcation we must have

$$f(0,0) = 0 \tag{5.31}$$

$$\frac{\partial f}{\partial x}(0,0) = 0 \tag{5.32}$$

$$\frac{\partial f}{\partial \mu}(0,0) \neq 0 \tag{5.33}$$

$$\frac{\partial^2 f}{\partial x^2}(0,0) \neq 0 \tag{5.34}$$

The first two conditions ensure a nonhyperbolic fixed point. Equation (5.33) implies that a unique curve of fixed points passes through $(x, \mu) = (0, 0)$, and (5.34) implies that the curve lies locally on one side of $\mu = 0$.

The Taylor expansion at $(x, \mu) = (0, 0)$ of the vector field (5.26) is given as follows

$$\begin{aligned} f(x,\mu) = {} & f(0,0) + f_x(0,0)x + f_\mu(0,0)\mu + \frac{1}{2}(f_{xx}(0,0)x^2 + 2f_{x\mu}(0,0)x\mu + f_{\mu\mu}(0,0)\mu^2) \\ & + \frac{1}{6}(f_{xxx}(0,0)x^3 + 3f_{xx\mu}(0,0)x^2\mu + 3f_{x\mu\mu}(0,0)x\mu^2 + f_{\mu\mu\mu}(0,0)\mu^3) + O(4) \end{aligned}$$

where $f_u(0,0)$ means the first partial derivative with respect to the variable u evaluated at $(x, \mu) = (0, 0)$.

The dynamics of the above equation near $(x, \mu) = (0, 0)$ satisfying the conditions (5.31), (5.32), (5.33) and (5.34) are qualitatively the same as one of the following vector fields

$$\dot{x} = \mu \pm ax^2 \tag{5.35}$$

where $a = \frac{1}{2}f_{xx}(0,0)$ is a constant.

Hence, (5.35) can be viewed as the normal form for saddle-node bifurcations.

5.2.7 Nondegeneracy Conditions for Transcritical Bifurcation

We again use the implicit function theorem to characterise the geometry of the curves of fixed points passing through the bifurcation point. For transcritical bifurcation, the orbit structure near the bifurcation point is characterised as follows.

1. Two curves of fixed points pass through $(x, \mu) = (0, 0)$.

2. Both curves of fixed points exist on both sides of $\mu = 0$.

3. The stability along each curve of fixed points changes on passing through $\mu = 0$.

Using these three points as a guide, we derive general conditions. We summarise the results as follows. In order for (5.26) to undergo a transcritical bifurcation we must have

$$f(0,0) = 0 \tag{5.36}$$
$$\frac{\partial f}{\partial x}(0,0) = 0 \tag{5.37}$$
$$\frac{\partial f}{\partial \mu}(0,0) = 0 \tag{5.38}$$
$$\frac{\partial^2 f}{\partial x \partial \mu}(0,0) \neq 0 \tag{5.39}$$
$$\frac{\partial^2 f}{\partial x^2}(0,0) \neq 0 \tag{5.40}$$

The first two conditions ensure a nonhyperbolic fixed point.

Thus, (5.36), (5.37), (5.38), (5.39) and (5.40) show that the orbit structure near $(x, \mu) = (0, 0)$ is qualitatively the same as the orbit structure near $(x, \mu) = (0, 0)$ of

$$\dot{x} = \mu x \pm a x^2 \tag{5.41}$$

where $a = \frac{1}{2} f_{xx}(0, 0)$ is a constant.

Equation (5.41) can be viewed as a normal form for the transcritical bifurcation.

5.2.8 Nondegeneracy Conditions for Pitchfork Bifurcation

The geometry of the curves of steady states associated with the pitchfork bifurcation has the following characteristics.

1. Two curves of steady states pass through $(x, \mu) = (0, 0)$, one given by $x = 0$, the other by $\mu = x^2$.

2. The curve $x = 0$ exists on both sides of $\mu = 0$; the curve $\mu = x^2$ exists on one side of $\mu = 0$.

3. The steady states on the curve $x = 0$ have different stability types on opposite sides of $\mu = 0$. The steady states on $\mu = x^2$ all have the same stability type.

In order for (5.26) to undergo a pitchfork bifurcation at $(x, \mu) = (0, 0)$, it is sufficient to have the following conditions which satisfy the above properties of the steady state curve:

$$\begin{aligned} f(0,0) &= 0 && (5.42)\\ \frac{\partial f}{\partial x}(0,0) &= 0 && (5.43)\\ \frac{\partial f}{\partial \mu}(0,0) &= 0 && (5.44)\\ \frac{\partial^2 f}{\partial x \partial \mu}(0,0) &\neq 0 && (5.45)\\ \frac{\partial^2 f}{\partial x^2}(0,0) &= 0 && (5.46)\\ \frac{\partial^3 f}{\partial x^3}(0,0) &\neq 0 && (5.47) \end{aligned}$$

We conclude by noting that (5.42), (5.43), (5.44), (5.45) (5.46) and (5.47) imply that the orbit structure of steady states near $(x, \mu) = (0, 0)$ is qualitatively the same as the orbit structure of steady states near $(x, \mu) = (0, 0)$ of the vector field

$$\dot{x} = \mu x \pm a x^3 \tag{5.48}$$

where $a = \frac{1}{6} f_{xxx}(0, 0)$ is a constant.

Thus, (5.48) can be viewed as a normal form for the pitchfork bifurcation.

5.3 Liapunov-Schmidt Reduction

The type of a bifurcation can be obtained by using the Liapunov-Schmidt reduction procedure. This procedure determines a mapping from the kernel of the linearisation of the original mapping into the complement of the image of the linearised mapping. The solutions along the new branch are tangent to the kernel.

The following derivation is from Golubitsky and Schaeffer (1990) pages 25-35. Consider a system of n equations

$$f_i(\mathbf{x}, \mu) = 0, \quad i = 1, \ldots, n \tag{5.49}$$

where $f_i : \mathbb{R}^n \times \mathbb{R} \to \mathbb{R}$ is a smooth mapping. The vector $\mathbf{x} = (x_1, \ldots, x_n)$ is the unknown to be solved for in Equation (5.49), and μ is a parameter.

Let $F = (f_1, \ldots, f_n)$ such that $F : \mathbb{R}^n \times \mathbb{R} \to \mathbb{R}^n$. We assume that $F(\mathbf{0}, 0) = \mathbf{0}$ and we attempt to describe the solution of this system locally near the origin.

Let $J = (dF)_{(\mathbf{0},0)}$ be the $n \times n$ Jacobian matrix $(\frac{\partial f_i}{\partial x_j}(\mathbf{0}, 0))$. If $\text{rank}(dF)_{(\mathbf{0},0)} = n$, the implicit function theorem implies that (5.49) may be solved uniquely for $\mathbf{x}$ as a function of μ. In other words, this is a nondegenerate case where no bifurcation occurs. We consider the *minimally* degenerate case, where

$$\text{rank}(dF)_{(\mathbf{0},0)} = n - 1 \tag{5.50}$$

We show that under the assumption (5.50) , solutions of the full system (5.49) may locally be put in one-to-one correspondence with solutions of a single equation

$$g(y, \mu) = 0 \tag{5.51}$$

where $g : \mathbb{R} \times \mathbb{R} \to \mathbb{R}$ and g is the restriction of F onto $\ker(J)$ about $(\mathbf{0}, 0)$. This is the Liapunov-Schmidt reduction for Equation (5.49).

We choose vector space complements M and N to $\ker(J)$ and $\text{range}(J)$, respectively, obtaining the decompositions:

$$\mathbb{R}^n = \ker(J) \oplus M \tag{5.52}$$

$$\mathbb{R}^n = N \oplus \text{range}(J) \tag{5.53}$$

From the dimension theorem,

$$\begin{aligned} \dim(\text{range}(J)) &= \dim(M) = n - 1 \\ \dim(\ker(J)) &= \dim(N) = 1 \end{aligned}$$

Let E be the projection map of $\mathbb{R}^n$ onto $\text{range}(J)$, with complementary projection map $I - E$, defined as follows:

$$\begin{aligned} E &: \mathbb{R}^n \to \text{range}(J) \quad \text{with} \quad \ker(E) = N \\ (I - E) &: \mathbb{R}^n \to N \quad \text{with} \quad \ker(I - E) = \text{range}(J) \end{aligned}$$

Observe that $F(\mathbf{x}, \mu) = \mathbf{0}$ if and only if the components of F in $\text{range}(J)$ and in N are zero:

$$EF(\mathbf{x}, \mu) = \mathbf{0} \tag{5.54}$$

$$(I - E)F(\mathbf{x}, \mu) = \mathbf{0} \tag{5.55}$$

To solve these equations, write

$$\mathbf{x} = \mathbf{v} + \mathbf{w}, \quad \mathbf{v} \in \ker(J), \mathbf{w} \in M$$

The implicit function theorem implies that (5.54) is uniquely solvable for $\mathbf{w}$ near the origin. Write this solution as $\mathbf{w} = W(\mathbf{v}, \mu)$; thus $W : \ker J \times \mathbb{R} \to M$ satisfies

$$EF(\mathbf{v} + W(\mathbf{v}, \mu), \mu) \equiv \mathbf{0}, \quad W(\mathbf{0}, 0) = 0 \tag{5.56}$$

Substitute $\mathbf{w}$ into (5.55) to obtain the reduced mapping $g : \ker J \times \mathbb{R} \to N$, where

$$g(\mathbf{v}, \mu) = (I - E)F(\mathbf{v} + W(\mathbf{v}, \mu), \mu) \tag{5.57}$$

Then the zeros of $g(\mathbf{v}, \mu)$ are in one-to-one correspondence with the zeros of $F(\mathbf{x}, \mu)$, being given by

$$g(\mathbf{v}, \mu) = 0 \Leftrightarrow F(\mathbf{v} + W(\mathbf{v}, \mu), \mu) = 0$$

since $F(\mathbf{v} + W(\mathbf{v}, \mu), \mu)$ is not a member of $\ker(I - E) = \text{range} J$ and $\mathbf{w}$ is uniquely determined by $\mathbf{v}$.

The reduced function g contains all the qualitative information that we need.

Now we choose arbitrary coordinates on $\ker J$ and N. Let $\mathbf{v}_0$ and $\mathbf{v}_0^*$ be nonzero vectors in $\ker J$ and $(\text{range} J)^\perp$, respectively. Any $\mathbf{v} \in \ker J$ may be written uniquely in the form $\mathbf{v} = x\mathbf{v}_0$ where $x \in \mathbb{R}$. Define $r : \mathbb{R} \times \mathbb{R} \to \mathbb{R}$ by

$$r(x, \mu) = < \mathbf{v}_0^*, g(x\mathbf{v}_0, \mu) > \tag{5.58}$$

where $< \cdot, \cdot >$ is the inner product. Since $g(x\mathbf{v}_0, \mu) \in N$,

$$r(x, \mu) = 0 \Leftrightarrow g(x\mathbf{v}_0, \mu) = 0$$

Thus the zeros of r are also in one-to-one correspondence with solutions of $F(\mathbf{x}, \mu) = 0$.

Now, we compute the derivatives of the reduced function $r(x, \mu)$ from derivatives of the original mapping $F(\mathbf{x}, \mu)$. The derivatives of r can be obtained if we know the derivatives of the function g. The derivatives of g evaluated at $(\mathbf{x}, \mu) = (\mathbf{0}, 0)$ are computed as follows. See Golubitsky and Schaeffer (1990) for a detail.

$$\begin{aligned}
g_x &= 0 \\
g_{xx} &= (I - E)\left\{d^2F(\mathbf{0}, 0)(\mathbf{v}_0, \mathbf{v}_0)\right\} \\
g_{xxx} &= (I - E)\left\{3d^2F(\mathbf{0}, 0)(\mathbf{v}_0, W_{xx}(\mathbf{0}, 0)) + d^3F(\mathbf{0}, 0)(\mathbf{v}_0, \mathbf{v}_0, \mathbf{v}_0)\right\} \\
g_\mu &= (I - E)\left\{F_\mu(\mathbf{0}, 0)\right\} \\
g_{\mu x} &= (I - E)\left\{d^2F(\mathbf{0}, 0)(\mathbf{v}_0, W_\mu(\mathbf{0}, 0)) + dF_\mu(\mathbf{0}, 0)(\mathbf{v}_0)\right\}
\end{aligned}$$

Moreover at $(\mathbf{x}, \mu) = (\mathbf{0}, 0)$

$$W_{xx}(\mathbf{0}, 0) = -J^{-1}Ed^2F(\mathbf{0}, 0)(\mathbf{v}_0, \mathbf{v}_0), \tag{5.59}$$

$$W_{\mu}(\mathbf{0}, 0) = -J^{-1}EF_{\mu}(\mathbf{0}, 0). \tag{5.60}$$

where $J^{-1} : \text{range}(J) \to M$ denote the inverse of the linear map $J|_M$.

We now recall that $\langle \mathbf{v}_0^*, (I - E)\mathbf{y} \rangle = \langle \mathbf{v}_0^*, \mathbf{y} \rangle$ since $\mathbf{v}_0^* \in (\text{range}J)^{\perp}$ and for any vector $\mathbf{y} \in \mathbb{R}^n$, $E\mathbf{y} \in \text{range}(J)$, so $\langle \mathbf{v}_0^*, E\mathbf{y} \rangle = 0$. Hence,

$$\langle \mathbf{v}_0^*, (I - E)\mathbf{y} \rangle = \langle \mathbf{v}_0^*, I\mathbf{y} - E\mathbf{y} \rangle = \langle \mathbf{v}_0^*, \mathbf{y} \rangle$$

Therefore, the resulting formulas are:

$$\begin{aligned}
r_x &= 0 \\
r_{xx} &= \langle \mathbf{v}_0^*, d^2F(\mathbf{0}, 0)(\mathbf{v}_0, \mathbf{v}_0) \rangle \\
r_{xxx} &= \langle \mathbf{v}_0^*, d^3F(\mathbf{0}, 0)(\mathbf{v}_0, \mathbf{v}_0, \mathbf{v}_0) - 3d^2F(\mathbf{0}, 0)(\mathbf{v}_0, J^{-1}Ed^2F(\mathbf{0}, 0)(\mathbf{v}_0, \mathbf{v}_0)) \rangle \\
r_{\mu} &= \langle \mathbf{v}_0^*, F_{\mu}(\mathbf{0}, 0) \rangle \\
r_{\mu x} &= \langle \mathbf{v}_0^*, dF_{\mu}(\mathbf{0}, 0)(\mathbf{v}_0) - d^2F(\mathbf{0}, 0)(\mathbf{v}_0, J^{-1}EF_{\mu}(\mathbf{0}, 0)) \rangle
\end{aligned}$$

Finally, since $\mathbf{x} = \mathbf{0}$ is a solution of the equation for all value of μ, i.e., $F(\mathbf{0}, \mu) \equiv 0$, $F_{\mu}(\mathbf{0}, 0) = 0$, so $W_{\mu}(\mathbf{0}, 0) = 0$. Hence, we can simplify the above formulas for synchrony-breaking codimension-one bifurcation of homogeneous networks as follows:

$$r_x = 0 \tag{5.61}$$

$$r_{xx} = \langle \mathbf{v}_0^*, d^2F(\mathbf{0}, 0)(\mathbf{v}_0, \mathbf{v}_0) \rangle \tag{5.62}$$

$$r_{xxx} = \langle \mathbf{v}_0^*, d^3F(\mathbf{0}, 0)(\mathbf{v}_0, \mathbf{v}_0, \mathbf{v}_0) - 3d^2F(\mathbf{0}, 0)(\mathbf{v}_0, J^{-1}Ed^2F(\mathbf{0}, 0)(\mathbf{v}_0, \mathbf{v}_0)) \rangle \tag{5.63}$$

$$r_{\mu} = 0 \tag{5.64}$$

$$r_{\mu x} = \langle \mathbf{v}_0^*, dF_{\mu}(\mathbf{0}, 0)(\mathbf{v}_0) \rangle \tag{5.65}$$

Proposition 5.1. *Let $\mathcal{G}$ be a regular homogeneous coupled cell network with one-dimensional internal dynamics for each cell. Let A be the $n \times n$ adjacency matrix associated with $\mathcal{G}$. Assume that A has simple eigenvalues. Let*

λ : *simple real eigenvalue of A*

$\mathbf{v}$: *corresponding eigenvector*

$\mathbf{u}$: *corresponding eigenvector of A^T*

Then

$$\langle \mathbf{v}_0^*, d^2F(\mathbf{0},0)(\mathbf{v}_0,\mathbf{v}_0)\rangle = \langle \mathbf{u}, \mathbf{v}^{[2]}\rangle, \tag{5.66}$$

$$\langle \mathbf{v}_0^*, d^3F(\mathbf{0},0)(\mathbf{v}_0,\mathbf{v}_0,\mathbf{v}_0)\rangle = \langle \mathbf{u}, \mathbf{v}^{[3]}\rangle, \tag{5.67}$$

$$\langle \mathbf{v}_0^*, d^2F(\mathbf{v}_0, J^{-1}Ed^2F(\mathbf{0},0)(\mathbf{v}_0,\mathbf{v}_0))\rangle = \langle \mathbf{u}, \mathbf{v} * A\mathbf{v}^{[2]}\rangle, \tag{5.68}$$

where $\mathbf{v}^{[2]} = (v_1^2, v_2^2, \ldots, v_n^2)$, $\mathbf{v}^{[3]} = (v_1^3, v_2^3, \ldots, v_n^3)$ *and* $\mathbf{x} * \mathbf{y} = (x_1y_1, x_2y_2, \ldots, x_ny_n)$.

Hence,

- *If* $\langle \mathbf{u}, \mathbf{v}^{[2]}\rangle \neq 0$, *then there exists a transcritical bifurcation.*
- *If* $\langle \mathbf{u}, \mathbf{v}^{[2]}\rangle = 0$, *then generically the bifurcation is a pitchfork, provided* $\langle \mathbf{u}, \mathbf{v}^{[3]}\rangle \neq 0$, $\langle \mathbf{u}, \mathbf{v} * A\mathbf{v}^{[2]}\rangle \neq 0$, *or* $\mathbf{v} * (A - \lambda I)^{-1}\mathbf{v}^{[2]} \neq 0$.

All three may vanish.

Proof. See Golubitsky and Stewart (2008) (to appear). □

5.4 Synchrony-Breaking Bifurcations

5.4.1 Generic Codimension-one Steady-state Bifurcations

We consider synchrony-breaking bifurcations from a fully synchronous equilibrium in a regular homogeneous coupled cell system; that is a coupled cell network with only one type of cell and one kind of arrow and all cells have the same number of input arrows.

Consider an n-cell regular homogeneous coupled cell network $\mathcal{G}$ and denote the total phase space by $P = (\mathbb{R}^k)^n$ where $\mathbb{R}^k$ is the phase space of each cell. For simplicity assume that the dimension k is 1. As noted in Leite and Golubitsky (2006), this assumption will not change the classification of codimension one bifurcations.

Let

$$\dot{X} = F(X, \mu) \tag{5.69}$$

where $X \in \mathbb{R}^n$, $\mu \in \mathbb{R}$ is a real bifurcation parameter and $F : \mathbb{R}^n \times \mathbb{R} \to \mathbb{R}^n$ is an admissible vector field for $\mathcal{G}$, where all coordinates of F are defined by the same function f. The diagonal subspace

$$\triangle = \{(x, x, \ldots, x) : x \in \mathbb{R}\}$$

is flow-invariant because $F(\triangle) \subseteq \triangle$ for all F. Moreover, the class of $\mathcal{G}$-admissible vector fields restricted to $\triangle$ is the set of all vector fields on $\triangle$. Thus, it is reasonable to assume that there

exists a synchronous equilibrium in $\triangle$, which we may assume, after a change of coordinates, is at the origin. Therefore, we assume

$$F(\mathbf{0}, \mu) \equiv \mathbf{0}$$

for all $\mu \in \mathbb{R}$. This means that the fully synchronous state exists for all bifurcation parameter value μ.

We define a function f associated to a regular homogeneous coupled cell network with valency r as follows:

$$f(x_i, \overline{x_{i_1}, \ldots, x_{i_r}}) : \mathbb{R} \times \underbrace{\mathbb{R} \times \cdots \times \mathbb{R}}_{r} \to \mathbb{R}$$

for $i = 1, \ldots, n$. The bar in $f(x_i, \overline{x_{i_1}, \ldots, x_{i_r}})$ indicates that the coupling from these external cells is symmetric.

Let $\mathbf{y} \in \mathbb{R}^n$ be a perturbation from $\mathbf{0} \in \triangle$. Let $\alpha = (d_{x_i} f)|_{(\mathbf{0},\mu)} \in \mathbb{R}$ be the linearised internal dynamics and let $\beta = (d_{x_{i_1}} f)|_{(\mathbf{0},\mu)} = \cdots = (d_{x_{i_r}} f)|_{(\mathbf{0},\mu)} \in \mathbb{R}$ be the linearised coupling. Let I_n be $n \times n$ identity matrix and A be the adjacency matrix of network G. Then

$$\begin{aligned} F(\mathbf{y}, \mu) &= F(\mathbf{0}, \mu) + (DF)|_{(\mathbf{0},\mu)} \cdot \mathbf{y} + O(2) \\ &= (\alpha I_n + \beta A) \cdot \mathbf{y} + O(2) \end{aligned}$$

Hence

$$(DF)|_{(\mathbf{0},\mu)} = \alpha I_n + \beta A$$

Every eigenvalue of $J_\mu = (DF)|_{(\mathbf{0},\mu)}$ has the form $\alpha + \lambda\beta$, where λ is an eigenvalue of A. For general $k \geq 1$, this result is stated in Leite and Golubitsky (2006) as the following proposition:

Proposition 5.2. *Let λ_i, $i = 1, \ldots, n$ be eigenvalues of adjacency matrix A. The eigenvalues of J_μ are the union of the eigenvalues of the n of $k \times k$ matrices $Q + \lambda_j R, j = 1, \ldots, n$, including algebraic multiplicity, where Q is the linearised internal dynamics and R be the linearised coupling. The eigenvectors of J_μ are the vectors $u \otimes w$, where $u \in \mathbb{C}^k$ is an eigenvector of Q and $w \in \mathbb{C}^n$ is an eigenvector of A.*

Proof. See Leite and Golubitsky (2006). □

Furthermore, eigenvalues of an adjacency matrix of a regular homogeneous networks have the following property:

Proposition 5.3. *Let $\mathcal{G}$ be an n-cell homogeneous network and A be the associated $n \times n$ adjacency matrix. Then A always has the largest eigenvalue $\lambda_0 = r$, where r is the valency of the network and corresponding synchronous eigenvector $\mathbf{v}_0 = (1, \cdots, 1)^t \in \mathbb{C}^{n \times 1}$ and the spectrum of eigenvalues of A is given by $|\lambda| \leq r$.*

Proof.

$$A\mathbf{v}_0 = \begin{pmatrix} a_{11} & a_{12} & \cdots & a_{1n} \\ a_{21} & a_{22} & \cdots & a_{2n} \\ \vdots & \ddots & \ddots & \vdots \\ a_{n1} & a_{n2} & \cdots & a_{nn} \end{pmatrix} \begin{pmatrix} 1 \\ 1 \\ \vdots \\ 1 \end{pmatrix} = \begin{pmatrix} a_{11} + a_{12} + \cdots + a_{1n} \\ a_{21} + a_{22} + \cdots + a_{2n} \\ \vdots \\ a_{n1} + a_{n2} + \cdots + a_{nn} \end{pmatrix} = r \begin{pmatrix} 1 \\ 1 \\ \vdots \\ 1 \end{pmatrix}$$

Therefore, r is an eigenvalue of A with the corresponding eigenvector $(1, \ldots, 1)^t \in \mathbb{C}^{n\times 1}$.

Next we show that the spectrum of eigenvalues of A is $|\lambda| \leq r$.

Let $\lambda \in \mathbb{C}$ be an eigenvalue of A and $\mathbf{v} \in \mathbb{C}^{n\times 1}$ be the corresponding eigenvector. Then

$$A\mathbf{v} = \lambda\mathbf{v} \tag{5.70}$$

k-th component of the equation (5.70) is expressed as:

$$\sum_{j=1}^{n} a_{kj} v_j = \lambda v_k$$

Suppose that each component of $\mathbf{v}$ satisfies $|v_j| \leq |v_k|$ for $\forall j = 1, \ldots, n$. Then

$$\begin{aligned} |\lambda||v_k| &= |\lambda v_k| \\ &= \left| \sum_{j=1}^{n} a_{kj} v_j \right| \\ &\leq \sum_{j=1}^{n} |a_{kj} v_j| \\ &= \sum_{j=1}^{n} a_{kj} \, |v_j| \\ &\leq \sum_{j=1}^{n} a_{kj} \, |v_k| \\ &= r|v_k| \end{aligned}$$

Therefore, $|\lambda| \leq r$. □

Remark 5.1. *This property in Proposition 5.3 is equivalent to a well known property of stochastic matrices.*

Define the centre subspace E^c of the Jacobian $J_\mu = (DF)|_{(\mathbf{0},\mu)}$ such as:

$$E^c = \text{span}\{\mathbf{e}_1, \ldots, \mathbf{e}_c\}$$

where $\{\mathbf{e}_1, \ldots, \mathbf{e}_c\}$ are the (generalised) eigenvectors of J_μ corresponding to the eigenvalues of J_μ having zero real part. By a **synchrony-breaking** bifurcation, we mean that at the origin

there is a critical eigenvector in the centre subspace E^c of the Jacobian $J_\mu = (DF)|_{(\mathbf{0},\mu)}$ that is not in $\triangle$.

Codimension-one bifurcations divide into **steady-state** (J_μ has a zero eigenvalue) and **Hopf** bifurcation (J_μ has purely imaginary eigenvalues). We focus on synchrony-breaking steady-state bifurcations from a synchronous equilibrium. In our bifurcation analysis we shall assume that the critical eigenvalues cross the imaginary axis with nonzero speed.

We have seen that, in general dynamical systems, a saddle-node bifurcation is the generic codimension-one bifurcation. However, because of the assumption $F(\mathbf{0}, \mu) \equiv 0$, i.e., $(0, 0, \ldots, 0)$ is a steady state for all $\mu \in \mathbb{R}$, we exclude the saddle-node bifurcation as a generic codimension-one synchrony-breaking bifurcation in regular homogeneous networks. By contrast, this assumption $F(\mathbf{0}, \mu) \equiv 0$ make a transcritical bifurcation generic. Therefore, we expect transcritical and pitchfork bifurcations as the generic codimension-one bifurcations for regular homogeneous coupled cell networks. When the Jacobian matrix has simple eigenvalues, we can reduce a system of n equations $F(X, \mu) = 0$ to a single equation $g(x, \mu) = 0$, where $g : \mathbb{R} \times \mathbb{R} \to \mathbb{R}$, by applying Liapunov-Schmidt reduction. The existence of transcritical and pitchfork bifurcating branches can then be shown by computing the derivatives of $g(x, \mu)$, as in Subsections 5.2.7 and 5.2.8.

5.4.2 Symmetric coupling constrains the form of the Taylor Expansion

Consider codimension-one bifurcation of a regular homogeneous coupled cell network $\mathcal{G}$ with valency 2, whose associated admissible vector field is defined by the function $f(u, \overline{v, w}, \mu)$. Let A be the $n \times n$ adjacency matrix A of $\mathcal{G}$ with its eigenvalues $\lambda_0, \ldots, \lambda_{n-1}$ and the corresponding eigenvectors $\mathbf{v}_0, \ldots, \mathbf{v}_{n-1}$, where $\lambda_0 = 2$ and $\mathbf{v}_0 = (1, \ldots, 1)$.

So far, we have derived general conditions using derivatives of a function evaluated at the origin $(u, \overline{v, w}, \lambda) = (0, \overline{0, 0}, 0)$ for the existence of each bifurcation branch. Let $\lambda_0, \ldots, \lambda_{n-1}$ be eigenvalues of an n-cell coupled cell networks, in general, there are at most $n - 1$ synchrony-breaking bifurcation points μ_i, $1 \leq i \leq n - 1$, which depend on the eigenvalues $\lambda_1, \ldots, \lambda_{n-1}$ of A. Hence when we prove the existence of various types of bifurcation branches, we consider derivatives of a function evaluated at each bifurcation point.

The $O(2)$ Taylor expansion evaluated at each bifurcation point $(u, v, w, \mu) = (0, 0, 0, \mu_i)$

is:

$$\begin{aligned} f(u,\overline{v,w},\mu) &= f(0,0,0,\mu_i) + f_u(0,0,0,\mu_i)u \\ &\quad + f_v(0,0,0,\mu_i)v + f_w(0,0,0,\mu_i)w + f_\mu(0,0,0,\mu_i)(\mu-\mu_i) \\ &\quad + \frac{1}{2}\left\{f_{uu}(0,0,0,\mu_i)u^2 + f_{vv}(0,0,0,\mu_i)v^2 + f_{ww}(0,0,0,\mu_i)w^2\right. \\ &\quad \left. + f_{\mu\mu}(0,0,0,\mu_i)(\mu-\mu_i)^2\right\} \\ &\quad + f_{uv}(0,0,0,\mu_i)uv + f_{uw}(0,0,0,\mu_i)uw + f_{u\mu}(0,0,0,\mu_i)u(\mu-\mu_i) \\ &\quad + f_{vw}(0,0,0,\mu_i)vw + f_{v\mu}(0,0,0,\mu_i)v(\mu-\mu_i) + f_{w\mu}(0,0,0,\mu_i)w(\mu-\mu_i) + O(3) \end{aligned}$$

Since $f(\mathbf{0},\mu) \equiv 0$, $f(0,0,0,\mu_i) = f_\mu(0,0,0,\mu_i) = f_{\mu\mu}(0,0,0,\mu_i) = 0$. Also some coefficients are equal because of the symmetry property $f(u,v,w,\mu) = f(u,w,v,\mu)$. Hence,

$$\begin{aligned} f(u,\overline{v,w},\mu) &= f_u(0,0,0,\mu_i)u + f_v(0,0,0,\mu_i)(v+w) \\ &\quad + \frac{1}{2}f_{uu}(0,0,0,\mu_i)u^2 + \frac{1}{2}f_{vv}(0,0,0,\mu_i)(v^2+w^2) \\ &\quad + f_{uv}(0,0,0,\mu_i)u(v+w) + f_{v\mu}(0,0,0,\mu_i)(\mu-\mu_i)(v+w) \\ &\quad + f_{u\mu}(0,0,0,\mu_i)u(\mu-\mu_i) + f_{vw}(0,0,0,\mu_i)vw + O(3) \end{aligned} \tag{5.71}$$

5.5 Conclusions

In regular homogeneous coupled cell systems, we expect generic steady-state synchrony-breaking bifurcation from a synchronous equilibrium is either transcritical or pitchfork. Liapunov-Schmidt reduction is applied to show the existence of transcritical and pitchfork bifurcating branches at simple real eigenvalues in Chapter 6 and Example 7.5 in Chapter 7.

Golubitsky and Stewart (2008) obtain necessary and sufficient conditions for generic synchrony-breaking steady-state bifurcation at a simple real eigenvalue to be transcritical or pitchfork. These conditions are expressed in terms of algebraic properties of the critical eigenvectors of the adjacency matrix of the network and its transpose. However, they show that these conditions are not always satisfied and there exist exceptional networks (one of them is 4-cell network of valency 736) for which generic steady-state bifurcation at a simple eigenvalue is more degenerate than transcritical or pitchfork. They speculate that this phenomenon seems to be a consequence of number-theoretic and combinatorial properties of the adjacency matrix, with a given valency, and its eigenvectors, rather than network topology as such.

Chapter 6

Homogeneous Two-cell Networks: Steady-state Bifurcation

6.1 Introduction

For a bifurcation analysis of n-cell regular homogeneous coupled cell networks, we consider the bifurcation behaviour of k-cell regular homogeneous coupled cell networks inductively, where $1 < k < n$.

There are five two-cell regular homogeneous coupled cell networks with valency 2 as shown in Figure 3.1 , Chapter 3. For each two-cell regular homogeneous network, we consider

$$\dot{X} = F(X, \mu)$$

where $F : \mathbb{R}^2 \times \mathbb{R} \to \mathbb{R}^2$ is an admissible vector field of two-cell valency 2 regular homogeneous coupled cell networks defined by the same function $f : \mathbf{R}^3 \times \mathbf{R} \to \mathbb{R}$.

We assume that $F(\mathbf{0}, \mu) \equiv 0$ for all bifurcation parameter μ and prove the existence of various synchrony-breaking bifurcating branches from the trivial solution $X = 0$, using either the Implicit Function Theorem or Liapunov-Schmidt reduction.

In these five networks, the conditions for the critical eigenvalues crossing the imaginary axis with nonzero speed are all satisfied.

6.2 Network #1

Consider 2-cell network #1 with valency 2, whose adjacency matrix, its eigenvalues, and the corresponding eigenvectors are shown in Table 6.1.

The admissible dynamical systems for this network have the form:

$$\begin{aligned} \dot{x}_1 &= f(x_1, \overline{x_2, x_2}, \mu) \\ \dot{x}_2 &= f(x_2, \overline{x_2, x_2}, \mu) \end{aligned}$$

Network #1	Adjacency matrix	Eigenvalues	Eigenvectors
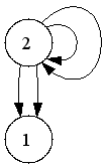	$\mathbf{A_1} = \begin{pmatrix} 0 & 2 \\ 0 & 2 \end{pmatrix}$	$\lambda_0 = 2$ $\lambda_1 = 0$	$(1,1)$ $(1,0)$

Table 6.1: Two-cell network #1

Since we are interested in finding non-trivial bifurcation branches, i.e., the eigenvector corresponding to a new branch is not $(1,1)$, we want to obtain the condition that the corresponding eigenvalue becomes zero. By Proposition 5.2, the critical eigenvalue for synchrony-breaking is:

$$f_u(0,\mu_1)\cdot 1 + f_v(0,\mu_1)\cdot \lambda_1 = f_u(0,\mu_1)$$

where μ_1 is a bifurcation point which depends on the eigenvalue λ_1.

Therefore, when this critical eigenvalue $f_u(0,\mu_1) = 0$ with $f_{u\mu}(0,\mu_1) \neq 0$, a codimension-one steady state bifurcation occurs.

Theorem 6.1. *Assume that the coupled cell system defined by $f(u,\overline{v,w},\mu)$ associated to network #1 satisfies the following conditions:*

$$f_u(\mathbf{0},\mu_1) = 0, \quad f_v(\mathbf{0},\mu_1) \neq 0, \quad f_{\mu u}(\mathbf{0},\mu_1) \neq 0, \quad f_{uu}(\mathbf{0},\mu_1) \neq 0.$$

Then there is one transcritical branch bifurcating from the trivial solution $(x_1,x_2,\mu) = (0,0,\mu_1)$ of the form

$$(x_1,x_2) = (X_1(\mu),0)$$

where $X_1(\mu_1) = 0$ and $X_1'(\mu_1) \neq 0$.

Proof. Using (5.71), the $O(2)$ Taylor expansion for four variables function evaluated at $(u,v,w,\mu) = (0,0,0,\mu_1)$ is given by:

$$\begin{aligned} f(u,\overline{v,w},\mu) \;\approx\; & f_u(\mathbf{0},\mu_1)u + f_v(\mathbf{0},\mu_1)(v+w) \\ & + f_{uv}(\mathbf{0},\mu_1)u(v+w) + f_{vw}(\mathbf{0},\mu_1)vw + f_{v\mu}(\mathbf{0},\mu_1)(\mu-\mu_1)(v+w) \\ & + f_{\mu u}(\mathbf{0},\mu_1)(\mu-\mu_1)u + \frac{1}{2}(f_{uu}(\mathbf{0},\mu_1)u^2 + f_{vv}(\mathbf{0},\mu_1)(v^2+w^2)) + O(3) \end{aligned}$$

where u is internal variable, v and w is external signal from neighbouring cells, and μ is a bifurcation parameter.

Since $f_u(\mathbf{0}, \mu_1) = 0$, the equation for cell 2 is:

$$\begin{aligned} f(x_2, \overline{x_2, x_2}, \mu) &\approx 2f_v(\mathbf{0}, \mu_1)x_2 \\ &\quad +2f_{uv}(\mathbf{0}, \mu_1)x_2^2 + f_{vw}(\mathbf{0}, \mu_1)x_2^2 + 2f_{v\mu}(\mathbf{0}, \mu_1)(\mu - \mu_1)x_2 \\ &\quad +f_{\mu u}(\mathbf{0}, \mu_1)(\mu - \mu_1)x_2 + \frac{1}{2}(f_{uu}(\mathbf{0}, \mu_1)x_2^2 + 2f_{vv}(\mathbf{0}, \mu_1)x_2^2) + O(3) \end{aligned}$$

Since $f_v(\mathbf{0}, \mu_1) \neq 0$, the first derivative for the function is

$$f'(\mathbf{0}, \mu_1) = 2f_v(\mathbf{0}, \mu_1) \neq 0$$

Therefore, by the Implicit Function Theorem, $x_2 = 0$ is the unique solution for the cell 2 equation.

Substituting $x_2 = 0$ into the cell 1 equation gives

$$f(x_1, \overline{0, 0}, \mu) = 0$$

Using the $O(2)$ Taylor expansion for this equation,

$$f(x_1, \overline{0, 0}, \mu) \approx f_{\mu u}(\mathbf{0}, \mu_1)(\mu - \mu_1)x_1 + \frac{1}{2}f_{uu}(\mathbf{0}, \mu_1)x_1^2 + O(3)$$

Therefore, the steady states are given by the equation $f(x_1, \overline{0, 0}, \mu) = 0$, that is,

$$x_1(f_{\mu u}(\mathbf{0}, \mu_1)(\mu - \mu_1) + \frac{1}{2}f_{uu}(\mathbf{0}, \mu_1)x_1) = 0$$

Since $f_{uu}(\mathbf{0}, \mu_1) \neq 0$ and $f_{\mu u}(\mathbf{0}, \mu_1) \neq 0$, we have $x_1 = 0$ or $x_1 = \frac{-2f_{\mu u}(\mathbf{0}, \mu_1)(\mu - \mu_1)}{f_{uu}(\mathbf{0}, \mu_1)}$.

When $x_1 = 0$, this gives the trivial solution $(x_1, x_2) = (0, 0)$.

We set $X_1(\mu) = \frac{-2f_{\mu u}(\mathbf{0}, \mu_1)(\mu - \mu_1)}{f_{uu}(\mathbf{0}, \mu_1)}$, then $X_1(\mu_1) = 0$ and $X_1'(\mu_1) = \frac{-2f_{\mu u}(\mathbf{0}, \mu_1)}{f_{uu}(\mathbf{0}, \mu_1)} \neq 0$. Therefore, the non-trivial branch that bifurcates from the trivial branch is transcritical. □

Alternatively, we can apply Liapunov-Schmidt reduction to the system

$$F(X, \mu) = (F_1(X, \mu), F_2(X, \mu)) = \mathbf{0}$$

where $F_1(X, \mu) = f(x_1, \overline{x_2, x_2}, \mu)$ and $F_2(X, \mu) = f(x_2, \overline{x_2, x_2}, \mu)$.

The reduced equation obtained by applying Liapunov-Schmidt reduction has the form

$$K(y, \mu) = 0$$

where $y \in \mathbb{R}$, $K : \mathbb{R} \times \mathbb{R} \to \mathbb{R}$ is smooth, $K_y(0, \mu_1) = 0$, $K_\mu(0, \mu_1) = 0$ and $K(0, \mu_1) = 0$. We calculate each derivative of this reduced equation to determine which bifurcation occurs.

The Jacobian J is given by:

$$J = f_u(\mathbf{0}, \mu_1)\begin{pmatrix} 1 & 0 \\ 0 & 1 \end{pmatrix} + f_v(\mathbf{0}, \mu_1)\begin{pmatrix} 0 & 2 \\ 0 & 2 \end{pmatrix} = f_v(\mathbf{0}, \mu_1)\begin{pmatrix} 0 & 2 \\ 0 & 2 \end{pmatrix}$$

where $f_v(\mathbf{0}, \mu_1) \neq 0$.

- **Obtaining $v_0 \in kerJ$ and $v_0^* \in (rangeJ)^\perp$:**

  Let (x, y) be any vector in $\mathbb{R}^2$.

$$f_v(\mathbf{0}, \mu_1) \begin{pmatrix} 0 & 2 \\ 0 & 2 \end{pmatrix} \begin{pmatrix} x \\ y \end{pmatrix} = f_v(\mathbf{0}, \mu_1) \begin{pmatrix} 2y \\ 2y \end{pmatrix} = \begin{pmatrix} 0 \\ 0 \end{pmatrix} \quad \Rightarrow \begin{pmatrix} x \\ y \end{pmatrix} = \begin{pmatrix} 1 \\ 0 \end{pmatrix}$$

  where $f_v(\mathbf{0}, \mu_1) \neq 0$.

  Therefore, $v_0 = (1, 0)$. Since $(1, 1) \in rangeJ$, $v_0^* = (1, -1) \in (rangeJ)^\perp$.

- **Computation of $K_{y\mu}(0, \mu_1)$:**

$$F_\mu = (f_\mu(x_1, \overline{x_2, x_2}, \mu), f_\mu(x_2, \overline{x_2, x_2}, \mu))$$

$$dF_\mu(v_0) = \begin{pmatrix} f_{\mu u} & 2f_{\mu v} \\ 0 & f_{\mu u} + 2f_{\mu v} \end{pmatrix} \begin{pmatrix} 1 \\ 0 \end{pmatrix} = \begin{pmatrix} f_{\mu u} \\ 0 \end{pmatrix}$$

  Therefore,

$$\begin{aligned} K_{y\mu}(0, \mu_1) = \langle v_0^*, dF_\mu(v_0) \rangle &= \begin{pmatrix} 1 \\ -1 \end{pmatrix} \cdot \begin{pmatrix} f_{\mu u}(\mathbf{0}, \mu_1) \\ 0 \end{pmatrix} \\ &= f_{\mu u}(\mathbf{0}, \mu_1) \end{aligned}$$

  which is generically nonzero.

- **Computation of $K_{yy}(0, \mu_1)$:**

  Since $v_0^* = (1, -1)$,

$$K_{yy}(0, \mu_1) = d^2F_1(v_0, v_0) - d^2F_2(v_0, v_0)$$

  Now

$$\begin{aligned} dF_1(v_0) &= \begin{pmatrix} f_u \\ 2f_v \end{pmatrix} \cdot \begin{pmatrix} 1 \\ 0 \end{pmatrix} = f_u(x_1, \overline{x_2, x_2}, \mu) \\ d^2F_1(v_0, v_0) &= \begin{pmatrix} f_{uu} \\ 2f_{uv} \end{pmatrix} \cdot \begin{pmatrix} 1 \\ 0 \end{pmatrix} = f_{uu}(\mathbf{0}, \mu_1) \\ dF_2(v_0) &= \begin{pmatrix} 0 \\ f_u + 2f_v \end{pmatrix} \cdot \begin{pmatrix} 1 \\ 0 \end{pmatrix} = 0 \\ d^2F_2(v_0, v_0) &= \begin{pmatrix} 0 \\ 0 \end{pmatrix} \cdot \begin{pmatrix} 1 \\ 0 \end{pmatrix} = 0 \end{aligned}$$

  Therefore, $K_{yy}(0, \mu_1) = f_{uu}(\mathbf{0}, \mu_1)$, which is generically non-zero.

Hence, the above conditions are the same as the conditions we found by using the Implicit Function Theorem, and they also guarantee the existence of a transcritical bifurcating branch from the trivial solution.

6.3 Network #2

Consider 2-cell network #2 with valency 2, whose adjacency matrix, its eigenvalues, and the corresponding eigenvectors are shown in Table 6.2.

Network #2	Adjacency matrix	Eigenvalues	Eigenvectors
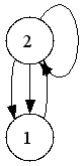	$\mathbf{A_2} = \begin{pmatrix} 0 & 2 \\ 1 & 1 \end{pmatrix}$	$\lambda_0 = 2$ $\lambda_1 = -1$	$(1,1)$ $(2,-1)$

Table 6.2: Two-cell network #2

The admissible dynamical systems for this network have the form:

$$\dot{x}_1 = f(x_1, \overline{x_2, x_2}, \mu)$$
$$\dot{x}_2 = f(x_2, \overline{x_2, x_1}, \mu)$$

The critical eigenvalue for synchrony-breaking is:

$$\begin{aligned} & f_u(\mathbf{0}, \mu_1) \cdot 1 + f_v(\mathbf{0}, \mu_1) \cdot \lambda_1 = 0 \\ \Rightarrow \quad & f_u(\mathbf{0}, \mu_1) - f_v(\mathbf{0}, \mu_1) = 0 \\ \Rightarrow \quad & f_u(\mathbf{0}, \mu_1) = f_v(\mathbf{0}, \mu_1) \end{aligned}$$

where μ_1 is determined by λ_1.

So, we can obtain the Jacobian:

$$\begin{aligned} J &= f_u(\mathbf{0}, \mu_1) I + f_v(\mathbf{0}, \mu_1) A \\ &= f_v(\mathbf{0}, \mu_1)(I + A) \\ &= f_v(\mathbf{0}, \mu_1) \begin{pmatrix} 1 & 2 \\ 1 & 2 \end{pmatrix} \end{aligned}$$

where $f_v(\mathbf{0}, \mu_1) \neq 0$.

Theorem 6.2. *Assume that the coupled cell system defined by $f(u, \overline{v, w}, \mu)$ associated to network #2 satisfies the following conditions:*

$$f_u(\mathbf{0}, \mu_1) = f_v(\mathbf{0}, \mu_1), \quad f_v(\mathbf{0}, \mu_1) \neq 0, \quad f_{\mu u}(\mathbf{0}, \mu_1) \neq f_{\mu v}(\mathbf{0}, \mu_1),$$
$$f_{uu}(\mathbf{0}, \mu_1) - 2f_{uv}(\mathbf{0}, \mu_1) + f_{vv}(\mathbf{0}, \mu_1) \neq 0.$$

Then there is one transcritical bifurcating branch from the trivial solution $(x_1, x_2, \mu) = (0, 0, \mu_1)$.

Proof. We apply Liapunov-Schmidt reduction to the system

$$F(X, \mu) = (F_1(X, \mu), F_2(X, \mu)) = \mathbf{0}$$

where $F_1(X, \mu) = f(x_1, \overline{x_2, x_2}, \mu)$ and $F_2(X, \mu) = f(x_2, \overline{x_2, x_1}, \mu)$.

The reduced equation has the form

$$K(y, \mu) = 0$$

where $y \in \mathbb{R}$, $K : \mathbb{R} \times \mathbb{R} \to \mathbb{R}$ is smooth, $K_y(0, \mu_1) = 0$, $K_\mu(0, \mu_1) = 0$ and $K(0, \mu_1) = 0$. We calculate each derivative of this reduced equation to determine which bifurcation occurs.

- **Obtaining** $v_0 \in kerJ$ **and** $v_0^* \in (rangeJ)^\perp$**:**

  Let (x, y) be any vector in $\mathbb{R}^2$.

  $$f_v(\mathbf{0}, \mu_1) \begin{pmatrix} 1 & 2 \\ 1 & 2 \end{pmatrix} \begin{pmatrix} x \\ y \end{pmatrix} = f_v(\mathbf{0}, \mu_1) \begin{pmatrix} x + 2y \\ x + 2y \end{pmatrix} = \begin{pmatrix} 0 \\ 0 \end{pmatrix} \quad \Rightarrow \begin{pmatrix} x \\ y \end{pmatrix} = \begin{pmatrix} 2 \\ -1 \end{pmatrix}$$

  Therefore, $v_0 = (2, -1)$. Since $(1, 1) \in rangeJ$, $v_0^* = (1, -1) \in (rangeJ)^\perp$.

- **Computation of** $K_{y\mu}(0, \mu_1)$**:**

  $$F_\mu = (f_\mu(x_1, \overline{x_2, x_2}, \mu), f_\mu(x_2, \overline{x_2, x_1}, \mu))$$

  $$dF_\mu(v_0) = \begin{pmatrix} f_{\mu u} & 2f_{\mu v} \\ f_{\mu v} & f_{\mu u} + f_{\mu v} \end{pmatrix} \begin{pmatrix} 2 \\ -1 \end{pmatrix} = \begin{pmatrix} 2f_{\mu u} - 2f_{\mu v} \\ f_{\mu v} - f_{\mu u} \end{pmatrix}$$

  Therefore,

  $$\begin{aligned} K_{y\mu}(0, \mu_1) = \langle v_0^*, dF_\mu(v_0) \rangle &= \begin{pmatrix} 1 \\ -1 \end{pmatrix} \cdot \begin{pmatrix} 2f_{\mu u}(\mathbf{0}, \mu_1) - 2f_{\mu v}(\mathbf{0}, \mu_1) \\ f_{\mu v}(\mathbf{0}, \mu_1) - f_{\mu u}(\mathbf{0}, \mu_1) \end{pmatrix} \\ &= 3(f_{\mu u}(\mathbf{0}, \mu_1) - f_{\mu v}(\mathbf{0}, \mu_1)) \end{aligned}$$

  which is nonzero if $f_{\mu u}(\mathbf{0}, \mu_1) \neq f_{\mu v}(\mathbf{0}, \mu_1)$.

- **Computation of** $K_{yy}(0, \mu_1)$**:**

  Since $v_0^* = (1, -1)$,

  $$K_{yy}(0, \mu_1) = d^2F_1(v_0, v_0) - d^2F_2(v_0, v_0)$$

Now

$$\begin{aligned}
dF_1(v_0) &= \begin{pmatrix} f_u \\ 2f_v \end{pmatrix} \cdot \begin{pmatrix} 2 \\ -1 \end{pmatrix} = 2f_u(x_1, \overline{x_2, x_2}, \mu) - 2f_v(x_1, \overline{x_2, x_2}, \mu) \\
d^2F_1(v_0, v_0) &= \begin{pmatrix} 2f_{uu} - 2f_{vu} \\ 4f_{uv} - 4f_{vv} \end{pmatrix} \cdot \begin{pmatrix} 2 \\ -1 \end{pmatrix} \\
&= 4f_{uu}(\mathbf{0}, \mu_1) - 8f_{uv}(\mathbf{0}, \mu_1) + 4f_{vv}(\mathbf{0}, \mu_1) \\
dF_2(v_0) &= \begin{pmatrix} f_v \\ f_u + f_v \end{pmatrix} \cdot \begin{pmatrix} 2 \\ -1 \end{pmatrix} = f_v(x_2, \overline{x_2, x_1}, \mu) - f_u(x_2, \overline{x_2, x_1}, \mu) \\
d^2F_2(v_0, v_0) &= \begin{pmatrix} f_{vv} - f_{uv} \\ f_{vu} + f_{vv} - f_{uu} - f_{uv} \end{pmatrix} \cdot \begin{pmatrix} 2 \\ -1 \end{pmatrix} \\
&= f_{vv}(\mathbf{0}, \mu_1) - 2f_{uv}(\mathbf{0}, \mu_1) + f_{uu}(\mathbf{0}, \mu_1)
\end{aligned}$$

Therefore, $K_{yy}(0, \mu_1) = 3(f_{uu}(\mathbf{0}, \mu_1) - 2f_{uv}(\mathbf{0}, \mu_1) + f_{vv}(\mathbf{0}, \mu_1))$, which is generically non-zero.

Therefore there is one transcritical branch bifurcating from the trivial solution. □

6.4 Network #3

Consider 2-cell network #3 with valency 2, whose adjacency matrix, its eigenvalues, and the corresponding eigenvectors are shown in Table 6.3.

Network #3	Adjacency matrix	Eigenvalues	Eigenvectors
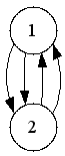	$\mathbf{A_3} = \begin{pmatrix} 0 & 2 \\ 2 & 0 \end{pmatrix}$	$\lambda_0 = 2$ $\lambda_1 = -2$	$(1, 1)$ $(1, -1)$

Table 6.3: Two-cell network #3

The admissible dynamical systems for this network have the form:

$$\begin{aligned}
\dot{x}_1 &= f(x_1, \overline{x_2, x_2}, \mu) \\
\dot{x}_2 &= f(x_2, \overline{x_1, x_1}, \mu)
\end{aligned}$$

The critical eigenvalue for synchrony-breaking is:

$$\begin{aligned}
& f_u(\mathbf{0}, \mu_1) \cdot 1 + f_v(\mathbf{0}, \mu_1) \cdot \lambda_1 = 0 \\
\Rightarrow \quad & f_u(\mathbf{0}, \mu_1) + f_v(\mathbf{0}, \mu_1) \cdot (-2) = 0 \\
\Rightarrow \quad & f_u(\mathbf{0}, \mu_1) = 2f_v(\mathbf{0}, \mu_1)
\end{aligned}$$

where μ_1 is determined by λ_1.

Therefore, the Jacobian is:

$$\begin{aligned} J &= f_u(\mathbf{0},\mu_1)I + f_v(\mathbf{0},\mu_1)A \\ &= f_v(\mathbf{0},\mu_1)(A+2I) \\ &= f_v(\mathbf{0},\mu_1)\begin{pmatrix} 2 & 2 \\ 2 & 2 \end{pmatrix} \end{aligned}$$

where $f_v(\mathbf{0},\mu_1) \neq 0$.

Theorem 6.3. *Assume that the coupled cell system defined by $f(u,\overline{v,w},\mu)$ associated to network #3 satisfies the following conditions:*

$$f_u(\mathbf{0},\mu_1) = 2f_v(\mathbf{0},\mu_1), \quad f_v(\mathbf{0},\mu_1) \neq 0, \quad f_{\mu u}(\mathbf{0},\mu_1) - 2f_{\mu v}(\mathbf{0},\mu_1) \neq 0, \quad A - 3B \neq 0.$$

where

$$\begin{aligned} A &= 2(f_{uuu}(\mathbf{0},\mu_1) - 6f_{uuv}(\mathbf{0},\mu_1) + 12f_{vvu}(\mathbf{0},\mu_1) - 8f_{vvv}(\mathbf{0},\mu_1)) \\ B &= \frac{(f_{uu}(\mathbf{0},\mu_1) - 4f_{uv}(\mathbf{0},\mu_1) + 4f_{vv}(\mathbf{0},\mu_1))}{2f_v(\mathbf{0},\mu_1)}(f_{uu}(\mathbf{0},\mu_1) - 4f_{vv}(\mathbf{0},\mu_1)) \end{aligned}$$

Then, a pitchfork branch bifurcates from the trivial solution $(x_1,x_2,\mu) = (0,0,\mu_1)$.

Proof. We apply Liapunov-Schmidt reduction to the system

$$F(X,\mu) = (F_1(X,\mu), F_2(X,\mu)) = 0$$

where $F_1(X,\mu) = f(x_1,\overline{x_2,x_2},\mu)$ and $F_2(X,\mu) = f(x_2,\overline{x_1,x_1},\mu)$.

The reduced equation has the form

$$K(y,\mu) = 0$$

where $y \in \mathbb{R}$, $K : \mathbb{R}\times\mathbb{R} \to \mathbb{R}$ is smooth, $K_y(0,\mu_1) = 0$, $K_\mu(0,\mu_1) = 0$ and $K(0,\mu_1) = 0$. We calculate each derivative of this reduced equation to determine which bifurcation occurs.

- **Obtaining $v_0 \in kerJ$ and $v_0^* \in (rangeJ)^\perp$:**

  Let (x,y) be any vector in $\mathbb{R}^2$.

  $$f_v(\mathbf{0},\mu_1)\begin{pmatrix} 2 & 2 \\ 2 & 2 \end{pmatrix}\begin{pmatrix} x \\ y \end{pmatrix} = f_v(\mathbf{0},\mu_1)\begin{pmatrix} 2(x+y) \\ 2(x+y) \end{pmatrix} = \begin{pmatrix} 0 \\ 0 \end{pmatrix} \quad \Rightarrow \begin{pmatrix} x \\ y \end{pmatrix} = \begin{pmatrix} 1 \\ -1 \end{pmatrix}$$

  Therefore $v_0 = (1,-1)$. Since $(1,1) \in rangeJ$, $v_0^* = (1,-1) \in (rangeJ)^\perp$.

- **Computation of $K_{y\mu}(0,\mu_1)$:**

$$F_\mu = (f_\mu(x_1, \overline{x_2, x_2}, \mu), f_\mu(x_2, \overline{x_1, x_1}, \mu))$$

$$dF_\mu(v_0) = \begin{pmatrix} f_{\mu u} & 2f_{\mu v} \\ 2f_{\mu v} & f_{\mu u} \end{pmatrix} \begin{pmatrix} 1 \\ -1 \end{pmatrix} = \begin{pmatrix} f_{\mu u} - 2f_{\mu v} \\ 2f_{\mu v} - f_{\mu u} \end{pmatrix}$$

Therefore

$$\begin{aligned} K_{y\mu}(0,\mu_1) = \langle v_0^*, dF_\mu(v_0)\rangle &= \begin{pmatrix} 1 \\ -1 \end{pmatrix} \cdot \begin{pmatrix} f_{\mu u} - 2f_{\mu v} \\ 2f_{\mu v} - f_{\mu u} \end{pmatrix} \\ &= 2f_{\mu u}(\mathbf{0},\mu_1) - 4f_{\mu v}(\mathbf{0},\mu_1) \end{aligned}$$

which is generically nonzero.

- **Computation of $K_{yy}(0,\mu_1)$:**

Since $v_0^* = (1,-1)$,

$$K_{yy}(0,\mu_1) = d^2F_1(v_0,v_0) - d^2F_2(v_0,v_0)$$

Now

$$\begin{aligned} dF_1(v_0) &= \begin{pmatrix} f_u \\ 2f_v \end{pmatrix} \cdot \begin{pmatrix} 1 \\ -1 \end{pmatrix} = f_u(x_1, \overline{x_2, x_2}, \mu) - 2f_v(x_1, \overline{x_2, x_2}, \mu) \\ d^2F_1(v_0,v_0) &= \begin{pmatrix} f_{uu} - 2f_{vu} \\ 2f_{uv} - 4f_{vv} \end{pmatrix} \cdot \begin{pmatrix} 1 \\ -1 \end{pmatrix} \\ &= f_{uu}(\mathbf{0},\mu_1) - 4f_{uv}(\mathbf{0},\mu_1) + 4f_{vv}(\mathbf{0},\mu_1) \\ dF_2(v_0) &= \begin{pmatrix} 2f_v \\ f_u \end{pmatrix} \cdot \begin{pmatrix} 1 \\ -1 \end{pmatrix} = 2f_v(x_2, \overline{x_1, x_1}, \mu) - f_u(x_2, \overline{x_1, x_1}, \mu) \\ d^2F_2(v_0,v_0) &= \begin{pmatrix} 4f_{vv} - 2f_{uv} \\ 2f_{vu} - f_{uu} \end{pmatrix} \cdot \begin{pmatrix} 1 \\ -1 \end{pmatrix} \\ &= 4f_{vv}(\mathbf{0},\mu_1) - 4f_{uv}(\mathbf{0},\mu_1) + f_{uu}(\mathbf{0},\mu_1) \end{aligned}$$

Therefore $K_{yy}(0,\mu_1) = 0$.

- **Computation of $K_{yyy}(0,\mu_1)$:**

We calculate $K_{yyy}(0,\mu_1)$ by first calculating

$$\begin{aligned} A &\equiv \langle v_0^*, d^3F(v_0,v_0,v_0)\rangle \\ B &\equiv \langle v_0^*, d^2F(v_0, J^{-1}Ed^2F(v_0,v_0))\rangle \end{aligned}$$

Since $v_0^* = (1,-1)$,

$$\begin{aligned} A &= d^3F_1(v_0,v_0,v_0) - d^3F_2(v_0,v_0,v_0) \\ B &= d^2F_1(v_0, J^{-1}Ed^2F(v_0,v_0)) - d^2F_2(v_0, J^{-1}Ed^2F(v_0,v_0)) \end{aligned}$$

Now

$$\begin{aligned} d^3F_1(v_0,v_0,v_0) &= \begin{pmatrix} f_{uuu}-4f_{uvu}+4f_{vvu} \\ 2f_{uuv}-8f_{uvv}+8f_{vvv} \end{pmatrix} \cdot \begin{pmatrix} 1 \\ -1 \end{pmatrix} \\ &= f_{uuu}(\mathbf{0},\mu_1)-6f_{uuv}(\mathbf{0},\mu_1)+12f_{vvu}(\mathbf{0},\mu_1)-8f_{vvv}(\mathbf{0},\mu_1) \\ d^3F_2(v_0,v_0,v_0) &= \begin{pmatrix} 8f_{vvv}-8f_{uvv}+2f_{uuv} \\ 4f_{vvu}-4f_{uvu}+f_{uuu} \end{pmatrix} \cdot \begin{pmatrix} 1 \\ -1 \end{pmatrix} \\ &= 8f_{vvv}(\mathbf{0},\mu_1)-12f_{uvv}(\mathbf{0},\mu_1)+6f_{uuv}(\mathbf{0},\mu_1)-f_{uuu}(\mathbf{0},\mu_1) \end{aligned}$$

Therefore, $A = 2(f_{uuu}(\mathbf{0},\mu_1)-6f_{uuv}(\mathbf{0},\mu_1)+12f_{vvu}(\mathbf{0},\mu_1)-8f_{vvv}(\mathbf{0},\mu_1))$.

To find B we need to know $J^{-1} : rangeJ \to M$ where M satisfies $\mathbb{R}^2 = kerJ \oplus M$. Now M and $rangeJ$ are spanned by $(1,1)$, so in this basis

$$J\begin{pmatrix} 1 \\ 1 \end{pmatrix} = f_v(\mathbf{0},\mu_1)\begin{pmatrix} 2 & 2 \\ 2 & 2 \end{pmatrix}\begin{pmatrix} 1 \\ 1 \end{pmatrix} = 4f_v(\mathbf{0},\mu_1)\begin{pmatrix} 1 \\ 1 \end{pmatrix}$$

Therefore, $J^{-1} = \frac{1}{4f_v(\mathbf{0},\mu_1)}$.

Given $v = (v_1,v_1) \in rangeJ$, $\overline{v} \in M$ has the form

$$\overline{v} = \frac{1}{4f_v(\mathbf{0},\mu_1)}(v_1,v_1)$$

Now

$$d^2F(v_0,v_0) = (a,a)$$

where $a = f_{uu}(\mathbf{0},\mu_1)-4f_{uv}(\mathbf{0},\mu_1)+4f_{vv}(\mathbf{0},\mu_1)$. Hence $d^2F(v_0,v_0) \in rangeJ$. Note that $E|_{rangeJ} = I$, so

$$u_0 = J^{-1}Ed^2F(v_0,v_0) = \frac{1}{4f_v(\mathbf{0},\mu_1)}(a,a)$$

Therefore

$$\begin{aligned} d^2F_1(v_0,u_0) &= \frac{1}{4f_v(\mathbf{0},\mu_1)}\begin{pmatrix} f_{uu}-2f_{vu} \\ 2f_{uv}-4f_{vv} \end{pmatrix}\begin{pmatrix} a \\ a \end{pmatrix} = \frac{a}{4f_v(\mathbf{0},\mu_1)}(f_{uu}(\mathbf{0},\mu_1)-4f_{vv}(\mathbf{0},\mu_1)) \\ d^2F_2(v_0,u_0) &= \frac{1}{4f_v(\mathbf{0},\mu_1)}\begin{pmatrix} 4f_{vv}-2f_{uv} \\ 2f_{uv}-f_{uu} \end{pmatrix}\begin{pmatrix} a \\ a \end{pmatrix} = \frac{a}{4f_v(\mathbf{0},\mu_1)}(4f_{vv}(\mathbf{0},\mu_1)-f_{uu}(\mathbf{0},\mu_1)) \end{aligned}$$

Hence

$$B = \frac{a}{2f_v(\mathbf{0},\mu_1)}(f_{uu}(\mathbf{0},\mu_1)-4f_{vv}(\mathbf{0},\mu_1))$$

Finally,

$$\begin{aligned} K_{yyy}(0,\mu_1) &= A - 3B \\ &= 2(f_{uuu}(\mathbf{0},\mu_1) - 6f_{uuv}(\mathbf{0},\mu_1) + 12f_{vvu}(\mathbf{0},\mu_1) - 8f_{vvv}(\mathbf{0},\mu_1)) \\ &\quad - \frac{3(f_{uu}(\mathbf{0},\mu_1) - 4f_{uv}(\mathbf{0},\mu_1) + 4f_{vv}(\mathbf{0},\mu_1))}{2f_v(\mathbf{0},\mu_1)}(f_{uu}(\mathbf{0},\mu_1) - 4f_{vv}(\mathbf{0},\mu_1)) \end{aligned}$$

which is generically non-zero.

Therefore, a pitchfork branch bifurcates from the trivial solution. □

6.5 Network #4

Consider 2-cell network #4 with valency 2, whose adjacency matrix, its eigenvalues, and the corresponding eigenvectors are shown in Table 6.4.

Network #4	Adjacency matrix	Eigenvalues	Eigenvectors
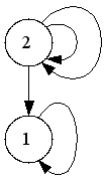	$\mathbf{A_4} = \begin{pmatrix} 1 & 1 \\ 0 & 2 \end{pmatrix}$	$\lambda_0 = 2$ $\lambda_1 = 1$	$(1,1)$ $(1,0)$

Table 6.4: Two-cell network #4

The admissible dynamical systems for this network have the form:

$$\dot{x}_1 = f(x_1, \overline{x_1, x_2}, \mu)$$
$$\dot{x}_2 = f(x_2, \overline{x_2, x_2}, \mu)$$

The critical eigenvalue for synchrony-breaking is:

$$\begin{aligned} & f_u(\mathbf{0},\mu_1)\cdot 1 + f_v(\mathbf{0},\mu_1)\cdot\lambda_1 = 0 \\ \Rightarrow\quad & f_u(\mathbf{0},\mu_1) + f_v(\mathbf{0},\mu_1) = 0 \\ \Rightarrow\quad & f_u(\mathbf{0},\mu_1) = -f_v(\mathbf{0},\mu_1) \end{aligned}$$

where μ_1 is determined by λ_1.

Therefore, we can obtain the Jacobian as follows :

$$\begin{aligned} J &= f_u(\mathbf{0},\mu_1)I + f_v(\mathbf{0},\mu_1)A \\ &= f_v(\mathbf{0},\mu_1)(A - I) \\ &= f_v(\mathbf{0},\mu_1)\begin{pmatrix} 0 & 1 \\ 0 & 1 \end{pmatrix} \end{aligned}$$

where $f_v(\mathbf{0},\mu_1) \neq 0$.

Theorem 6.4. *Assume that the coupled cell system defined by $f(u, \overline{v, w}, \mu)$ associated to network #4 satisfies the following conditions:*

$$f_u(\mathbf{0}, \mu_1) = -f_v(\mathbf{0}, \mu_1), \quad f_v(\mathbf{0}, \mu_1) \neq 0, \quad f_{\mu u}(\mathbf{0}, \mu_1) \neq -f_{\mu v}(\mathbf{0}, \mu_1),$$
$$f_{uu}(\mathbf{0}, \mu_1) + 2f_{uv}(\mathbf{0}, \mu_1) + f_{vv}(\mathbf{0}, \mu_1) \neq 0.$$

Then a transcritical branch bifurcates from the trivial solution $(x_1, x_2, \mu) = (0, 0, \mu_1)$.

Proof. We apply Liapunov-Schmidt reduction to the system

$$F(X, \mu) = (F_1(X, \mu), F_2(X, \mu)) = 0$$

where $F_1(X, \mu) = f(x_1, \overline{x_1, x_2}, \mu)$ and $F_2(X, \mu) = f(x_2, \overline{x_2, x_2}, \mu)$.

The reduced equation has the form

$$K(y, \mu) = 0$$

where $y \in \mathbb{R}$, $K : \mathbb{R} \times \mathbb{R} \to \mathbb{R}$ is smooth, $K_y(0, \mu_1) = 0$, $K_\mu(0, \mu_1) = 0$ and $K(0, \mu_1) = 0$. We calculate each derivative of this reduced equation to determine which bifurcation occurs.

- **Obtaining $v_0 \in kerJ$ and $v_0^* \in (rangeJ)^\perp$:**

  Let (x, y) be any vector in $\mathbb{R}^2$.

$$f_v(\mathbf{0}, \mu_1) \begin{pmatrix} 0 & 1 \\ 0 & 1 \end{pmatrix} \begin{pmatrix} x \\ y \end{pmatrix} = f_v(\mathbf{0}, \mu_1) \begin{pmatrix} y \\ y \end{pmatrix} = \begin{pmatrix} 0 \\ 0 \end{pmatrix} \quad \Rightarrow \begin{pmatrix} x \\ y \end{pmatrix} = \begin{pmatrix} 1 \\ 0 \end{pmatrix}$$

  Therefore $v_0 = (1, 0)$. Since $(1, 1) \in rangeJ$, $v_0^* = (1, -1) \in (rangeJ)^\perp$.

- **Computation of $K_{y\mu}(0, \mu_1)$:**

$$F_\mu = (f_\mu(x_1, \overline{x_1, x_2}, \mu), f_\mu(x_2, \overline{x_2, x_2}, \mu))$$

$$dF_\mu(v_0) = \begin{pmatrix} f_{\mu u} + f_{\mu v} & f_{\mu v} \\ 0 & f_{\mu u} + 2f_{\mu v} \end{pmatrix} \begin{pmatrix} 1 \\ 0 \end{pmatrix} = \begin{pmatrix} f_{\mu u} + f_{\mu v} \\ 0 \end{pmatrix}$$

  Therefore

$$\begin{aligned} K_{y\mu}(0, \mu_1) = \langle v_0^*, dF_\mu(v_0) \rangle &= \begin{pmatrix} 1 \\ -1 \end{pmatrix} \cdot \begin{pmatrix} f_{\mu u} + f_{\mu v} \\ 0 \end{pmatrix} \\ &= f_{\mu u}(\mathbf{0}, \mu_1) + f_{\mu v}(\mathbf{0}, \mu_1) \end{aligned}$$

  which is nonzero if $f_{\mu u}(\mathbf{0}, \mu_1) \neq -f_{\mu v}(\mathbf{0}, \mu_1)$.

- **Computation of $K_{yy}(0,\mu_1)$:**

  Since $v_0^* = (1,-1)$,

$$K_{yy}(0,\mu_1) = d^2F_1(v_0,v_0) - d^2F_2(v_0,v_0)$$

  Now

$$\begin{aligned}
dF_1(v_0) &= \begin{pmatrix} f_u + f_v \\ f_v \end{pmatrix} \cdot \begin{pmatrix} 1 \\ 0 \end{pmatrix} = f_u(x_1, \overline{x_1, x_2}, \mu) + f_v(x_1, \overline{x_1, x_2}, \mu) \\
d^2F_1(v_0,v_0) &= \begin{pmatrix} f_{uu} + f_{uv} + f_{vu} + f_{vv} \\ f_{uv} + f_{vv} \end{pmatrix} \cdot \begin{pmatrix} 1 \\ 0 \end{pmatrix} \\
&= f_{uu}(\mathbf{0},\mu_1) + 2f_{uv}(\mathbf{0},\mu_1) + f_{vv}(\mathbf{0},\mu_1) \\
dF_2(v_0) &= \begin{pmatrix} 0 \\ f_u + 2f_v \end{pmatrix} \cdot \begin{pmatrix} 1 \\ 0 \end{pmatrix} = 0 \\
d^2F_2(v_0,v_0) &= \begin{pmatrix} 0 \\ 0 \end{pmatrix} \cdot \begin{pmatrix} 1 \\ 0 \end{pmatrix} \\
&= 0
\end{aligned}$$

  Therefore $K_{yy}(0,\mu_1) = f_{uu}(\mathbf{0},\mu_1) + 2f_{uv}(\mathbf{0},\mu_1) + f_{vv}(\mathbf{0},\mu_1)$, which is generically non-zero.

Therefore there exists a transcritical branch bifurcating from the trivial solution. □

Alternatively, we can derive the same conditions using the. Implicit function theorem. Since $f(\mathbf{0},\mu_1) = 0$ and $f_u(\mathbf{0},\mu_1) = -f_v(\mathbf{0},\mu_1)$, the equation for cell 2 is:

$$\begin{aligned}
f(x_2, \overline{x_2, x_2}, \mu) &\approx f_v(\mathbf{0},\mu_1)x_2 \\
&\quad +2f_{uv}(\mathbf{0},\mu_1)x_2^2 + f_{vw}(\mathbf{0},\mu_1)x_2^2 + 2f_{v\mu}(\mathbf{0},\mu_1)x_2(\mu-\mu_1) \\
&\quad +f_{\mu u}(\mathbf{0},\mu_1)(\mu-\mu_1)x_2 + \frac{1}{2}(f_{uu}(\mathbf{0},\mu_1)x_2^2 + 2f_{vv}(\mathbf{0},\mu_1)x_2^2) + O(3)
\end{aligned}$$

Since $f_v(\mathbf{0},\mu_1) \neq 0$, the Implicit Function theorem implies that the equation for cell 2 has the unique solution $x_2 = 0$.

Substituting $x_2 = 0$ into the equation for cell 1 gives:

$$\begin{aligned}
f(x_1, \overline{0, x_1}, \mu) &\approx (f_u(\mathbf{0},\mu_1)x_1 + f_v(\mathbf{0},\mu_1)x_1) \\
&\quad +(f_{v\mu}(\mathbf{0},\mu_1)x_1(\mu-\mu_1) + f_{\mu u}(\mathbf{0},\mu_1)(\mu-\mu_1)x_1 + f_{uv}(\mathbf{0},\mu_1)x_1^2) \\
&\quad +\frac{1}{2}(f_{uu}(\mathbf{0},\mu_1)x_1^2 + f_{vv}(\mathbf{0},\mu_1)x_1^2) \\
&= x_1\{[\frac{1}{2}(f_{uu}(\mathbf{0},\mu_1) + f_{vv}(\mathbf{0},\mu_1)) + f_{uv}(\mathbf{0},\mu_1)]x_1 \\
&\quad +(f_{v\mu}(\mathbf{0},\mu_1) + f_{\mu u}(\mathbf{0},\mu_1))(\mu-\mu_1)\}
\end{aligned}$$

as $f_u(\mathbf{0},\mu_1) + f_v(\mathbf{0},\mu_1) = 0$.

Therefore, two roots of this equation are:

$$x_1 = 0, \quad x_1 = \frac{-\{(f_{v\mu}(\mathbf{0},\mu_1) + f_{\mu u}(\mathbf{0},\mu_1))(\mu - \mu_1)\}}{\frac{1}{2}(f_{uu}(\mathbf{0},\mu_1) + f_{vv}(\mathbf{0},\mu_1)) + f_{uv}(\mathbf{0},\mu_1)}$$

Therefore, if

$$\begin{aligned} f_{v\mu}(\mathbf{0},\mu_1) + f_{\mu u}(\mathbf{0},\mu_1) &\neq 0 \\ f_{uu}(\mathbf{0},\mu_1) + f_{vv}(\mathbf{0},\mu_1) + 2f_{uv}(\mathbf{0},\mu_1) &\neq 0 \end{aligned}$$

then a transcritical branch bifurcates from the trivial solution. This condition is the same as the one that we found by applying Liapunov-Schmidt reduction.

6.6 Network #5

Consider 2-cell network #5 with valency 2, whose adjacency matrix, its eigenvalues, and the corresponding eigenvectors are shown in Table 6.5.

Network #5	Adjacency matrix	Eigenvalues	Eigenvectors
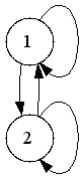	$\mathbf{A_5} = \begin{pmatrix} 1 & 1 \\ 1 & 1 \end{pmatrix}$	$\lambda_0 = 2$ $\lambda_1 = 0$	$(1,1)$ $(1,-1)$

Table 6.5: Two-cell network #5

The admissible dynamical systems for this network have the form:

$$\begin{aligned} \dot{x}_1 &= f(x_1, \overline{x_1, x_2}, \mu) \\ \dot{x}_2 &= f(x_2, \overline{x_1, x_2}, \mu) \end{aligned}$$

The critical eigenvalue for synchrony-breaking is:

$$\begin{aligned} & f_u(\mathbf{0},\mu_1)\cdot 1 + f_v(\mathbf{0},\mu_1)\cdot\lambda_1 = 0 \\ \Rightarrow \quad & f_u(\mathbf{0},\mu_1) + f_v(\mathbf{0},\mu_1)\cdot 0 = 0 \\ \Rightarrow \quad & f_u(\mathbf{0},\mu_1) = 0 \end{aligned}$$

where μ_1 is determined by λ_1.

Therefore, the Jacobian is :

$$\begin{aligned} J &= f_u(\mathbf{0},\mu_1)I + f_v(\mathbf{0},\mu_1)A \\ &= f_v(\mathbf{0},\mu_1)A \\ &= f_v(\mathbf{0},\mu_1)\begin{pmatrix} 1 & 1 \\ 1 & 1 \end{pmatrix} \end{aligned}$$

where $f_v(\mathbf{0},\mu_1) \neq 0$.

Theorem 6.5. *Assume that the coupled cell system defined by $f(u, \overline{v, w}, \mu)$ associated to network #5 satisfies the following conditions:*

$$f_u(\mathbf{0}, \mu_1) = 0, \quad f_v(\mathbf{0}, \mu_1) \neq 0, \quad f_{\mu u}(\mathbf{0}, \mu_1) \neq 0, \quad A - 3B \neq 0.$$

where

$$\begin{aligned} A &= 2f_{uuu}(\mathbf{0}, \mu_1) \\ B &= \frac{f_{uu}(\mathbf{0}, \mu_1)}{f_v(\mathbf{0}, \mu_1)}(f_{uu}(\mathbf{0}, \mu_1) + 2f_{uv}(\mathbf{0}, \mu_1)) \end{aligned}$$

Then a pitchfork branch bifurcates from the trivial solution $(x_1, x_2, \mu) = (0, 0, \mu_1)$.

Proof. We apply Liapunov-Schmidt reduction to the system

$$F(X, \mu) = (F_1(X, \mu), F_2(X, \mu)) = 0$$

where $F_1(X, \mu) = f(x_1, \overline{x_1, x_2}, \mu)$ and $F_2(X, \mu) = f(x_2, \overline{x_1, x_2}, \mu)$.

The reduced equation has the form

$$K(y, \mu) = 0$$

where $y \in \mathbb{R}$, $K : \mathbb{R} \times \mathbb{R} \to \mathbb{R}$ is smooth, $K_y(0, \mu_1) = 0$, $K_\mu(0, \mu_1) = 0$ and $K(0, \mu_1) = 0$. We calculate each derivative of this reduced equation to determine which bifurcation occurs.

- **Obtaining $v_0 \in kerJ$ and $v_0^* \in (rangeJ)^\perp$:**

  Let (x, y) be any vector in $\mathbb{R}^2$.

  $$f_v(\mathbf{0}, \mu_1) \begin{pmatrix} 1 & 1 \\ 1 & 1 \end{pmatrix} \begin{pmatrix} x \\ y \end{pmatrix} = f_v(\mathbf{0}, \mu_1) \begin{pmatrix} x + y \\ x + y \end{pmatrix} = \begin{pmatrix} 0 \\ 0 \end{pmatrix} \quad \Rightarrow \begin{pmatrix} x \\ y \end{pmatrix} = \begin{pmatrix} 1 \\ -1 \end{pmatrix}$$

  Therefore $v_0 = (1, -1)$. Since $(1, 1) \in rangeJ$, $v_0^* = (1, -1) \in (rangeJ)^\perp$.

- **Computation of $K_{y\mu}(0, \mu_1)$:**

  $$F_\mu = (f_\mu(x_1, \overline{x_1, x_2}, \mu), f_\mu(x_2, \overline{x_1, x_2}, \mu))$$

  $$dF_\mu(v_0) = \begin{pmatrix} f_{\mu u} + f_{\mu v} & f_{\mu v} \\ f_{\mu v} & f_{\mu u} + f_{\mu v} \end{pmatrix} \begin{pmatrix} 1 \\ -1 \end{pmatrix} = \begin{pmatrix} f_{\mu u} \\ -f_{\mu u} \end{pmatrix}$$

  Therefore

  $$\begin{aligned} K_{y\mu}(0) = \langle v_0^*, dF_\mu(v_0) \rangle &= \begin{pmatrix} 1 \\ -1 \end{pmatrix} \cdot \begin{pmatrix} f_{\mu u} \\ -f_{\mu u} \end{pmatrix} \\ &= 2f_{\mu u}(\mathbf{0}, \mu_1) \end{aligned}$$

  which is generically nonzero.

- **Computation of $K_{yy}(0,\mu_1)$:**

  Since $v_0^* = (1,-1)$,

$$K_{yy}(0,\mu_1) = d^2F_1(v_0,v_0) - d^2F_2(v_0,v_0)$$

  Now

$$\begin{aligned}
dF_1(v_0) &= \begin{pmatrix} f_u + f_v \\ f_v \end{pmatrix} \cdot \begin{pmatrix} 1 \\ -1 \end{pmatrix} = f_u(x_1, \overline{x_1, x_2}, \mu) \\
d^2F_1(v_0,v_0) &= \begin{pmatrix} f_{uu} + f_{uv} \\ f_{uv} \end{pmatrix} \cdot \begin{pmatrix} 1 \\ -1 \end{pmatrix} \\
&= f_{uu}(\mathbf{0},\mu_1) \\
dF_2(v_0) &= \begin{pmatrix} f_v \\ f_u + f_v \end{pmatrix} \cdot \begin{pmatrix} 1 \\ -1 \end{pmatrix} = -f_u(x_2, \overline{x_1, x_2}, \mu) \\
d^2F_2(v_0) &= \begin{pmatrix} -f_{uv} \\ -f_{uu} - f_{uv} \end{pmatrix} \cdot \begin{pmatrix} 1 \\ -1 \end{pmatrix} \\
&= f_{uu}(\mathbf{0},\mu_1)
\end{aligned}$$

  Therefore $K_{yy}(0,\mu_1) = 0$.

- **Computation of $K_{yyy}(0,\mu_1)$:**

  We calculate $K_{yyy}(0,\mu_1)$ by first calculating

$$\begin{aligned}
A &\equiv \langle v_0^*, d^3F(v_0,v_0,v_0)\rangle \\
B &\equiv \langle v_0^*, d^2F(v_0, J^{-1}Ed^2F(v_0,v_0))\rangle
\end{aligned}$$

  Since $v_0^* = (1,-1)$,

$$\begin{aligned}
A &= d^3F_1(v_0,v_0,v_0) - d^3F_2(v_0,v_0,v_0) \\
B &= d^2F_1(v_0, J^{-1}Ed^2F(v_0,v_0)) - d^2F_2(v_0, J^{-1}Ed^2F(v_0,v_0))
\end{aligned}$$

  Now

$$\begin{aligned}
d^3F_1(v_0,v_0,v_0) &= \begin{pmatrix} f_{uuu} + f_{uuv} \\ f_{uuv} \end{pmatrix} \cdot \begin{pmatrix} 1 \\ -1 \end{pmatrix} \\
&= f_{uuu}(\mathbf{0},\mu_1) \\
d^3F_2(v_0,v_0,v_0) &= \begin{pmatrix} f_{uuv} \\ f_{uuu} + f_{uuv} \end{pmatrix} \cdot \begin{pmatrix} 1 \\ -1 \end{pmatrix} \\
&= -f_{uuu}(\mathbf{0},\mu_1)
\end{aligned}$$

Therefore $A = 2f_{uuu}(\mathbf{0}, \mu_1)$.

To find B we need to know $J^{-1} : rangeJ \to M$ where M satisfies $\mathbb{R}^2 = kerJ \oplus M$. Now M and $rangeJ$ are spanned by $(1, 1)$, so in this basis

$$J\begin{pmatrix}1\\1\end{pmatrix} = f_v(\mathbf{0}, \mu_1)\begin{pmatrix}1 & 1\\ 1 & 1\end{pmatrix}\begin{pmatrix}1\\1\end{pmatrix} = 2f_v(\mathbf{0}, \mu_1)\begin{pmatrix}1\\1\end{pmatrix}$$

Therefore, $J^{-1} = \frac{1}{2f_v(\mathbf{0},\mu_1)}$.

Given $v = (v_1, v_1) \in rangeJ$, $\overline{v} \in M$ has the form

$$\overline{v} = \frac{1}{2f_v(\mathbf{0}, \mu_1)}(v_1, v_1)$$

Now

$$d^2F(v_0, v_0) = (a, a)$$

where $a = f_{uu}(\mathbf{0}, \mu_1)$. Hence $d^2F(v_0, v_0) \in rangeJ$. Note that $E|_{rangeJ} = I$, so

$$u_0 = J^{-1}Ed^2F(v_0, v_0) = \frac{1}{2f_v(\mathbf{0}, \mu_1)}(a, a)$$

Therefore,

$$\begin{aligned} d^2F_1(v_0, u_0) &= \frac{a}{2f_v(\mathbf{0}, \mu_1)}(f_{uu}(\mathbf{0}, \mu_1) + 2f_{uv}(\mathbf{0}, \mu_1)) \\ d^2F_2(v_0, u_0) &= \frac{a}{2f_v(\mathbf{0}, \mu_1)}(-f_{uu}(\mathbf{0}, \mu_1) - 2f_{uv}(\mathbf{0}, \mu_1)) \end{aligned}$$

Hence

$$B = \frac{a}{f_v(\mathbf{0}, \mu_1)}(f_{uu}(\mathbf{0}, \mu_1) + 2f_{uv}(\mathbf{0}, \mu_1))$$

Finally,

$$\begin{aligned} K_{yyy}(0, \mu_1) &= A - 3B \\ &= 2f_{uuu}(\mathbf{0}, \mu_1) - \frac{3f_{uu}(\mathbf{0}, \mu_1)}{f_v(\mathbf{0}, \mu_1)}(f_{uu}(\mathbf{0}, \mu_1) + 2f_{uv}(\mathbf{0}, \mu_1)) \end{aligned}$$

which is generically non-zero.

Therefore a pitchfork branch bifurcates from the trivial solution. □

6.7 Conclusions

We summarise the results in the following:

network	bifurcation type	generic conditions
#1 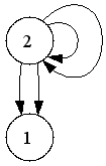	transcritical	$f_u(\mathbf{0},\mu_1)=0$, $f_v(\mathbf{0},\mu_1)\neq 0$, $f_{\mu u}(\mathbf{0},\mu_1)\neq 0$, $f_{uu}(\mathbf{0},\mu_1)\neq 0$
#2 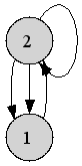	transcritical	$f_u(\mathbf{0},\mu_1)=f_v(\mathbf{0},\mu_1)$, $f_v(\mathbf{0},\mu_1)\neq 0$, $f_{\mu u}(\mathbf{0},\mu_1)\neq f_{\mu v}(\mathbf{0},\mu_1)$, $f_{uu}(\mathbf{0},\mu_1)-2f_{uv}(\mathbf{0},\mu_1)+f_{vv}(\mathbf{0},\mu_1)\neq 0$
#3 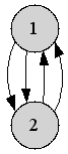	pitchfork	$f_u(\mathbf{0},\mu_1)=2f_v(\mathbf{0},\mu_1)$, $f_v(\mathbf{0},\mu_1)\neq 0$, $f_{\mu u}(\mathbf{0},\mu_1)-2f_{\mu v}(\mathbf{0},\mu_1)\neq 0$, $A-3B\neq 0$, where $A=2(f_{uuu}(\mathbf{0},\mu_1)-6f_{uuv}(\mathbf{0},\mu_1)+12f_{vvu}(\mathbf{0},\mu_1)-8f_{vvv}(\mathbf{0},\mu_1))$, $B=\frac{(f_{uu}(\mathbf{0},\mu_1)-4f_{uv}(\mathbf{0},\mu_1)+4f_{vv}(\mathbf{0},\mu_1))}{2f_v(\mathbf{0},\mu_1)}(f_{uu}(\mathbf{0},\mu_1)-4f_{vv}(\mathbf{0},\mu_1))$
#4 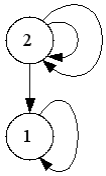	transcritical	$f_u(\mathbf{0},\mu_1)=-f_v(\mathbf{0},\mu_1)$, $f_v(\mathbf{0},\mu_1)\neq 0$, $f_{\mu u}(\mathbf{0},\mu_1)\neq -f_{\mu v}(\mathbf{0},\mu_1)$, $f_{uu}(\mathbf{0},\mu_1)+2f_{uv}(\mathbf{0},\mu_1)+f_{vv}(\mathbf{0},\mu_1)\neq 0$
#5 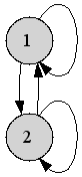	pitchfork	$f_u(\mathbf{0},\mu_1)=0$, $f_v(\mathbf{0},\mu_1)\neq 0$, $f_{\mu u}(\mathbf{0},\mu_1)\neq 0$, $A-3B\neq 0$, where $A=2f_{uuu}(\mathbf{0},\mu_1)$, $B=\frac{f_{uu}(\mathbf{0},\mu_1)}{f_v(\mathbf{0},\mu_1)}(f_{uu}(\mathbf{0},\mu_1)+2f_{uv}(\mathbf{0},\mu_1))$

Remark 6.1. *Strongly connected networks are shaded, namely networks #2, #3 and #5.*

Although networks #1 and #4 are topologically distinct, we expect their dynamical behaviour to be equivalent (They are called ODE-equivalent (Dias and Stewart, 2005)). Similarly, network #3 and #5 also have equivalent dynamical behaviour despite with their distinct topology.

Chapter 7

Steady-state Bifurcation Analysis using the Lattice

7.1 Introduction

In Chapter 4, we computed all balanced equivalence relations of any regular homogeneous coupled cell network $\mathcal{G}$, using just the adjacency matrix, and constructed a lattice, denoted by $\Lambda_{\mathcal{G}}$ in this chapter, that consists of these balanced equivalence relations. Each balanced equivalence relation $\bowtie \in \Lambda_{\mathcal{G}}$ is associated with a subspace $\triangle_{\bowtie} \subseteq P$, called the **balanced polydiagonal** corresponding to $\bowtie$. A coupled cell network restricted to this subspace $\triangle_{\bowtie}$ determines a quotient network $\mathcal{G}/_{\bowtie}$ whose dynamics correspond to synchronous dynamics of $\mathcal{G}$. In this Chapter, we firstly define two further lattices, $V_{\mathcal{G}}^P$ with balanced polydiagonals as elements, and $U_{\mathcal{G}}^P$ with sets of eigenvalues of quotient networks as elements. We show the three lattices for a given network in the following example.

Example 7.1. Consider regular homogeneous four-cell valency 2 network #326, denoted by $\mathcal{G}$. The associated adjacency matrix has four distinct (and therefore simple) eigenvalues, as shown in Table 7.1. There are two non-trivial quotient networks as shown in Figure 7.1. The three different lattices for $\mathcal{G}$ (discussed above) are shown in Figure 7.2. $\diamond$

We then show that there are lattice generators of $V_{\mathcal{G}}^P$ for any coupled cell network where the associated adjacency matrix has distinct eigenvalues. These lattice generators are constructed from the eigenvector structures of corresponding distinct eigenvalues. In Example 7.1, equivalence relations (the corresponding balanced polydiagonals) generated from eigenvectors $\mathbf{v}_1$ (or equivalently $\mathbf{v}_2$) and $\mathbf{v}_3$ are possible lattice generators. All other non-trivial lattice elements can be constructed by a join of lattice generators. All possible lattice structures for 3-cell and 4-cell regular homogeneous networks of any valency, but with simple eigenvalues, are constructed.

Network #326	Adjacency matrix	Eigenvalues	Eigenvectors
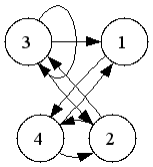	$\begin{pmatrix} 0 & 0 & 1 & 1 \\ 0 & 0 & 1 & 1 \\ 0 & 1 & 1 & 0 \\ 1 & 1 & 0 & 0 \end{pmatrix}$	$\lambda_0 = 2$ $\lambda_1 = \frac{-1-\sqrt{5}}{2}$ $\lambda_2 = \frac{-1+\sqrt{5}}{2}$ $\lambda_3 = 0$	$\mathbf{v}_0 = (1,1,1,1)$ $\mathbf{v}_1 = (\frac{-1-\sqrt{5}}{4}, \frac{-1-\sqrt{5}}{4}, \frac{-1+\sqrt{5}}{4}, 1)$ $\mathbf{v}_2 = (\frac{-1+\sqrt{5}}{4}, \frac{-1+\sqrt{5}}{4}, \frac{-1-\sqrt{5}}{4}, 1)$ $\mathbf{v}_3 = (-1,1,-1,1)$

Table 7.1: Four-cell valency 2 network #326, its adjacency matrix, eigenvalues and the corresponding eigenvectors.

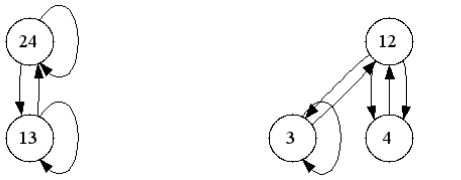

$\{2, 0\}$ $\{2, \frac{-1-\sqrt{5}}{2}, \frac{-1+\sqrt{5}}{2}\}$

Figure 7.1: Two quotient networks of four-cell valency 2 network #326. The sets of eigenvalues of each quotient network are shown.

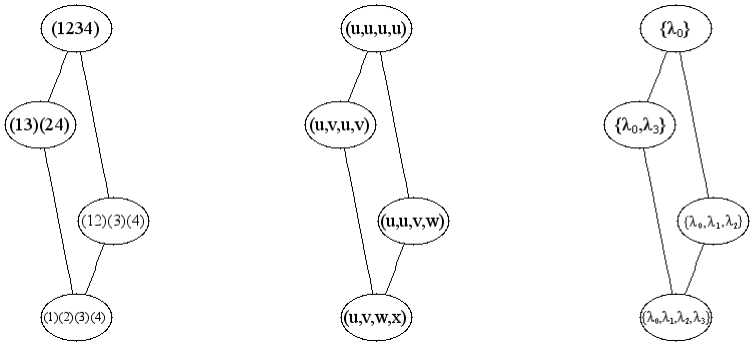

$\Lambda_{\mathcal{G}}$ $V_{\mathcal{G}}^P$ $U_{\mathcal{G}}^P$

Figure 7.2: Three different lattices for four-cell valency 2 network #326, here denoted as $\mathcal{G}$. Firstly $\Lambda_{\mathcal{G}}$, a lattice of balanced equivalence relations. Secondly $V_{\mathcal{G}}^P$, which depends on the total phase space P, consists of the balanced polydiagonals $\triangle_{\bowtie}$ corresponding to $\bowtie \in \Lambda_{\mathcal{G}}$. The third lattice $U_{\mathcal{G}}^P$ consists of the sets of eigenvalues of the adjacency matrices of the quotient networks $\mathcal{G}/_{\bowtie}$.

The lattice $U_{\mathcal{G}}^{P}$ has an important role in the determination of bifurcation branches as it shows where synchrony-breaking steady-state bifurcation occurs and in which polydiagonals bifurcating branches lie. Corollary 7.2 states that all quotient networks of a simple eigenvalue network are topologically distinct. Since an eigenspace corresponding to a simple eigenvalue is one-dimensional and the Jacobian evaluated at the bifurcation point is singular, this guarantees a unique bifurcating branch at a simple real eigenvalue. The bifurcation type is uniquely determined by a topologically distinct quotient network. The existence of synchrony-breaking steady-state bifurcation branches is shown schematically for 3 and 4-cell simple eigenvalue networks.

7.2 Preliminaries

7.2.1 Lattice Theory: Part 2

The following definitions are from Davey and Priestley (1990).

Definition 7.1. *Let $\langle P, \leq_P \rangle$ and $\langle Q, \leq_Q \rangle$ be ordered sets and let $f : P \to Q$ be a map. Then f is order-preserving if and only if for all $p_1, p_2 \in P$*

$$p_1 \leq_P p_2 \Rightarrow f(p_1) \leq_Q f(p_2)$$

Definition 7.2. *Let P and Q be ordered sets and let $\phi : P \to Q$ be a map. Then ϕ is an order-isomorphism if and only if*

1. *ϕ is order-preserving,*
2. *ϕ has an inverse ϕ^{-1},*
3. *ϕ^{-1} is order-preserving.*

The ordered sets P and Q are order-isomorphic if and only if there is an order-isomorphism $\phi : P \to Q$.

Definition 7.3. *Let P be an ordered set and let $Q \subseteq P$. Then*

1. *$a \in Q$ is the **greatest** element of Q if $a \geq x$ for every $x \in Q$.*
2. *$a \in Q$ is the **least** element of Q if $a \leq x$ for every $x \in Q$.*

Definition 7.4. *Let P be an ordered set. The greatest element of P, if it exists, is called the **top element** of P and written $\top$ ('top'). Similarly, the least element of P, if such exists, is called the **bottom element** and denoted $\bot$ ('bottom').*

For example, in regular homogeneous coupled cell networks, $\top = (x, \ldots, x) \subseteq \mathbb{R}^n$ and $\bot = P$.

Definition 7.5. *Let $\langle L, \leq \rangle$ be a lattice. A non-empty subset F of L is called a **filter** if*

1. *$x, y \in F$ imply $x \wedge y \in F$,*
2. *if $x \in F$ and $y \in L$ with $y \geq x$, then $y \in F$.*

(That is, F is closed under finite meets and closed under going up.)

7.3 Three Lattices: $\Lambda_{\mathcal{G}}$, $V_{\mathcal{G}}^P$ and $U_{\mathcal{G}}^P$

7.3.1 Lattice of Balanced Equivalence Relations and Polydiagonals

The following notations and definitions are from Stewart (2007).

Suppose that $\mathcal{G}$ is a coupled cell network with cells $\mathcal{C}$ and a choice of total phase space P. Let $M_{\mathcal{G}}$ be the complete lattice of all equivalence relations on $\mathcal{C}$. Associated with each equivalence relation $\bowtie \in M_{\mathcal{G}}$ is a polysynchronous subspace $\triangle_{\bowtie} \subseteq P$, called the **polydiagonal** corresponding to $\bowtie$.

Define $W_{\mathcal{G}}^P$ to be the set of all polydiagonals for this choice of P and $\mathcal{G}$. There is a bijection

$$\delta : M_{\mathcal{G}} \to W_{\mathcal{G}}^P \quad \delta(\bowtie) = \triangle_{\bowtie}$$

Lemma 7.1. *The map δ is a lattice anti-isomorphism, that is, an isomorphism that reverses order, and hence interchanges meet and join.*

Proof. See Stewart (2007). □

Let $\bowtie_1, \bowtie_2 \in M_{\mathcal{G}}$. Recall that $\bowtie_1$ refines $\bowtie_2$, denoted by $\bowtie_1 \prec \bowtie_2$, if and only if

$$c \bowtie_1 d \Rightarrow c \bowtie_2 d \quad \text{where} \quad c, d \in \mathcal{C}$$

That is, the partition of $\mathcal{C}$ defined by $\bowtie_1$ is finer than that defined by $\bowtie_2$ in the sense that for any $c \in \mathcal{C}$

$$[c]_1 \subseteq [c]_2$$

where $[c]_j$ is the $\bowtie_j$-equivalence class of c for $j = 1, 2$.

As in Lemma 7.1, forming polydiagonals reverses order:

$$\bowtie_1 \prec \bowtie_2 \Leftrightarrow \triangle_{\bowtie_1} \supset \triangle_{\bowtie_2}$$

Let $\Lambda_{\mathcal{G}}$ be the set of all balanced equivalence relations for $\mathcal{G}$, and denote the set of all balanced polydiagonals for $\mathcal{G}$ by $V_{\mathcal{G}}^P$. Then

$$\Lambda_{\mathcal{G}} \subseteq M_{\mathcal{G}} \quad V_{\mathcal{G}}^P \subseteq W_{\mathcal{G}}^P$$

Next, we define the rank of an element in $M_{\mathcal{G}}$ and the corresponding dimension of an element in $W_{\mathcal{G}}^P$ using an anti-isomorphism δ.

7.3.2 Rank and Dimension of a Partition Lattice

The rank is a parameter that indicates the *height* at which one can find an element in an ordered set (Schröder, 1990). We particularly consider the rank and corresponding dimension in a finite partition lattice.

Definition 7.6. *Let P be a finite partition lattice and let $n \in \mathbb{N}$. For $p \in P$, define the **rank** of p to be the number of equivalence classes in p. That is, if the partition p has n equivalence classes, then rank$(p) = n$.*

Since $M_{\mathcal{G}}$ is a finite partition lattice, the bijection δ lets us define the dimension of the corresponding element in $W_{\mathcal{G}}^P$ as in the following Theorem 7.1:

Theorem 7.1. *Let $\bowtie \in M_{\mathcal{G}}$ and let $\triangle_{\bowtie} \in W_{\mathcal{G}}^P$ be the corresponding polysynchronous subspace. Then*

$$dim(\triangle_{\bowtie}) = rank(\bowtie)$$

Proof. If rank$(\bowtie) = n$, then it means there are n equivalence classes in $\bowtie$. Since the subspace $\triangle_{\bowtie}$ is defined as:

$$\triangle_{\bowtie} = \{x \in P : c, d \in \mathcal{C} \quad \text{and} \quad c \bowtie d \Rightarrow x_c = x_d\}.$$

and $\delta(\bowtie) = \triangle_{\bowtie}$ by a bijection δ, $\triangle_{\bowtie}$ has n distinct components, $v_1, v_2, \ldots, v_n$. For each component v_i, $i = 1, 2, \ldots, n$, there is a natural basis vector which has either 1 for the position of v_i or 0 for the position of $v_j, j \neq i$ as elements. This leads that the n basis vectors complement each other, therefore, they are linearly independent. Hence, the n linearly independent vectors form a basis of $\triangle_{\bowtie}$. Therefore the dimension of $\triangle_{\bowtie}$ is n, which is the same as the rank of the corresponding equivalence relation $\bowtie$. □

7.3.3 Lattice of Eigenvalues of Adjacency Matrices of Quotient Networks

Any balanced equivalence relation $\bowtie$ on a network $\mathcal{G}$ determines a quotient network $\mathcal{G}/_{\bowtie}$ (Subsection 4.2.6) in which all cells of any equivalence class are identified. The dynamics of $\mathcal{G}/_{\bowtie}$ correspond to synchronous dynamics of $\mathcal{G}$; that is, dynamics restricted to $\triangle_{\bowtie}$.

The number of cells of a quotient network $\mathcal{G}/_{\bowtie}$ is the same as the dimension of $\triangle_{\bowtie} \in V_{\mathcal{G}}^P$, which is equal to the rank of $\bowtie \in \Lambda_{\mathcal{G}}^P$ by Theorem 7.1.

Lemma 7.2. *Let $\bowtie_1, \bowtie_2 \in \Lambda_{\mathcal{G}}$. If $\bowtie_1 \prec \bowtie_2$, then $\mathcal{G}/_{\bowtie_2}$ is a quotient network of $\mathcal{G}/_{\bowtie_1}$.*

Proof. By Lemma 7.1, $\bowtie_1 \prec \bowtie_2 \Leftrightarrow \triangle_{\bowtie_1} \supset \triangle_{\bowtie_2}$. Hence $\mathcal{G}/_{\bowtie_2}$ is a quotient network of $\mathcal{G}/_{\bowtie_1}$ restricted to a subspace $\triangle_{\bowtie_2}$ of $\triangle_{\bowtie_1}$. □

Now we construct a lattice of the sets of eigenvalues of adjacency matrices of quotient networks. In the following, we will define $L_{\bowtie}$ as the set of eigenvalues of the adjacency matrix of a quotient network $\mathcal{G}/_{\bowtie}$:

Definition 7.7. *Let $\mathcal{G}$ be an n-cell regular homogeneous coupled network associated with an $n \times n$ adjacency matrix A. Let $\mathcal{G}/_{\bowtie}$ be a k-cell quotient network of $\mathcal{G}$ restricted to a k-dimensional balanced polydiagonal $\triangle_{\bowtie} \in V_{\mathcal{G}}^P$ associated with a $k \times k$ adjacency matrix $A_{\bowtie}$. Define $L_{\bowtie}$ to be the set of eigenvalues of $A_{\bowtie}$ with k elements, including repeated eigenvalues.*

Next, we will define $U_{\mathcal{G}}^P$ as the set of sets $L_{\bowtie}$ as follows:

Definition 7.8. *Define $U_{\mathcal{G}}^P$ to be the set of all sets $L_{\bowtie}$ for all balanced equivalence relations $\bowtie \in \Lambda_{\mathcal{G}}$ on a regular homogeneous coupled cell network $\mathcal{G}$.*

Definition 7.9. *Let $\mathcal{G}$ be a regular homogeneous coupled cell network and let $\mathcal{G}/_{\bowtie}$ be the quotient network of $\mathcal{G}$ associated with a balanced equivalence relation $\bowtie$. Let $L_{\bowtie}$ be the set of eigenvalues of the adjacency matrix of $\mathcal{G}/_{\bowtie}$. We denote the number of distinct eigenvalues in $L_{\bowtie}$ by $|L_{\bowtie}|$.*

The following Lemma 7.3 shows an order in the set $U_{\mathcal{G}}^P$. It shows that the set of eigenvalues of the adjacency matrix $A_{\bowtie_2}$ is contained in the set of eigenvalues of the adjacency matrix $A_{\bowtie_1}$ if $\bowtie_1 \prec \bowtie_2$.

Lemma 7.3. *Let $A_{\bowtie_l}$ be the $k_l \times k_l$ adjacency matrix of a k_l-cell regular homogeneous coupled network $\mathcal{G}$ and let $L_{\bowtie_l}$ be the set of eigenvalues of $A_{\bowtie_l}$. If $\bowtie_l \prec \bowtie_m$, then $L_{\bowtie_l} \supset L_{\bowtie_m}$ for $l, m \in \mathbb{N}$.*

Proof. Without loss of generality, set $l = 1$ and $m = 2$. Since $\bowtie_1 \prec \bowtie_2$, we have $k_1 > k_2$. Let $\{\mathbf{v}_0, \ldots, \mathbf{v}_{k_2-1}\}$ be the basis vectors of $\triangle_{\bowtie_2}$ where $\mathbf{v}_i \in \mathbb{R}^{n \times 1}$, $i = 0, \ldots, k_2 - 1$ and $\mathbf{v}_0 = (1, 1, \ldots, 1)$ as every $\triangle_{\bowtie}$ is expressed as a sum with the fully synchronous eigenspace $\mathbf{R}\{(1, 1, \ldots, 1)\}$. Complete this basis with $\{\mathbf{v}_{k_2}, \ldots, \mathbf{v}_{k_1-1}\}$ for $\mathbb{R}^{n \times 1}$. Since $\triangle_{\bowtie_2}$ is invariant under $A_{\bowtie_1}$, $A_{\bowtie_1}$ with respect to the above basis has the structure:

$$A_{\bowtie_1} = \begin{pmatrix} A_{\bowtie_2} & B \\ \mathbf{0} & D \end{pmatrix}$$

where $A_{\bowtie_2}$ is a $k_2 \times k_2$ matrix which is the restriction of $A_{\bowtie_1}$ to $\triangle_{\bowtie_2}$. The matrix $A_{\bowtie_2}$ corresponds to the quotient network of $\mathcal{G}/_{\bowtie_1}$ by Lemma 7.2. Further, B is a $k_2 \times (k_1 - k_2)$ matrix and D is a $(k_1 - k_2) \times (k_1 - k_2)$ square matrix.

Since $A_{\bowtie_1}$ is upper triangular, the set of eigenvalues of $A_{\bowtie_1}$ is the union of the eigenvalues of the diagonal block matrices $A_{\bowtie_2}$ and D. Therefore the set of eigenvalues of $A_{\bowtie_2}$ is a subset of the set of eigenvalues of $A_{\bowtie_1}$, equivalently, $L_{\bowtie_1} \supset L_{\bowtie_2}$. □

Now, we show that there is an order-preserving map between $\Lambda_{\mathcal{G}}$ (equivalently, $V_{\mathcal{G}}^P$ using a bijection δ) and $U_{\mathcal{G}}^P$.

Proposition 7.1. *Let $V_{\mathcal{G}}^P$ be the set of all balanced polydiagonals of a regular homogeneous coupled cell network $\mathcal{G}$. Let $U_{\mathcal{G}}^P$ be a set of sets $L_{\bowtie}$ of quotient networks $\mathcal{G}/_{\bowtie}$ associated with for all $\triangle_{\bowtie} \in V_{\mathcal{G}}^P$. Then, there is a order-preserving map*

$$f : V_{\mathcal{G}}^P \to U_{\mathcal{G}}^P \quad f(\triangle_{\bowtie}) = L_{\bowtie}$$

Proof. Each balanced polydiagonal $\triangle_{\bowtie} \in V_{\mathcal{G}}^P$ generates a quotient network $\mathcal{G}/_{\bowtie}$. There is the corresponding adjacency matrix $A_{\bowtie}$ to a quotient network $\mathcal{G}/_{\bowtie}$. Let $\triangle_{\bowtie_1}, \triangle_{\bowtie_2} \in V_{\mathcal{G}}^P$ and $\triangle_{\bowtie_1} \subset_V \triangle_{\bowtie_2}$, then $\mathcal{G}/_{\bowtie_1}$ is a quotient network of $\mathcal{G}/_{\bowtie_2}$ restricted on $\triangle_{\bowtie_1}$. Hence, by the Lemma 7.3, $f(\triangle_{\bowtie_1}) \subset_U f(\triangle_{\bowtie_2})$. □

As a consequence, $U_{\mathcal{G}}^P$ forms a lattice.

7.4 Steady-state Bifurcation Analysis of Simple Eigenvalue Networks

So far we have discussed three different lattices, $\Lambda_{\mathcal{G}}$, $V_{\mathcal{G}}^P$ and $U_{\mathcal{G}}^P$, of a given network, regardless network's eigenvalue structure (simple eigenvalues or non-simple eigenvalues). For the rest of this Chapter, we consider only regular homogeneous networks where the associated adjacency matrices have distinct eigenvalues (which are therefore simple).

7.4.1 Simple Quotient Networks

Lemma 7.4. *Let $\mathcal{G}$ be an n-cell regular homogeneous coupled network with $n \times n$ adjacency matrix A, and let $\mathcal{G}/_{\bowtie}$ be the corresponding quotient network to $\bowtie$. Let $L_{\bowtie}$ be the set of eigenvalues of the adjacency matrix of $\mathcal{G}/_{\bowtie}$ and $U_{\mathcal{G}}^P$ be the lattice of $L_{\bowtie}$. If A has n distinct eigenvalues, then*

$$|L_{\bowtie}| = rank(\bowtie), \quad \forall L_{\bowtie} \in U_{\mathcal{G}}^P \tag{7.1}$$

Proof. By Lemma 7.3, it follows that the eigenvalues of the adjacency matrix $A_{\bowtie}$ of the quotient network $\mathcal{G}/_{\bowtie}$ are a subset of the eigenvalues of the adjacency matrix A of $\mathcal{G}$. Therefore, if A has n distinct eigenvalues, then $A_{\bowtie}$ has k distinct eigenvalues, where k is the size of the quotient network $\mathcal{G}/_{\bowtie}$; that is rank($\bowtie$). Hence,

$$|L_{\bowtie}| = \text{rank}(\bowtie), \quad \forall L_{\bowtie} \in U_{\mathcal{G}}^{P}$$

□

Proposition 7.2. *If the adjacency matrix of a regular homogeneous coupled cell network $\mathcal{G}$ has simple eigenvalues, then the adjacency matrices of all quotient networks $\mathcal{G}/_{\bowtie}$ also have simple eigenvalues.*

Proof. This follows from Lemma 7.3. □

7.4.2 Polysynchronous subspaces and Eigenvectors of A

Let $\mathbf{v} = (v)_{c\in\mathcal{C}}$ be an eigenvector of the adjacency matrix A of a regular homogeneous coupled cell network $\mathcal{G}$. For a given eigenvector $\mathbf{v}$, there is an equivalence relation associated with $\mathbf{v}$ as follows:

$$c \bowtie_{\mathbf{v}} d \Leftrightarrow v_c = v_d$$

The corresponding polydiagonal subspace is defined by

$$\triangle_{\bowtie_{\mathbf{v}}} = \{\mathbf{x} \in P : c \bowtie_{\mathbf{v}} d \Leftrightarrow x_c = x_d\}$$

Lemma 7.5. *Let $\mathbf{v} = (v)_{c\in\mathcal{C}}$ be an eigenvector of the adjacency matrix A of a regular homogeneous coupled cell network $\mathcal{G}$. For a given eigenvector $\mathbf{v}$ we have $\triangle \oplus \mathbb{R}\{\mathbf{v}\} \subseteq \triangle_{\bowtie_{\mathbf{v}}}$, where $\triangle = \mathbb{R}\{(1,\ldots,1)\}$ is the synchronous eigenspace.*

Proof. There is a unique coarsest (top) element $\bowtie_{\top} \in \Lambda_{\mathcal{G}}$ such that

$$c \bowtie_{\top} d \Leftrightarrow x_c = x_d \quad \text{for all} \quad c, d \in \mathcal{C} \tag{7.2}$$

and

$$\bowtie_i \prec \bowtie_{\top} \quad \text{for all} \quad \bowtie_i \in \Lambda_{\mathcal{G}}, i \neq \top \tag{7.3}$$

(7.3) implies that

$$\bowtie_{\mathbf{v}} \prec \bowtie_{\top} \quad \text{where} \quad \mathbf{v} \neq (1,\ldots,1) \tag{7.4}$$

The polydiagonal corresponding to the coarsest element is the smallest polydiagonal $\triangle = \mathbb{R}\{(1,\ldots,1)\}$ by (7.2).

By Lemma 7.1, forming polydiagonals reverses order, so by (7.4)

$$\bowtie_{\mathbf{v}} \prec \bowtie_{\top} \Leftrightarrow \triangle_{\bowtie_{\mathbf{v}}} \supset \triangle$$

Hence $\triangle \subset \triangle_{\bowtie_{\mathbf{v}}}$.

Since $c \bowtie_{\mathbf{v}} d \Leftrightarrow v_c = v_d$ for any given eigenvector $\mathbf{v}$, it easily follows that $\mathbb{R}\{\mathbf{v}\} \subseteq \triangle_{\bowtie_{\mathbf{v}}}$. Therefore, the direct sum $\triangle \oplus \mathbb{R}\{\mathbf{v}\}$ of the subspaces $\triangle$ and $\mathbb{R}\{\mathbf{v}\}$ is also a subspace in $\triangle_{\bowtie_{\mathbf{v}}}$, that is $\triangle \oplus \mathbb{R}\{\mathbf{v}\} \subseteq \triangle_{\bowtie_{\mathbf{v}}}$. □

Lemma 7.6. *Let $\mathcal{G}$ be an n-cell regular homogeneous coupled network with $n \times n$ adjacency matrix A. Let $\mathbf{v}$ be any eigenvector of A. If $\mathbf{v}$ has only two distinct entries, then $\triangle_{\bowtie_{\mathbf{v}}} = \triangle \oplus \mathbb{R}\{\mathbf{v}\}$.*

Proof. By Lemma 7.5, $\triangle \oplus \mathbb{R}\{\mathbf{v}\} \subseteq \triangle_{\bowtie_{\mathbf{v}}}$. Now we show that $\triangle \oplus \mathbb{R}\{\mathbf{v}\} \supseteq \triangle_{\bowtie_{\mathbf{v}}}$.

Writing the two distinct entries of $\mathbf{v}$ as $x, y \in \mathbb{R}$, where $x \neq y$, with a suitable ordering of cells we can express $\mathbf{v}$ as:

$$\mathbf{v} = (\underbrace{x, x, \ldots, x}_{k}, \underbrace{y, y, \ldots, y}_{n-k})$$

We now consider any polydiagonal $\mathbf{p} \in \triangle_{\bowtie_{\mathbf{v}}}$, which can be expressed as:

$$\mathbf{p} = (\underbrace{x', x', \ldots, x'}_{k}, \underbrace{y', y', \ldots, y'}_{n-k}), \quad \text{where} \quad x', y' \in \mathbb{R} \tag{7.5}$$

Now we express $\mathbf{p}$ as a sum of the form:

$$\mathbf{p} = a(\underbrace{1, 1, \ldots, 1}_{k}, \underbrace{1, 1, \ldots, 1}_{n-k}) + b(\underbrace{x, x, \ldots, x}_{k}, \underbrace{y, y, \ldots, y}_{n-k}) \tag{7.6}$$

Comparing coefficients in Equations (7.5) and (7.6)

$$\begin{aligned} a + bx &= x' \\ a + by &= y' \end{aligned}$$

These simultaneous equations can be solved for $a, b \in \mathbb{R}$ regardless of the values of x', y', and there is no contradiction. Hence any vector $\mathbf{p} \in \triangle_{\bowtie_{\mathbf{v}}}$ can be written as $\mathbf{q} + \mathbf{r}$, where $\mathbf{q} \in \triangle$ and $\mathbf{r} \in \mathbb{R}\{\mathbf{v}\}$, that is, $\triangle \oplus \mathbb{R}\{\mathbf{v}\} \supseteq \triangle_{\bowtie_{\mathbf{v}}}$. Therefore, $\triangle_{\bowtie_{\mathbf{v}}} = \triangle \oplus \mathbb{R}\{\mathbf{v}\}$. □

Since both eigenvectors and balanced polydiagonals are A-invariant, we expect there is a relationship between them. The following Lemma 7.7 shows that, for some cases, an equivalence relation associated with the eigenvector structure is balanced.

Lemma 7.7. *Let $\mathcal{G}$ be an n-cell homogeneous coupled network with $n \times n$ adjacency matrix A. Let $\mathbf{v}$ be any eigenvector of A. If $\mathbf{v}$ has only two distinct entries, then $\bowtie_{\mathbf{v}}$ is balanced.*

Proof. We show that $\triangle_{\bowtie_{\mathbf{v}}}$ is an A-invariant polydiagonal. This implies that the associated equivalence relation $\bowtie_{\mathbf{v}}$ is balanced.

If $\mathbf{v}$ has only two distinct entries, then by Lemma 7.6, the subspace $\triangle_{\bowtie_{\mathbf{v}}}$ generated by $\bowtie_{\mathbf{v}}$ is a direct sum of two eigenspaces:

$$\begin{aligned} \triangle_{\bowtie_{\mathbf{v}}} &= \mathbb{R}\{(1,1,\ldots,1)\} \oplus \mathbb{R}\{\mathbf{v}\} \\ &= \triangle \oplus \mathbb{R}\{\mathbf{v}\} \end{aligned}$$

Since both $(1,1,\ldots,1)$ and $\mathbf{v}$ are eigenvectors of A, the direct sum of these eigenspaces, that is $\triangle_{\bowtie_{\mathbf{v}}}$, is A invariant. Hence $A(\triangle_{\bowtie_{\mathbf{v}}}) \subseteq \triangle_{\bowtie_{\mathbf{v}}}$ and the associated equivalence relation $\bowtie_{\mathbf{v}}$ is balanced.

□

However, if $\mathbf{v}$ has more than two distinct entries, polydiagonals generated by eigenvector structures are not always balanced, as the following example shows.

Example 7.2. Consider strongly connected four-cell regular homogeneous network #295 with the associated 4×4 adjacency matrix A shown in Figure 7.3:

Network #295 Adjacency matrix A

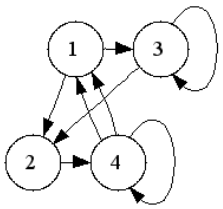

$$A = \begin{pmatrix} 0 & 0 & 0 & 2 \\ 1 & 0 & 1 & 0 \\ 1 & 0 & 1 & 0 \\ 0 & 1 & 0 & 1 \end{pmatrix}$$

Figure 7.3: Strongly connected four-cell network #295 with the associated adjacency matrix.

The admissible ODEs associated with this network are those of the form:

$$\begin{aligned} \dot{x_1} &= f(x_1, \overline{x_4, x_4}) \\ \dot{x_2} &= f(x_2, \overline{x_1, x_3}) \\ \dot{x_3} &= f(x_3, \overline{x_1, x_3}) \\ \dot{x_4} &= f(x_4, \overline{x_2, x_4}) \end{aligned}$$

The table below shows eigenvalues and corresponding eigenvectors of the adjacency matrix. The last column shows predicted balanced equivalence relations from the eigenvector structures:

Eigenvalues	Eigenvectors	Partition	Polysynchronous subspace
$\mu_0 = 2$	$\mathbf{v}_0 = (1, 1, 1, 1)$	$\{1, 2, 3, 4\}$	$\{x, x, x, x\}$
$\mu_1 = 0$	$\mathbf{v}_1 = (1, 0, -1, 0)$	$\{1\}, \{3\}, \{2, 4\}$	$\{x, y, z, y\}$
$\mu_2 = i$	$\mathbf{v}_2 = (-2i, -1 + i, -1 + i, 1)$	$\{1\}, \{2, 3\}, \{4\}$	$\{x, y, y, z\}$
$\mu_3 = -i$	$\mathbf{v}_3 = (2i, -1 - i, -1 - i, 1)$	$\{1\}, \{2, 3\}, \{4\}$	$\{x, y, y, z\}$

Now we show that the second equivalence relation $\bowtie$ is not balanced, therefore, the corresponding polysynchronous subspace $\triangle_{\bowtie} = (x, y, z, y)$ is not robust.

The projection map $P_{\bowtie}$ on $\triangle_{\bowtie}$ is:

$$P_{\bowtie} = \begin{pmatrix} 1 & 0 & 0 & 0 \\ 0 & 1 & 0 & 0 \\ 0 & 0 & 1 & 0 \\ 0 & 1 & 0 & 0 \end{pmatrix}.$$

Then

$$\begin{aligned} P_{\bowtie} A P_{\bowtie} &= P_{\bowtie} (A P_{\bowtie}) \\ &= \begin{pmatrix} 1 & 0 & 0 & 0 \\ 0 & 1 & 0 & 0 \\ 0 & 0 & 1 & 0 \\ 0 & 1 & 0 & 0 \end{pmatrix} \left\{ \begin{pmatrix} 0 & 0 & 0 & 2 \\ 1 & 0 & 1 & 0 \\ 1 & 0 & 1 & 0 \\ 0 & 1 & 0 & 1 \end{pmatrix} \begin{pmatrix} 1 & 0 & 0 & 0 \\ 0 & 1 & 0 & 0 \\ 0 & 0 & 1 & 0 \\ 0 & 1 & 0 & 0 \end{pmatrix} \right\} \\ &= \begin{pmatrix} 1 & 0 & 0 & 0 \\ 0 & 1 & 0 & 0 \\ 0 & 0 & 1 & 0 \\ 0 & 1 & 0 & 0 \end{pmatrix} \left\{ \begin{pmatrix} 0 & 2 & 0 & 0 \\ 1 & 0 & 1 & 0 \\ 1 & 0 & 1 & 0 \\ 0 & 2 & 0 & 0 \end{pmatrix} \right\} \\ &= \begin{pmatrix} 0 & 2 & 0 & 0 \\ 1 & 0 & 1 & 0 \\ 1 & 0 & 1 & 0 \\ 1 & 0 & 1 & 0 \end{pmatrix} \end{aligned}$$

Therefore, $P_{\bowtie} A P_{\bowtie} \neq A P_{\bowtie}$ and, by Proposition 4.2, $\triangle_{\bowtie}$ is not A-invariant.

This means $\triangle_{\bowtie}$ is not a robust polysynchronous subspace, either. We verify this as follows.

$$A(\triangle_{\bowtie}) = \begin{pmatrix} 0 & 0 & 0 & 2 \\ 1 & 0 & 1 & 0 \\ 1 & 0 & 1 & 0 \\ 0 & 1 & 0 & 1 \end{pmatrix} \begin{pmatrix} x \\ y \\ z \\ y \end{pmatrix}$$

$$= \begin{pmatrix} 2y \\ x+z \\ x+z \\ 2y \end{pmatrix} \not\subseteq \triangle_{\bowtie}$$

Therefore, from Proposition 4.1, $\triangle_{\bowtie}$ is not robustly polysynchronous. ◇

Hence the eigenspaces do not directly specify balanced equivalence relations.

7.4.3 Order-Isomorphism between $V_{\mathcal{G}}^P$ and $U_{\mathcal{G}}^P$

In the following lemmas, we show that the three lattices $\Lambda_{\mathcal{G}}$, $V_{\mathcal{G}}^P$ and $U_{\mathcal{G}}^P$ are order-isomorphic if the associated regular homogeneous coupled cell networks has simple eigenvalues.

Lemma 7.8. *Let $\mathcal{G}$ be a regular homogeneous coupled cell network with adjacency matrix A, and suppose that A has simple eigenvalues. Then*

$$L_{\bowtie_1} = L_{\bowtie_2} \Leftrightarrow \triangle_{\bowtie_1} = \triangle_{\bowtie_2}$$

Proof. $\triangle_{\bowtie_1} = \triangle_{\bowtie_2} \Rightarrow L_{\bowtie_1} = L_{\bowtie_2}$ is trivial. We show the converse.

Let $\lambda_0, \ldots, \lambda_{n-1}$ be the distinct eigenvalues of A and $\mathbf{v}_0, \ldots, \mathbf{v}_{n-1}$ be the corresponding eigenvectors. Since $\mathbf{v}_0, \ldots, \mathbf{v}_{n-1}$ are linearly independent, $\{\mathbf{v}_0, \ldots, \mathbf{v}_{n-1}\}$ forms a basis of $\mathbb{R}^n$. Suppose the space $\mathbb{R}^n$ is decomposed into a direct sum of two subspaces, one of which is A-invariant. Consider two different decomposition of $\mathbb{R}^n$ as follows:

$$\mathbb{R}^n = \mathcal{L}_1 \dot{+} \mathcal{L}_2 \tag{7.7}$$

$$\mathbb{R}^n = \mathcal{L}'_1 \dot{+} \mathcal{L}'_2 \tag{7.8}$$

where $\triangle_{\bowtie_1} = \mathcal{L}_1$ and $\triangle_{\bowtie_2} = \mathcal{L}'_1$ are both A-invariant, but $\mathcal{L}_1 \neq \mathcal{L}'_1$.

It suffices to consider the case when $\dim(\mathcal{L}_1) = \dim(\mathcal{L}'_1)$, because if the dimensions of subspaces are different, the cardinalities of the sets $L_{\bowtie_1}$ and $L_{\bowtie_2}$ are different, so $L_{\bowtie_1} \neq L_{\bowtie_2}$.

Since $\mathcal{L}_1 \neq \mathcal{L}'_1$, there are two different bases for $\mathcal{L}_1$ and $\mathcal{L}'_1$ from $\{\mathbf{v}_0, \ldots, \mathbf{v}_{n-1}\}$ such as:

$$\mathcal{L}_1 = \text{span}\{\mathbf{v}_0, \mathbf{v}_2, \ldots, \mathbf{v}_{k-1}\} \quad \text{and} \quad \mathcal{L}_2 = \text{span}\{\mathbf{v}_k, \ldots, \mathbf{v}_{n-1}\} \tag{7.9}$$

$$\mathcal{L}'_1 = \text{span}\{\mathbf{v}'_0, \mathbf{v}'_2, \ldots, \mathbf{v}'_{k-1}\} \quad \text{and} \quad \mathcal{L}'_2 = \text{span}\{\mathbf{v}'_k, \ldots, \mathbf{v}'_{n-1}\} \tag{7.10}$$

in $\mathbb{R}^n$, where $k = \dim(\mathcal{L}_1) = \dim(\mathcal{L}'_1)$ and the first k elements constitute a basis in $\mathcal{L}_1$ and $\mathcal{L}'_1$, respectively with $\{\mathbf{v}_0, \ldots, \mathbf{v}_{k-1}\} \neq \{\mathbf{v'}_0, \ldots, \mathbf{v'}_{k-1}\}$.

Since $\mathcal{L}_1$ and $\mathcal{L}'_1$ are A-invariant, $A(\mathbf{v}_j) \in \mathcal{L}_1$ and $A(\mathbf{v'}_j) \in \mathcal{L}'_1$ for $j = 0, \ldots, k-1$. In general, we can write

$$A(\mathbf{v}_j) = \sum_{i=0}^{k-1} a_{ij}\mathbf{v}_i, \quad j = 0, \ldots, k-1.$$

Similarly,

$$A(\mathbf{v'}_j) = \sum_{i=0}^{k-1} a'_{ij}\mathbf{v'}_i, \quad j = 0, \ldots, k-1.$$

However,

$$A(\mathbf{v}_j) = \lambda_j\mathbf{v}_j, \quad j = 0, \ldots, k-1.$$

Similarly,

$$A(\mathbf{v'}_j) = \lambda'_j\mathbf{v'}_j, \quad j = 0, \ldots, k-1.$$

as $\mathbf{v}_j$ and $\mathbf{v'}_j$ are eigenvectors of A.

Hence the matrix $A = (a_{ij})_{i,j=1}^n$ with respect to the basis $\{\mathbf{v}_0, \mathbf{v}_2, \ldots, \mathbf{v}_{k-1}\}$ with its complement has the form,

$$A = \left(\begin{array}{ccc|c} \lambda_0 & \cdots & 0 & \\ \vdots & \ddots & \vdots & B \\ 0 & \cdots & \lambda_{k-1} & \\ \hline & \mathbf{0} & & D \end{array}\right).$$

Similarly, the matrix $A = (a_{ij})_{i,j=1}^n$ with respect to the basis $\{\mathbf{v}'_0, \mathbf{v}'_2, \ldots, \mathbf{v}'_{k-1}\}$ with its complement has the form

$$A = \left(\begin{array}{ccc|c} \lambda'_0 & \cdots & 0 & \\ \vdots & \ddots & \vdots & B' \\ 0 & \cdots & \lambda'_{k-1} & \\ \hline & \mathbf{0} & & D' \end{array}\right).$$

The upper-left $k \times k$ matrices are similar matrices to $A_{\bowtie_1}$ and $A_{\bowtie_2}$, respectively. Since $\{\mathbf{v}_0, \ldots, \mathbf{v}_{k-1}\} \neq \{\mathbf{v'}_0, \ldots, \mathbf{v'}_{k-1}\}$, the two sets of eigenvalues $L_{\bowtie_1} \neq L_{\bowtie_2}$ for quotient networks $\mathcal{G}/_{\bowtie_1}$ and $\mathcal{G}/_{\bowtie_2}$. Hence, if $\triangle_{\bowtie_1} \neq \triangle_{\bowtie_2}$ then $L_{\bowtie_1} \neq L_{\bowtie_2}$. Equivalently, if $L_{\bowtie_1} = L_{\bowtie_2}$ then $\triangle_{\bowtie_1} = \triangle_{\bowtie_2}$. $\square$

On the contrary, if the eigenvalues of A are not simple, there can be more than one balanced polydiagonal which gives the same set of eigenvalues for the quotient network. This is the reason why there is more than one topologically identical quotient network in the double and triple eigenvalue cases.

We now show the converse of Lemma 7.3 is true if the associated adjacency matrix of a given network has distinct eigenvalues.

Lemma 7.9. *Let A be the adjacency matrix of a regular homogeneous coupled cell network G with simple eigenvalues. If $L_{\bowtie_1} \supset L_{\bowtie_2}$, then $\bowtie_1 \prec \bowtie_2$.*

Proof. Let $|L_{\bowtie_1}| = k_1$. Since A has simple eigenvalues, there are k_1 distinct eigenvalues in $L_{\bowtie_1}$ and these eigenvalues correspond to k_1 linearly independent eigenvectors, $\mathbf{v}_1, \ldots, \mathbf{v}_{k_1}$. Hence the corresponding balanced polydiagonal $\triangle_{\bowtie_1}$ to the balanced equivalence relation $\bowtie_1$ is spanned by $\mathbf{v}_1, \ldots, \mathbf{v}_{k_1}$.

Since $L_{\bowtie_1} \supset L_{\bowtie_2}$, the corresponding balanced polydiagonal $\triangle_{\bowtie_2}$ to the balanced equivalence relation $\bowtie_2$ is spanned by some of the vectors $\mathbf{v}_1, \ldots, \mathbf{v}_{k_1}$. Hence $\triangle_{\bowtie_1} \supset \triangle_{\bowtie_2}$. Using an anti-isomorphism in Lemma 7.1, this implies $\bowtie_1 \prec \bowtie_2$. □

In Proposition 7.1, we showed that there exists an order-preserving map from $V_{\mathcal{G}}^P$ to $U_{\mathcal{G}}^P$. We now show that $V_{\mathcal{G}}^P$ (equivalently $\Lambda_{\mathcal{G}}$) and $U_{\mathcal{G}}^P$ are order-isomorphic if the adjacency matrices of networks have simple eigenvalues.

Lemma 7.10. *Let A be the adjacency matrix of a regular homogeneous coupled cell network $\mathcal{G}$. If A has simple eigenvalues, then there exist an order-isomorphism $f : V_{\mathcal{G}}^P \to U_{\mathcal{G}}^P$.*

Proof. In Proposition 7.1, we showed $f : V_{\mathcal{G}}^P \to U_{\mathcal{G}}^P$ is an order-preserving map for any Jordan normal forms of A. To show f is an order-isomorphism when A has simple eigenvalues, we show there exists $f^{-1} : U_{\mathcal{G}}^P \to V_{\mathcal{G}}^P$ and it is an order-preserving map.

Since each quotient network is uniquely determined by the corresponding balanced polydiagonal, for any $L_{\bowtie} \in U_{\mathcal{G}}^P$ there exists an element $\triangle_{\bowtie} \in V_{\mathcal{G}}^P$ such that $f(\triangle_{\bowtie}) = L_{\bowtie}$. Hence f is a surjection.

If A has simple eigenvalues, by Lemma 7.8, f is an injection. Therefore there exists $f^{-1} : U_{\mathcal{G}}^P \to V_{\mathcal{G}}^P$ since f is a bijection.

Now we show that $f^{-1} : U_{\mathcal{G}}^P \to V_{\mathcal{G}}^P$ is an order-preserving map. Let $L_{\bowtie_1} \supset L_{\bowtie_2}$ and let $\triangle_{\bowtie_1}$ and $\triangle_{\bowtie_2}$ be the corresponding balanced polydiagonals, respectively. We want to show that $\triangle_{\bowtie_1} \supset \triangle_{\bowtie_2}$.

By Lemma 7.9, if $L_{\bowtie_1} \supset L_{\bowtie_2}$, then $\bowtie_1 \prec \bowtie_2$. Using the anti-isomorphism in Lemma 7.1, $\triangle_{\bowtie_1} \supset \triangle_{\bowtie_2}$. □

7.4.4 Lattice Generators of Simple Eigenvalue Networks

In Subsection 7.4.2 we showed that the equivalence relation defined by an eigenvector is balanced if the eigenvector has only two distinct entries. However, an equivalence relation generated by an eigenvector which has more than two distinct entries is not always balanced. The following

Theorem 7.2 shows the condition

$$P_{\bowtie} A P_{\bowtie} = A P_{\bowtie}$$

where $P_{\bowtie}$ is a projection matrix onto a polydiagonal subspace $\triangle_{\bowtie}$, must be satisfied so that a given equivalence relation (equivalently the corresponding polydiagonal), which is generated by an eigenvector is balanced.

Theorem 7.2. *Let $\mathcal{G}$ be an n-cell regular homogeneous coupled network with $n \times n$ adjacency matrix A and total phase space $P = \mathbb{R}^n$. Let $V_{\mathcal{G}}^P$ be the set of all balanced polydiagonals for this choice of P and $\mathcal{G}$. If A has simple eigenvalues, then there exists a subset $\widetilde{V}_{\mathcal{G}}^P \subseteq V_{\mathcal{G}}^P$ such that all $\triangle_{\bowtie} \in \widetilde{V}_{\mathcal{G}}^P$ are generated by equivalence relations of eigenvectors of A.*

Proof. Let $\lambda_0 \neq \lambda_1 \neq \cdots \neq \lambda_{n-1}$ be the n distinct eigenvalues of A and let $\mathbf{v}_0, \cdots, \mathbf{v}_{n-1}$ be the corresponding eigenvectors, where $\mathbf{v}_0 = (1, 1, \ldots, 1)$ is associated with λ_0.

Since $\mathbf{v}_0, \cdots, \mathbf{v}_{n-1}$ are linearly independent, $\mathbb{R}^n$ can be decomposed as:

$$\mathbb{R}^n = \mathbb{R}\{\mathbf{v}_0\} \oplus \cdots \oplus \mathbb{R}\{\mathbf{v}_{n-1}\}$$

where $\mathbb{R}\{\mathbf{v}_i\} = \{k\mathbf{v}_i : k \in \mathbb{R}\}$ is the one-dimensional eigenspace spanned by $\mathbf{v}_i$.

For the equivalence relation $\bowtie_{\mathbf{v}_i}$ associated with $\mathbf{v}_i$, where $i = 1, \ldots, n-1$, the corresponding polydiagonal subspace is

$$\triangle_{\bowtie_{\mathbf{v}_i}} = \{\mathbf{x} \in P : c \bowtie_{\mathbf{v}_i} d \Leftrightarrow x_c = x_d\}$$

For $i = 1, \ldots, n-1$, consider the direct sum of a one-dimensional eigenspace $\mathbb{R}\{\mathbf{v}_i\}$ and the synchronous eigenspace $\mathbb{R}\{\mathbf{v}_0\}$:

$$\mathbb{R}\{\mathbf{v}_0\} \oplus \mathbb{R}\{\mathbf{v}_i\} = \{x + y : x \in \mathbb{R}\{\mathbf{v}_0\} \quad \text{and} \quad y \in \mathbb{R}\{\mathbf{v}_i\}\}$$

By Lemma 7.5, this direct sum is a subspace of the polydiagonal $\triangle_{\bowtie_{\mathbf{v}_i}}$.

Note that it is possible for different eigenspaces to be complements to $\mathbb{R}\{\mathbf{v}_0\}$ for the same polydiagonal. We let $\{\triangle_{\bowtie_{\mathbf{v}_1}}, \cdots, \triangle_{\bowtie_{\mathbf{v}_s}}\} \subseteq W_{\mathcal{G}}^P$, where $s \leq n-1$, be the set of distinct polydiagonals in $\{\triangle_{\bowtie_{\mathbf{v}_1}}, \cdots, \triangle_{\bowtie_{\mathbf{v}_{n-1}}}\}$.

Now, $\triangle_{\bowtie_{\mathbf{v}_i}}$ is invariant under A because this is the sum of two invariant subspaces. For $\triangle_{\bowtie_{\mathbf{v}_i}}$ to be a balanced polydiagonal, we need to check the following condition.

Theorem 4.4 states that $\triangle_{\bowtie}$ is a balanced polydiagonal if and only if $P_{\bowtie} A P_{\bowtie} = A P_{\bowtie}$, where $P_{\bowtie}$ is the projection on $\triangle_{\bowtie}$. Here, we define a projection map $\pi_{\mathcal{G}}$ of polydiagonals to itself such that

$$\pi_{\mathcal{G}}(\triangle_{\bowtie_{\mathbf{v}_i}}) = \begin{cases} \triangle_{\bowtie_{\mathbf{v}_i}} & \text{if} \quad P_{\bowtie} A P_{\bowtie} = A P_{\bowtie} \\ 0 & \text{otherwise} \end{cases}$$

and therefore

$$\text{range}(\pi_{\mathcal{G}}) = \widetilde{V}_{\mathcal{G}}^P \subseteq V_{\mathcal{G}}^P \subseteq W_{\mathcal{G}}^P$$

which is the set of balanced polydiagonals. Hence $\widetilde{V}_{\mathcal{G}}^P \subseteq V_{\mathcal{G}}^P$. □

We now define a corresponding balanced equivalence relation $\bowtie$ to a balanced polydiagonal $\triangle_{\bowtie}$. When $\pi_{\mathcal{G}}(\triangle_{\bowtie_{\mathbf{v}_i}}) \neq 0$, using δ^{-1}:

$$\delta^{-1} : \widetilde{V}_{\mathcal{G}}^P \to \widetilde{\Lambda}_{\mathcal{G}} \quad \delta^{-1}(\triangle_{\bowtie_{\mathbf{v}_i}}) = \bowtie_{\mathbf{v}_i}$$

where $\widetilde{\Lambda}_{\mathcal{G}} \subseteq \Lambda_{\mathcal{G}}$.

So far we have found generators for the lattice of balanced equivalence relations. Every lattice of balanced equivalence relations of regular homogeneous networks contains two trivial relations: all cells are equivalent and all cells are different. Therefore, we will construct the rest of non-trivial balanced equivalence relations in the lattice using these generators.

Lemma 7.11. *Let $\widetilde{V}_{\mathcal{G}}^P = \{\triangle_{\bowtie_1}, \ldots, \triangle_{\bowtie_s}\}$, where $s < n$, be the set of balanced polydiagonals generated from the eigenvectors of the $n \times n$ adjacency matrix A of a given n-cell regular homogeneous network $\mathcal{G}$. If A has simple eigenvalues, then all other non-trivial lattice elements of balanced polydiagonals (if they exist) are generated by $\langle \widetilde{V}_{\mathcal{G}}, \vee \rangle$ which satisfy*

$$dim(\triangle_{\bowtie}) = rank(\bowtie).$$

Proof. Let $\widetilde{U}_{\mathcal{G}}^P = \{L_{\bowtie_1}, \ldots, L_{\bowtie_s}\}$ be the set of eigenvalue sets. Each $L_{\bowtie}$ corresponds to the set of eigenvalues of the adjacency matrix of a quotient network $\mathcal{G}/_{\bowtie}$. Let $\mathcal{S} = \bigcup_{i=1}^s L_{\bowtie_i}$ which is the collection of eigenvalues correspond to the generators of $\widetilde{V}_{\mathcal{G}}^P$, and let $\mathcal{T} = \{\lambda_0, \ldots, \lambda_{n-1}\}$ be n distinct eigenvalues of A. If there exists a balanced polydiagonal $\triangle_{\bowtie} \in V_{\mathcal{G}}^P \setminus \widetilde{V}_{\mathcal{G}}^P$, then, by an order-isomorphism f, there are three cases for the corresponding set of eigenvalues $L_{\bowtie}$:

1. $L_{\bowtie} \notin \widetilde{U}_{\mathcal{G}}^P$ and $\exists \lambda \in L_{\bowtie}$ such that $\lambda \in \mathcal{T} \backslash \mathcal{S}$,
2. $L_{\bowtie} \in \widetilde{U}_{\mathcal{G}}^P$, but the corresponding $\triangle_{\bowtie} \notin \widetilde{V}_{\mathcal{G}}^P$,
3. $L_{\bowtie} \notin \widetilde{U}_{\mathcal{G}}^P$. $\forall \lambda \in L_{\bowtie}$, $\lambda \in \mathcal{S}$, but the corresponding $\triangle_{\bowtie} \notin \widetilde{V}_{\mathcal{G}}^P$.

The first case does not happen because the polydiagonal generated by $\lambda \in \mathcal{T} \setminus \mathcal{S}$ is not balanced. The second case also does not happen since, by Lemma 7.8, there is a one-to-one relationship between $L_{\bowtie}$ and $\triangle_{\bowtie}$.

Therefore, the third case is the only possibility. Since $\forall \lambda \in L_{\bowtie}$, $\lambda \in \mathcal{S}$, $L_{\bowtie}$ is generated by the join operation of elements in $\widetilde{U}_{\mathcal{G}}^P$ which satisfy $|L_{\bowtie}| = \text{rank}(\bowtie)$. Note that we can exclude the case of a meet operation as smaller sets of eigenvalues must have been found already in $\widetilde{U}_{\mathcal{G}}^P$.

Using an order-isomorphism f, the corresponding polydiagonal $\triangle_{\bowtie} \notin \widetilde{V}_{\mathcal{G}}^{P}$ is generated by the join operation of the corresponding elements in $\widetilde{V}_{\mathcal{G}}^{P}$ which satisfy $\dim(\triangle_{\bowtie}) = \text{rank}(\bowtie)$. This polydiagonal is the sum of balanced polydiagonals, firstly it is A-invariant. To be a balanced polydiagonal, this must satisfy

$$P_{\bowtie} A P_{\bowtie} = A P_{\bowtie}$$

where $P_{\bowtie}$ is projection onto $\triangle_{\bowtie}$.

Hence if there exists a polydiagonal $\triangle_{\bowtie} \notin \widetilde{V}_{\mathcal{G}}^{P}$, then it can be generated only by $\langle \widetilde{V}_{\mathcal{G}}, \vee \rangle$ which satisfy

$$\dim(\triangle_{\bowtie}) = \text{rank}(\bowtie).$$

□

Definition 7.10. *Define $V_{\vee}$ to be the set of balanced polydiagonals which are generated by the join operation applied to elements $\triangle_{\bowtie} \in \widetilde{V}_{\mathcal{G}}^{P}$.*

Theorem 7.3. *Let $\mathcal{G}$ be a regular homogeneous coupled cell network with adjacency matrix A and total phase space P. If the adjacency matrix A associated with the coupled cell network $\mathcal{G}$ has simple eigenvalues, then $V_{\mathcal{G}}^{P} = \left(\widetilde{V}_{\mathcal{G}}^{P} \cup V_{\vee}\right) \cup (\triangle \cup P)$.*

Proof. From Lemma 7.11, no other non-trivial balanced polydiagonals exist. Hence, the set of all non-trivial balanced polydiagonals is the union of the set of balanced polydiagonals generated by eigenvector structures (which is $\widetilde{V}_{\mathcal{G}}^{P}$) and the set of balanced polydiagonals generated by the join operation (which is $V_{\vee}$). Also $V_{\mathcal{G}}^{P}$ contains two trivial balanced polydiagonals $\triangle$ and P. Hence, $V_{\mathcal{G}}^{P} = \left(\widetilde{V}_{\mathcal{G}}^{P} \cup V_{\vee}\right) \cup (\triangle \cup P)$. □

Corollary 7.1. *Let $\mathcal{G}$ be a regular homogeneous coupled cell network with adjacency matrix A. Let $\widetilde{\Lambda}_{\mathcal{G}}$ be the set of balanced equivalence relations associated with eigenvectors of A. If the adjacency matrix A associated with the coupled cell network $\mathcal{G}$ has simple eigenvalues, then all other non-trivial balanced equivalence relations (if they exist) are generated by $\langle \widetilde{\Lambda}_{\mathcal{G}}, \wedge \rangle$.*

Proof. Applying the anti-isomorphism $\delta^{-1} : W_{\mathcal{G}}^{P} \to M_{\mathcal{G}}$ to $\widetilde{V}_{\mathcal{G}}^{P}$ gives:

$$\widetilde{\Lambda}_{\mathcal{G}} = \{\delta^{-1}(\triangle_{\bowtie}) : \forall \triangle_{\bowtie} \in \widetilde{V}_{\mathcal{G}}^{P}\}$$

Other non-trivial balanced equivalence relations, if they exist, correspond to $\delta^{-1}(\triangle_{\bowtie})$ where $\triangle_{\bowtie} \in V_{\vee}$. Since δ^{-1} interchanges meet and join, they are generated by the meet operation of elements in $\widetilde{\Lambda}_{\mathcal{G}}$. □

Network #297	Adjacency matrix	Eigenvalues	Eigenvectors
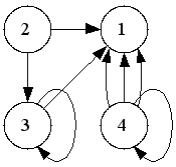	$\begin{pmatrix} 0 & 0 & 0 & 2 \\ 1 & 0 & 1 & 0 \\ 1 & 0 & 1 & 0 \\ 1 & 0 & 0 & 1 \end{pmatrix}$	2 1 0 -1	$(1,1,1,1)$ $(0,1,1,0)$ $(0,1,0,0)$ $(-2,1,1,1)$

Table 7.2: Four-cell network #297

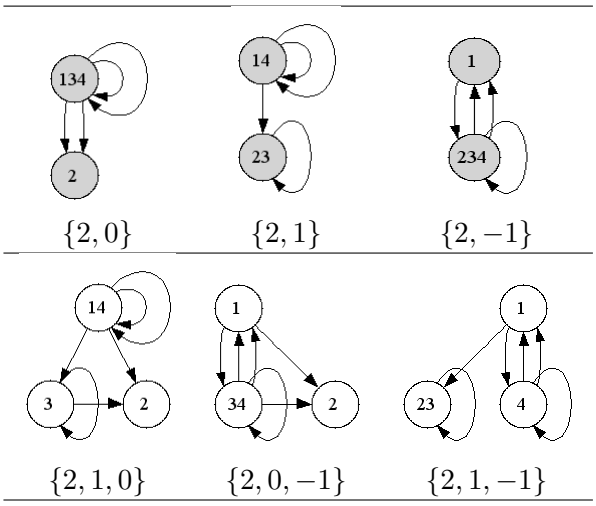

Figure 7.4: The six quotient networks and corresponding eigenvalues of four-cell network #297, where shaded networks are generated by non-trivial balanced equivalence relations associated with eigenvectors.

Example 7.3. Consider 4-cell valency 2 regular homogeneous network #297, whose adjacency matrix has simple eigenvalues (Table 7.2). This has six quotient networks shown in Figure 7.4, with their corresponding eigenvalues. The resulting lattice is shown in Figure 7.5.

◇

7.4.5 Existence of Bifurcating Branches

The above discussion is valid for real and complex simple eigenvalues. However, note that some statements below consider only simple real eigenvalues, since we restrict attention to synchrony-breaking steady-state bifurcations.

We now define the number of independent (distinct) eigenvalues in each $L_{\bowtie} \in U_{\mathcal{G}}^{P}$. These independent eigenvalues correspond to critical eigenvalues of the Jacobian of a coupled cell system. Bifurcation points are determined by these critical eigenvalues and there exist bifurcating branches either along the balanced polydiagonal $\triangle_{\bowtie}$ or outside these balanced polydiagonals.

First we define the number of independent eigenvalues for each element $p \in U_{\mathcal{G}}^{P}$. This

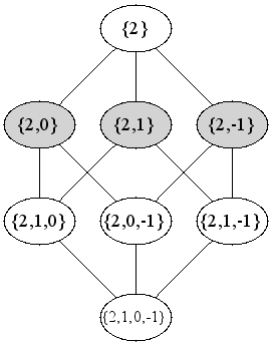

Figure 7.5: Lattice of the eigenvalues of quotient networks for four-cell network #297, where the shaded non-trivial lattice points are generated by eigenvectors.

number will be used for the construction of the minimum lattice of balanced polydiagonals.

Definition 7.11. *For $p \in U_{\mathcal{G}}^P$, define the number of independent eigenvalues $\eta(p) \in \mathbb{N}_0$ recursively as follows. Consider the filter with p as bottom element. If $p = \top$, define $\eta(p) := 1$. Let $\mathcal{F}(p)$ be the filter with bottom element p; that is $\mathcal{F}(p) = \{x | x \geq p, x \in U_{\mathcal{G}}^P\}$. Then define $\eta(p)$ by:*

$$\eta(p) = rank(p) - \sum_{e \in \mathcal{F}(p), e \neq p} \eta(e)$$

Proposition 7.3. *Let n be the number of cells in a regular homogeneous coupled cell network $\mathcal{G}$. Then*

$$\sum_{p \in U_{\mathcal{G}}^P} \eta(p) = n \tag{7.11}$$

where $\eta(p) := 1$ if $p = \top$ and $0 \leq \eta(p) \leq rank(p) - 1$ if $p \neq \top$.

Proof. This follows directly from the definition of $\eta(p)$. In fact, $\eta(p)$ counts the number of eigenvalues in a set of eigenvalues in $p = L_{\bowtie}$ which does not come from connecting higher lattice points. Since there are n eigenvalues (including repeated eigenvalues), $\sum_{p \in U_{\mathcal{G}}^P} \eta(p)$ sums to n. □

Example 7.4. Given the following lattice structure, we assign numbers $\eta(p)$ to each lattice point p as in Definition 7.11:

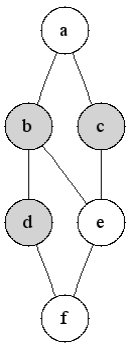

a = 1 since a is the top.
b = 2-1 = 1
c = 2-1 = 1
d = 3-(1+1)=1
e = 3-(1+1+1)=0
f = 4-(1+0+1+1+1)=0

◇

Lemma 7.12. *Let $\mathcal{G}$ be a coupled cell network with associated adjacency matrix A, which has simple real eigenvalues. Let $L_{\bowtie} \in U_{\mathcal{G}}^{P}$. If $\eta(L_{\bowtie}) \neq 0$, then there exists a unique synchrony-breaking steady-state bifurcating branch which lies in the corresponding balanced polydiagonal $\triangle_{\bowtie}$ and its bifurcation type is determined by the quotient network $\mathcal{G}/_{\bowtie}$.*

Proof. If $\eta(L_{\bowtie}) \neq 0$, then there exists an eigenvalue λ of A which determines a synchrony-breaking bifurcation point μ through the equation:

$$h(\mu) + \lambda k(\mu) = 0 \tag{7.12}$$

where h and k are functions of μ, determined by the linearised internal and external dynamics of the admissible vector field of $\mathcal{G}$, respectively. Therefore, synchrony-breaking bifurcation occurs at μ, where Equation (7.12) is satisfied with the derivative of a critical eigenvalue with respect to μ; that is $h'(\mu) + \lambda k'(\mu)$, is nonzero.

Since the centre eigenspace corresponding to λ (and μ) is one-dimensional, it is contained in the synchronous subspace $\triangle_{\bowtie}$ associated with the quotient network $\mathcal{G}/_{\bowtie}$. Moreover, the Jacobian evaluated at the bifurcation point, corresponding to a simple eigenvalue, is singular, therefore, there exists a unique synchrony-breaking bifurcating branch lying in $\triangle_{\bowtie}$. Finally, the type of generic bifurcation of the synchronous state in $\triangle_{\bowtie}$ is determined by the corresponding quotient network. □

For a specific eigenvector structure (eigenvectors with only two distinct entries), the existence of a unique synchrony-breaking bifurcating branch is guaranteed. The following Lemma is equivalent to the result shown in Wang and Golubitsky (2005) for lattice dynamical systems. This paper considers four types of planar lattice dynamical system. It shows that for a given balanced two-colouring in these lattice dynamical systems, there is a codimension one bifurcation from a synchronous equilibrium to a branch of equilibria with that two-colouring.

Lemma 7.13. *Let $\mathcal{G}$ be an n-cell regular homogeneous network and let the associated system of the form*

$$\dot{X} = F(X, \mu)$$

where $\mu \in \mathbb{R}$ is a bifurcation parameter. Assume that $F(\mathbf{0}, \mu) = \mathbf{0}$ for all μ. Let $\alpha A + \beta I$, where $\alpha, \beta \in \mathbb{R}$, be a linear admissible vector field of the system. Let $\mathbf{v}$ be an eigenvector of A that has only two distinct entries in $\mathbb{R}$. Then there exists a unique synchrony-breaking bifurcating branch bifurcating from the fully synchronous state $X = \mathbf{0}$ such that the bifurcating branch is in $\triangle_{\bowtie_\mathbf{v}}$, where $\triangle_{\bowtie_\mathbf{v}}$ is the polydiagonal generated by $\mathbf{v}$.

Proof. By Lemma 7.7, if $\mathbf{v}$ has only two distinct entries, the equivalence relation defined by $\mathbf{v}$ is always balanced. By Lemma 7.12, balanced equivalence relations determined by an eigenvector structures always have nonzero values for $\eta(p)$, and this guarantee the existence of a bifurcating branch from the fully synchronous state. The bifurcating branch is unique since this bifurcates at a simple eigenvalue. □

Let $\perp$ to be the bottom element in $U_\mathcal{G}^P$. Now:

$$\eta(\perp) = \dim(\ker(\pi_\mathcal{G})) + \#(\text{trivial polydiagonal} = P)$$

Therefore, $\eta(\perp)$ is equal to the number of non-balanced polydiagonals plus the trivial polydiagonal P. Now we define

Definition 7.12. *If $\eta(\perp) = 0$, we call the lattice $U_\mathcal{G}^P$ nondegenerate. If $\eta(\perp) \neq 0$, we call the lattice $U_\mathcal{G}^P$ degenerate.*

Theorem 7.4. *Let $\mathcal{G}$ be a regular homogeneous coupled cell network with adjacency matrix A, which has simple real eigenvalues. If $U_\mathcal{G}^P$ is nondegenerate, then synchrony-breaking steady-state bifurcations of a network $\mathcal{G}$ can be deduced solely from those quotient networks for which $\eta(L_\bowtie) \neq 0$. If $U_\mathcal{G}^P$ is degenerate, there may be bifurcating branches outside the balanced polydiagonals.*

Proof. If $U_\mathcal{G}^P$ is nondegenerate, by Lemma 7.12, all synchrony-breaking bifurcation points are determined by the simple eigenvalues of A and their bifurcation is determined by the corresponding quotient network.

If $U_\mathcal{G}^P$ is degenerate, there exists an eigenvalue λ of A where a synchrony-breaking bifurcation occurs; however, the centre eigenspace corresponding to λ is not in any synchronous subspace. Hence, there may be synchrony-breaking bifurcating branches outside the balanced polydiagonal. □

Theorem 7.5. *If $\mathcal{G}_1$ and $\mathcal{G}_2$ are n-cell regular homogeneous coupled cell networks and their adjacency matrices A_1 and A_2 are not similar (have different Jordan Normal Forms), then $\mathcal{G}_1 \ncong \mathcal{G}_2$; that is $\mathcal{G}_1$ and $\mathcal{G}_2$ are topologically distinct.*

Proof. Assume $\mathcal{G}_1 \cong \mathcal{G}_2$. Then there exists a permutation matrix P such that

$$PA_1P^{-1} = A_2$$

This means that A_1 and A_2 are similar. Equivalently, if A_1 and A_2 are not similar, then $\mathcal{G}_1 \ncong \mathcal{G}_2$. □

As a Corollary of Theorem 7.5, we prove that all quotient networks corresponding to elements in $U_{\mathcal{G}}^P$ are topologically distinct.

Corollary 7.2. *Let A be the $n \times n$ adjacency matrix associated with an n-cell regular homogeneous coupled cell network $\mathcal{G}$. Let $\triangle_{\bowtie} \in V_{\mathcal{G}}^P$ and let $\mathcal{G}/_{\bowtie}$ be the corresponding quotient network. If all eigenvalues of the adjacency matrix A are distinct, then all quotient networks $\mathcal{G}/_{\bowtie}$ are topologically distinct.*

Proof. Assume $\mathcal{G}/_{\bowtie_1} \cong \mathcal{G}/_{\bowtie_2}$ with $L_{\bowtie_1} \neq L_{\bowtie_1}$, consequently $\triangle_{\bowtie_1} \neq \triangle_{\bowtie_1}$. Then there exists a permutation matrix P such that

$$PA_{\bowtie_1}P^{-1} = A_{\bowtie_2}$$

where $A_{\bowtie_1}$ and $A_{\bowtie_2}$ are adjacency matrices of $\mathcal{G}/_{\bowtie_1}$ and $\mathcal{G}/_{\bowtie_2}$. This means that $A_{\bowtie_1}$ is similar to $A_{\bowtie_2}$. However, $A_{\bowtie_1}$ and $A_{\bowtie_2}$ have different sets of distinct eigenvalues (spectrums), therefore, they are not similar. This is contradiction. Hence there does not exist such a permutation matrix P, so $\mathcal{G}/_{\bowtie_1}$ and $\mathcal{G}/_{\bowtie_2}$ are topologically distinct. □

Therefore, quotient networks of regular homogeneous coupled cell networks with simple eigenvalues are all topologically different. Bifurcation types (e.g., transcritical, pitchfork) which lie in the corresponding polysynchronous subspaces are determined from the corresponding quotient networks.

7.4.6 Lattice Determination of 3 and 4-cell Networks with Simple Eigenvalues

Proposition 7.4. *Let $\mathcal{G}$ be a 3-cell regular homogeneous coupled cell network with any valency r, and let A be the corresponding 3×3 adjacency matrix. If A has 3 distinct eigenvalues, then there are just 3 possible lattice structures, shown in Figure 7.6, which satisfy Equation (7.11) in Proposition 7.3.*

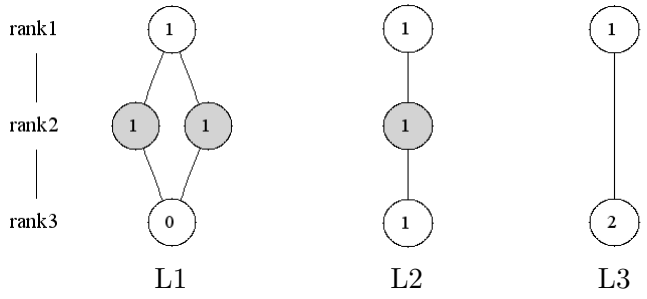

Figure 7.6: The three lattice structures for 3-cell networks with simple eigenvalues. The shaded lattice nodes are (non-trivial) lattice generators constructed from the eigenvector structures.

Proof. A lattice always has a top element $\top$ and a bottom element $\bot$, whose corresponding elements in $V_{\mathcal{G}}^P$ are the fully synchronous state $(1,\ldots,1)$ and total phase space P, respectively. The top element has $\eta(\top) = 1$ since, by Proposition 5.3, r is always an eigenvalue of homogeneous coupled cell networks, with eigenvector $(1,\ldots,1)$.

Equation (7.11) requires $\sum_{p\in U_{\mathcal{G}}^P} \eta(p) = 3$. The top element $\top$ contributes $\eta(\top) = 1$ to this sum, with the rest from the bottom element $\bot$ and any rank 2 elements. There are three possibilities for the rank 2 elements corresponding to the three lattice structures shown in Figure 7.6:

1. If there are two lattice elements of rank 2, then by Definition 7.11, $\eta(p) = 2-1 = 1$ for both these lattice elements, and $\eta(\bot) = 3-(1+1+1) = 0$. This leads to L1.

2. If there is one lattice element of rank 2 with $\eta(p) = 2-1 = 1$, then $\eta(\bot) = 3-(1+1) = 1$. This leads to L2.

3. If there is no lattice element of rank 2, then $\eta(\bot) = 3-1 = 2$. This leads to L3.

We can exclude the possibility of there being more than two rank 2 lattice elements, as these would each have $\eta(p) = 1$. It would then follow that $\eta(\bot) < 0$ which is invalid. □

Proposition 7.5. *Let $\mathcal{G}$ be a 4-cell regular homogeneous coupled cell network with any valency r, and let A be the corresponding 4×4 adjacency matrix. If A has 4 distinct eigenvalues, then the lattice of balanced equivalence relations must be one of the 14 structures shown in Figure 7.7.*

Proof. As in the proof of Proposition 7.4, a lattice always has a top element $\top$ with $\eta(\top) = 1$ and a bottom element $\bot$. To satisfy $\sum_{p\in U_{\mathcal{G}}^P} \eta(p) = 4$, there can be at most three lattice elements of rank 2. More than this would require $\eta(\bot) < 0$ which is invalid. We consider the following cases:

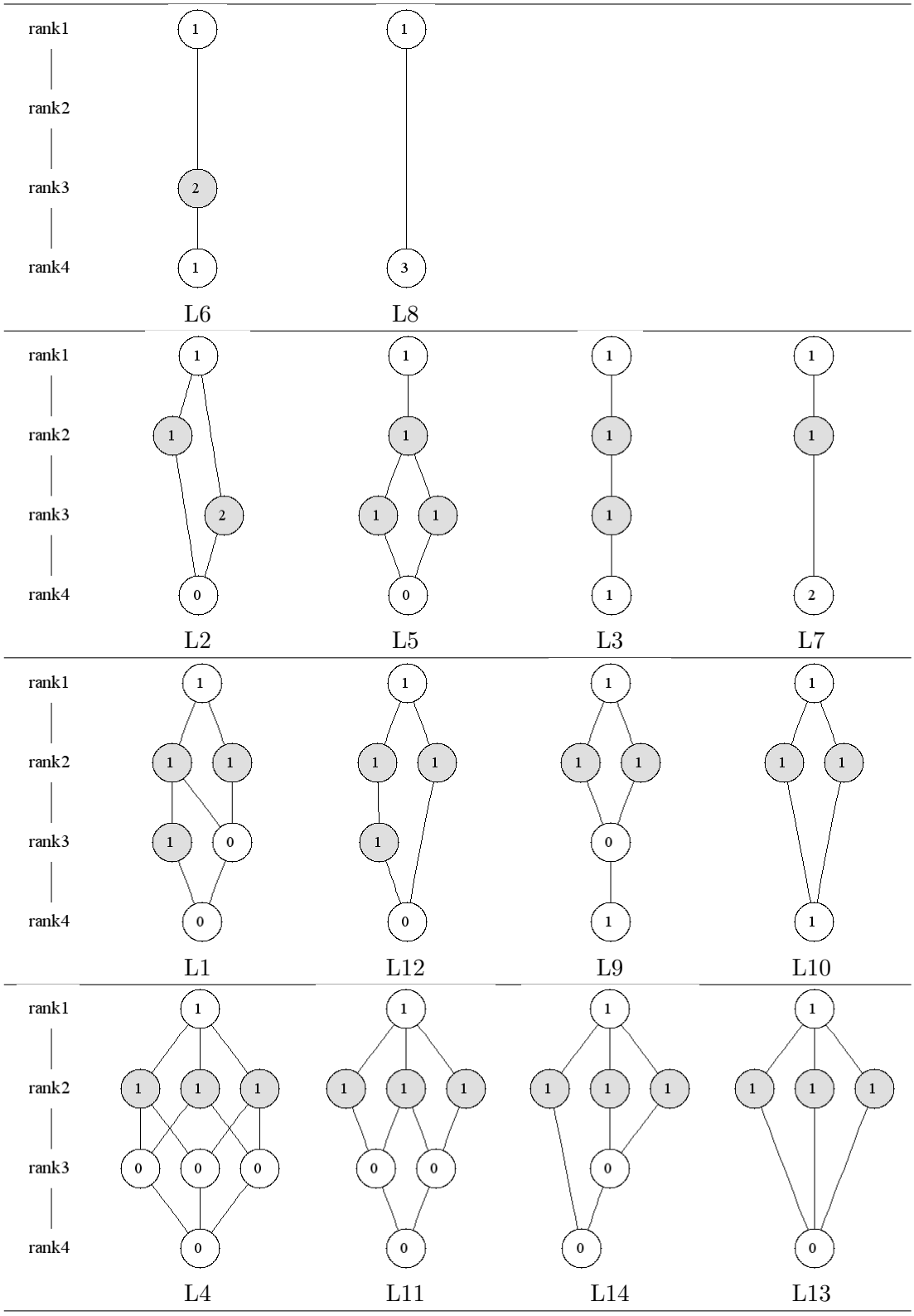

Figure 7.7: The 14 possible lattice structures for four-cell networks with simple eigenvalues. The number in each node p is $\eta(p)$. The shaded lattice nodes correspond to non-trivial balanced equivalence relations generated from the eigenvector structures (which are equivalently lattice generators).

1. **There are three lattice elements of rank 2:**

   All three lattice elements of rank 2 have $\eta(p) = 2 - 1 = 1$. Since $\sum \eta(p) = 4$ already, $\eta(\perp) = 0$ and $\eta(p) = 0$ for all other lattice elements, if they exist. Since lattices $\Lambda_{\mathcal{G}}$ and $U_{\mathcal{G}}^{P}$ are isomorphic, then by applying Corollary 7.1 to $\Lambda_{\mathcal{G}}$, we may consider all possible lattice elements as the result of a meet operation using the above three lattice elements as lattice generators.

   In order to satisfy $\eta(p) = 0$, any lattice element p of rank 3 must have exactly two edges from elements of rank 2. There are the following cases to consider:

   (a) If all possible intersections (as a result of a meet operation) of the three balanced equivalence relations of rank 2 are balanced, then there are three lattice elements of rank 3. This is labelled as $L4$.

   (b) If only two possible intersections of the three balanced equivalence relations are balanced, then this corresponds to $L11$.

   (c) If only one intersection of the three balanced equivalence relations is balanced, then this corresponds to $L14$.

   (d) If none of the intersections of the three balanced equivalence relations is balanced, then this leads to $L13$.

2. **There are two lattice elements of rank 2:**

   Two lattice elements of rank 2 have $\eta(p) = 2 - 1 = 1$. To satisfy $\sum \eta(p) = 4$, we have a lattice element with $\eta(p) = 1$ either of rank 3 or rank 4.

   (a) If there exists a lattice element of rank 3, this lattice must have one edge from a lattice element of rank 2, so that $\eta(p) = 3 - (1 + 1) = 1$. In this case there are two possibilities, as follows:

      i. If the intersection of two lattice elements of rank 2 is balanced with $\eta(p) = 0$, then this leads to $L1$.

      ii. If the intersection of two lattice elements of rank 2 is not balanced, then this leads to $L12$.

   (b) If there is no lattice element with $\eta(p) = 1$ of rank 3, then $\eta(\perp) = 4 - (1 + 1 + 1) = 1$. In this case, there are two possibilities:

      i. If the intersection of two lattice elements of rank 2 is balanced with $\eta(p) = 0$, then this leads to $L9$.

ii. If the intersection of two lattice elements of rank 2 is not balanced, then this leads to $L10$.

3. **There is one lattice element of rank 2:**

   One lattice element of rank 2 will have $\eta(p) = 2 - 1 = 1$.

   (a) If the total value of $\eta(p)$ is 2 for rank 3, then $\eta(\perp) = 4 - (1 + 1 + 2) = 0$. There are two possibilities for this case:

      i. If there is a lattice element of rank 3, which is directly connected to $\top$, then $\eta(p) = 3 - 1 = 2$. This corresponds to $L2$.

      ii. If there are two lattice elements of rank 3, each with a single edge from rank 2, then each of them has $\eta(p) = 3 - (1 + 1) = 1$. This leads to $L5$.

   (b) If there is only one lattice element with $\eta(p) = 3 - (1 + 1) = 1$ of rank 3, then $\eta(\perp) = 4 - (1 + 1 + 1) = 1$. This corresponds to $L3$.

   (c) Finally, if there is no lattice element of rank 3, then $\eta(\perp) = 4 - (1 + 1) = 2$. This corresponds to $L7$.

4. **There is no lattice element of rank 2:**

   If there exists a lattice element of rank 3, then $\eta(p) = 3 - 1 = 2$. In this case, $\eta(\perp) = 4 - (1 + 2) = 1$; that is $L6$. Otherwise, $\eta(\perp) = 4 - 1 = 3$ which leads to $L8$. Two or more lattice elements of rank 3 would contradict $\sum \eta(p) = 4$.

□

Remark 7.1. *There are two lattice structures which we can not observe in four-cell regular homogeneous networks of valency* 2*.*

(i) *Lattice structure* $L13$ *appears for the first time when the valency is* 3 *for the four-cell network shown in Figure 7.8.*

(ii) *The lattice structure* $L14$ *does not occur for any four-cell network of valency* ≤ 5*. We do not know whether it can occur for higher valency.*

The 14 lattice structures for four-cell regular homogeneous networks (Figure 7.7) are possible minimum lattice topologies and we can't reduce the lattice size any further. When an adjacency matrix has any repeated eigenvalues with algebraic multiplicity more than 1, the size of lattice would be larger – up to 15 nodes, and quotient networks corresponding to the nodes in the lattice are not isomorphic.

	Adjacency matrix	Eigenvalues
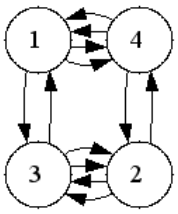	$\begin{pmatrix} 0 & 0 & 1 & 2 \\ 0 & 0 & 2 & 1 \\ 1 & 2 & 0 & 0 \\ 2 & 1 & 0 & 0 \end{pmatrix}$	$\begin{pmatrix} 3 \\ 1 \\ -1 \\ -3 \end{pmatrix}$

Figure 7.8: A four-cell network of valency 3 with lattice structure L13.

7.4.7 Example: Four-cell Simple Eigenvalue Network

We show an example which contrast the results from Liapunov-Schmidt reduction and from the lattice method for the determination of the existence of synchrony-breaking branches from a trivial solution. We also show an numerical analysis using a specific function form for Xppaut simulation in Example 7.6.

Example 7.5 *(The Existence of Branches from Liapunov-Schmidt Reduction).* Consider the following 4-cell valency 2 regular homogeneous network #10 (denoted by $\mathcal{G}$ for lattices). The associated adjacency matrix, its eigenvalues, and the corresponding eigenvectors are shown in Table 7.3.

Network #10	Adjacency matrix	Eigenvalues	Eigenvectors
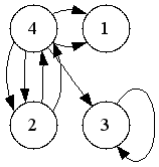	$\mathbf{A_{10}} = \begin{pmatrix} 0 & 0 & 0 & 2 \\ 0 & 0 & 0 & 2 \\ 0 & 0 & 1 & 1 \\ 0 & 2 & 0 & 0 \end{pmatrix}$	$\lambda_0 = 2$ $\lambda_1 = 1$ $\lambda_2 = 0$ $\lambda_3 = -2$	$(1,1,1,1)$ $(0,0,1,0)$ $(1,0,0,0)$ $(-3,-3,-1,3)$

Table 7.3: Four-cell network #10 of valency 2.

All balanced equivalence relation are computed and its lattice is shown as $\Lambda_{\mathcal{G}}$. Each balanced equivalence relation $\bowtie$ in $\Lambda_{\mathcal{G}}$ defines a balanced polydiagonal $\triangle_{\bowtie}$ and the admissible vector field restricted to $\triangle_{\bowtie}$ determines the quotient network $\mathcal{G}/_{\bowtie}$. The lattice of eigenvalues of quotient networks is defined as U_G^P. These lattices are shown in Figure 7.9.

The lattice $U_{\mathcal{G}}^P$ has L1 structure in Figure 7.7. Hence we expect to have three unique synchrony-breaking branches bifurcate from three distinct bifurcation points μ_1, μ_2 and μ_3. Each bifurcation type is determined by the corresponding quotient network and the bifurcating branch lies in the corresponding balanced polydiagonal. We now find nondegeneracy conditions for each synchrony-breaking bifurcating branch.

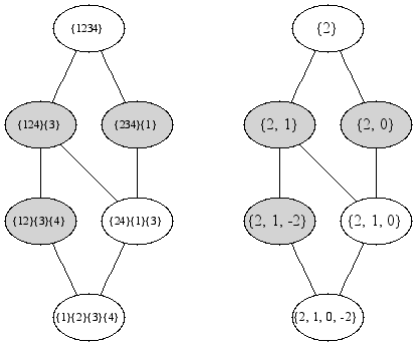

Figure 7.9: Lattices $\Lambda_{\mathcal{G}}$ and U_G^P of network #10. Shaded lattice nodes are generated by eigenvectors of A_{10}.

The admissible dynamical systems for this network have the form:

$$\begin{aligned}
\dot{x}_1 &= f(x_1, \overline{x_4, x_4}, \mu) \\
\dot{x}_2 &= f(x_2, \overline{x_4, x_4}, \mu) \\
\dot{x}_3 &= f(x_3, \overline{x_4, x_3}, \mu) \\
\dot{x}_4 &= f(x_4, \overline{x_2, x_2}, \mu)
\end{aligned}$$

where $\mu \in \mathbb{R}$ is a bifurcation parameter.

We apply Liapunov-Schmidt reduction to the system

$$F(X, \mu) = (F_1(X, \mu), F_2(X, \mu), F_3(X, \mu), F_4(X, \mu)) = \mathbf{0}$$

where $F_1(X, \mu) = f(x_1, \overline{x_4, x_4}, \mu)$, $F_2(X, \mu) = f(x_2, \overline{x_4, x_4}, \mu)$, $F_3(X, \mu) = f(x_3, \overline{x_4, x_3}, \mu)$, and $F_4(X, \mu) = f(x_4, \overline{x_2, x_2}, \mu)$.

The reduced equation obtained by applying Liapunov-Schmidt reduction has the form

$$K(y, \mu) = 0$$

where $y \in \mathbb{R}$, $K : \mathbb{R} \times \mathbb{R} \to \mathbb{R}$ is smooth.

The critical eigenvalue μ_i for synchrony-breaking associated with the eigenvalue λ_i, $i = 1, 2, 3$ is given by

$$f_u(\mathbf{0}, \mu_i) + \lambda_i f_v(\mathbf{0}, \mu_i)$$

Hence the Jacobian J is:

$$J = f_u(\mathbf{0}, \mu_i) \begin{pmatrix} 1 & 0 & 0 & 0 \\ 0 & 1 & 0 & 0 \\ 0 & 0 & 1 & 0 \\ 0 & 0 & 0 & 1 \end{pmatrix} + f_v(\mathbf{0}, \mu_i) \begin{pmatrix} 0 & 0 & 0 & 2 \\ 0 & 0 & 0 & 2 \\ 0 & 0 & 1 & 1 \\ 0 & 2 & 0 & 0 \end{pmatrix}$$

We calculate each derivative of the reduced equation to determine which bifurcation occurs at each synchrony-breaking bifurcation point. In the following, we assume that

$$f_{\mu u}(\mathbf{0}, \mu_i) + \lambda_i f_{\mu v}(\mathbf{0}, \mu_i) \neq 0 \tag{7.13}$$

at each bifurcation point μ_i[1].

1. **When $f_u(\mathbf{0}, \mu_1) = -f_v(\mathbf{0}, \mu_1)$:**

   Since $f_u(\mathbf{0}, \mu_1) = -f_v(\mathbf{0}, \mu_1)$, the Jacobian is:

$$J = f_v(\mathbf{0}, \mu_1)(A_{10} - I_4) = f_v(\mathbf{0}, \mu_1) \begin{pmatrix} -1 & 0 & 0 & 2 \\ 0 & -1 & 0 & 2 \\ 0 & 0 & 0 & 1 \\ 0 & 2 & 0 & -1 \end{pmatrix}$$

   where $f_v(\mathbf{0}, \mu_1) \neq 0$.

   - **Obtaining $\mathbf{v}_0 \in kerJ$ and $\mathbf{v}_0^* \in (rangeJ)^\perp$:**

     Let (x, y, z, w) be any vector in $\mathbb{R}^4$.

$$f_v(\mathbf{0}, \mu_1) \begin{pmatrix} -1 & 0 & 0 & 2 \\ 0 & -1 & 0 & 2 \\ 0 & 0 & 0 & 1 \\ 0 & 2 & 0 & -1 \end{pmatrix} \begin{pmatrix} x \\ y \\ z \\ w \end{pmatrix} = f_v(\mathbf{0}, \mu_1) \begin{pmatrix} -x + 2w \\ -y + 2w \\ w \\ 2y - w \end{pmatrix} = \begin{pmatrix} 0 \\ 0 \\ 0 \\ 0 \end{pmatrix}$$

$$\Rightarrow \quad \begin{pmatrix} x \\ y \\ z \\ w \end{pmatrix} = \begin{pmatrix} 0 \\ 0 \\ \alpha \\ 0 \end{pmatrix}$$

     where $\alpha \in \mathbb{R}$.

     Therefore, $\mathbf{v}_0 = (0, 0, 1, 0)$. By solving $\ker(J^t)$, we obtain $\mathbf{v}_0^* = (0, 2, -3, 1) \in (rangeJ)^\perp$.

   - **Computation of $K_{y\mu}(0, \mu_1)$:**

$$F_\mu = (f_\mu(x_1, \overline{x_4, x_4}, \mu), f_\mu(x_2, \overline{x_4, x_4}, \mu), f_\mu(x_3, \overline{x_4, x_3}, \mu), f_\mu(x_4, \overline{x_2, x_2}, \mu))$$

$$dF_\mu(\mathbf{v}_0) = \begin{pmatrix} f_{\mu u} & 0 & 0 & 2f_{\mu v} \\ 0 & f_{\mu u} & 0 & 2f_{\mu v} \\ 0 & 0 & f_{\mu u} + f_{\mu v} & f_{\mu v} \\ 0 & 2f_{\mu v} & 0 & f_{\mu u} \end{pmatrix} \begin{pmatrix} 0 \\ 0 \\ 1 \\ 0 \end{pmatrix} = \begin{pmatrix} 0 \\ 0 \\ f_{\mu u} + f_{\mu v} \\ 0 \end{pmatrix}$$

[1] This condition is actually satisfied as the same condition for $K_{\mu y}(0, \mu_i) \neq 0$.

Therefore,

$$\begin{aligned} K_{y\mu}(0,\mu_1) = \langle \mathbf{v}_0^*, dF_\mu(\mathbf{v}_0)\rangle &= \begin{pmatrix} 0 \\ 2 \\ -3 \\ 1 \end{pmatrix} \cdot \begin{pmatrix} 0 \\ 0 \\ f_{\mu u} + f_{\mu v} \\ 0 \end{pmatrix} \\ &= -3(f_{\mu u}(\mathbf{0},\mu_1) + f_{\mu v}(\mathbf{0},\mu_1)) \end{aligned}$$

which is generically nonzero if $f_{\mu u}(\mathbf{0},\mu_1) \neq -f_{\mu v}(\mathbf{0},\mu_1)$.

- **Computation of $K_{yy}(0,\mu_1)$:**

  Since $\mathbf{v}_0^* = (0,2,-3,1)$,

$$K_{yy}(0,\mu_1) = 2d^2F_2(\mathbf{v}_0,\mathbf{v}_0) - 3d^2F_3(\mathbf{v}_0,\mathbf{v}_0) + d^2F_4(\mathbf{v}_0,\mathbf{v}_0)$$

  Now

$$\begin{aligned} dF_1(\mathbf{v}_0) &= \begin{pmatrix} f_u \\ 0 \\ 0 \\ 2f_v \end{pmatrix} \cdot \begin{pmatrix} 0 \\ 0 \\ 1 \\ 0 \end{pmatrix} = 0 \\ d^2F_1(\mathbf{v}_0,\mathbf{v}_0) &= 0 \\ dF_2(\mathbf{v}_0) &= \begin{pmatrix} 0 \\ f_u \\ 0 \\ 2f_v \end{pmatrix} \cdot \begin{pmatrix} 0 \\ 0 \\ 1 \\ 0 \end{pmatrix} = 0 \\ d^2F_2(\mathbf{v}_0,\mathbf{v}_0) &= 0 \\ dF_3(\mathbf{v}_0) &= \begin{pmatrix} 0 \\ 0 \\ f_u + f_v \\ f_v \end{pmatrix} \cdot \begin{pmatrix} 0 \\ 0 \\ 1 \\ 0 \end{pmatrix} = f_u(x_3,\overline{x_3,x_4},\mu) + f_v(x_3,\overline{x_3,x_4},\mu) \\ d^2F_3(\mathbf{v}_0,\mathbf{v}_0) &= \begin{pmatrix} 0 \\ 0 \\ f_{uu} + 2f_{uv} + f_{vv} \\ f_{uv} + f_{vv} \end{pmatrix} \cdot \begin{pmatrix} 0 \\ 0 \\ 1 \\ 0 \end{pmatrix} = f_{uu} + 2f_{uv} + f_{vv} \end{aligned}$$

$$dF_4(\mathbf{v}_0) = \begin{pmatrix} 0 \\ 2f_v \\ 0 \\ f_u \end{pmatrix} \cdot \begin{pmatrix} 0 \\ 0 \\ 1 \\ 0 \end{pmatrix} = 0$$

$$d^2F_4(\mathbf{v}_0, \mathbf{v}_0) = 0$$

Therefore, $K_{yy}(0, \mu_1) = -3(f_{uu}(\mathbf{0}, \mu_1) + 2f_{uv}(\mathbf{0}, \mu_1) + f_{vv}(\mathbf{0}, \mu_1))$, which is generically nonzero if $f_{uu}(\mathbf{0}, \mu_1) + 2f_{uv}(\mathbf{0}, \mu_1) + f_{vv}(\mathbf{0}, \mu_1) \neq 0$.

The above conditions guarantee the existence of a transcritical bifurcating branch from the trivial solution $(x_1, x_2, x_3, x_4, \mu) = (0, 0, 0, 0, \mu_1)$. Note that these conditions are the same as we found in two-cell quotient network # 4 in Table 7.4. The transcritical branch lies in the two-dimensional polydiagonal $(x_1, x_2, x_3, x_4) = (u, u, v, u)$.

2. **When $f_u(\mathbf{0}, \mu_2) = 0$:**
   Since $f_u(\mathbf{0}, \mu_1) = 0$, the Jacobian is:

$$J = f_v(\mathbf{0}, \mu_2)A_{10} = f_v(\mathbf{0}, \mu_2) \begin{pmatrix} 0 & 0 & 0 & 2 \\ 0 & 0 & 0 & 2 \\ 0 & 0 & 1 & 1 \\ 0 & 2 & 0 & 0 \end{pmatrix}$$

   where $f_v(\mathbf{0}, \mu_2) \neq 0$.

   - **Obtaining $\mathbf{v}_0 \in kerJ$ and $\mathbf{v}_0^* \in (rangeJ)^\perp$:**
     Let (x, y, z, w) be any vector in $\mathbb{R}^4$.

$$f_v(\mathbf{0}, \mu_2) \begin{pmatrix} 0 & 0 & 0 & 2 \\ 0 & 0 & 0 & 2 \\ 0 & 0 & 1 & 1 \\ 0 & 2 & 0 & 0 \end{pmatrix} \begin{pmatrix} x \\ y \\ z \\ w \end{pmatrix} = f_v(\mathbf{0}, \mu_2) \begin{pmatrix} 2w \\ 2w \\ z + w \\ 2y \end{pmatrix} = \begin{pmatrix} 0 \\ 0 \\ 0 \\ 0 \end{pmatrix}$$

$$\Rightarrow \begin{pmatrix} x \\ y \\ z \\ w \end{pmatrix} = \begin{pmatrix} \alpha \\ 0 \\ 0 \\ 0 \end{pmatrix}$$

     where $\alpha \in \mathbb{R}$,

Therefore, $\mathbf{v}_0 = (1,0,0,0)$. By solving $\ker(J^t)$, we obtain $\mathbf{v}_0^* = (1,-1,0,0) \in (rangeJ)^{\perp}$.

- **Computation of $K_{y\mu}(0,\mu_2)$:**

$$F_\mu = (f_\mu(x_1, \overline{x_4, x_4}, \mu), f_\mu(x_2, \overline{x_4, x_4}, \mu), f_\mu(x_3, \overline{x_4, x_3}, \mu), f_\mu(x_4, \overline{x_2, x_2}, \mu))$$

$$dF_\mu(\mathbf{v}_0) = \begin{pmatrix} f_{\mu u} & 0 & 0 & 2f_{\mu v} \\ 0 & f_{\mu u} & 0 & 2f_{\mu v} \\ 0 & 0 & f_{\mu u} + f_{\mu v} & f_{\mu v} \\ 0 & 2f_{\mu v} & 0 & f_{\mu u} \end{pmatrix} \begin{pmatrix} 1 \\ 0 \\ 0 \\ 0 \end{pmatrix} = \begin{pmatrix} f_{\mu u} \\ 0 \\ 0 \\ 0 \end{pmatrix}$$

Therefore,

$$\begin{aligned} K_{y\mu}(0,\mu_2) = \langle \mathbf{v}_0^*, dF_\mu(\mathbf{v}_0) \rangle &= \begin{pmatrix} 1 \\ -1 \\ 0 \\ 0 \end{pmatrix} \cdot \begin{pmatrix} f_{\mu u} \\ 0 \\ 0 \\ 0 \end{pmatrix} \\ &= f_{\mu u}(\mathbf{0}, \mu_2) \end{aligned}$$

which is generically nonzero .

- **Computation of $K_{yy}(0,\mu_2)$:**

Since $\mathbf{v}_0^* = (1,-1,0,0)$,

$$K_{yy}(0,\mu_2) = d^2F_1(\mathbf{v}_0, \mathbf{v}_0) - d^2F_2(\mathbf{v}_0, \mathbf{v}_0)$$

Now

$$\begin{aligned} dF_1(\mathbf{v}_0) &= \begin{pmatrix} f_u \\ 0 \\ 0 \\ 2f_v \end{pmatrix} \cdot \begin{pmatrix} 1 \\ 0 \\ 0 \\ 0 \end{pmatrix} = f_u(x_1, \overline{x_4, x_4}, \mu) \\ d^2F_1(\mathbf{v}_0, \mathbf{v}_0) &= \begin{pmatrix} f_{uu} \\ 0 \\ 0 \\ 2f_{uv} \end{pmatrix} \cdot \begin{pmatrix} 1 \\ 0 \\ 0 \\ 0 \end{pmatrix} = f_{uu}(\mathbf{0}, \mu_2) \end{aligned}$$

$$dF_2(\mathbf{v}_0) = \begin{pmatrix} 0 \\ f_u \\ 0 \\ 2f_v \end{pmatrix} \cdot \begin{pmatrix} 1 \\ 0 \\ 0 \\ 0 \end{pmatrix} = 0$$

$$d^2F_2(\mathbf{v}_0, \mathbf{v}_0) = 0$$

Therefore, $K_{yy}(0, \mu_2) = f_{uu}(\mathbf{0}, \mu_2)$, which is generically nonzero.

The above conditions guarantee the existence of a transcritical bifurcating branch from the trivial solution $(x_1, x_2, x_3, x_4, \mu) = (0, 0, 0, 0, \mu_2)$. Note that these conditions are the same as we found in two-cell quotient network # 1 in Table 7.4. The transcritical branch lies in the two-dimensional polydiagonal $(x_1, x_2, x_3, x_4) = (u, v, v, v)$.

3. **When $f_u(\mathbf{0}, \mu_3) = 2f_v(\mathbf{0}, \mu_3)$:**

   Since $f_u(\mathbf{0}, \mu_3) = 2f_v(\mathbf{0}, \mu_3)$, the Jacobian is:

$$J = f_v(\mathbf{0}, \mu_3)(A_{10} + 2I_4) = f_v(\mathbf{0}, \mu_3) \begin{pmatrix} 2 & 0 & 0 & 2 \\ 0 & 2 & 0 & 2 \\ 0 & 0 & 3 & 1 \\ 0 & 2 & 0 & 2 \end{pmatrix}$$

   where $f_v(\mathbf{0}, \mu_3) \neq 0$.

   - **Obtaining $\mathbf{v}_0 \in ker J$ and $\mathbf{v}_0^* \in (range J)^\perp$:**

     Let (x, y, z, w) be any vector in $\mathbb{R}^4$.

$$f_v(\mathbf{0}, \mu_3) \begin{pmatrix} 2 & 0 & 0 & 2 \\ 0 & 2 & 0 & 2 \\ 0 & 0 & 3 & 1 \\ 0 & 2 & 0 & 2 \end{pmatrix} \begin{pmatrix} x \\ y \\ z \\ w \end{pmatrix} = f_v(\mathbf{0}, \mu_3) \begin{pmatrix} 2x + 2w \\ 2y + 2w \\ 3z + w \\ 2y + 2w \end{pmatrix} = \begin{pmatrix} 0 \\ 0 \\ 0 \\ 0 \end{pmatrix}$$

$$\Rightarrow \begin{pmatrix} x \\ y \\ z \\ w \end{pmatrix} = \begin{pmatrix} 3\alpha \\ 3\alpha \\ \alpha \\ -3\alpha \end{pmatrix}$$

     where $\alpha \in \mathbb{R}$.

     Therefore, $\mathbf{v}_0 = (3, 3, 1, -3)$. By solving $\ker(J^t)$, we obtain $\mathbf{v}_0^* = (0, 1, 0, -1) \in (range J)^\perp$.

- **Computation of $K_{y\mu}(0,\mu_3)$:**

$$F_\mu = (f_\mu(x_1, \overline{x_4, x_4}, \mu), f_\mu(x_2, \overline{x_4, x_4}, \mu), f_\mu(x_3, \overline{x_4, x_3}, \mu), f_\mu(x_4, \overline{x_2, x_2}, \mu))$$

$$dF_\mu(\mathbf{v}_0) = \begin{pmatrix} f_{\mu u} & 0 & 0 & 2f_{\mu v} \\ 0 & f_{\mu u} & 0 & 2f_{\mu v} \\ 0 & 0 & f_{\mu u} + f_{\mu v} & f_{\mu v} \\ 0 & 2f_{\mu v} & 0 & f_{\mu u} \end{pmatrix} \begin{pmatrix} 3 \\ 3 \\ 1 \\ -3 \end{pmatrix} = \begin{pmatrix} 3f_{\mu u} - 6f_{\mu v} \\ 3f_{\mu u} - 6f_{\mu v} \\ f_{\mu u} - 2f_{\mu v} \\ 6f_{\mu v} - 3f_{\mu u} \end{pmatrix}$$

Therefore,

$$\begin{aligned} K_{y\mu}(0,\mu_3) = \langle \mathbf{v}_0^*, dF_\mu(\mathbf{v}_0) \rangle &= \begin{pmatrix} 0 \\ 1 \\ 0 \\ -1 \end{pmatrix} \cdot \begin{pmatrix} 3f_{\mu u} - 6f_{\mu v} \\ 3f_{\mu u} - 6f_{\mu v} \\ f_{\mu u} - 2f_{\mu v} \\ 6f_{\mu v} - 3f_{\mu u} \end{pmatrix} \\ &= 6(f_{\mu u}(\mathbf{0},\mu_3) - 2f_{\mu v}(\mathbf{0},\mu_3)) \end{aligned}$$

which is generically nonzero if $f_{\mu u}(\mathbf{0},\mu_3) \neq 2f_{\mu v}(\mathbf{0},\mu_3)$.

- **Computation of $K_{yy}(0,\mu_3)$:**

Since $\mathbf{v}_0^* = (0,1,0,-1)$,

$$K_{yy}(0,\mu_3) = d^2F_2(\mathbf{v}_0,\mathbf{v}_0) - d^2F_4(\mathbf{v}_0,\mathbf{v}_0)$$

Now

$$dF_2(\mathbf{v}_0) = \begin{pmatrix} 0 \\ f_u \\ 0 \\ 2f_v \end{pmatrix} \cdot \begin{pmatrix} 3 \\ 3 \\ 1 \\ -3 \end{pmatrix} = 3f_u(x_2, \overline{x_4, x_4}, \mu) - 6f_v(x_2, \overline{x_4, x_4}, \mu)$$

$$\begin{aligned} d^2F_2(\mathbf{v}_0,\mathbf{v}_0) &= \begin{pmatrix} 0 \\ 3f_{uu} - 6f_{uv} \\ 0 \\ 6f_{uv} - 12f_{vv} \end{pmatrix} \cdot \begin{pmatrix} 3 \\ 3 \\ 1 \\ -3 \end{pmatrix} \\ &= 9f_{uu}(\mathbf{0},\mu_3) - 36f_{uv}(\mathbf{0},\mu_3) + 36f_{vv}(\mathbf{0},\mu_3) \end{aligned}$$

$$
\begin{aligned}
dF_4(\mathbf{v}_0) &= \begin{pmatrix} 0 \\ 2f_v \\ 0 \\ f_u \end{pmatrix} \cdot \begin{pmatrix} 3 \\ 3 \\ 1 \\ -3 \end{pmatrix} = 6f_v(x_4, \overline{x_2, x_2}, \mu) - 3f_u(x_4, \overline{x_2, x_2}, \mu) \\
d^2F_4(\mathbf{v}_0, \mathbf{v}_0) &= \begin{pmatrix} 0 \\ 12f_{vv} - 6f_{uv} \\ 0 \\ 6f_{uv} - 3f_{uu} \end{pmatrix} \cdot \begin{pmatrix} 3 \\ 3 \\ 1 \\ -3 \end{pmatrix} \\
&= 36f_{vv}(\mathbf{0}, \mu_3) - 36f_{uv}(\mathbf{0}, \mu_3) + 9f_{uu}(\mathbf{0}, \mu_3)
\end{aligned}
$$

Therefore, $K_{yy}(0, \mu_3) = 0$.

- **Computation of $K_{yyy}(0, \mu_3)$:**

  We calculate $K_{yyy}(0, \mu_3)$ by first calculating

$$
\begin{aligned}
A &\equiv \langle \mathbf{v}_0^*, d^3F(\mathbf{v}_0, \mathbf{v}_0, \mathbf{v}_0) \rangle \\
B &\equiv \langle \mathbf{v}_0^*, d^2F(\mathbf{v}_0, J^{-1}Ed^2F(\mathbf{v}_0, \mathbf{v}_0)) \rangle
\end{aligned}
$$

  Since $\mathbf{v}_0^* = (0, 1, 0, -1)$,

$$
\begin{aligned}
A &= d^3F_2(\mathbf{v}_0, \mathbf{v}_0, \mathbf{v}_0) - d^3F_4(\mathbf{v}_0, \mathbf{v}_0, \mathbf{v}_0) \\
B &= d^2F_2(\mathbf{v}_0, J^{-1}Ed^2F(\mathbf{v}_0, \mathbf{v}_0)) - d^2F_4(\mathbf{v}_0, J^{-1}Ed^2F(\mathbf{v}_0, \mathbf{v}_0))
\end{aligned}
$$

  Now

$$
\begin{aligned}
d^3F_2(\mathbf{v}_0, \mathbf{v}_0, \mathbf{v}_0) &= \begin{pmatrix} 0 \\ 9f_{uuu} - 36f_{uvu} + 36f_{vvu} \\ 0 \\ 18f_{uuv} - 72f_{uvv} + 72f_{vvv} \end{pmatrix} \cdot \begin{pmatrix} 3 \\ 3 \\ 1 \\ -3 \end{pmatrix} \\
&= 27f_{uuu}(\mathbf{0}, \mu_3) - 108f_{uuv}(\mathbf{0}, \mu_3) + 108f_{vvu}(\mathbf{0}, \mu_3) \\
&\quad -54f_{uuv}(\mathbf{0}, \mu_3) + 216f_{uvv}(\mathbf{0}, \mu_3) - 216f_{vvv}(\mathbf{0}, \mu_3) \\
d^3F_4(\mathbf{v}_0, \mathbf{v}_0, \mathbf{v}_0) &= \begin{pmatrix} 0 \\ 72f_{vvv} - 72f_{uvv} + 18f_{uuv} \\ 0 \\ 36f_{vvu} - 36f_{uvu} + 9f_{uuu} \end{pmatrix} \cdot \begin{pmatrix} 3 \\ 3 \\ 1 \\ -3 \end{pmatrix} \\
&= 216f_{vvv}(\mathbf{0}, \mu_3) - 216f_{uvv}(\mathbf{0}, \mu_3) + 54f_{uuv}(\mathbf{0}, \mu_3) \\
&\quad -108f_{vvu}(\mathbf{0}, \mu_3) + 108f_{uvu}(\mathbf{0}, \mu_3) - 27f_{uuu}(\mathbf{0}, \mu_3)
\end{aligned}
$$

Therefore

$$A = 2\left\{27f_{uuu}(\mathbf{0},\mu_3) - 162f_{uuv}(\mathbf{0},\mu_3) + 324f_{uvv}(\mathbf{0},\mu_3) - 216f_{vvv}(\mathbf{0},\mu_3)\right\} \qquad (7.14)$$

To find B we need to know $J^{-1} : rangeJ \to M$ where M satisfies $\mathbb{R}^4 = kerJ \oplus M$. Now M and $rangeJ$ are spanned by $\{(1,0,0,0),(0,1,0,1),(0,0,1,0)\}$, so in this basis

$$\begin{pmatrix} 2 & 0 & 0 & 2 \\ 0 & 2 & 0 & 2 \\ 0 & 0 & 3 & 1 \\ 0 & 2 & 0 & 2 \end{pmatrix}\begin{pmatrix} 1 \\ 0 \\ 0 \\ 0 \end{pmatrix} = \begin{pmatrix} 2 \\ 0 \\ 0 \\ 0 \end{pmatrix} = 2\begin{pmatrix} 1 \\ 0 \\ 0 \\ 0 \end{pmatrix} + 0\begin{pmatrix} 0 \\ 1 \\ 0 \\ 1 \end{pmatrix} + 0\begin{pmatrix} 0 \\ 0 \\ 1 \\ 0 \end{pmatrix}$$

$$\begin{pmatrix} 2 & 0 & 0 & 2 \\ 0 & 2 & 0 & 2 \\ 0 & 0 & 3 & 1 \\ 0 & 2 & 0 & 2 \end{pmatrix}\begin{pmatrix} 0 \\ 1 \\ 0 \\ 1 \end{pmatrix} = \begin{pmatrix} 2 \\ 4 \\ 1 \\ 4 \end{pmatrix} = 2\begin{pmatrix} 1 \\ 0 \\ 0 \\ 0 \end{pmatrix} + 4\begin{pmatrix} 0 \\ 1 \\ 0 \\ 1 \end{pmatrix} + 1\begin{pmatrix} 0 \\ 0 \\ 1 \\ 0 \end{pmatrix}$$

$$\begin{pmatrix} 2 & 0 & 0 & 2 \\ 0 & 2 & 0 & 2 \\ 0 & 0 & 3 & 1 \\ 0 & 2 & 0 & 2 \end{pmatrix}\begin{pmatrix} 0 \\ 0 \\ 1 \\ 0 \end{pmatrix} = \begin{pmatrix} 0 \\ 0 \\ 3 \\ 0 \end{pmatrix} = 0\begin{pmatrix} 1 \\ 0 \\ 0 \\ 0 \end{pmatrix} + 0\begin{pmatrix} 0 \\ 1 \\ 0 \\ 1 \end{pmatrix} + 3\begin{pmatrix} 0 \\ 0 \\ 1 \\ 0 \end{pmatrix}$$

Hence J restricted to M has the form:

$$J = \begin{pmatrix} 2 & 2 & 0 \\ 0 & 4 & 0 \\ 0 & 1 & 3 \end{pmatrix}$$

and the inverse of J exists such as:

$$J^{-1} = \frac{1}{12}\begin{pmatrix} 6 & -3 & 0 \\ 0 & 3 & 0 \\ 0 & -1 & 4 \end{pmatrix}$$

$\mathbf{v} = (v_1, v_2, v_3, v_2) \in \text{range}(J)$ can be written as:

$$\begin{pmatrix} v_1 \\ v_2 \\ v_3 \\ v_2 \end{pmatrix} = v_1\begin{pmatrix} 1 \\ 0 \\ 0 \\ 0 \end{pmatrix} + v_2\begin{pmatrix} 0 \\ 1 \\ 0 \\ 1 \end{pmatrix} + v_3\begin{pmatrix} 0 \\ 0 \\ 1 \\ 0 \end{pmatrix}$$

The coordinate of $\mathbf{v}$ in M is:

$$J^{-1}\begin{pmatrix} v_1 \\ v_2 \\ v_3 \end{pmatrix} = \frac{1}{12}\begin{pmatrix} 6v_1 - 3v_2 \\ 3v_2 \\ -v_2 + 4v_3 \end{pmatrix}$$

Hence for a given $\mathbf{v} \in \text{range}(J)$, $\overline{\mathbf{v}} \in M$ has the form

$$\overline{\mathbf{v}} = \frac{1}{12}(6v_1 - 3v_2)\begin{pmatrix} 1 \\ 0 \\ 0 \\ 0 \end{pmatrix} + \frac{1}{12}3v_2\begin{pmatrix} 0 \\ 0 \\ 1 \\ 0 \end{pmatrix} + \frac{1}{12}(-v_2 + 4v_3)\begin{pmatrix} 0 \\ 0 \\ 1 \\ 0 \end{pmatrix} \tag{7.15}$$

Now

$$\begin{aligned} d^2F_1(\mathbf{v}_0, \mathbf{v}_0) &= \begin{pmatrix} 3f_{uu} - 6f_{uv} \\ 0 \\ 0 \\ 6f_{uv} - 12f_{vv} \end{pmatrix} \cdot \begin{pmatrix} 3 \\ 3 \\ 1 \\ -3 \end{pmatrix} \\ &= 9f_{uu}(\mathbf{0}, \mu_3) - 36f_{uv}(\mathbf{0}, \mu_3) + 36f_{vv}(\mathbf{0}, \mu_3) \\ dF_3(\mathbf{v}_0) &= \begin{pmatrix} 0 \\ 0 \\ f_u + f_v \\ f_v \end{pmatrix} \cdot \begin{pmatrix} 3 \\ 3 \\ 1 \\ -3 \end{pmatrix} = f_u(x_3, \overline{x_3, x_4}, \mu) - 2f_v(x_3, \overline{x_3, x_4}, \mu) \\ d^2F_3(\mathbf{v}_0) &= \begin{pmatrix} 0 \\ 0 \\ f_{uu} - f_{uv} - 2f_{vv} \\ f_{uv} - 2f_{vv} \end{pmatrix} \cdot \begin{pmatrix} 3 \\ 3 \\ 1 \\ -3 \end{pmatrix} \\ &= f_{uu}(\mathbf{0}, \mu_3) - 4f_{uv}(\mathbf{0}, \mu_3) + 4f_{vv}(\mathbf{0}, \mu_3) \end{aligned}$$

Therefore

$$d^2F(\mathbf{v}_0, \mathbf{v}_0) = \begin{pmatrix} 9f_{uu}(\mathbf{0}, \mu_3) - 36f_{uv}(\mathbf{0}, \mu_3) + 36f_{vv}(\mathbf{0}, \mu_3) \\ 9f_{uu}(\mathbf{0}, \mu_3) - 36f_{uv}(\mathbf{0}, \mu_3) + 36f_{vv}(\mathbf{0}, \mu_3) \\ f_{uu}(\mathbf{0}, \mu_3) - 4f_{uv}(\mathbf{0}, \mu_3) + 4f_{vv}(\mathbf{0}, \mu_3) \\ 9f_{uu}(\mathbf{0}, \mu_3) - 36f_{uv}(\mathbf{0}, \mu_3) + 36f_{vv}(\mathbf{0}, \mu_3) \end{pmatrix} = \begin{pmatrix} a \\ a \\ b \\ a \end{pmatrix} \in \text{range}(J)$$

where

$$\begin{aligned} a &= 9f_{uu}(\mathbf{0}, \mu_3) - 36f_{uv}(\mathbf{0}, \mu_3) + 36f_{vv}(\mathbf{0}, \mu_3) \\ b &= f_{uu}(\mathbf{0}, \mu_3) - 4f_{uv}(\mathbf{0}, \mu_3) + 4f_{vv}(\mathbf{0}, \mu_3) \end{aligned}$$

Therefore, use the form of $\overline{\mathbf{v}} \in M$ and note that $E|_{\text{range}(J)} = I$ to obtain

$$\mathbf{u}_0 = J^{-1}Ed^2F(\mathbf{v}_0, \mathbf{v}_0) = \frac{1}{4}\begin{pmatrix} a \\ a \\ -\frac{1}{3}a + \frac{4}{3}b \\ a \end{pmatrix}$$

as $v_1 = v_2 = a$ and $v_3 = b$ in Equation (7.15). We calculate $d^2F_2(\mathbf{v}_0, \mathbf{u}_0)$ and $d^2F_4(\mathbf{v}_0, \mathbf{u}_0)$ as follows:

$$\begin{aligned} d^2F_2(\mathbf{v}_0, \mathbf{u}_0) &= \frac{1}{4}\begin{pmatrix} 0 \\ 3f_{uu} - 6f_{uv} \\ 0 \\ 6f_{uv} - 12f_{vv} \end{pmatrix}\begin{pmatrix} a \\ a \\ -\frac{1}{3}a + \frac{4}{3}b \\ a \end{pmatrix} \\ &= \frac{1}{4}(3af_{uu}(\mathbf{0}, \mu_3) - 12af_{vv}(\mathbf{0}, \mu_3)) \\ d^2F_4(\mathbf{v}_0, \mathbf{u}_0) &= \begin{pmatrix} 0 \\ 12f_{vv} - 6f_{uv} \\ 0 \\ 6f_{uv} - 3f_{uu} \end{pmatrix}\begin{pmatrix} a \\ a \\ -\frac{1}{3}a + \frac{4}{3}b \\ a \end{pmatrix} \\ &= \frac{1}{4}(12af_{vv}(\mathbf{0}, \mu_3) - 3af_{uu}(\mathbf{0}, \mu_3)) \end{aligned}$$

Therefore

$$B = \frac{3}{2}a(f_{uu}(\mathbf{0}, \mu_3) - 4f_{vv}(\mathbf{0}, \mu_3)) \tag{7.16}$$

Generically, $K_{yyy}(0, \mu_3) = A - 3B$ is nonzero.

The above conditions guarantee the existence of a pitchfork bifurcating branch from the trivial solution $(x_1, x_2, x_3, x_4, \mu) = (0, 0, 0, 0, \mu_3)$. Note that these conditions are the same as we found in 3-cell quotient network # 10 shown in Table 7.4. The pitchfork branch lies in the three-dimensional polydiagonal $(x_1, x_2, x_3, x_4) = (u, u, v, w)$.

The following Table 7.4 summarises the relations of nondegeneracy conditions among quotient networks in the lattice. Since all quotient networks of a simple eigenvalue network also have simple eigenvalues, all nondegeneracy conditions for each quotient network are also calculated by using Liapunov-Schmidt reduction.

◇

two-cell quotient network # 4		two-cell quotient network # 1	
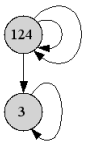		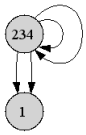	
critical eigenvalue: $f_u(\mathbf{0},\mu_1) = -f_v(\mathbf{0},\mu_1)$	Bif. type: transcritical	critical eigenvalue: $f_u(\mathbf{0},\mu_2) = 0$	Bif. type: transcritical
nondegeneracy conditions: $f_v(\mathbf{0},\mu_1) \neq 0$ $f_{\mu u}(\mathbf{0},\mu_1) \neq -f_{\mu v}(\mathbf{0},\mu_1)$ $f_{uu}(\mathbf{0},\mu_1) + 2f_{uv}(\mathbf{0},\mu_1) + f_{vv}(\mathbf{0},\mu_1) \neq 0$		nondegeneracy conditions: $f_v(\mathbf{0},\mu_2) \neq 0$ $f_{\mu u}(\mathbf{0},\mu_2) \neq 0$ $f_{uu}(\mathbf{0},\mu_2) \neq 0$	
three-cell quotient network # 10		three-cell quotient network # 5	
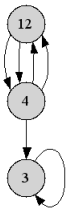		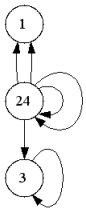	
critical eigenvalue: $f_u(\mathbf{0},\mu_1) = -f_v(\mathbf{0},\mu_1)$	Bif. type: transcritical	critical eigenvalue: $f_u(\mathbf{0},\mu_1) = -f_v(\mathbf{0},\mu_1)$	Bif. type: transcritical
nondegeneracy conditions: $f_v(\mathbf{0},\mu_1) \neq 0$ $f_{\mu u}(\mathbf{0},\mu_1) \neq -f_{\mu v}(\mathbf{0},\mu_1)$ $f_{uu}(\mathbf{0},\mu_1) + 2f_{uv}(\mathbf{0},\mu_1) + f_{vv}(\mathbf{0},\mu_1) \neq 0$		nondegeneracy conditions: $f_v(\mathbf{0},\mu_1) \neq 0$ $f_{\mu u}(\mathbf{0},\mu_1) \neq -f_{\mu v}(\mathbf{0},\mu_1)$ $f_{uu}(\mathbf{0},\mu_1) + 2f_{uv}(\mathbf{0},\mu_1) + f_{vv}(\mathbf{0},\mu_1) \neq 0$	
critical eigenvalue: $f_u(\mathbf{0},\mu_3) = 2f_v(\mathbf{0},\mu_3)$	Bif. type: pitchfork	critical eigenvalue: $f_u(\mathbf{0},\mu_2) = 0$	Bif. type: transcritical
nondegeneracy conditions: $f_v(\mathbf{0},\mu_3) \neq 0$ $f_{\mu u}(\mathbf{0},\mu_3) \neq 2f_{\mu v}(\mathbf{0},\mu_3)$ $A - 3B \neq 0$		nondegeneracy conditions: $f_v(\mathbf{0},\mu_2) \neq 0$ $f_{\mu u}(\mathbf{0},\mu_2) \neq 0$ $f_{uu}(\mathbf{0},\mu_2) \neq 0$	

Table 7.4: Quotient networks of four-cell network #10 and their nondegeneracy conditions from Liapunov-Schmidt reduction. A and B are given Equation (7.14) and (7.16). The shaded quotient networks are determined by the balanced polydiagonals which are generated from the eigenvector structures of the adjacency matrix of the network.

Example 7.6 *(Numerical Analysis).* We numerically analyse synchrony-breaking steady-state bifurcations of the same four-cell valency 2 network #10 using a specific function form.

From the above Example 7.5, we expect to have three unique bifurcating branches from three distinct bifurcation points, that is:

1. a transcritical branch in a polydiagonal subspace $(x_1, x_2, x_3, x_4) = (u, u, v, u)$,
2. a transcritical branch in a polydiagonal subspace $(x_1, x_2, x_3, x_4) = (u, v, v, v)$,
3. a pitchfork branch in a polydiagonal subspace $(x_1, x_2, x_3, x_4) = (u, u, v, w)$.

No other branches are expected.

We choose a function form which satisfies the nondegeneracy conditions for all bifurcation points so that we expect to see all predicted bifurcating branches at all three synchrony-breaking bifurcation points. For example, the function form

$$f(u, \overline{v, w}, \mu) = \mu u - (u + v + w) + u^2 - u^3 \tag{7.17}$$

has the following derivatives:

$$\begin{aligned}
f_u(\mathbf{0}, \mu) &= \mu - 1, \\
f_{\mu u}(\mathbf{0}, \mu) &= 1, \\
f_v(\mathbf{0}, \mu) &= -1, \\
f_{\mu v}(\mathbf{0}, \mu) &= 0, \\
f_{uu}(\mathbf{0}, \mu) &= 2, \\
f_{uv}(\mathbf{0}, \mu) &= 0, \\
f_{vv}(\mathbf{0}, \mu) &= 0, \\
f_{uuu}(\mathbf{0}, \mu) &= -6, \\
f_{uuv}(\mathbf{0}, \mu) &= 0, \\
f_{uvv}(\mathbf{0}, \mu) &= 0, \\
f_{vvv}(\mathbf{0}, \mu) &= 0.
\end{aligned}$$

Three synchrony-breaking bifurcation points are:

Eigenvalue of A	Bifurcation point
$\lambda_1 = 1$	$f_u(\mathbf{0}, \mu_1) + \lambda_1 f_v(\mathbf{0}, \mu_1) = 0 \Rightarrow \mu_1 = 2$
$\lambda_2 = 0$	$f_u(\mathbf{0}, \mu_2) + \lambda_2 f_v(\mathbf{0}, \mu_2) = 0 \Rightarrow \mu_2 = 1$
$\lambda_3 = -2$	$f_u(\mathbf{0}, \mu_3) + \lambda_3 f_v(\mathbf{0}, \mu_3) = 0 \Rightarrow \mu_3 = -1$

All nondegeneracy conditions at every μ_i, $i = 1, 2, 3$ are satisfied.

Using the function form (7.17), the system of ODEs for the network #10 has the form:

$$\begin{aligned}
\dot{x}_1 &= \mu x_1 - (x_1 + x_4 + x_4) + x_1^2 - x_1^3 \\
\dot{x}_2 &= \mu x_2 - (x_2 + x_4 + x_4) + x_2^2 - x_2^3 \\
\dot{x}_3 &= \mu x_3 - (x_3 + x_3 + x_4) + x_3^2 - x_3^3 \\
\dot{x}_4 &= \mu x_4 - (x_4 + x_2 + x_2) + x_4^2 - x_4^3
\end{aligned}$$

Table 7.5 shows steady states close to each bifurcation point $(x_1, x_2, x_3, x_4, \mu) = (0, 0, 0, 0, \mu_i)$, $i = 1, 2, 3$. $\bowtie$ shows the patterns of synchrony and the corresponding polydiagonals in which bifurcating branches lie. The existence of generic bifurcations is guaranteed by nondegeneracy conditions. "P" means a "pitchfork" bifurcation and "T" means a "transcritical" bifurcation in the last column.

Bifurcation parameter $\mu_3 = -0.9999$

x_1	x_2	x_3	x_4	$\bowtie$	Bif.
-0.0140908	-0.0140908	-0.00472295	0.0141908	$(12)(3)(4)$	P
0.0141908	0.0141908	0.00470444	-0.0140908		

Bifurcation parameter $\mu_2 = 1.0001$

x_1	x_2	x_3	x_4	$\bowtie$	Bif.
-0.00009999	0	0	0	$(234)(1)$	T

Bifurcation parameter $\mu_1 = 2.0001$

x_1	x_2	x_3	x_4	$\bowtie$	Bif.
0	0	-0.00009999	0	$(124)(3)$	T

Table 7.5: Steady states of four-cell network #10 at very close to each bifurcation point.

These numerical solutions show three bifurcation branches in the expected polydiagonal and their bifurcation types.

Four bifurcation diagrams are shown in Figure 7.10. Each axis x (as x_1), y (as x_2), z (as x_3) and w (as x_4) corresponds to a state variable for cell "1", cell "2", cell "3" and cell "4", respectively with the bifurcation parameter axis r (as μ).

By comparing the bifurcation diagrams in Figure 7.10 for each variable with Table 7.5, we can see how the four states x_1, x_2, x_3 and x_4 are coupled as steady state solutions and three synchrony-breaking bifurcating branches lie in three distinct polydiagonals. This result is shown schematically in Figure 7.12, L1 lattice.

$\diamond$

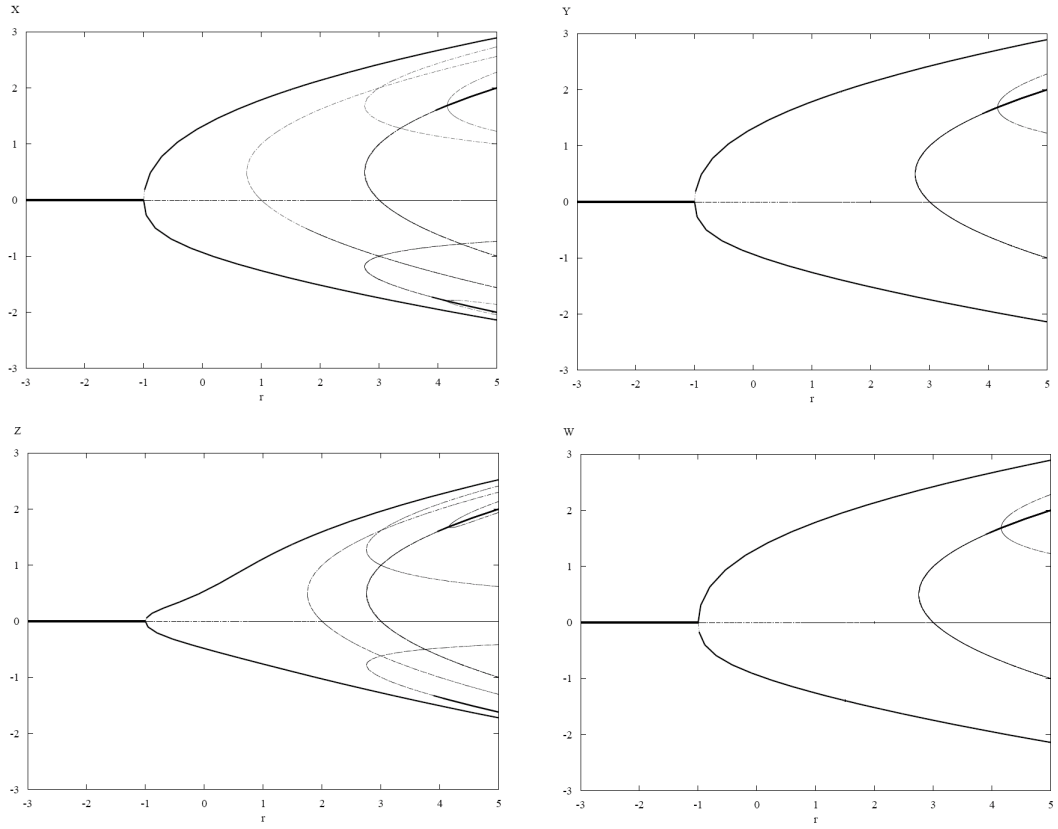

Figure 7.10: Bifurcation diagrams of four-cell valency 2 network #10 for cell "1", "2", "3" and "4" state variables.

7.4.8 Bifurcation Diagrams of 3 and 4-cell Networks with Simple Eigenvalues

The following schematic Figure 7.11 shows the existence of synchrony-breaking steady-state bifurcating branches, for the three lattice structures observed in 3-cell regular homogeneous networks with simple real eigenvalues. Because there are three distinct eigenvalues, there are three corresponding distinct bifurcation points. There have been marked on the horizontal axis from left to right as μ_0, μ_1 and μ_2. This ordering on the axis does not reflect their numerical values[2].

The bifurcation point μ_0 corresponds to the synchrony-preserving bifurcating point (i.e., the eigenvalue equal to a valency of the network), and therefore has no synchrony-breaking bifurcation branches.

The vertical axis does not represent any particular variable, but is a simplified representation of directions in the relevant balanced polydiagonals. The shape and direction of the curves shown has no significance in these schematic figures. Synchrony-breaking bifurcation branches

[2]If we want to study the equivalence of two bifurcation diagrams, we need to consider the spectrum of eigenvalues. Then the order of μ_0, μ_1 and μ_2 does matter.

lie in a particular balanced polydiagonal direction, which has been labelled. For example P_2 indicates two conjugacy classes, e.g. $(x, y, z) = (u, u, v)$, while for P_3 we have three conjugacy classes, i.e. $(x, y, z) = (u, v, w)$.

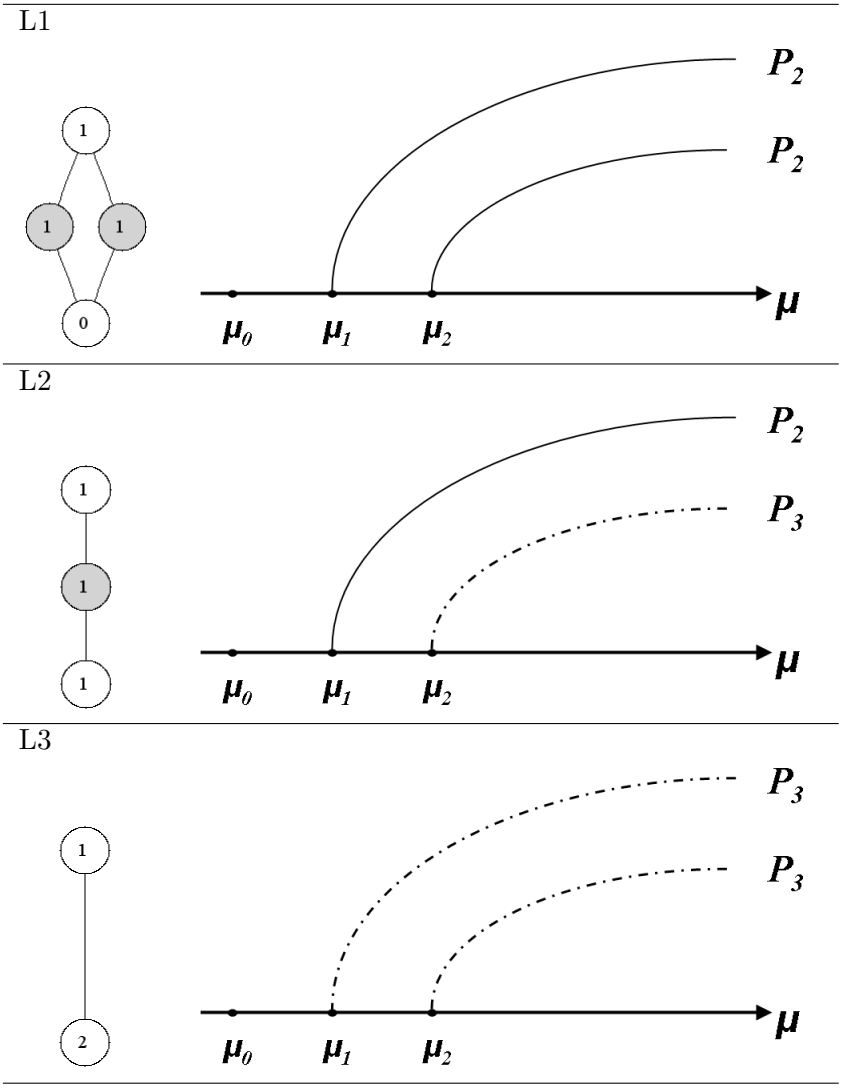

Figure 7.11: Existence of bifurcating branches for each 3-cell network lattice structure. The shaded lattice nodes correspond to non-trivial balanced equivalence relations generated from the eigenvector structures (which are equivalently lattice generators).

Similarly, Figure 7.12 shows the existence of synchrony-breaking steady-state bifurcation branches schematically, for the fourteen lattice structures of 4-cell regular homogeneous networks with simple real eigenvalues listed in Figure 7.7.

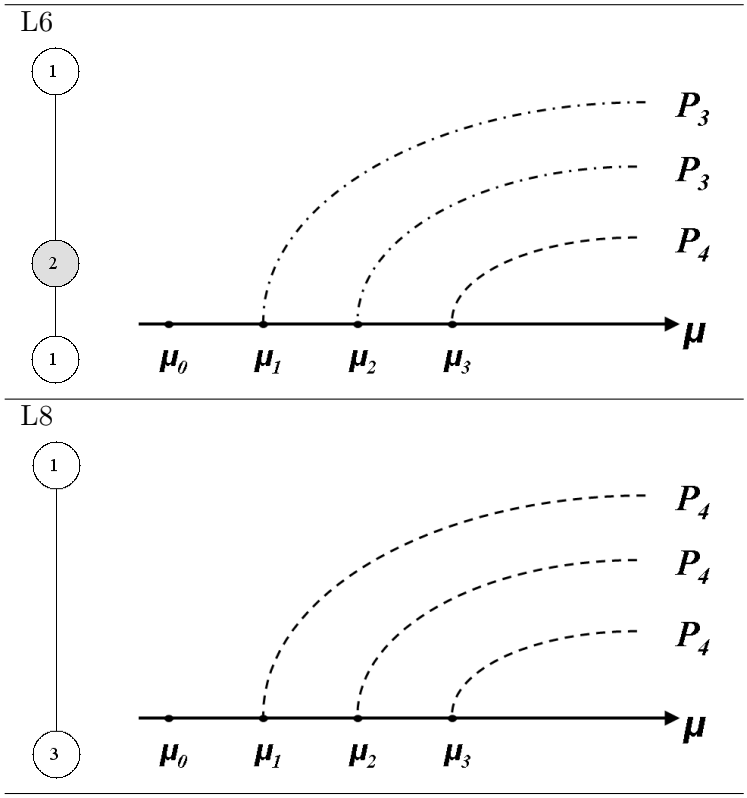

Figure 7.12: Existence of bifurcating branches for 4-cell network lattice structures shown in Figure 7.7 (split over four pages). The shaded lattice nodes correspond to non-trivial balanced equivalence relations generated from the eigenvector structures (which are equivalently lattice generators).

L2

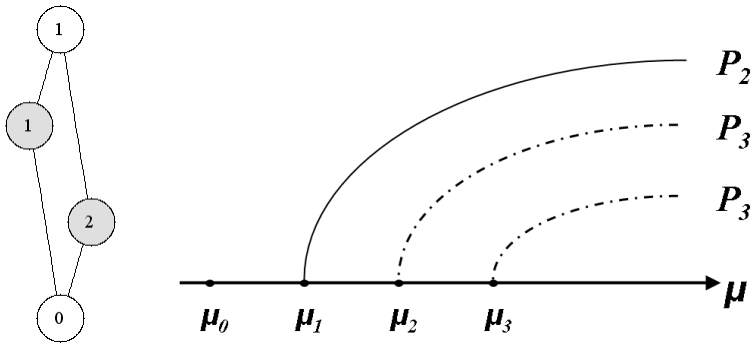
1
1
2
0
P2
P3
P3
μ
μ0
μ1
μ2
μ3

L5

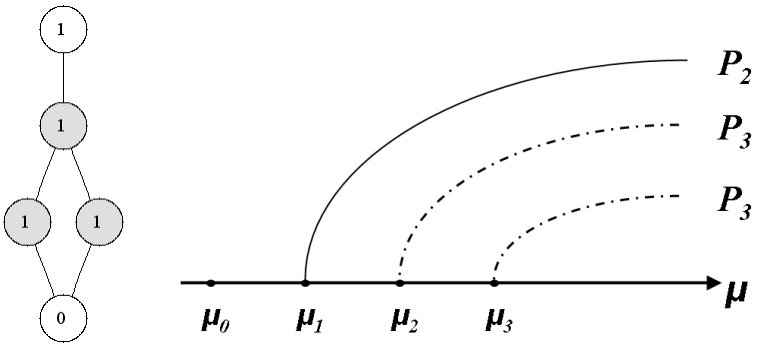
1
1
1
1
0
P2
P3
P3
μ
μ0
μ1
μ2
μ3

L3

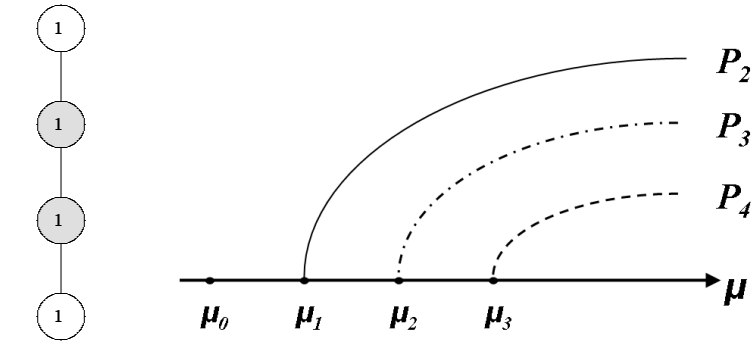
1
1
1
1
P2
P3
P4
μ
μ0
μ1
μ2
μ3

L7

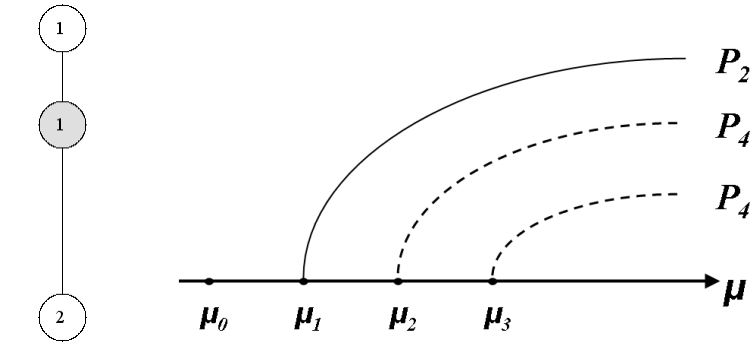
1
1
2
P2
P4
P4
μ
μ0
μ1
μ2
μ3

L1

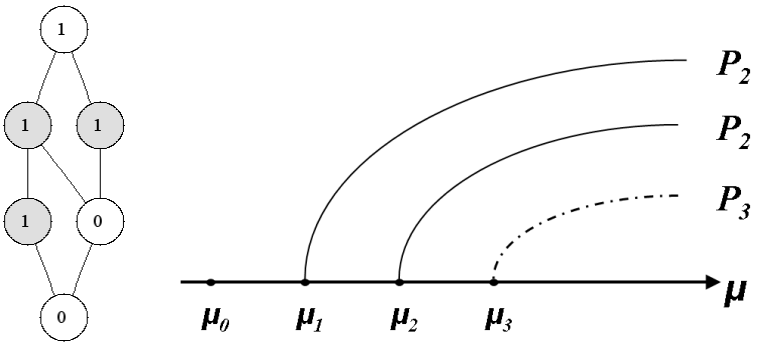
1
1
1
1
0
0
P2
P2
P3
μ
μ0
μ1
μ2
μ3

L12

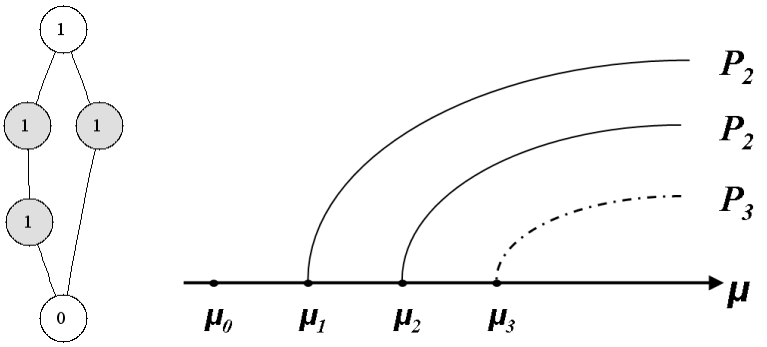
1
1
1
1
0
P2
P2
P3
μ
μ0
μ1
μ2
μ3

L9

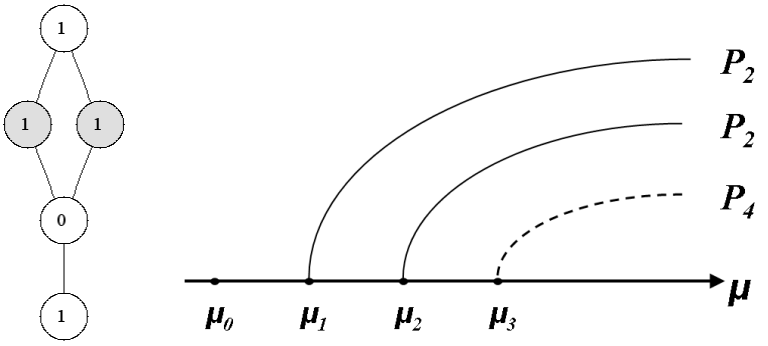
1
1
1
0
1
P2
P2
P4
μ
μ0
μ1
μ2
μ3

L10

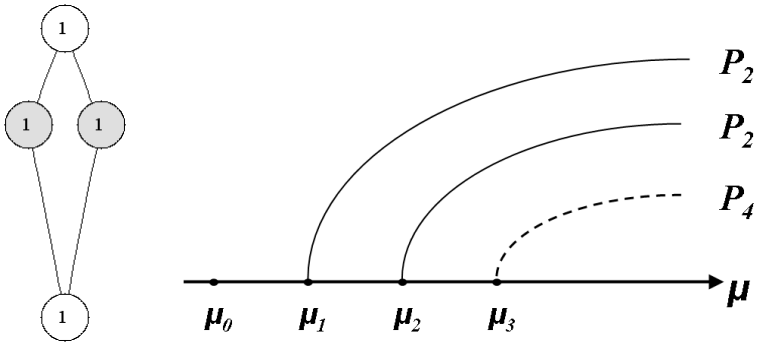
1
1
1
1
P2
P2
P4
μ
μ0
μ1
μ2
μ3

L4

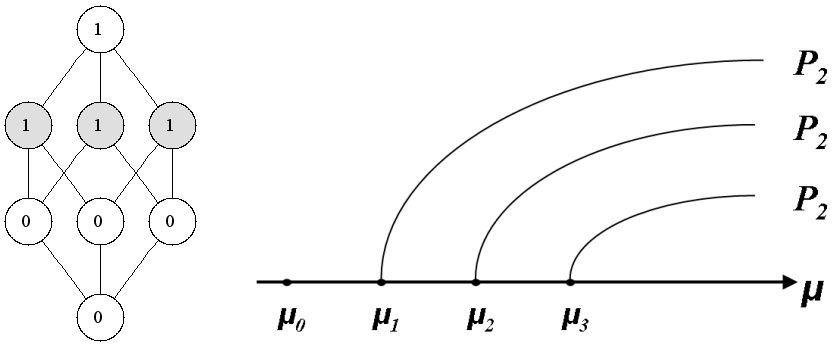

L11

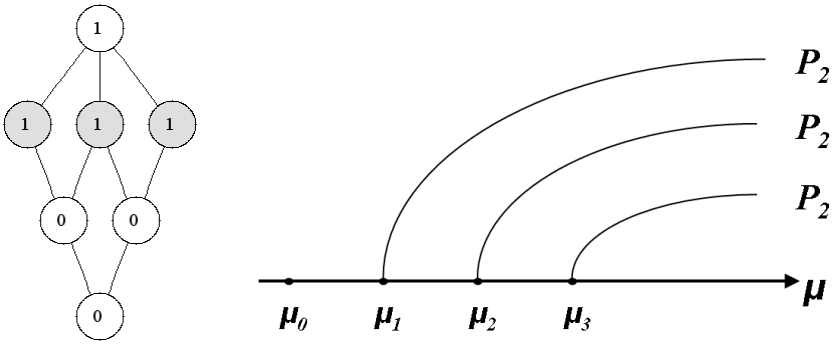

L14

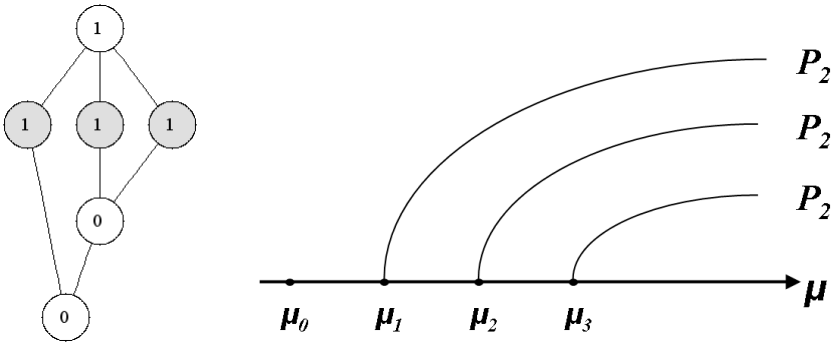

L13

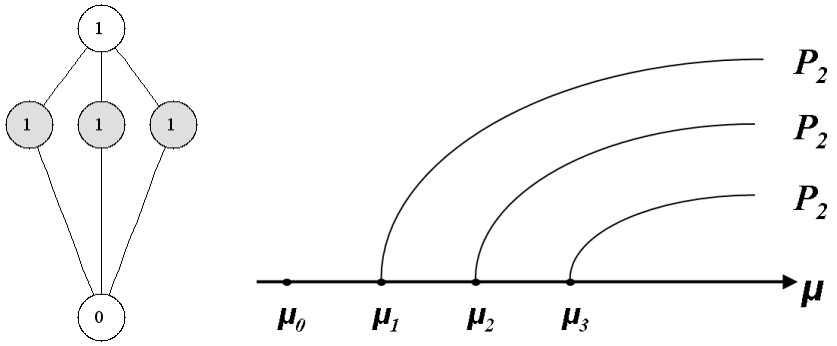

7.5 Conclusions

For both simple eigenvalue networks and non-simple eigenvalue networks, we defined three lattices: lattice of balanced equivalence relations, lattice of balanced polydiagonals and lattice of the set of eigenvalues of quotient networks, denoted by $\Lambda_{\mathcal{G}}$, $V_{\mathcal{G}}^P$ and $U_{\mathcal{G}}^P$, respectively. We showed that these three lattices are order-isomorphic if the adjacency matrices of networks have simple eigenvalues. However, when the adjacency matrix has repeated eigenvalues, $V_{\mathcal{G}}^P$ is isomorphic to $\Lambda_{\mathcal{G}}$ but there is only an order-preserving map between $U_{\mathcal{G}}^P$ and $\Lambda_{\mathcal{G}}$ (or equivalently $V_{\mathcal{G}}^P$).

We then showed that there exist lattice generators for simple networks and these generators can be constructed from the eigenvector structures of the adjacency matrices of the networks. The rest of the lattice elements in $V_{\mathcal{G}}^P$ were constructed by a join of lattice generators.

All possible lattice structures for three and four-cell regular homogeneous networks of any valency with simple eigenvalues are determined. If balanced equivalence relations $\bowtie$ are defined by lattice generators, then synchrony-breaking bifurcating branches exist in the corresponding balanced polydiagonals $\triangle_{\bowtie}$ at a simple real eigenvalue. From lattice structures, the existence of bifurcating branches and their bifurcating directions was determined. In particular, the number of the bottom element, $\eta(\perp)$, in a lattice elucidates the existence of bifurcating branches outside the possible balanced polydiagonals.

Schematic bifurcation diagrams which show the existence of bifurcating branches and their bifurcating directions (the dimension of balanced polydiagonals) were listed for all possible lattice structures of all three and four-cell regular homogeneous networks with simple real eigenvalues.

Bifurcation diagrams of four-cell network lattices $L1$ and $L12$ have the same number of synchrony-breaking branches in $P2$ and in $P3$. Similarly, $L9$ and $L10$ are the same, and $L4$, $L11$, $L14$ and $L13$ are the same. These groupings share the same number of nonzero lattice nodes in each rank. Note that $L2$ and $L5$ have the same number of synchrony-breaking branches in $P2$ and $P3$, however, in $L2$ two 3-dimensional polydiagonals are identical and in $L5$ two 3-dimensional polydiagonals are distinct. They are slightly different from the above groupings.

Although in these diagrams the position of bifurcation points is not considered, we can elucidate that the existence of their bifurcating branches are topologically similar. When two networks $\mathcal{G}_1$ and $\mathcal{G}_2$ share the same bifurcation diagram (in the above sense), this means that we can expect the same number of bifurcating branches in each dimension (e.g. $P2$ or $P3$). For example, if $\mathcal{G}_1$ has two branches in $P2$ and one branch in $P3$, then so will $\mathcal{G}_2$. However, from which bifurcation point these branches occur may be different.

For a more detailed classification of bifurcation behaviour, such as which branch is a

transcritical or pitchfork, we need to determine the corresponding quotient networks in balanced polydiagonals. This is summarised in Appendix B for all four-cell regular homogeneous networks of valency 2 with simple eigenvalues (both real and complex).

Chapter 8

Steady-state Bifurcation Analysis: Non-Simple Eigenvalue Networks

8.1 Introduction

When an $n \times n$ adjacency matrix A of a regular homogeneous network has n distinct eigenvalues (which are therefore simple), the corresponding n eigenvectors are linearly independent. Each of the n eigenspaces is spanned by one eigenvector, and is therefore one-dimensional. One-dimensional eigenspaces can generate at most one balanced polydiagonal, which is either balanced or not.

However, when an adjacency matrix has a repeated eigenvalue λ (i.e., the algebraic multiplicity of λ is more than one) with geometric multiplicity $g(\lambda) > 1$, the dimension of the corresponding eigenspace $\ker(A - \lambda I_n)$ is more than one. In this case, $\ker(A - \lambda I_n)$ might be able to generate more than $g(\lambda)$ balanced polydiagonals, or equivalently quotient networks which have the same set of eigenvalues. This leads to the fact that some lattice nodes correspond to possibly topologically identical quotient networks with different balanced equivalence relations, which we do not observe in networks with simple eigenvalues (proved in Proposition 7.2). Also these additional lattice nodes make the lattice size of non-simple eigenvalue networks larger than those of simple eigenvalue networks.

Example 8.1. Regular homogeneous three-cell valency 2 network #27 from Table 8.1.

Network #27	Adjacency matrix	Eigenvalues	Eigenvectors
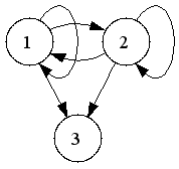	$\begin{pmatrix} 1 & 1 & 0 \\ 1 & 1 & 0 \\ 1 & 1 & 0 \end{pmatrix}$	2 0 0	$(1,1,1)$ $\left.\begin{matrix}\\ \\ \end{matrix}\right\}$ $(\alpha, -\alpha, \beta)$

Table 8.1: Three-cell network #27. α,$\beta \in \mathbb{R}$

The geometric multiplicity of the eigenvector $(\alpha, -\alpha, \beta)$, corresponding to the double eigenvalue 0, is two. From the eigenvector structure, there are three possible equivalence relations as follows:

Case I If $\alpha = 0$, $(x_1, x_2, x_3) = (u, u, v)$, i.e., $\bowtie_1 = (12)(3)$,

Case II If $\alpha = \beta$, $(x_1, x_2, x_3) = (u, v, u)$, i.e., $\bowtie_2 = (13)(2)$,

Case III If $-\alpha = \beta$, $(x_1, x_2, x_3) = (u, v, v)$, i.e., $\bowtie_3 = (1)(23)$,

where $u, v \in \mathbf{R}$.

In this example, all three equivalence relations are balanced and the restrictions of the admissible vector fields to the corresponding balanced polydiagonals generate three associated quotient networks. For example, the balanced equivalence relation $\bowtie_1 = (12)(3)$ generates a two-cell quotient network with one cell, made by merging cell 1 and 2 in the original three-cell network and the second cell corresponding to cell 3. The three quotient network are as follows:

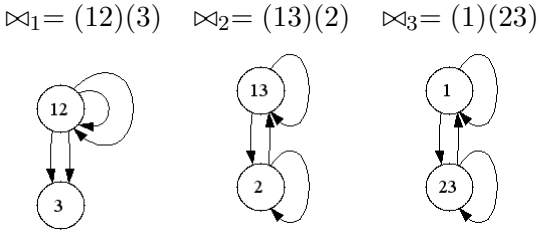

Figure 8.1: Three two-cell quotient networks of network #27.

The two quotient networks generated by $\bowtie_2$ and $\bowtie_3$ are topologically identical. From the adjacency matrix computation as we discussed in Chapter 4, we observe that these three two-cell quotient networks correspond to all of the non-trivial quotient networks for the three-cell network #27. Hence, the lattice of balanced equivalence relations, shown in Figure 8.2, consists of five lattice nodes; two of them correspond to trivial balanced equivalence relations and the other three nodes are as above. Each lattice node describes which cell coordinates are equal to generate the corresponding quotient network.

There are three lattice nodes in rank 2, although we had a maximum of two lattice nodes in rank 2 for simple eigenvalue three-cell networks.

$\diamond$

The questions we want to answer are:

1. In which balanced polydiagonals do bifurcating branches exist?

2. How many branches exist at each bifurcation point?

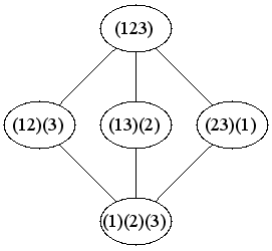

Figure 8.2: Lattice of balanced equivalence relations of three-cell network #27. The node labels show the equivalence classes. For example (12)(3) means that there are two equivalence classes and cell 1 and cell 2 are in the same equivalence class while cell 3 is in the other class, that is $(x_1, x_2, x_3) = (u, u, v)$

3. Are there any other bifurcating branches outside the balanced polydiagonals?

If we can assign $\eta(p)$ to each lattice node as we did for lattices of networks with simple eigenvalues, it would enable us to answer Question 1 and 3. However, we cannot directly apply the same method for the lattices of non-simple eigenvalue networks, because an eigenvector which corresponds to a repeated eigenvalue might generate more balanced polydiagonals than its algebraic multiplicity. *How can we exclude these additional lattice nodes to assign the correct number $\eta(p)$?* The approach taken here is to clump these extra lattice nodes together and reduce the original lattice to one of the lattices observed in networks with simple eigenvalues. This procedure is equivalent to taking the intersection of balanced polydiagonals with generalised eigenspaces. Note that to identify the existence of bifurcating branches outside of balanced polydiagonals, we need to check if enough balanced polydiagonals are generated from eigenspaces, which have more than one dimension.

To answer Question 2, we simply go back to the original lattices to observe how many balanced polydiagonals are generated by the same eigenvalue.

8.2 Preliminaries

Let an $n \times n$ matrix A_B represent a linear map

$$T : V \to V$$

for $V = \mathbb{R}^n$ with a basis $B = \{\mathbf{b}_1, \mathbf{b}_2, \ldots, \mathbf{b}_n\}$. We can represent A_B with respect to different bases. If

$$B' = \{\mathbf{b}'_1, \mathbf{b}'_2, \ldots, \mathbf{b}'_n\}$$

is a basis, then the matrix $A_{B'}$ representing A_B with respect to B' is

$$A_{B'} = P^{-1} A_B P$$

where P is the transition matrix from the basis B' to the basis B. If there exists such a nonsingular matrix P, then A_B and $A_{B'}$ are said to be **similar**. In particular, if P is a permutation matrix, then A_B and $A_{B'}$ are said to be **permutation similar**.

Given a general matrix A_B, the problem of finding a similar matrix $A_{B'} = P^{-1}A_BP$ with a simpler form thus becomes the same as that of finding a nice basis. For example, consider a basis B' consisting entirely of eigenvectors of A. By constructing a transition matrix P using these basis vectors as columns, $P^{-1}A_BP$ becomes a diagonal matrix with the eigenvalues along the diagonal. This diagonalisation happens exactly when there are n linearly independent eigenvectors, or equivalently, when the minimal polynomial has no repeated roots. The theory of the Jordan normal (or canonical) form generalises this diagonalisation process to the situation where some of the roots might have multiplicities.

8.2.1 Minimal Polynomial of a Matrix

Let A be an $n \times n$ matrix with s distinct eigenvalues $\lambda_1, \lambda_2, \ldots, \lambda_s$, where $s \leq n$. Let

$$f(\lambda) = \det(A - \lambda I_n) = \lambda^n + a_{n-1}\lambda^{n-1} + \cdots + a_1\lambda + a_0 = \prod_{i=1}^{s}(\lambda - \lambda_i)^{d_i}$$

be the characteristic polynomial of A, where d_i is the algebraic multiplicity of the eigenvalue λ_i. Then, the Cayley-Hamilton theorem states that

$$A^n + a_{n-1}A^{n-1} + \cdots + a_1A + a_0I_n = \mathbf{0}$$

which is one of **annihilating polynomials** of A, that is $f(A) = \mathbf{0}$.

The **minimal polynomial** of a matrix A is the monic polynomial $m(\lambda) = \sum_{i=0}^{l} c_i\lambda^i$, where $c_l = 1$, of the smallest degree $l \leq n$ such that

$$m(A) = \sum_{i=0}^{l} c_iA^i = \mathbf{0}$$

The minimal polynomial divides any polynomial $p(\lambda)$ satisfying $p(A) = \mathbf{0}$. In particular, the minimal polynomial $m(\lambda)$ divides the characteristic polynomial so that

$$m(\lambda) = \prod_{i=1}^{s}(\lambda - \lambda_i)^{m_i}$$

for some positive integers $m_i \leq d_i$. The exponent m_i associated with the eigenvalue λ_i is unique and it is known as the **index** of λ_i.[1]

A matrix A is diagonalisable if and only if its minimal polynomial is equal to $\prod_{i=1}^{s}(\lambda - \lambda_i)$, where $\lambda_1, \ldots, \lambda_s$ are the distinct eigenvalues of A. Therefore, when a matrix A has simple

[1] We show later that the indices m_i are the maximal sizes of Jordan blocks associated with the eigenvalues λ_i.

eigenvalues, the minimal polynomial does not have repeated roots and furthermore, the minimal polynomial of A coincides with its characteristic polynomial.

Note that any two similar matrices have the same minimal polynomial because

$$\prod_{i=1}^{s}(P^{-1}AP - \lambda_i I)^{m_i} = P^{-1}\left(\prod_{i=1}^{s}(A - \lambda_i I)^{m_i}\right)P$$

for any invertible matrix P. Hence, the indices of each λ_i with respect to A and $P^{-1}AP$ are equal.

In the next subsection 8.2.2, we show that the subspaces $\ker(A-\lambda_i I)^{m_i}$ with $i = 1, \ldots, s$ play an important role for the construction of Jordan normal forms of A and vector space $V = \mathbb{R}^n$ can be decomposed as a direct sum of these subspaces.

8.2.2 Generalised Eigenspaces

Let $E_{\lambda,r} = Ker(A-\lambda I)^r$, where r varies over the set of nonnegative integers. For a finite vector space $\mathbb{R}^n$, subspaces $E_{\lambda,r}$ have the following property:

$$\{\mathbf{0}\} = E_{\lambda,0} \subset E_{\lambda,1} \subset \cdots \subset E_{\lambda,p} = E_{\lambda,p+1} = \cdots \subset \mathbb{R}^n \tag{8.1}$$

for some positive integer p. Note that $E_{\lambda,1}$ is the eigenspace of A associated with λ.

The subspace $E_{\lambda,r}(1 \leq r \leq p)$ in (8.1) is referred to as a **generalised eigenspace** of A of order r associated with the eigenvalue λ. Also, a nonzero element $\mathbf{x}_r$ such that $\mathbf{x}_r \in E_{\lambda,r}$, but $\mathbf{x}_r \notin E_{\lambda,r-1}$ is said to be a **generalised eigenvector** of A of order r corresponding to the eigenvalue λ, that is

$$\mathbf{x}_r \in \ker(A-\lambda I)^r, \quad \text{but} \quad \mathbf{x}_r \notin \ker(A-\lambda I)^{r-1}$$

In particular, eigenvectors of A can be viewed as generalised eigenvectors of A of order 1 corresponding to the same eigenvalue.

Let $m(\lambda)$ be the minimal polynomial of matrix A with the distinct eigenvalues $\lambda_1, \lambda_2, \ldots, \lambda_s$ as follows:

$$m(\lambda) = \prod_{i=1}^{s}(\lambda - \lambda_i)^{m_i}$$

for some positive indices m_i, possibly equal to 1.

We can decompose the vector space V as a direct sum of A-invariant subspaces such as:

$$V = E_{\lambda_1,m_1} \oplus E_{\lambda_2,m_2} \oplus \cdots E_{\lambda_s,m_s}$$

where E_{λ_i,m_i} are the generalised eigenspaces of order m_i corresponding to the eigenvalue λ_i. Each generalised eigenspace is A-invariant because if

$$(A-\lambda_i I)^{m_i}(\mathbf{x}_{m_i}) = \mathbf{0}$$

then

$$(A - \lambda_i I)^{m_i}(A\mathbf{x}_{m_i}) = A(A - \lambda_i I)^{m_i}(\mathbf{x}_{m_i}) = A(\mathbf{0}) = \mathbf{0}$$

As a consequence, when we choose bases B_i for each E_{λ_i,m_i} separately and combine them to make a basis $B = B_1 \cup B_2 \cup \cdots \cup B_s$ for V as a whole, then the matrix of A will take the block diagonal form

$$\left(\begin{array}{c|c|c|c|c} A_{B_1} & 0 & \cdots & \cdots & 0 \\ \hline 0 & A_{B_2} & 0 & \cdots & 0 \\ \hline \vdots & \ddots & \ddots & \ddots & \vdots \\ \hline \vdots & \ddots & \ddots & A_{B_{s-1}} & 0 \\ \hline 0 & \cdots & \cdots & 0 & A_{B_s} \end{array}\right)$$

where the spectrum of A_{B_i} for $i = 1, \ldots, s$, consists of one point only, in fact λ_i. Moreover, the sizes of A_{B_i}, $1 \leq i \leq s$, are the algebraic multiplicities of the eigenvalues λ_i.[2]

Thus, to find a nice form A_B, it suffices to find a nice form for each A_{B_i} separately and combine them.

In the following subsection 8.2.3, we show that generalised eigenspaces E_{λ_i,m_i} can be decomposed further. This means that each A_{B_i} can be decomposed into a diagonal matrix whose diagonal elements are one or several smaller blocks, called **Jordan blocks**. We next find a basis for each generalised eigenspace E_{λ_i,m_i} for this decomposition.

8.2.3 Jordan Normal Forms

We note the following:

Lemma 8.1. $\mathbf{x}_r$ *is a generalised eigenvector of* A *of order* $r \geq 2$ *if and only if the element* $\mathbf{x}_{r-1} = (A - \lambda I)(\mathbf{x}_r)$ *is a generalised eigenvector of* A *of order* $r - 1$*, or, equivalently,*

$$A(\mathbf{x}_r) = \lambda \mathbf{x}_r + \mathbf{x}_{r-1} \tag{8.2}$$

where $\mathbf{x}_{r-1} \in E_{\lambda,r-1}$*,* $\mathbf{x}_{r-1} \notin E_{\lambda,r-2}$*.*

Proof. See Lancaster and Tismenetsky (1985). □

Lemma 8.2. $\mathbf{x}_r$ *is a generalised eigenvector of* A *of order* $r \geq 1$ *if and only if the vector* $(A - \lambda I)^{r-1}(\mathbf{x}_r)$ *is an eigenvector of* A *or, equivalently,*

$$(A - \lambda I)^k(\mathbf{x}_r) = \mathbf{0} \quad \textit{for} \quad k \geq r.$$

Proof. See Lancaster and Tismenetsky (1985). □

[2]Later, A_{B_i} will be denoted as $J(\lambda_i)$.

Using Lemma 8.1, observe that if $\mathbf{x}_r$ is a generalised eigenvector of A of order r, then there are vectors $\mathbf{x}_{r-1}, \ldots, \mathbf{x}_2, \mathbf{x}_1$ for which

$$\begin{aligned} A(\mathbf{x}_1) &= \lambda \mathbf{x}_1, \\ A(\mathbf{x}_2) &= \lambda \mathbf{x}_2 + \mathbf{x}_1, \\ &\vdots \\ A(\mathbf{x}_r) &= \lambda \mathbf{x}_r + \mathbf{x}_{r-1}, \end{aligned}$$

where $\mathbf{x}_j \in E_{\lambda,j}$, $\mathbf{x}_j \notin E_{\lambda,j-1}$ for $j = 1, 2, \ldots, r$. Such a sequence $\mathbf{x}_1, \mathbf{x}_2, \ldots, \mathbf{x}_r$ is called a **Jordan chain of length** r associated with the eigenvalue λ. Observe that the above equations imply

$$(A - \lambda I)\mathbf{x}_j = \mathbf{x}_{j-1} \quad \text{for} \quad j = 2, 3 \ldots, n-1 \tag{8.3}$$

From this point of view, the vectors $\mathbf{x}_2, \ldots, \mathbf{x}_r$ are generated by successively solving the above equations as long as there exist solutions to the nonhomogeneous equation (8.3). The vectors of a Jordan chain are linearly independent. See Lancaster and Tismenetsky (1985) for the proof.

The subspace generated by the elements of a Jordan chain of A of length r:

$$\mathcal{J}_r = \operatorname{span}\{\mathbf{x}_1, \mathbf{x}_2, \ldots, \mathbf{x}_r\} \tag{8.4}$$

is defined as the **Jordan subspace**.

Any Jordan subspace for A contains only one (linearly independent) eigenvector and it is A-invariant.

Let $A : V \to V$ be a linear transformation and let the subspace $V_0 \subset V$ be A-invariant. If $\mathbf{x} \in V_0$ and there exists a basis in V_0 of the form

$$\{\mathbf{x}, A(\mathbf{x}), \ldots, A^{k-1}(\mathbf{x})\}, \quad k = \dim(V_0) \tag{8.5}$$

then V_0 is said to be a **cyclic subspace** of V (with respect to A or $A|_{V_0}$).

By induction, $A^j(\mathbf{x}_r)$ is a linear combination of $\mathbf{x}_1, \mathbf{x}_2, \ldots, \mathbf{x}_r$. Hence the set (8.5) is also a basis of the Jordan subspace. Since the Jordan subspace is A-invariant and $\mathbf{x}_r$ is in this subspace, it follows that the Jordan subspace is cyclic with respect to A.

Let $A : V \to V$ and let $E_p = \operatorname{Ker}(A - \lambda I)^p$ be the generalised eigenspace of A of maximal order p associated with the eigenvalue λ, that is, $E_{p-1} \neq E_p = E_{p+1}$.

Theorem 8.1. *There exists a unique decomposition*

$$E_p = \sum_{i=1}^{t_p} \cdot \mathcal{J}_p^{(i)} \oplus \sum_{i=1}^{t_{p-1}} \cdot \mathcal{J}_{p-1}^{(i)} \oplus \cdots \oplus \sum_{i=1}^{t_1} \cdot \mathcal{J}_1^{(i)}$$

where $\mathcal{J}_j^{(i)}$, $1 \leq j \leq p$, $1 \leq i \leq t_j$ is a cyclic Jordan subspace of dimension j and $\sum_{i=1}^{t_j} \cdot \mathcal{J}_j^{(i)}$ means a direct sum of t_j cyclic Jordan subspaces $\mathcal{J}_j^{(i)}$, which are j-dimensional.

Proof. See Lancaster and Tismenetsky (1985). □

Theorem 8.1 implies that there exists a basis in $\ker(A-\lambda I)^p$ consisting of Jordan chains; each chain is a basis in a cyclic Jordan subspace $\mathcal{J}_j^{(i)}$. Starting with $j=p$, we have the basis

$$
\begin{array}{l||llllll}
\mathcal{J}_p^{(1)} & \mathbf{x}_1^{(1)}, & \mathbf{x}_2^{(1)}, & \ldots, & \mathbf{x}_{p-1}^{(1)}, & \mathbf{x}_p^{(1)}, \\
\vdots & \vdots & \vdots & & \vdots & \vdots \\
\mathcal{J}_p^{(t_p)} & \mathbf{x}_1^{(t_p)}, & \mathbf{x}_2^{(t_p)}, & \ldots, & \mathbf{x}_{p-1}^{(t_p)}, & \mathbf{x}_p^{(t_p)}, \\
\mathcal{J}_{p-1}^{(t_p+1)} & \mathbf{x}_1^{(t_p+1)}, & \mathbf{x}_2^{(t_p+1)}, & \ldots, & \mathbf{x}_{p-1}^{(t_p+1)}, & \\
\vdots & \vdots & \vdots & & \vdots & \\
\mathcal{J}_{p-1}^{(t_p+t_{p-1})} & \mathbf{x}_1^{(t_p+t_{p-1})}, & \mathbf{x}_2^{(t_p+t_{p-1})}, & \ldots, & \mathbf{x}_{p-1}^{(t_p+t_{p-1})}, & \\
\vdots & \vdots & & & & \\
\vdots & \vdots & & & & \\
\mathcal{J}_1^{(t-t_1+1)} & \mathbf{x}_1^{(t-t_1+1)}, & & & & \\
\vdots & \vdots & & & & \\
\mathcal{J}_1^{(t)} & \mathbf{x}_1^{(t)}, & & & &
\end{array}
\tag{8.6}
$$

where $t=\sum_{j=1}^{p} t_j$ and the elements of each row form a Jordan chain of maximal possible length. Also, the elements of column r in (8.6) are generalised eigenvectors of A of order r associated with λ. The basis (8.6) of $\ker(A-\lambda I)^p$ is called a **Jordan basis** of the generalised eigenspace.

The cyclic Jordan subspace of dimension r, $\mathcal{J}_r$, is spanned by

$$
(A-\lambda_i I)^{r-1}(\mathbf{x}), \ldots, (A-\lambda_i I)(\mathbf{x}), \mathbf{x} \tag{8.7}
$$

where λ_i is an eigenvalue of A and $\mathbf{x}$ is a generalised eigenvector of A of order r associated with λ_i. Denote $\mathbf{x}_j=(A-\lambda_i I)^{r-j}(\mathbf{x})$. Then the above basis is expressed as

$$
\mathbf{x}_1, \mathbf{x}_2, \ldots, \mathbf{x}_r
$$

Since

$$
\begin{aligned}
A(\mathbf{x}_1) &= \lambda \mathbf{x}_1, \\
A(\mathbf{x}_2) &= \lambda \mathbf{x}_2 + \mathbf{x}_1, \\
&\vdots \\
A(\mathbf{x}_r) &= \lambda \mathbf{x}_r + \mathbf{x}_{r-1},
\end{aligned}
$$

the representation $J_r = (\alpha_{ij})_{i,j=1}^r$ of $A|_{\mathcal{J}_r}$ with respect to the basis (8.7) is

$$J_r = \begin{pmatrix} \lambda_i & 1 & 0 & \cdots & 0 \\ 0 & \lambda_i & 1 & \cdots & \vdots \\ \vdots & \ddots & \ddots & \ddots & 0 \\ \vdots & \ddots & \ddots & \ddots & 1 \\ 0 & \cdots & \cdots & 0 & \lambda_i \end{pmatrix} \tag{8.8}$$

which is called a **Jordan block** of order r corresponding to the eigenvalue λ_i. A Jordan block has λ_i's on the main diagonal, 1's on the superdiagonal, and 0's elsewhere.

Let $A : V \to V$ with distinct eigenvalues $\lambda_1, \ldots, \lambda_s$. Choosing in each generalised eigenspace $E_{\lambda_i, m_i} = \ker(A - \lambda_i I)^{m_i}$, $1 \leq i \leq s$, a Jordan basis of the form (8.6), we obtain a Jordan basis for the whole space V as a union of Jordan bases. This union is described as a **A-Jordan basis** for V.

Theorem 8.2. *In the notation of the preceding paragraph, the representation of A with respect to a A-Jordan basis is the matrix*

$$J = diag[J(\lambda_1), J(\lambda_2), \ldots, J(\lambda_s)] \tag{8.9}$$

where for $1 \leq i \leq s$,

$$J(\lambda_i) = diag[J_p^{(i)}, \ldots, J_p^{(i)}, J_{p-1}^{(i)}, \ldots, J_{p-1}^{(i)}, \ldots, J_1^{(i)}, \ldots, J_1^{(i)}] \tag{8.10}$$

in which the $j \times j$ matrix $J_j^{(i)}$ of the form (8.8) appears $t_j^{(i)}$ times in (8.10).

Proof. See Lancaster and Tismenetsky (1985). □

Note that the number of Jordan blocks in $J(\lambda_i)$ is equal to the number of rows in (8.6), that is, to the geometric multiplicity of the eigenvalue λ_i. The sum of the dimensions of all Jordan blocks associated with λ_i is equal to the algebraic multiplicity of λ_i.

The representation of J in (8.9) and (8.10) is called a **Jordan normal form** of the transformation A.

Corollary 8.1. *Any complex square matrix A is similar to a Jordan normal form that is uniquely determined by A up to the permutation of the matrices $J(\lambda_i)$ in (8.9) and the Jordan blocks in (8.10).*

Proof. See Lancaster and Tismenetsky (1985). □

8.2.4 Lattice Theory: Part 3

An equivalence relation θ on a lattice L which is compatible with both join and meet is called a **congruence** on L; that is for all $a, b, c, d \in L$

$$a \equiv b(\mathrm{mod}\theta) \quad \text{and} \quad c \equiv d(\mathrm{mod}\theta)$$

imply

$$a \vee c \equiv b \vee d(\mathrm{mod}\theta) \quad \text{and} \quad a \wedge c \equiv b \wedge d(\mathrm{mod}\theta)$$

A congruence on a lattice L can be indicated on a diagram by placing a loop or square around the elements in each block of the corresponding partition.

Given an equivalence relation θ on a lattice L there is a natural way to try to define operations $\vee$ and $\wedge$ on the set

$$L/\theta := \{[a]_\theta | a \in L\}$$

of blocks. Namely, for all $a, b \in L$, we define

$$[a]_\theta \vee [b]_\theta := [a \vee b]_\theta \quad \text{and} \quad [a]_\theta \wedge [b]_\theta := [a \wedge b]_\theta$$

This will produce well-defined operations precisely when the definitions are independent of the elements chosen to represent the equivalence classes, that is, when

$$[a_1]_\theta = [a_2]_\theta \quad \text{and} \quad [b_1]_\theta = [b_2]_\theta$$

imply

$$[a_1 \vee b_1]_\theta = [a_2 \vee b_2]_\theta \quad \text{and} \quad [a_1 \wedge b_1]_\theta = [a_2 \wedge b_2]_\theta$$

for all $a, b \in L$. Since, for all $a_1, a_2 \in L$,

$$[a_1]_\theta = [a_2]_\theta \Leftrightarrow a_1 \in [a_2]_\theta \Leftrightarrow (a_1, a_2) \in \theta \Leftrightarrow a_1 \equiv a_2(\mathrm{mod}\theta)$$

It follows that $\vee$ and $\wedge$ are well defined on L/θ if and only if θ is a congruence. When θ is a congruence on L, we call $\langle L/\theta; \vee, \wedge \rangle$ the **quotient lattice of L modulo θ**.

When considering the blocks of a congruence θ on L, it is best to think of each block as an entity in its own right rather than as the block $[a]_\theta$ associated with some $a \in L$. Intuitively, the quotient lattice L/θ is obtained by collapsing each block to a point.

Lemma 8.3. *Let θ be a congruence on the lattice L. Then $\langle L/\theta; \vee, \wedge \rangle$ is a lattice and the natural quotient map $q : L \to L/\theta$, defined by $q(a) := [a]_\theta$ is a homomorphism.*

Proof. See Davey and Priestley (1990). □

8.2.5 n Repeated Eigenvalues of n-cell Networks

The following result is trivial, however, we provide a proof here.

Proposition 8.1. *Let $\mathcal{G}$ be an n-cell regular homogeneous coupled cell network of valency r associated with the $n \times n$ adjacency matrix A. Let $\lambda_0, \lambda_1, \ldots, \lambda_{n-1}$ be the n eigenvalues of A, including repeated eigenvalues. If $\lambda_0 = \lambda_1 = \cdots = \lambda_{n-1} = r$, then $\mathcal{G}$ is disconnected.*

Proof. If $(\lambda_0, \ldots, \lambda_{n-1}) = (r, \ldots, r)$, then A is similar to the following diagonal matrix:

$$\begin{pmatrix} r & 0 & 0 & \cdots & 0 \\ 0 & r & 0 & \cdots & 0 \\ \vdots & \ddots & \ddots & \ddots & \vdots \\ 0 & \cdots & 0 & r & 0 \\ 0 & \cdots & 0 & 0 & r \end{pmatrix} = rI_n$$

This matrix describes n isolated nodes with r self-coupling to themselves, hence it is a disconnected network. Since the identity matrix is similar only to itself, there is no other connected homogeneous network which is similar to A. □

8.3 Isomorphic Quotient Networks

We firstly show that a double eigenvalue with geometric multiplicity two generates multiple polydiagonals from its eigenvector structure.

Proposition 8.2. *Let A be a 3×3 adjacency matrix with double eigenvalue λ. If there exist two linearly independent eigenvectors $\mathbf{v}_1$ and $\mathbf{v}_2$ associated with the eigenvalue λ, then $\mathbf{v}_1$ and $\mathbf{v}_2$ generate three non-trivial balanced equivalence relations.*

Proof. Up to the permutation of the positions of coordinates, the eigenvector with geometric multiplicity two can be written as:

$$(x_1, x_2, x_3) = (\alpha, \beta, l\alpha + m\beta), \tag{8.11}$$

where $\alpha, \beta \in \mathbb{R}$ and l, m are any scalars for α and β.

Since $\triangle = \{(x_1, x_2, x_3) | x_1 = x_2 = x_3\}$ is always an eigenvector of a given regular homogeneous network with eigenvalue equal to the valency, any eigenvector expressed in (8.11) must be linearly independent of vectors in $\triangle$.

There are three possible pattern of synchrony (excluding trivial balanced equivalence relations) depending on the values of α, β and their scalars such as

$$\begin{aligned}(x_1, x_2, x_3) &= (u, u, v) \quad \text{if} \quad \alpha = \beta,\\ (x_1, x_2, x_3) &= (u, v, u) \quad \text{if} \quad \alpha = l\alpha + m\beta,\\ (x_1, x_2, x_3) &= (v, u, u) \quad \text{if} \quad \beta = l\alpha + m\beta.\end{aligned}$$

which are linearly independent of the diagonal subspace $\triangle$.

These three forms of the eigenvector have only two distinct entries. Therefore, by Lemma 7.7, the corresponding equivalence relations generated from above three eigenvector structures are balanced.

Hence, if the corresponding eigenvector to the double eigenvalue λ has geometric multiplicity two, there exist three non-trivial balanced equivalence relations (or equivalently three non-trivial balanced polydiagonals). □

This result shows that a 2-dimensional eigenspace can generate 3 balanced polydiagonals, which is more than the algebraic multiplicity of the corresponding eigenvalue.

Lemma 7.8, states that

$$L_{\bowtie_1} = L_{\bowtie_2} \Rightarrow \triangle_{\bowtie_1} = \triangle_{\bowtie_2}$$

is true when the associated matrix of a given regular homogeneous has distinct eigenvalues (simple). However, this is not always true for networks with non-simple eigenvalues. We now show that non-simple eigenvalue networks can generate the same set of eigenvalues of quotient networks from different balanced equivalence relations.

Lemma 8.4. *Let A be the $n \times n$ adjacency matrix of an n-cell regular homogeneous coupled cell network $\mathcal{G}$. If A has repeated eigenvalues, then there exist equivalence relations $\bowtie_1 \neq \bowtie_2$ with rank($\bowtie_1$) = rank($\bowtie_2$) such that $L_{\bowtie_1} = L_{\bowtie_2}$.*

Proof. Let $\lambda_1, \ldots, \lambda_k$ where $k < n$ be the distinct eigenvalues of A. Then Jordan normal form of A is:

$$\begin{pmatrix} J(\lambda_1) & \mathbf{0} & \cdots & \cdots & \mathbf{0} \\ \mathbf{0} & J(\lambda_2) & \mathbf{0} & \cdots & \mathbf{0} \\ \vdots & \ddots & \ddots & \ddots & \mathbf{0} \\ \mathbf{0} & \cdots & \cdots & \mathbf{0} & J(\lambda_k) \end{pmatrix}$$

where $J(\lambda_i)$, $i = 1, \ldots, k$ has $g(\lambda_i)$ Jordan blocks, where $g(\lambda_i)$ is the geometric multiplicity of the eigenvalue λ_i.

Jordan blocks associated with the eigenvalue λ_i have the form:

$$\begin{pmatrix} \lambda_i & 1 & \cdots & \cdots & 0 \\ 0 & \lambda_i & 1\cdots & \cdots & 0 \\ \vdots & \ddots & \ddots & \ddots & 0 \\ 0 & \cdots & \cdots 0 & \lambda_i & 1 \\ 0 & \cdots & \cdots & 0 & \lambda_i \end{pmatrix}$$

where all superdiagonal elements are ones and all unmarked elements are zeros.

Since there is a bijection between $\bowtie \in \Lambda_{\mathcal{G}}$ and $\triangle_{\bowtie} \in V_{\mathcal{G}}^P$, there are the corresponding balanced polydiagonals $\triangle_{\bowtie_1}$ and $\triangle_{\bowtie_2}$ for the balanced equivalence relations $\bowtie_1$ and $\bowtie_1$, respectively, which satisfy $\triangle_{\bowtie_1} \neq \triangle_{\bowtie_2}$ with $\dim(\triangle_{\bowtie_1}) = \dim(\triangle_{\bowtie_2})$. Let $\mathbf{v}_1, \ldots, \mathbf{v}_n$ be n generalised eigenvectors of the $n \times n$ adjacency matrix A. Let $s = \dim(\triangle_{\bowtie_1}) = \dim(\triangle_{\bowtie_2})$. Suppose $\triangle_{\bowtie_1}$ and $\triangle_{\bowtie_2}$ are spanned by

$$\begin{aligned} \triangle_{\bowtie_1} &= \text{span}\{\mathbf{v}_1^1, \mathbf{v}_2^1, \ldots, \mathbf{v}_s^1\} \quad \text{and} \\ \triangle_{\bowtie_2} &= \text{span}\{\mathbf{v}_1^2, \mathbf{v}_2^2, \ldots, \mathbf{v}_s^2\} \end{aligned}$$

where $\{\mathbf{v}_1^1, \ldots, \mathbf{v}_s^1\} \neq \{\mathbf{v}_1^2, \ldots, \mathbf{v}_s^2\}$ are sets of s vectors chosen from $\{\mathbf{v}_1, \ldots, \mathbf{v}_n\}$ as a basis of $\triangle_{\bowtie_1}$ and $\triangle_{\bowtie_2}$, respectively. We can complete the above bases of $\triangle_{\bowtie_i}$ to obtain bases of $\mathbb{R}^n$. The matrix A with respect to these bases has the structures:

$$\left(\begin{array}{c|c} A_{\bowtie_1} & B_1 \\ \hline \mathbf{0} & D_1 \end{array}\right), \quad \text{and} \quad \left(\begin{array}{c|c} A_{\bowtie_2} & B_2 \\ \hline \mathbf{0} & D_2 \end{array}\right)$$

respectively, where $A_{\bowtie_i}$ is the $s \times s$ adjacency matrix of the quotient network $\mathcal{G}/_{\bowtie_i}$ for $i = 1, 2$.

There are $s \times s$ Jordan normal forms which are similar to $A_{\bowtie_1}$ and $A_{\bowtie_2}$. Since A has repeated eigenvalues, some diagonal elements in its Jordan blocks are equal. Hence $A_{\bowtie_1}$ and $A_{\bowtie_2}$ can have the same set of eigenvalues. Therefore, there exist $\triangle_{\bowtie_1} \neq \triangle_{\bowtie_2}$, equivalently $\bowtie_1 \neq \bowtie_2$ such that $L_{\bowtie_1} = L_{\bowtie_2}$. □

Furthermore, some quotient networks can be topologically identical. The following proposition follows from Lemma 8.4:

Proposition 8.3. *Let A be the $n \times n$ adjacency matrix of an n-cell regular homogeneous network $\mathcal{G}$. Let $\mathcal{G}/_{\bowtie}$ be a quotient network of $\mathcal{G}$ restricted to a balanced polydiagonal $\triangle_{\bowtie}$. If A has repeated eigenvalues, there exist $\bowtie_1 \neq \bowtie_2$ such that $\mathcal{G}/_{\bowtie_1} \cong \mathcal{G}/_{\bowtie_2}$.*

Proof. Lemma 8.4 states that there exist $\bowtie_1 \neq \bowtie_2$ with $\text{rank}(\bowtie_1) = \text{rank}(\bowtie_2)$ such that $L_{\bowtie_1} = L_{\bowtie_2}$. Now we show that for such $L_{\bowtie_1}$ and $L_{\bowtie_2}$, the corresponding quotient networks $\mathcal{G}/_{\bowtie_1}$

and $\mathcal{G}/_{\bowtie_2}$ can be topologically identical. Theorem 7.5 states that if $\mathcal{G}/_{\bowtie_1} \cong \mathcal{G}/_{\bowtie_2}$, then the corresponding adjacency matrices $A_{\bowtie_1}$ and $A_{\bowtie_2}$ are similar. The converse is not always true, however, it is true if $A_{\bowtie_1}$ and $A_{\bowtie_2}$ are permutation similar. Hence, there exist $\bowtie_1 \neq \bowtie_2$ such that $\mathcal{G}/_{\bowtie_1} \cong \mathcal{G}/_{\bowtie_2}$. □

8.4 Reduction of Lattices

So far, we have shown that an eigenspace which has dimension more than one can generate more balanced equivalence relations than the algebraic multiplicity of the corresponding eigenvalue (Proposition 8.2). Proposition 8.3 states that these balanced equivalence relations generated from the eigenvector structure whose geometric multiplicity is more than one can lead to topologically identical quotient networks. Now we consider a method to exclude additional balanced equivalence relations (or equivalently topologically identical quotient networks) from the lattice using a congruence relation. We motivate our discussion in the following example.

Example 8.2. Consider regular homogeneous four-cell valency 2 network #1. The associated adjacency matrix has a triple eigenvalue $\lambda_1 = \lambda_2 = \lambda_3 = 0$ and the corresponding eigenvector has the geometric multiplicity three as shown in Table 8.2. The lattice of balanced equivalence

Network #1	Adjacency matrix	Eigenvalues	Eigenvectors
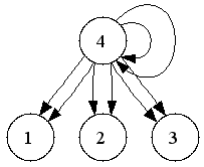	$\begin{pmatrix} 0 & 0 & 0 & 2 \\ 0 & 0 & 0 & 2 \\ 0 & 0 & 0 & 2 \\ 0 & 0 & 0 & 2 \end{pmatrix}$	$\lambda_0 = 2$ $\lambda_1 = 0$ $\lambda_2 = 0$ $\lambda_3 = 0$	$(1,1,1,1)$ $\Big\}(\alpha,\beta,\gamma,0)$

Table 8.2: Four-cell network #1 with a triple eigenvalue and three eigenvectors.

relations of this network is the same as the partition lattice of the set of four elements as shown in Figure 8.3. This shows there are seven two-cell quotient networks and six three-cell quotient networks corresponding to non-trivial balanced equivalence relations. The reason why there are so many balanced equivalence relations is because of the degree of freedom of the eigenvector structure $(\alpha, \beta, \gamma, 0)$ corresponding to the triple eigenvalue. However, we observe that all seven two-cell quotient networks are topologically identical, as are all six three-cell quotient networks, as shown in Figure 8.4. This poses a question: *can we simplify the lattice?*

The eigenvalue structure $(\alpha, \beta, \gamma, 0)$ corresponding to the triple eigenvalue $\lambda_1 = \lambda_2 = \lambda_3 = 0$ shows there are seven possible coordinate structures which have only two distinct entries, e.g. $(1,0,0,0), (1,1,0,0), \ldots$. As shown in Lemma 7.7, all equivalence relations generated from these seven eigenvector structures are balanced. Furthermore, we observe that the six balanced

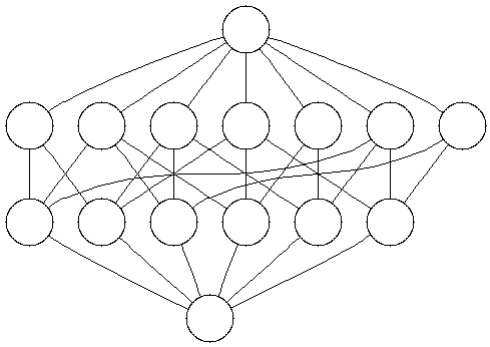

Figure 8.3: The lattice of balanced equivalence relations of four-cell network #1, which has the same structure as the partition lattice of the set of four elements.

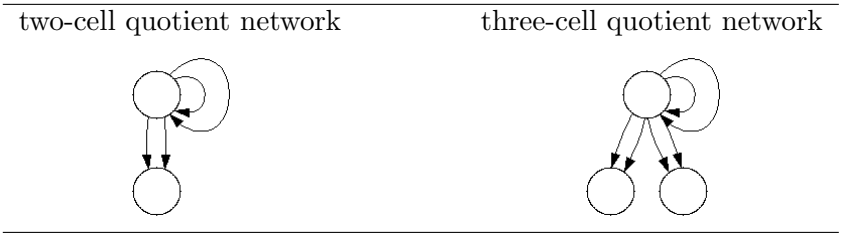

Figure 8.4: Two-cell and three-cell quotient network topology of four-cell network #1.

equivalence relations in rank 3 are generated by taking several combinations of intersections from balanced equivalence relations in rank 2 as shown in Corollary 7.1. Therefore the seven balanced equivalence relations are considered to be lattice generators.

In simple eigenvalue networks, lattice generators have a one-to-one relationship with eigenvectors. However, for this non-simple eigenvalue network #1, we have seven lattice generators versus three linearly independent eigenvectors.

In simple eigenvalue networks, we showed that all quotient network are topologically distinct (Corollary 7.2). So if we try to simplify the original lattice by merging all topologically identical quotient networks and assign $\eta(p)$ for each lattice node, we have a reduced lattice in Figure 8.5. The lattice of the sets of eigenvalues of quotient networks is shown next to the reduced lattice. The eigenvalue inheritance does not look right. For example, a double eigenvalue in rank 3 should be inherited from eigenvalues in rank 2, but the lattice of the sets of eigenvalues shows it comes from itself.

Instead, we consider weaker reduction by merging topologically identical quotient network without losing the dimension of eigenspace (three) as in Figure 8.6. This reduced lattice shows three lattice generators and the sets of eigenvalues of three-cell quotient networks shows their double eigenvalues are inherited from eigenvalues of two-cell quotient networks.

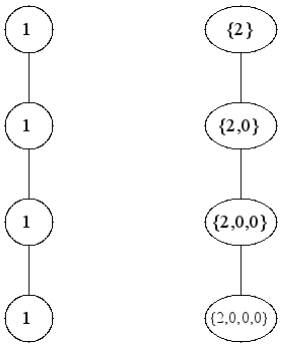

Figure 8.5: A fully reduced version of the lattice in Figure 8.3 for four-cell network #1, constructed by merging all lattice nodes with topologically identical quotient networks.

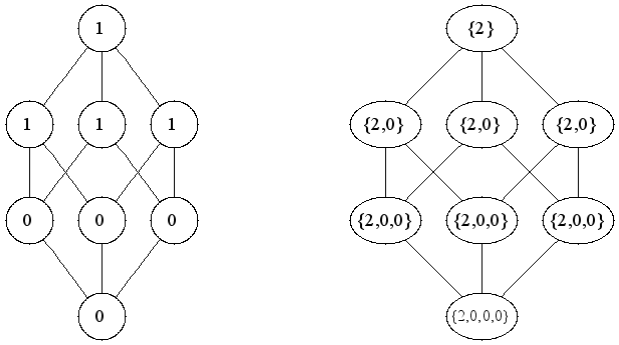

Figure 8.6: A minimally reduced version of the lattice in Figure 8.3, which unlike Figure 8.5, preserves the dimension of the eigenspace.

Finally, remember that the three lattice nodes in rank 2 represent seven balanced equivalence relations, which are generated from eigenvectors with two distinct entries. Hence there exist seven bifurcating branches from a bifurcation point corresponding to the triple eigenvalue (Lemma 7.13).

◇

Now we formalise the reduction method described in Example 8.2 as follows.

Let $\Lambda_{\mathcal{G}}$ be a lattice of balanced equivalence relations of a regular homogeneous network $\mathcal{G}$ with total phase space P. Each balanced equivalence relation $\bowtie \in \Lambda_{\mathcal{G}}$ determines the corresponding balanced polydiagonal $\triangle_{\bowtie}$. Let $Q^P_{\mathcal{G}}$ be the set of quotient networks of $\mathcal{G}$. Since a quotient network $\mathcal{G}/_{\bowtie}$ is uniquely determined by the equivalence relation $\bowtie$, there is a bijection between $\Lambda_{\mathcal{G}}$ and $Q^P_{\mathcal{G}}$, hence, $Q^P_{\mathcal{G}}$ forms a lattice. Meet and join operations in $Q^P_{\mathcal{G}}$ are defined by taking a meet and join operation of the corresponding balanced equivalence relations and determine a quotient network restricted to the corresponding balanced polydiagonal.

Lemma 8.5. *The graph isomorphism is a congruence on* $Q^P_{\mathcal{G}}$.

Proof. The graph isomorphism is trivially an equivalence relation. We show that the graph isomorphism is compatible with both join and meet.

Let $\mathcal{G}_{\bowtie_a} \cong \mathcal{G}_{\bowtie_b}$ and $\mathcal{G}_{\bowtie_c} \cong \mathcal{G}_{\bowtie_d}$, where $\mathcal{G}_{\bowtie_a}, \mathcal{G}_{\bowtie_b}, \mathcal{G}_{\bowtie_c}, \mathcal{G}_{\bowtie_d} \in Q^P_{\mathcal{G}}$.

If $\mathcal{G}_{\bowtie_a} \cong \mathcal{G}_{\bowtie_b}$, then the corresponding adjacency matrices $A_{\bowtie_a}$ and $A_{\bowtie_b}$ are similar, hence, $L_{\bowtie_a} = L_{\bowtie_b}$, where $L_{\bowtie_a}, L_{\bowtie_b} \in U^P_{\mathcal{G}}$. Similarly, $L_{\bowtie_c} = L_{\bowtie_d}$ for $L_{\bowtie_c}, L_{\bowtie_d} \in U^P_{\mathcal{G}}$. Therefore,

$$(L_{\bowtie_a} \vee L_{\bowtie_c}) = (L_{\bowtie_b} \vee L_{\bowtie_d}) \quad \text{and} \quad (L_{\bowtie_a} \wedge L_{\bowtie_c}) = (L_{\bowtie_b} \wedge L_{\bowtie_d})$$

Since there is an order-preserving map from $\bowtie \in \Lambda_{\mathcal{G}}$ to $L_{\bowtie} \in U^P_{\mathcal{G}}$, there are the corresponding elements in $\Lambda_{\mathcal{G}}$ such as:

$$(\bowtie_a \vee \bowtie_c) = (\bowtie_b \vee \bowtie_d) \quad \text{and} \quad (\bowtie_a \wedge \bowtie_c) = (\bowtie_b \wedge \bowtie_d)$$

Using a bijection map from $\Lambda_{\mathcal{G}}$ to $Q^P_{\mathcal{G}}$, we furthermore have

$$(\mathcal{G}_{\bowtie_a} \vee \mathcal{G}_{\bowtie_c}) \cong (\mathcal{G}_{\bowtie_b} \vee \mathcal{G}_{\bowtie_d}) \quad \text{and} \quad (\mathcal{G}_{\bowtie_a} \wedge \mathcal{G}_{\bowtie_c}) \cong (\mathcal{G}_{\bowtie_b} \wedge \mathcal{G}_{\bowtie_d})$$

Hence both join and meet operations are preserved and the graph isomorphism is a congruence on $Q^P_{\mathcal{G}}$. □

Once we find a congruence on a lattice $Q^P_{\mathcal{G}}$, we are free to choose which elements in each block (congruence) collapse to a single point. Because each lattice node contains information about the dimension of an eigenspace, we should not collapse too much. Now we define a **minimal reduced lattice** in the following:

Definition 8.1 (Reduction of Lattice). *Starting from rank 2, choose lattice elements from each congruence block, which is the set of topologically identical quotient networks. Then reduce the lattice size by clumping them accordingly clumping corresponding lattice elements in higher ranks. Repeat this procedure until the lattice has the same structure as one of simple eigenvalue network lattice structures. We define this lattice as a* ***minimal reduced lattice*** *of the original lattice.*

Definition 8.2. *Define the congruence defined in Lemma 8.5 as $\circledast$. Define the congruence described in 8.1 as $\underline{\circledast}$, which covered by $\circledast$; that is $\underline{\circledast} \prec \circledast$.*

By Lemma 8.3, the quotient map $q : Q^P_{\mathcal{G}} \to Q^P_{\mathcal{G}}/\underline{\circledast}$ is a homomorphism, which means both meet and join operations are preserved. In lattice $U^P_{\mathcal{G}}$, this reduction minimally merges sets which contain the same set of eigenvalues. Hence, the reduced lattice structure contains the same information in simple eigenvalue network lattice structures to determine from which lattice node independent eigenvalues appear. Therefore, using reduced lattice structures, we assign $\eta(p)$ to each lattice node as defined in (7.11) to determine the existence of bifurcating branches.

8.5 Three-cell Networks: Lattice Structures and Steady-state Bifurcations

Leite and Golubitsky (2006) classified the possible generic steady-state bifurcations of regular homogeneous three-cell networks using an eigenvalue structure and the corresponding eigenvector structure of a 3×3 adjacency matrix of a network as follows:

S1	simple eigenvalues
S2	double eigenvalues and two eigenvectors
S3	double eigenvalues and one eigenvector
S4	double eigenvalues and one eigenvector in $\triangle$ (fully synchronous subspace)

Note that we can exclude the possibility that all eigenvalues are equal by Proposition 8.1.

We use the same notation for three-cell network classification for the rest of the analysis. In Chapter 7, we showed that all adjacency matrices of quotient networks have simple eigenvalues when the original network has an adjacency matrix with simple eigenvalues, i.e., type $S1$ networks have type $S1$ quotient networks. On the contrary, networks with non-simple eigenvalues can have combinations of different types of networks as quotient networks.

In this section, we consider the reduction of lattices of three-cell networks. We show that only type $S2$ three-cell networks need a reduction of lattices. Then we determine the existence of bifurcation branches from their reduced lattice structures. These results from lattice structure match those of Leite and Golubitsky (2006) using graph decomposition and the implicit function theorem.

8.5.1 S2: Double Eigenvalues and Two Eigenvectors

Proposition 8.4. *There are two possible lattice structures for type $S2$ three-cell networks, shown in Figure 8.7.*

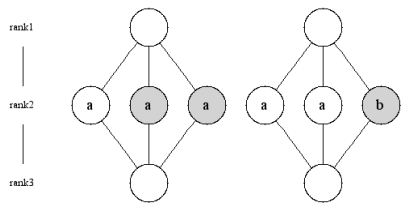

Figure 8.7: Lattices of balanced equivalence relations of three-cell networks of type $S2$. Shaded lattice nodes correspond to the balanced equivalence relations generated by eigenvector structures.

Proof. There are three balanced equivalence relations in rank 2 for $S2$ networks as shown in Proposition 8.2. Since Proposition 8.3 implies the existence of topologically identical quotient networks, there are three possibilities for the topology of quotient networks in rank 2.

The first case is all three two-cell quotient networks are topologically identical as shown on the left lattice in Figure 8.7.

The second case is two-cell quotient networks are topologically identical and the third two-cell quotient network is topologically distinct from other two networks as shown on the right lattice as shown in Figure 8.7.

The third case is all three two-cell quotient networks are topologically distinct. However, we can exclude this possibility since there are at most two topologically distinct 2-cell networks with the same spectrum (shown in Chapter 6).

Hence if there are three 2-cell quotient networks with the same set of eigenvalues, then at least two of them are topologically identical.

The labels "a" and "b" in rank 2 describe quotient network topology. When all three lattice nodes have the same label "a", this means all three two-cell quotient networks are topologically identical (although their equivalence relations are different). On the other hand, two lattice nodes labelled "a" and the third node labelled "b" means two of two-cell quotient networks are topologically identical, but the third two-cell quotient network is topologically distinct from other two networks. □

We did not observe the above lattice structures in three-cell networks with simple eigenvalues. Also these lattice structure break the dimension rule as the bottom lattice node has three edges from rank 2 nodes. We now reduce these lattice structures to one of 3 lattice structures observed in simple eigenvalue three-cell networks and determine the existence of bifurcating branches and its types. We show this procedure through an example.

Example 8.3. Consider three-cell valency 2 regular homogeneous network #1, which has repeated eigenvalue 0 with the algebraic multiplicity 2 and the geometric multiplicity 2 shown in Table 8.3.

Network #1	Adjacency matrix	Eigenvalues	Eigenvectors
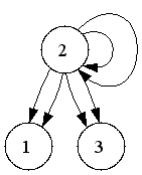	$\begin{pmatrix} 0 & 2 & 0 \\ 0 & 2 & 0 \\ 0 & 2 & 0 \end{pmatrix}$	$\lambda_0 = 2$ $\lambda_1 = 0$ $\lambda_2 = 0$	$(1,1,1)$ $\}(\alpha, 0, \beta)$

Table 8.3: Three-cell network #1. α,$\beta \in \mathbb{R}$

Figure 8.8 is the lattice of balanced equivalence relations. Each lattice describes which

cell coordinates are equal to generate a corresponding quotient network. The lattice nodes are labelled as in Example 8.1.

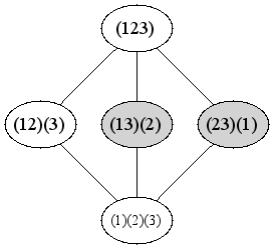

Figure 8.8: Lattice of balanced equivalence relations of three-cell network #1. Shaded lattice nodes are generated from the eigenvector structures.

Three two-cell quotient networks corresponding to the three balanced equivalence relations in Figure 8.8 are listed in Figure 8.9. Observe that all three quotient networks are topologically identical.

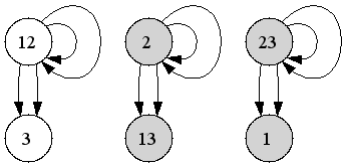

Figure 8.9: Topologically identical three two-cell quotient networks. Shaded quotient networks are determined by the balanced equivalence relations generated by the eigenvector structures.

Now, we reduce the lattice structure of Figure 8.8 by merging the lattice nodes, which corresponds to topologically identical quotient networks, but keeping the same number of nodes as the dimension of eigenspace (in this case, the dimension is two) as described in Definition 8.1.

In this example there are three nodes with topologically identical corresponding quotient networks, but we only merge two of them, as illustrated in Figure 8.10.

The congruence block is expressed by placing a rectangle box in Figure 8.10. We then assign $\eta(p)$ for each lattice node in the minimal reduced lattice.

In the reduced lattice, the label "1_a" means there exists one bifurcating branch whose bifurcation type is determined by a quotient network structure labelled by "a" and which lie in the corresponding balanced polydiagonal.

Since $\eta(\perp) = 0$, from Theorem 7.4, all synchrony-breaking bifurcating branches are analysed from quotient networks and there are not any other bifurcating branches.

In the original lattice, there are three balanced equivalence relations, equivalently three

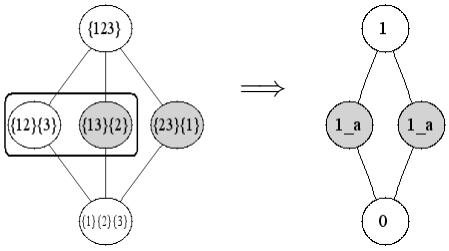

Figure 8.10: Reduction of lattice by merging the lattice nodes corresponding to topologically identical quotient networks.

balanced polydiagonals $(x_1, x_2, x_3) = (u, u, v), (u, v, u), (v, u, u)$, generated by double eigenvalue 0. Therefore, we expect there exist three synchrony-breaking bifurcation branches, along above three polydiagonals, whose bifurcation types are determined by the two-cell quotient networks in Figure 8.9. In chapter 5, we showed the corresponding two-cell network shows the existence of transcritical bifurcation. Hence, we expect there are three transcritical bifurcation branches from the trivial solution at the bifurcation point corresponding to the eigenvalue $\lambda_1 = \lambda_2 = 0$, which lie on three different polysynchronous subspaces $(x_1, x_2, x_3) = (u, u, v), (u, v, u), (v, u, u)$, where $u, v \in \mathbb{R}$.

$\diamond$

Leite and Golubitsky (2006) show that $S2$ bifurcations lead to multiple nontrivial bifurcating branches as opposed to $S1$ bifurcations which lead to a unique nontrivial branch. In their analysis of three-cell network #1 (number four in their notation which is ODE-equivalent to network #1), there exist three transcritical branches bifurcating from the trivial solution. This agrees with the above analysis from the lattice structure.

8.5.2 S3: Double Eigenvalues and One Eigenvector

The following Figure 8.11 shows observed lattice structure of type $S3$ three-cell networks of valency 2 with double eigenvalues and one eigenvector.

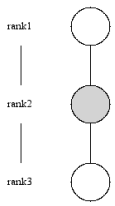

Figure 8.11: Lattice of balanced equivalence relations of three-cell networks of type S3, where shaded nodes correspond to the balanced equivalence relations generated by eigenvector structures.

Since the dimension of the eigenspace associated with the double eigenvalue is one, unlike $S2$ networks, the one-dimensional eigenspace does not generate multiple possible polydiagonals. Hence a reduction of lattices is not necessary for type $S3$ networks. We can assign $\eta(p)$ for each lattice node directly as the following example shows.

Example 8.4. Consider three-cell valency 2 regular homogeneous network #28 shown in Table 8.4.

Network #28	Adjacency matrix	Eigenvalues	Eigenvectors
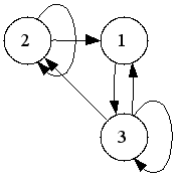	$\begin{pmatrix} 0 & 1 & 1 \\ 0 & 1 & 1 \\ 1 & 0 & 1 \end{pmatrix}$	$\lambda_0 = 2$ $\lambda_1 = 0$ $\lambda_2 = 0$	$(1,1,1)$ $(\alpha,\alpha,-\alpha)$

Table 8.4: Three-cell network #28. $\alpha \in \mathbb{R}$

The geometric multiplicity of eigenvector corresponding to the double eigenvalue $\lambda_1 = \lambda_2 = 0$ is one.

Figure 8.12 shows the lattice of balanced equivalence relations on the left. $\eta(p)$ is assigned for each lattice node on the right figure.

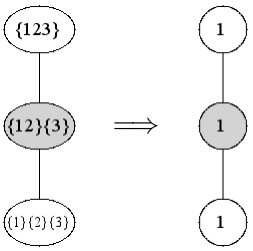

Figure 8.12: Lattice of balanced equivalence relations of three-cell network #28 (left) and the assigned $\eta(p)$ values (right). The shaded balanced equivalence relation is generated from the eigenvector structure associated with the double eigenvalue 0.

There is only one two-cell quotient network shown in Figure 8.13, which guarantee the existence of a pitchfork bifurcation.

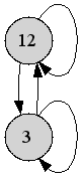

Figure 8.13: Two-cell quotient network of three-cell network #28.

Since there is non-zero lattice node in rank 2 and rank 3, we expect to have two synchrony-breaking bifurcating branches from the trivial solution: one is a pitchfork branch in a balanced polydiagonal $(x_1, x_2, x_3) = (u, u, v)$ and the other does not lie in none of synchronous subspace, i.e., all three state variables are different, and its bifurcation type would be obtained by the analysis of the original three-cell network. Both branches bifurcate from the bifurcation point corresponding to the eigenvalue $\lambda_1 = \lambda_2 = 0$.

$\diamond$

Leite and Golubitsky (2006) show that $S3$ bifurcations lead to two non-trivial bifurcating branches. Their analysis shows that three-cell network #28 (six in their reference numbering) has two branches of asynchronous solutions bifurcating from the trivial solution; when viewed in cell 3 one is transcritical and the other is pitchfork in a polydiagonal $(x_1, x_2, x_3) = (u, u, v)$.

8.5.3 S4: Double Eigenvalues and One Eigenvector in $\triangle$

Proposition 8.5. *Let $\mathcal{G}$ be an n-cell regular homogeneous network with valency r with $n \times n$ adjacency matrix A. If A has a double eigenvalue $\lambda_0 = \lambda_1 = r$, as a consequence one eigenvector associated with the double eigenvalue is in a fully synchronous subspace $\triangle$, then the eigenvector associated with this double eigenvalue generates at most one non-trivial balanced polydiagonal.*

Proof. There are two possibilities for the geometric multiplicity for the eigenvector corresponding to the valency double eigenvalue; either one or two. If the geometric multiplicity is one, then the eigenvector is $(1, 1, \ldots, 1) = \triangle$ as this is always the eigenvector associated with the valency eigenvalue of a homogeneous network.

Now we consider the case of the geometric multiplicity being two. One of eigenvectors can be taken as the fully synchronous subspace, i.e., $\triangle$ and we will write $\mathbf{v}$ for the second eigenvector. Any polydiagonal generated from an eigenvector $\mathbf{v}$ is given by $\mathbb{R}\{(1, \ldots, 1), \mathbf{v}\}$. Hence if there is any non-trivial polydiagonal generated from the eigenvector associated with a double eigenvalue, it is expressed as $\mathbb{R}\{(1, \ldots, 1), \mathbf{v}\}$. Whether this is balanced or not depends on the linear transformation described by the matrix A. Hence there is at most one non-trivial balanced polydiagonal generated from the double eigenvalue and one eigenvector in $\triangle$. $\square$

As a consequence of Proposition 8.5, the reduction of lattices for type $S4$ networks is not required because two linearly independent eigenvectors generate at most one non-trivial balanced equivalence relation.

Figure 8.14 shows observed lattice of balanced equivalence relations of type $S4$ three-cell regular homogeneous networks of valency 2 with double eigenvalues and one eigenvectors in $\triangle$.

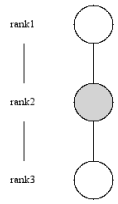

Figure 8.14: Lattice of balanced equivalence relations of three-cell networks of type S4, where the shaded nodes correspond to the balanced equivalence relations generated by eigenvector structures.

Example 8.5. Consider three-cell valency 2 regular homogeneous network #30 shown in Table 8.5.

Network #30	Adjacency matrix	Eigenvalues	Eigenvectors
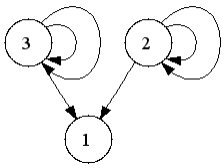	$\begin{pmatrix} 0 & 1 & 1 \\ 0 & 2 & 0 \\ 0 & 0 & 3 \end{pmatrix}$	$\lambda_0 = 2$ $\lambda_1 = 2$ $\lambda_2 = 0$	$\left.\begin{matrix} \\ \\ \end{matrix}\right\} (\alpha, \beta, -\alpha + 2\beta)$ $(1, 0, 0)$

Table 8.5: Three-cell network #30, its adjacency matrix, eigenvalues and the corresponding eigenvectors. $\alpha, \beta \in \mathbb{R}$

This network has $\lambda_0 = 2$ as a double eigenvalue and the corresponding two-dimensional eigenvector is expressed as $(\alpha, \beta, -\alpha + 2\beta)$, where $\alpha, \beta \in \mathbb{R}$. The only possible pattern of synchrony is $(x_1, x_2, x_3) = (u, u, u)$, i.e., a fully synchronous state with $\alpha = \beta$. Hence, the three coordinates of the second possible eigenvector (for $\lambda_0 = \lambda_1 = 2$) are independent of each other and thus it cannot express any non-trivial pattern of synchrony. As a result, this eigenvector structure does not generate any non-trivial balanced equivalence relation.

Figure 8.15 shows the lattice of balanced equivalence relations on the left. The shaded node is generated from the eigenvector structure associated with the distinct eigenvalue $\lambda_2 = 0$. This balanced equivalence relation determine two-cell quotient network shown in Figure 8.16.

Without any reduction, $\eta(p)$ is assigned for each lattice node on the right figure.

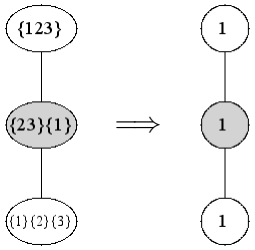

Figure 8.15: Lattice of balanced equivalence relations of three-cell network #30.

The two-cell quotient network in Figure 8.16 guarantees the existence of a transcritical

bifurcation.

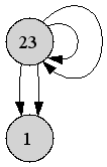

Figure 8.16: Two-cell quotient network of three-cell network #30.

Since there is one non-zero $\eta(p)$ in rank 2 and also in rank 3, we expect there exist two synchrony-breaking bifurcating branches from the trivial solution: one is a transcritical branch in a balanced polydiagonal $(x_1, x_2, x_3) = (u, v, v)$ bifurcating from the bifurcation point corresponding to the eigenvalue $\lambda_2 = 0$ and the second synchrony-breaking branch which does not lie in any synchronous subspace, i.e., all three state variables are different, occurs at the bifurcation point corresponding to the eigenvalues $\lambda_0 = \lambda_1 = 2$, and the type of this bifurcating branch can be obtained by the analysis of the original three-cell network.

$\diamond$

8.5.4 Bifurcation Diagrams of S2, S3, and S4 Networks

The following figures show schematically the existence of synchrony-breaking steady-state bifurcating branches from the synchronous state.

μ_0 is the bifurcation point where the synchrony-preserving bifurcating branch originates, hence there is no synchrony-breaking bifurcation branch unless one of the eigenvectors is in $\triangle$.

Red nodes correspond to balanced equivalence relations generated from the eigenvector structures of repeated eigenvalues. The bifurcation point associated with this "red" double eigenvalue is plotted as μ_1 on the horizontal axis, where we can observe multiple bifurcating branches.

The green node in $S4$ network corresponds to the balanced equivalence relation generated from the eigenvector structure whose corresponding eigenvalue is not repeated. The bifurcation point associated with this "green" single eigenvalue is plotted as μ_1 on the horizontal axis.

In reduced lattices, each lattice node p has labelled with $\eta(p)$. Additionally, some lattice node also include a letter "a" or "b" in rank 2. These letters describe sets of equal quotient network topologies. If lattice nodes in rank 2 are labelled "1_a" this means that their bifurcating branches will be constrained by having the same network structure, and therefore their bifurcation types should be the same. Other notations are used as in Chapter 7.

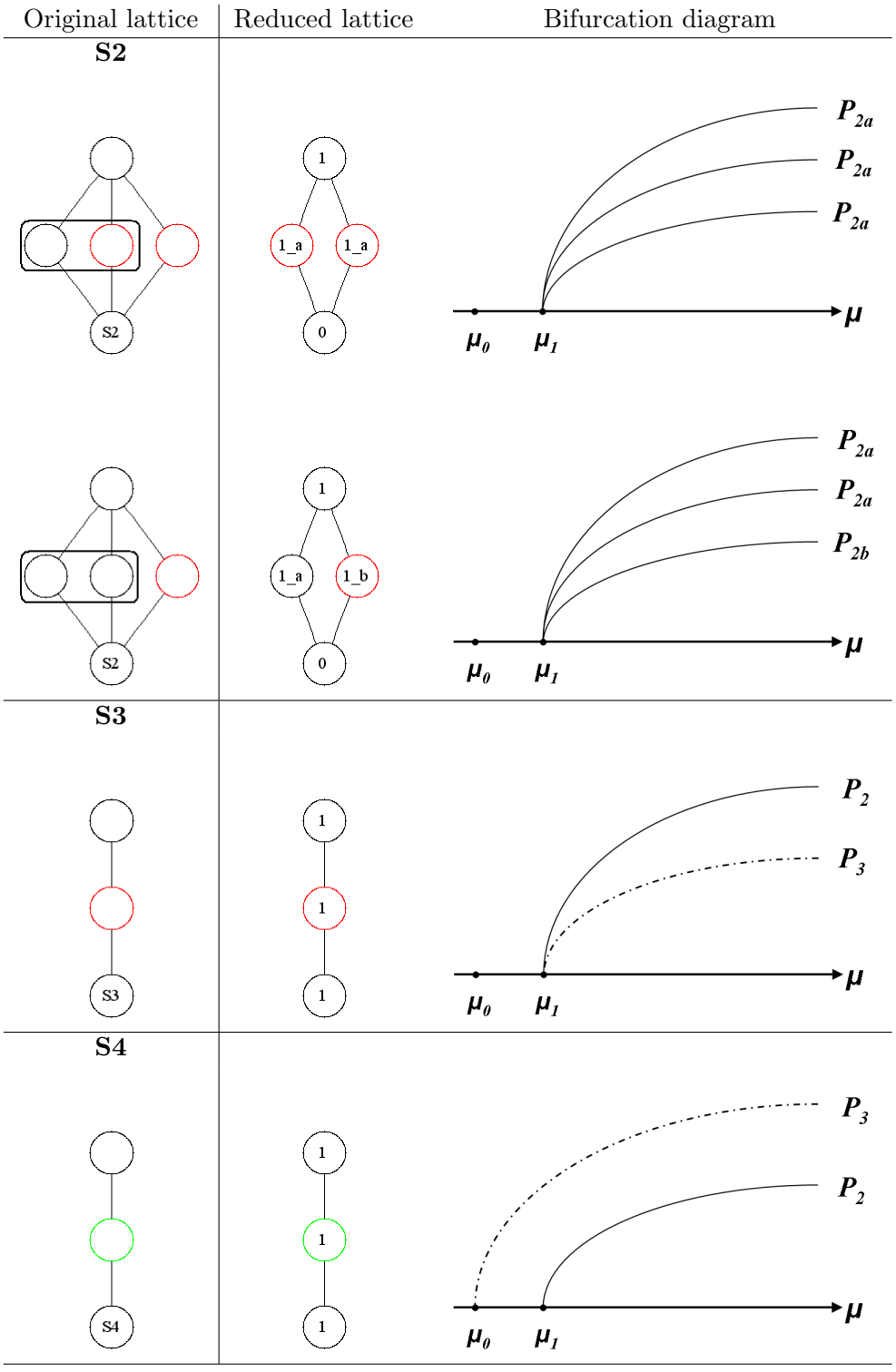

Figure 8.17: Existence of bifurcating branches for 3-cell valency 2 regular homogeneous networks with non-simple eigenvalues.

8.6 Four-cell Networks: Reduced Lattice Structures

There are eight four-cell regular homogeneous network types, which are classified by their adjacency matrix eigenvalue and eigenvector structures as follows:

1	simple eigenvalues
2	double eigenvalues and two eigenvectors
3	double eigenvalues and one eigenvector
4	pair of double eigenvalues and one eigenvector in $\triangle$ (fully synchronous subspace)
5	double eigenvalues and one eigenvector in $\triangle$ (fully synchronous subspace)
6	triple eigenvalues and three eigenvectors
7	triple eigenvalues and two eigenvectors
8	triple eigenvalues and one eigenvector

We consider non-simple eigenvalue cases; that is type 2 to 8. Reduction of lattices would be required for type 2, 4, 6, and 7 since the geometric multiplicities of eigenvalues are more than one and this may generate more balanced equivalence relations than the algebraic multiplicity of the eigenvalues (the number of generalised eigenvectors). Thus in the following, we only consider the types 2, 4, 6 and 7.

A lattice of four-cell networks contains lattices of three-cell networks. Therefore, for each non-simple eigenvalue network type, we firstly consider which three-cell network types can be seen in a given four-cell valency 2 regular homogeneous network. This simplifies how we can reduce a lattice structure as we know which three-cell network type need a reduction.

8.6.1 Double Eigenvalues and Two Eigenvectors

Proposition 8.6. *Let $\mathcal{G}$ be a four-cell regular homogeneous network with adjacency matrix A. If A has a double eigenvalue λ_2 with two linearly independent eigenvectors, then three-cell quotient networks $\mathcal{G}/_{\bowtie}$ of $\mathcal{G}$ are either type $S1$ or $S2$.*

Proof. Let λ_0, λ_1, and λ_2 are distinct eigenvalues of A, where λ_2 is a double eigenvalue with the geometric multiplicity two eigenvector. Then the Jordan normal form of A is

$$J = \begin{pmatrix} \lambda_0 & 0 & 0 & 0 \\ 0 & \lambda_1 & 0 & 0 \\ 0 & 0 & \lambda_2 & 0 \\ 0 & 0 & 0 & \lambda_2 \end{pmatrix}$$

An adjacency matrix associated with a homogeneous coupled cell network always has the eigenvalue which is equal to the valency. Hence for each balanced equivalence relations with

rank 3 (i.e. three equivalence classes), the Jordan normal form is decomposed either into

$$J_{\bowtie} = \begin{pmatrix} \lambda_0 & 0 & 0 \\ 0 & \lambda_1 & 0 \\ 0 & 0 & \lambda_2 \end{pmatrix}$$

which is a similar matrix to adjacency matrices of $S1$ networks, or

$$J_{\bowtie} = \begin{pmatrix} \lambda_0 & 0 & 0 \\ 0 & \lambda_2 & 0 \\ 0 & 0 & \lambda_2 \end{pmatrix}$$

which is a similar matrix to the adjacency matrices of $S2$ networks.

Hence three-cell quotient networks are either of type $S1$ or $S2$. □

Example 8.6. Consider four-cell valency 2 regular homogeneous network #2 which has a double eigenvalue $\lambda_1 = \lambda_2 = 0$ with the geometric multiplicity 2 eigenvector shown in Table 8.6.

Network #2	Adjacency matrix	Eigenvalues	Eigenvectors
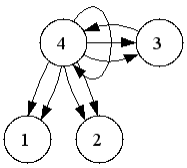	$\begin{pmatrix} 0 & 0 & 0 & 2 \\ 0 & 0 & 0 & 2 \\ 0 & 0 & 0 & 2 \\ 0 & 0 & 1 & 1 \end{pmatrix}$	$\lambda_0 = 2$	$(1,1,1,1)$
		$\lambda_1 = 0$	$\}$ $(\alpha, \beta, 0, 0)$
		$\lambda_2 = 0$	
		$\lambda_3 = -1$	$(-2,-2,-2,1)$

Table 8.6: Four-cell network #2 with a double eigenvalue and two eigenvectors.

There are eight quotient networks. Figure 8.18 shows these quotient networks and the corresponding eigenvalues:

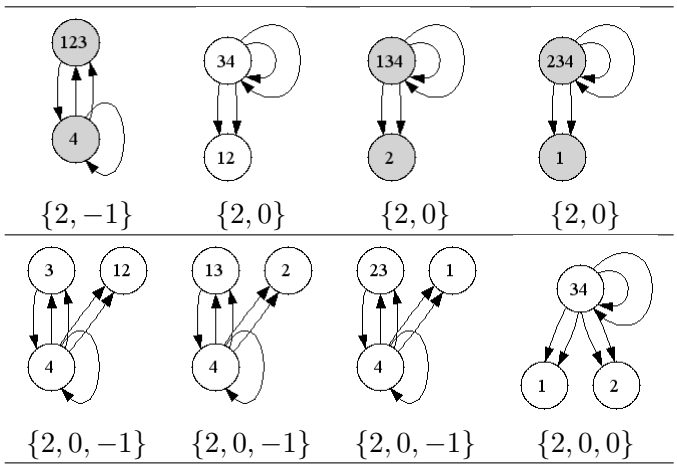

Figure 8.18: Eight quotient networks of four-cell network #2. For each quotient network, the set of eigenvalues of adjacency matrices are shown.

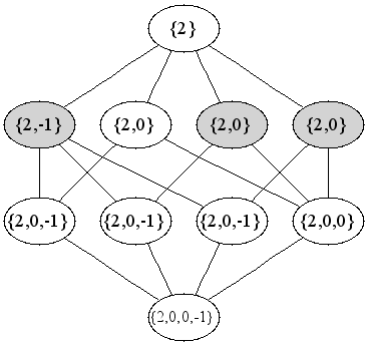

Figure 8.19: Lattice $U_{\mathcal{G}}^{P}$ of the sets of eigenvalues of quotient networks, where shaded lattice points were generated by eigenvector structures.

Figure 8.19 shows eigenvalue structure of three type $S1$ 3-cell quotient networks and one type $S2$ 3-cell quotient network. If we look at each lattice node in rank 3 and go up to the top element, we observe that there are three type $S1$ lattice structures and one type $S2$ lattice structure (before reduction).

We need a lattice reduction for lattice nodes corresponding to type $S2$ three-cell quotient network as it contains three lattice nodes in rank 2. In Figure 8.20, the "green" lattice node is generated by the eigenvector structures corresponding to a distinct eigenvalue $\lambda_3 = -1$ and "red" lattice nodes is generated by the eigenvector structure corresponding to a double eigenvalue $\lambda_1 = \lambda_2 = 0$. Now we make a minimal reduced lattice by clumping each of the blocks in Figure 8.20 to a single point. Firstly, we merge two lattice nodes in rank 2, which correspond to type $S2$ lattice structure. Because of this merging, two lattice nodes in rank 3 in the box become identical, hence, we merge them. This reduced lattice is the same as $L4$ lattice structure for simple eigenvalue networks. Then, we assign $\eta(p)$ to each lattice element.

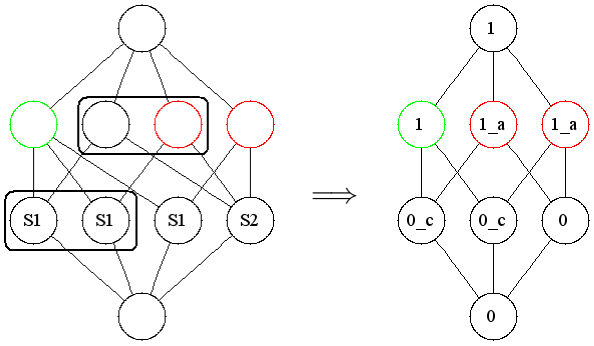

Figure 8.20: Minimal reduced lattice of four-cell network #2.

The lattice of eigenvalues of quotient networks is reduced as in Figure 8.21.

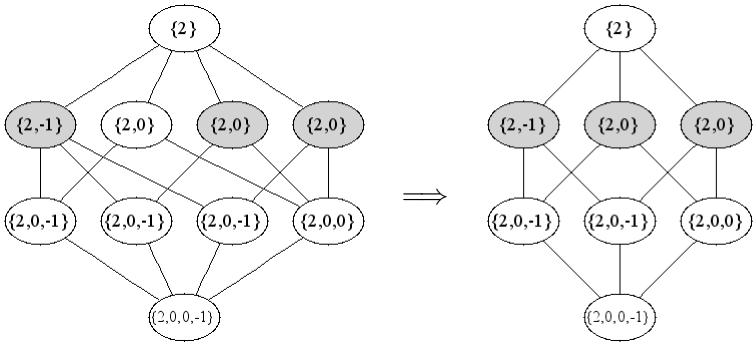

Figure 8.21: Lattice $U_{\mathcal{G}}^{P}$ of the sets of eigenvalues of quotient networks, where shaded lattice points were generated by eigenvector structures.

Both two topologically distinct 2-cell quotient networks in rank 2 guarantee the existence of transcritical bifurcating branches from the trivial solution $(x_1, x_2, x_3, x_4) = (0, 0, 0, 0)$. To determine how many bifurcating branches exist from a certain bifurcation point, we return to the original lattice. There are three balanced polydiagonals associated with the eigenvalue 0 and one balanced polydiagonal associated with the eigenvalue -1. Hence we expect to have three transcritical branches bifurcating from a bifurcation point corresponding to the eigenvalue 0 and one transcritical branches bifurcating from a bifurcation point corresponding to the eigenvalue -1. The schematic bifurcation diagram is shown in Section 8.7.

$\diamond$

Definition 8.3. *Let $\mathcal{G}$ be a four-cell regular homogeneous network associated with an adjacency matrix A. Let A have a double eigenvalue λ with corresponding eigenvector of geometric multiplicity two. Define a lattice which is already the minimal reduced lattice without any reduction or a lattice which is not reduced to one of* 14 *lattice structures of simple eigenvalue networks after reduction as a defective lattice.*

Conjecture 8.1. *In a defective lattice, the number $\eta(\perp)$ is non-zero.*

Xppaut simulations and Mathematica computations show the existence of additional solution branches outside the balanced polydiagonals determined from lattice structures.

For defective lattices, we set 1 as a default number for $\eta(\perp)$.

Remark 8.1. *There are five defective lattices; four-cell valency* 2 *regular homogeneous networks #*29*, #*51*,#*293*, #*303*, and #*76*.*

8.6.2 A Pair of Double Eigenvalues and One Eigenvector in $\triangle$

Let $(\lambda_0, \lambda_0, \lambda_1, \lambda_1)$ be the four eigenvalues of the adjacency matrix of a four-cell regular homogeneous network, where one eigenvector associated with the double eigenvalue λ_0 (which is

equal to the valency) is in $\triangle$. By Proposition 8.5, the double eigenvalue λ_0 does not generate multiple balanced polydiagonals. Hence the reduction of a lattice would be required depending on the eigenvector structures corresponding to the other double eigenvalue λ_1. Let $g(\lambda_1)$ be the geometric multiplicity of the eigenvector associated with the eigenvalue λ_1. There are two cases as follows:

Case I: $g(\lambda_1) = 2$,

Case II: $g(\lambda_1) = 1$

Hence, the reduction can be necessary only for case I.

Example 8.7. Consider four-cell valency 2 regular homogeneous network #315 which has a pair of double eigenvalues shown in Table 8.7.

Network #315	Adjacency matrix	Eigenvalues	Eigenvectors
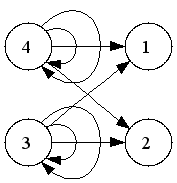	$\begin{pmatrix} 0 & 0 & 1 & 1 \\ 0 & 0 & 1 & 1 \\ 0 & 0 & 2 & 0 \\ 0 & 0 & 0 & 2 \end{pmatrix}$	$\lambda_0 = 2$ $\lambda_1 = 2$ $\lambda_2 = 0$ $\lambda_3 = 0$	$\}$ $(\alpha, \alpha, \beta, 2\alpha - \beta)$ $\}$ $(\gamma, \delta, 0, 0)$

Table 8.7: Four-cell network #315 and its associated adjacency matrix with eigenvalues and the corresponding eigenvectors. $\alpha, \beta, \gamma, \delta \in \mathbb{R}$.

There are two double eigenvalues $\lambda_0 = \lambda_1 = 2$ with two linearly independent eigenvectors and $\lambda_2 = \lambda_3 = 0$ with two linearly independent eigenvectors (Case I).

There are five quotient networks. Figure 8.22 shows these quotient networks and the corresponding eigenvalues.

In Figure 8.23, the lattice of the left shows there is one type $S4$ 3-cell quotient network and one type $S2$ 3-cell quotient network in rank 3. Now we make a minimal reduced lattice by clumping the blocks in the Figure 8.23 to a single point and assign $\eta(p)$ to each lattice element.

Figure 8.24 shows the lattice of eigenvalues of quotient networks and its reduced structure.

Topologically identical two-cell quotient networks in rank 2 guarantee the existence of transcritical bifurcating branches from the trivial solution $(x_1, x_2, x_3, x_4) = (0, 0, 0, 0)$. To determine how many bifurcating branches exist from a bifurcation point corresponding to the double eigenvalue $\lambda_2 = \lambda_3 = 0$, we return to the original lattice. There are three balanced polydiagonals associated with this double eigenvalue. Hence we expect to have three transcritical branches

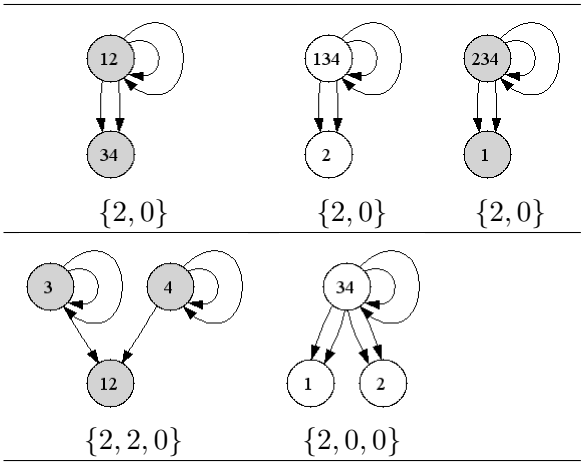

Figure 8.22: Five quotient networks of four-cell network #315. The sets of eigenvalues of each quotient network are shown.

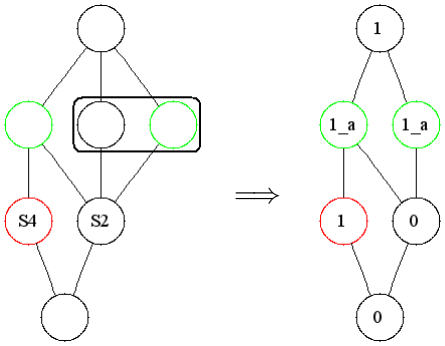

Figure 8.23: Minimal reduced lattice of four-cell network #315.

bifurcating from a bifurcation point corresponding to the double eigenvalue 0. One 3-cell quotient network in rank 3 guarantee the existence of a saddle-node bifurcation (analysed in (Leite and Golubitsky, 2006)). Hence there are three synchrony-preserving bifurcating branches from a bifurcation point corresponding to the eigenvalue $\lambda_2 = \lambda_3 = 0$ and one synchrony-breaking bifurcating branch from a bifurcation point corresponding to the eigenvalue $\lambda_0 = \lambda_1 = 2$. The schematic bifurcation diagram is shown in Section 8.7. Only synchrony-breaking bifurcating branches are shown.

$\diamond$

8.6.3 Triple Eigenvalues and Three Eigenvectors

Proposition 8.7. *Let $\mathcal{G}$ be a four-cell regular homogeneous network with adjacency matrix A. If A have a triple eigenvalue λ_1 with three linearly independent eigenvectors, then all of the three-cell quotient networks $\mathcal{G}/_{\bowtie}$ of $\mathcal{G}$ are type $S2$.*

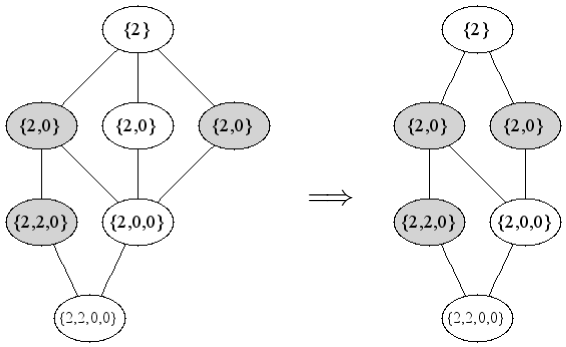

Figure 8.24: The lattice of the sets of eigenvalues of quotient networks $U_{\mathcal{G}}^{P}$ of four-cell network #315. Some sets, which have the same set of eigenvalues are merged into a single lattice node. Shaded lattice nodes are generated from the eigenvector structures.

Proof. Let λ_0, λ_1 be distinct eigenvalues of A, where λ_1 is a triple eigenvalue with the geometric multiplicity three eigenvector. Then the Jordan normal form of A is

$$J = \begin{pmatrix} \lambda_0 & 0 & 0 & 0 \\ 0 & \lambda_1 & 0 & 0 \\ 0 & 0 & \lambda_1 & 0 \\ 0 & 0 & 0 & \lambda_1 \end{pmatrix}$$

An adjacency matrix associated with a regular homogeneous coupled cell network has an eigenvalue which is equal to the valency. Hence for each balanced equivalence relations with rank 3 (i.e. three equivalence classes), the Jordan normal form is uniquely decomposed into

$$J_{\bowtie} = \begin{pmatrix} \lambda_0 & 0 & 0 \\ 0 & \lambda_1 & 0 \\ 0 & 0 & \lambda_1 \end{pmatrix}$$

which is a similar matrix to the adjacency matrices of $S2$ networks.

Hence all of the three-cell quotient networks are type $S2$. □

We consider regular homogeneous four-cell valency 2 network #311 which has a triple eigenvalue with the corresponding eigenvector with the geometric multiplicity three. We show how to reduce the original lattice to the minimal reduced lattice in the following.

Colour each lattice element in rank 2 either blue or yellow. Two colours express two topologically distinct two-cell quotient networks. Figure 8.25 shows there are three topologically identical two-cell quotient networks (coloured by blue) and four topologically identical two-cell quotient networks (coloured by yellow). Similarly, six three-cell quotient networks in total in rank

3 are coloured with two colours. Only one of quotient network (coloured by red) is topologically different from the rest of five quotient networks (coloured by green).

The minimal reduced lattice is obtained by clumping topologically identical networks as little as possible. Once we obtain the minimal reduced lattice, we assign $\eta(p)$ to each lattice node to determine the existence of bifurcating branches.

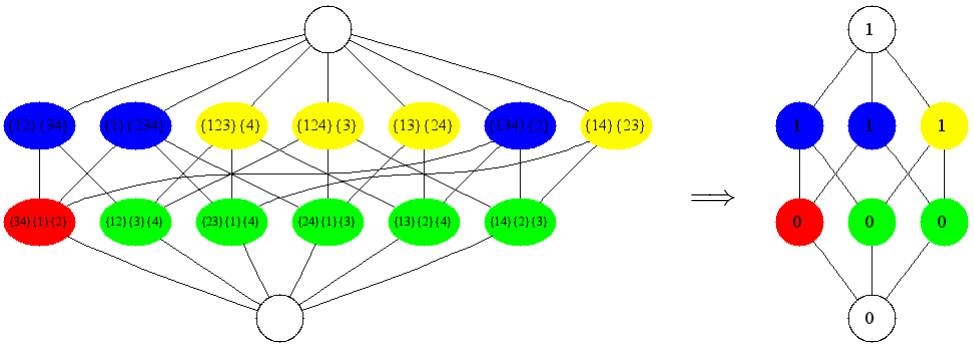

Figure 8.25: Minimal reduced lattice of four-cell network #311.

From the reduced lattice, we expect to have bifurcating branches only from rank 2 lattice elements. The two-cell quotient network coloured by blue guarantees the existence of a transcritical branch and the two-cell quotient network coloured by yellow guarantees the existence of a pitchfork branch. By looking at the original lattice, there are three blue lattice elements and four yellow lattice elements. Hence, we expect there to be seven bifurcating branches from the trivial solution; three of them are transcritical and four of them are pitchfork. These seven bifurcating branches lie in the corresponding two-dimensional balanced polydiagonals. A schematic bifurcation diagram is shown in Section 8.7.

8.6.4 Triple Eigenvalues and Two Eigenvectors

Proposition 8.8. *Let $\mathcal{G}$ be a four-cell regular homogeneous network with adjacency matrix A. If A have a triple eigenvalue λ_1 with two linearly independent eigenvectors, then three-cell quotient networks $\mathcal{G}/_{\bowtie}$ of $\mathcal{G}$ are either type $S2$ or $S3$.*

Proof. Let λ_0, λ_1 be distinct eigenvalues of A, where λ_1 is a triple eigenvalue with the geometric multiplicity two eigenvector. Then the Jordan normal form of A is

$$J = \begin{pmatrix} \lambda_0 & 0 & 0 & 0 \\ 0 & \lambda_1 & 0 & 0 \\ 0 & 0 & \lambda_1 & 1 \\ 0 & 0 & 0 & \lambda_1 \end{pmatrix}$$

An adjacency matrix associated with a regular homogeneous coupled cell network always has an eigenvalue equal to the valency. Hence for each balanced equivalence relations with rank 3 (i.e. three equivalence classes), the Jordan normal form is decomposed either as

$$J_{\bowtie} = \begin{pmatrix} \lambda_0 & 0 & 0 \\ 0 & \lambda_1 & 0 \\ 0 & 0 & \lambda_1 \end{pmatrix}$$

which is a similar matrix to adjacency matrices of $S2$ networks, or as

$$J_{\bowtie} = \begin{pmatrix} \lambda_0 & 0 & 0 \\ 0 & \lambda_1 & 1 \\ 0 & 0 & \lambda_1 \end{pmatrix}$$

which is a similar matrix to the adjacency matrices of $S3$ networks.

Hence three-cell quotient networks are either of type $S2$ or $S3$. □

Remark 8.2. *Four-cell valency* 2 *regular homogeneous networks* #343*,* #6*,* #13*,* #270*,* #410*,* #344 *have exceptional structures. The existence of bifurcating branches outside the balanced polydiagonals in lattices are analysed by xppaut and mathematica.*

8.7 Bifurcation Diagrams of Four-cell Networks

The following figures show schematically the existence of synchrony-breaking bifurcating branches from the synchronous state. The minimal reduced lattices are labelled from MRL1 to MRL46 with the corresponding simple eigenvalue network lattice structure, one of L1 to L14, in brackets.

There are several choices how to merge lattice nodes in each congruence block unless there are some constraints of quotient network topologies. Note that the order of the lattice $U_{\mathcal{G}}^P$ (the sets of eigenvalues of adjacency matrices of quotient networks) and the lattice $Q_{\mathcal{G}}^P$ (the set of quotient networks) are preserved under the reduction, however, the order of balanced equivalence relations is not.

8.7.1 Double Eigenvalues with Geometric Multiplicity 2

Let $(\lambda_0, \lambda_1, \lambda_2, \lambda_2)$ be a set of eigenvalues of the adjacency matrix of a given four-cell regular homogeneous network $\mathcal{G}$. λ_0 is equal to the valency of the network and λ_2 is a repeated eigenvalue with the geometric multiplicity two. The bifurcation points μ_i correspond to each λ_i.

μ_0 is the bifurcation point where the synchrony-preserving bifurcating branch originates, hence there is no synchrony-breaking bifurcation branch unless one of the eigenvectors is in $\triangle$.

The green node in each lattice corresponds to the balanced equivalence relation generated from the eigenvector structure whose corresponding eigenvalue has geometric multiplicity one (λ_1). The bifurcation point associated with this "green" single eigenvalue is plotted as μ_1 on the horizontal axis.

Red nodes correspond to balanced equivalence relations generated from eigenvector structures of the double eigenvalue (λ_2). The bifurcation point associated with this "red" double eigenvalue is plotted as μ_2 on the horizontal axis, where we can observe multiple bifurcating branches.

In the minimal reduced lattices (labelled MRL with the corresponding simple eigenvalue network lattice structure), each lattice node p is labelled with $\eta(p)$. Additionally, some lattice nodes also include a letter a or b in rank 2 and c or d in rank 3. These letters describe sets of equal quotient network topologies. If lattice nodes in rank 2 are labelled 1_a this means that their bifurcating branches will be constrained by having the same network structure, and therefore their bifurcation types should be the same.

Some of the structures shown in the "original lattices" column are identical except for the colouring of the nodes. For example, the original lattices leading to MRL1 and MRL2 have the same structure, but the location of one red node is different. This leads to differences in the number of topologically distinct quotient networks. Therefore, we list all possible coloured variations of the original lattices in turn, and the possible reduced lattices in each case. For example MRL2 and MLR3 both come from the same original lattice.

The final column shows a schematic bifurcation diagram, where the number of branches can be inferred from the clumping used to construct the reduced lattice, but the bifurcation types (labelled using a or b) can be determined from the minimal reduced lattice directly. To emphasize that MLR1 to MLR8 cover only two distinct bifurcation diagrams, these have been labelled with type (i) or (ii).

Three of the following exceptional lattices have been labelled with four-cell valency 2 network numbers; namely networks #29, #51, #293, #303, #76 and #327.

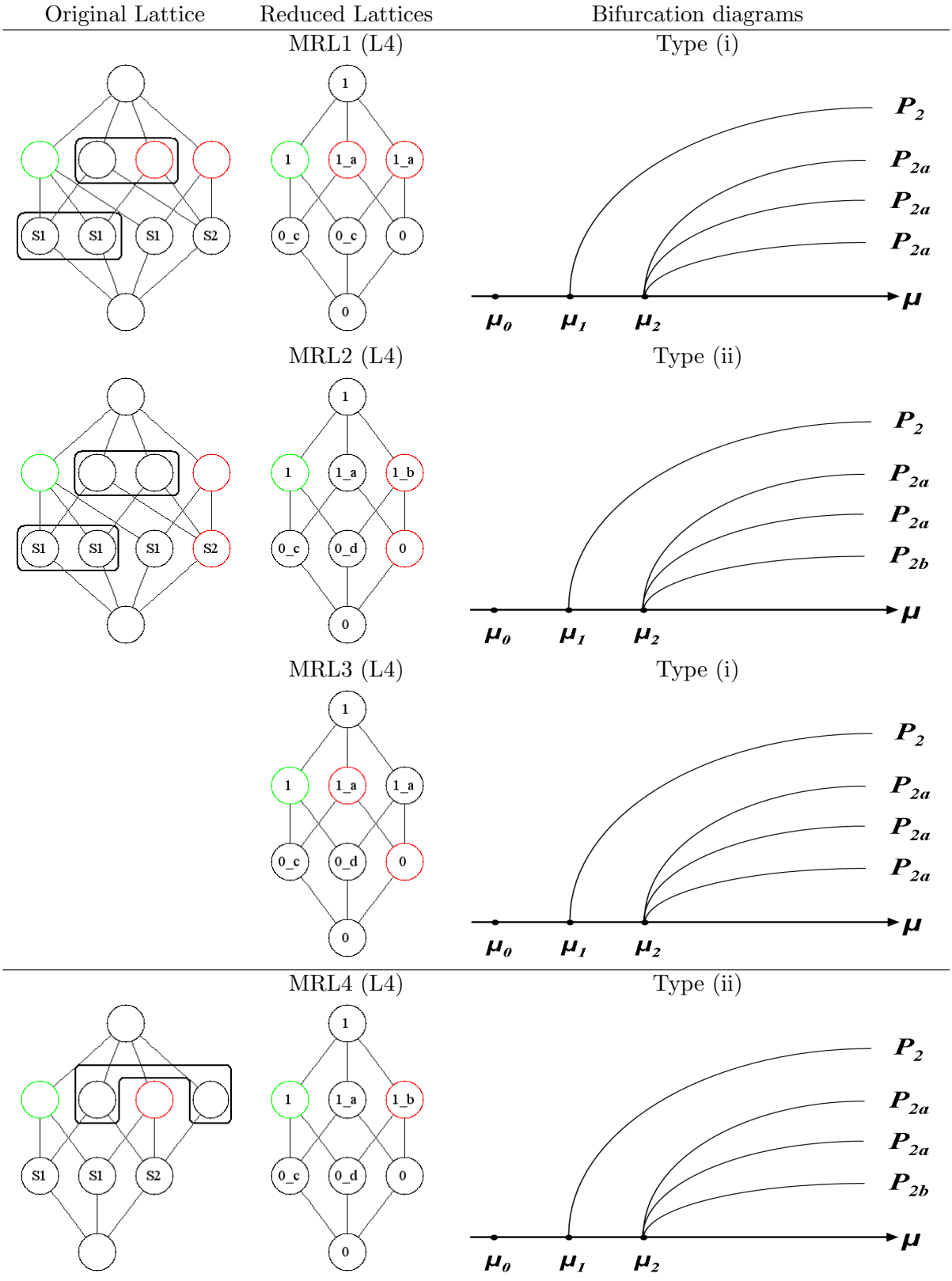

Figure 8.26: Existence of bifurcating branches for 4-cell valency 2 regular homogeneous networks with double eigenvalues and two eigenvectors (split over five pages).

MRL5 (L4)

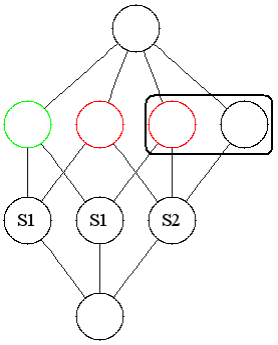

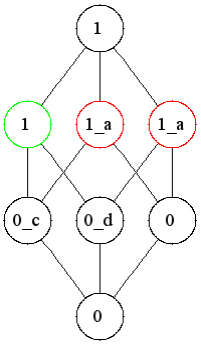

Type (i)

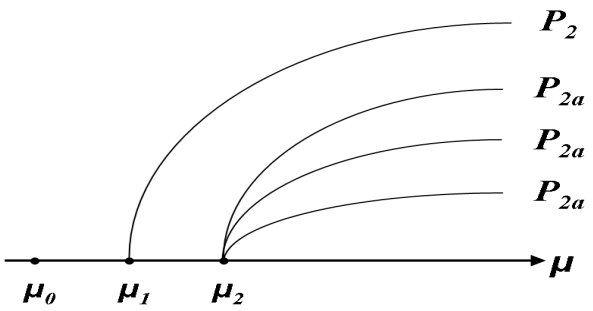

MRL6 (L4)

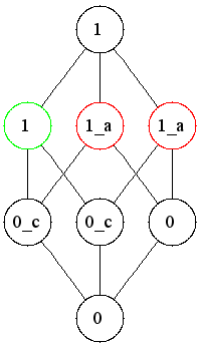

Type (i)

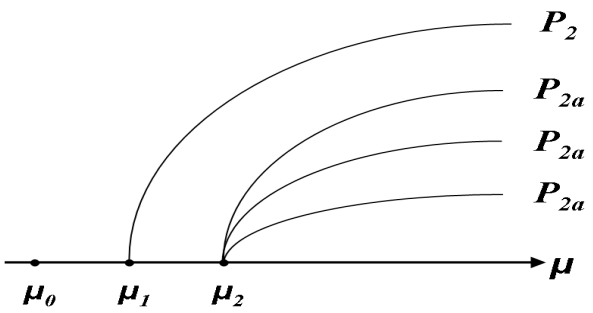

MRL7 (L4)

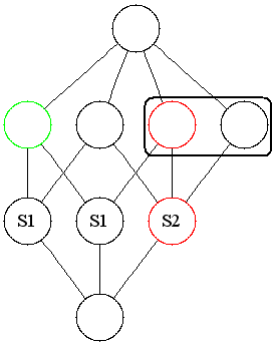

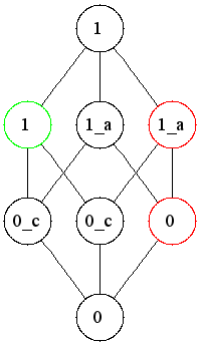

Type (i)

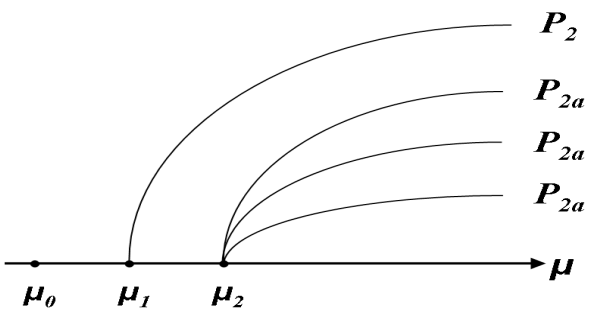

MRL8 (L4)

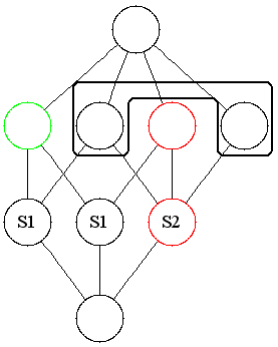

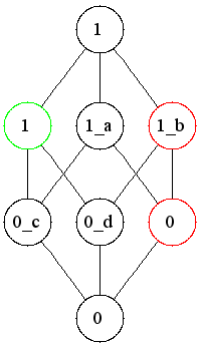

Type (ii)

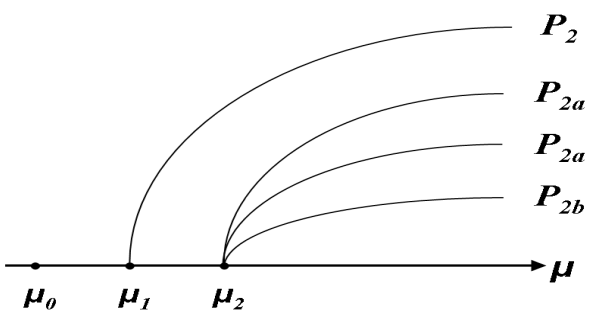

MRL9 (L1)

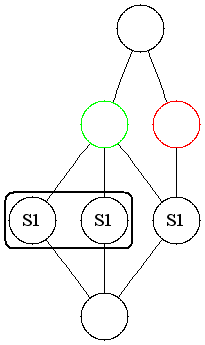

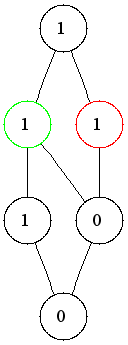

MRL10 (L1)

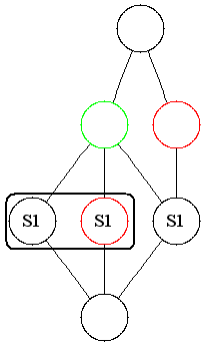

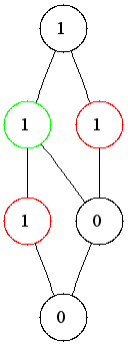

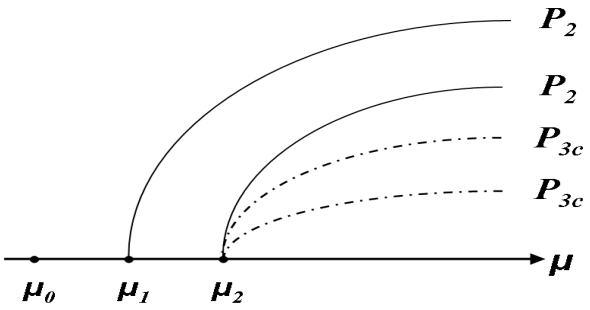

MRL11 (L1)

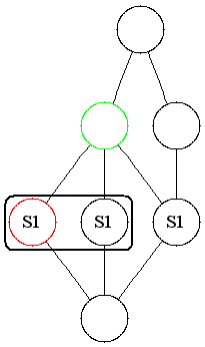

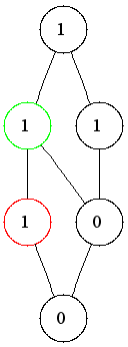

#29, #51, #293, #303 MRL12

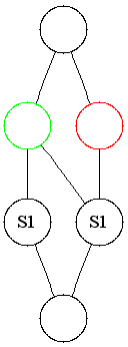

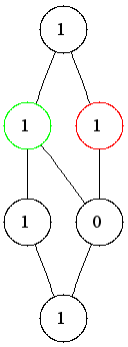

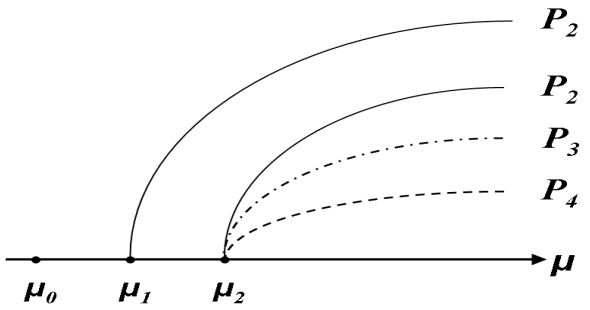

MRL13 (L1)

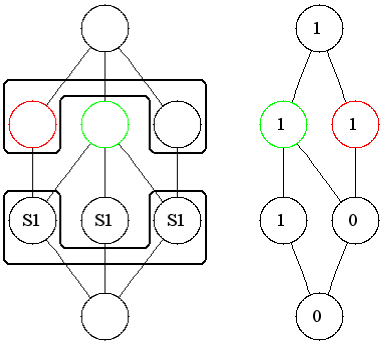

MRL14 (L1)

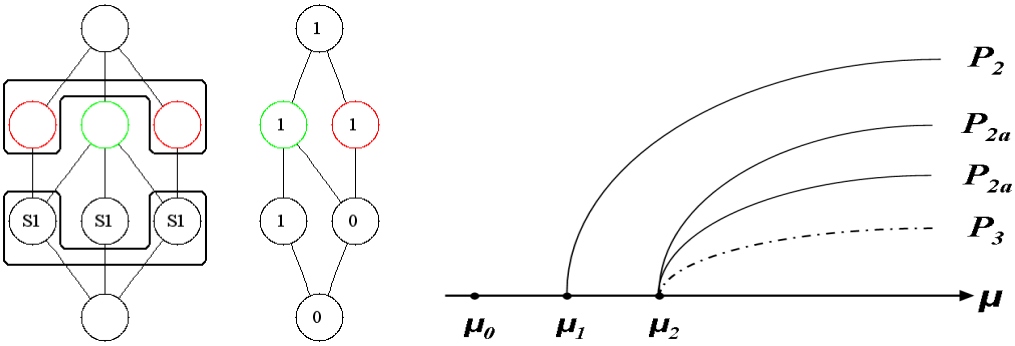

MRL15 (L1)

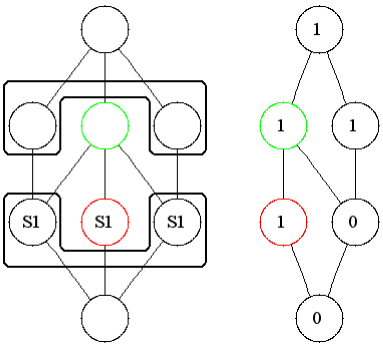

MRL16 (L9)

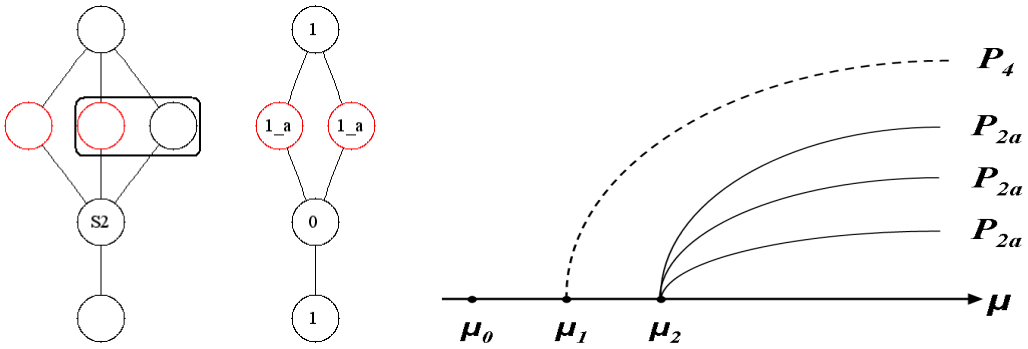

MRL17 (L1)

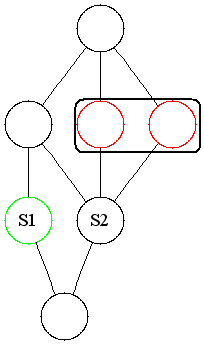

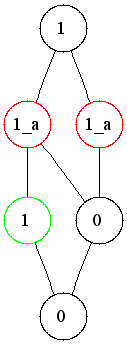

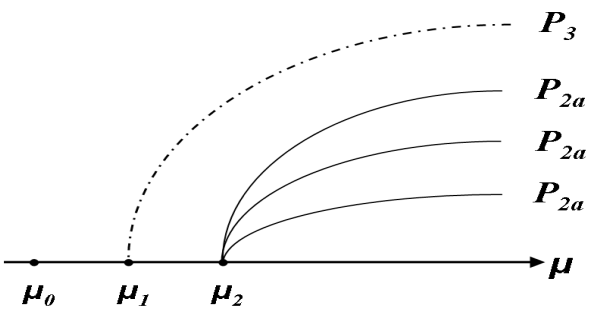

MRL18 (L1)

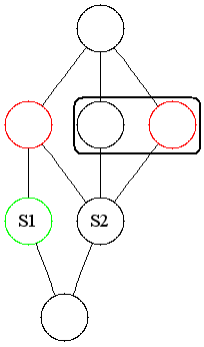

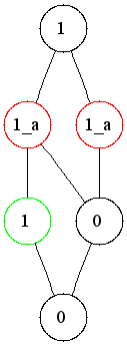

#76 MRL19

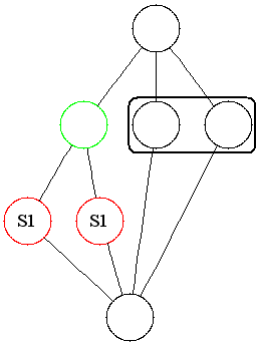

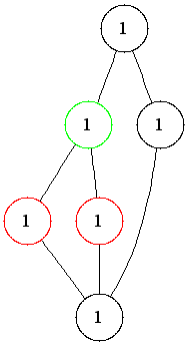

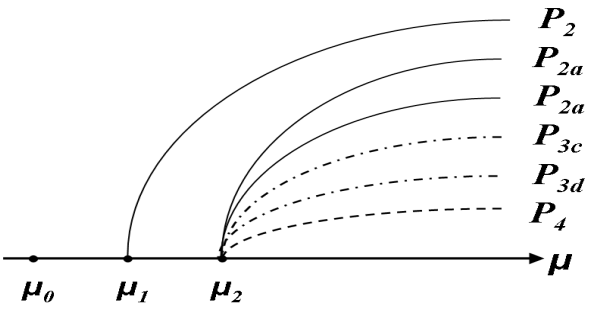

#327 MRL20 (L12)

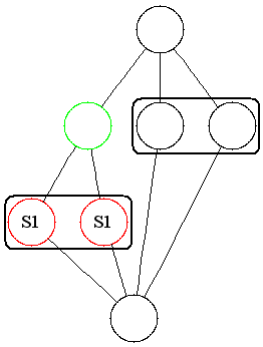

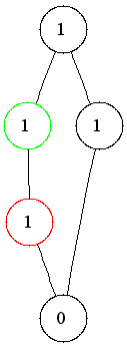

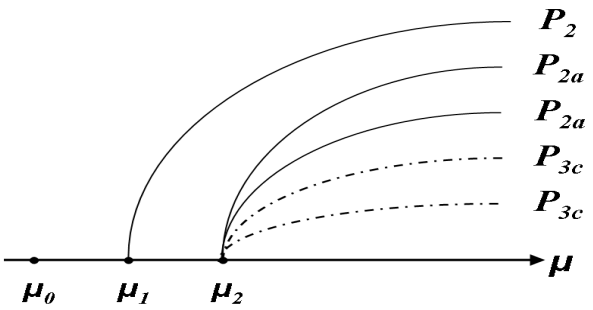

8.7.2 Double Eigenvalues with Geometric Multiplicity 1

Let $(\lambda_0, \lambda_1, \lambda_2, \lambda_2)$ be a set of eigenvalues of the adjacency matrix of a given four-cell regular homogeneous network $\mathcal{G}$. λ_0 is equal to the valency of the network and λ_2 is a repeated eigenvalue with the geometric multiplicity one. The bifurcation points μ_i correspond to each λ_i.

The green node in each lattice corresponds to the balanced equivalence relation generated from the eigenvector structure whose corresponding eigenvalue has geometric multiplicity one (λ_1). The bifurcation point associated with this "green" single eigenvalue is plotted as μ_1 on the horizontal axis.

Red nodes correspond to balanced equivalence relations generated from eigenvector structures of the double eigenvalue (λ_2) with only one linearly independent eigenvector. The bifurcation point associated with this "red" double eigenvalue is plotted as μ_2 on the horizontal axis, where we can observe multiple bifurcating branches.

Note that the reduced lattices are the same as the original lattices. Since there is only one linearly independent eigenvector for the corresponding double eigenvalue, the reduction is not required for this type of networks.

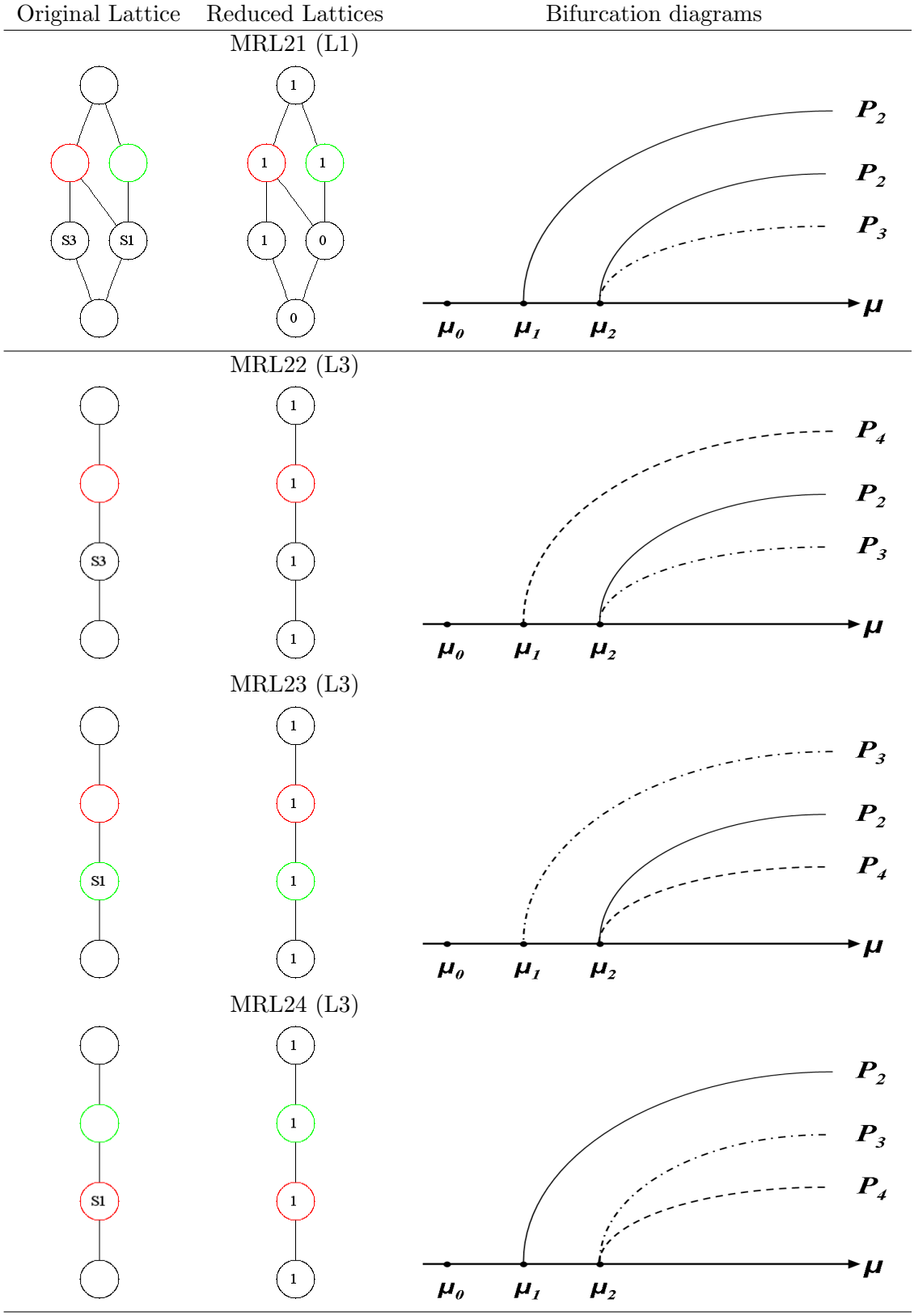

Figure 8.27: Existence of bifurcating branches for 4-cell valency 2 regular homogeneous networks with double eigenvalues and one eigenvector (split over two pages).

MRL25 (L5)

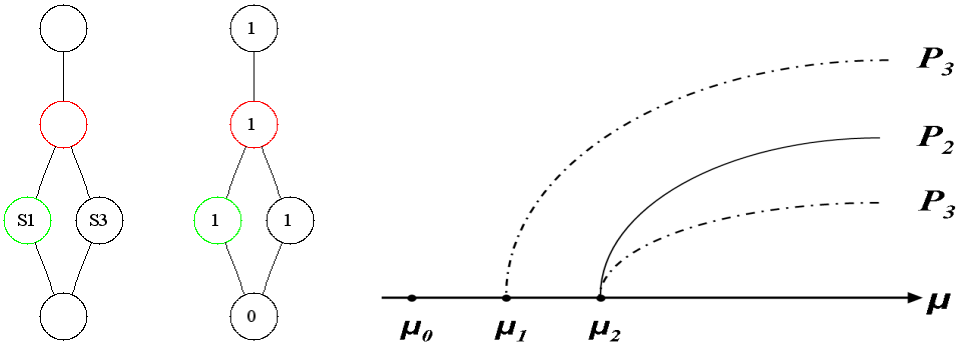

MRL26 (L9)

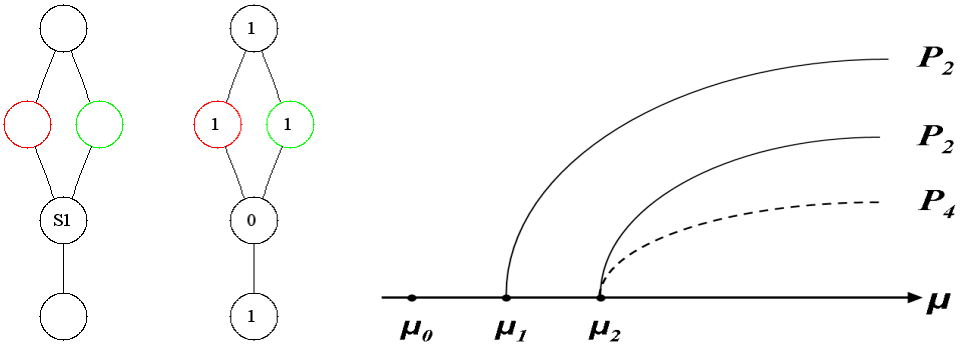

MRL27 (L7)

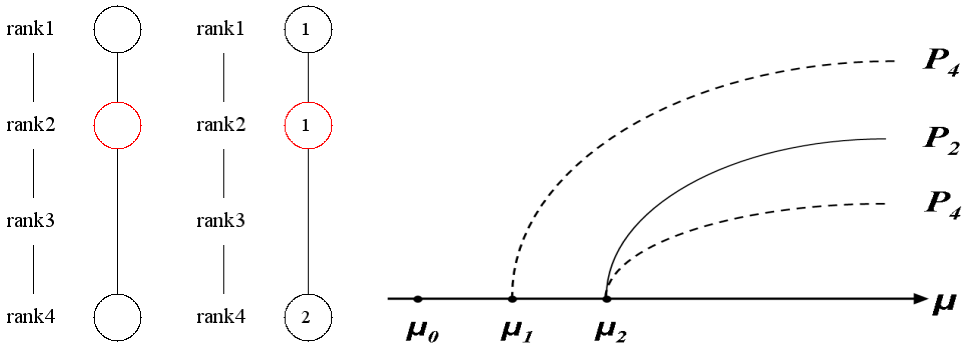

MRL28 (L8)

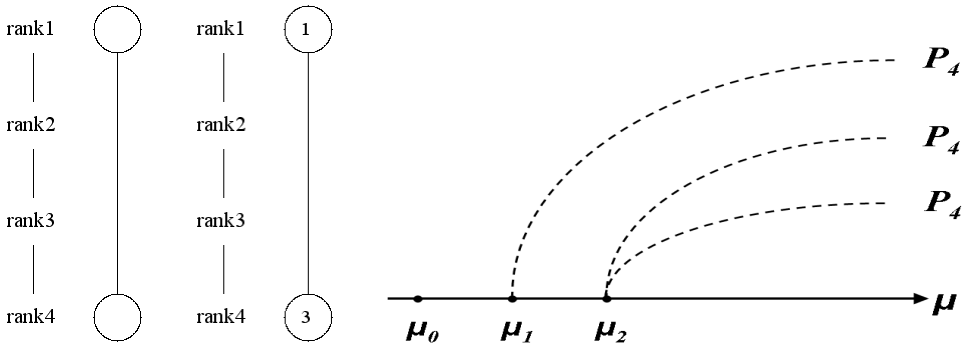

8.7.3 A Pair of Double Eigenvalues and one eigenvector in $\triangle$

Let $(\lambda_0, \lambda_0, \lambda_1, \lambda_1)$ be a set of a pair of double eigenvalues of a given four-cell regular network $\mathcal{G}$. λ_0 is equal to the valency of the network with the one of the corresponding eigenvectors is $(1, 1, 1, 1) \in \triangle$.

The green node in each lattice corresponds to the balanced equivalence relation generated from the eigenvector structure whose corresponding eigenvalue is λ_1. The bifurcation point associated with this "green" single eigenvalue is plotted as μ_1 on the horizontal axis.

Red nodes correspond to balanced equivalence relations generated from eigenvector structures of the double eigenvalue λ_0. The bifurcation point associated with this "red" double eigenvalue is plotted as μ_0 on the horizontal axis, where it is not shown but there exists a synchrony-preserving bifurcating branch.

The reduction would be required if the corresponding eigenvector to the double eigenvalue λ_1 has the geometric multiplicity two (Case I).

Case I: $(\lambda_0, \lambda_0, \lambda_1, \lambda_1)$ **with** $g(\lambda_1) = 2$

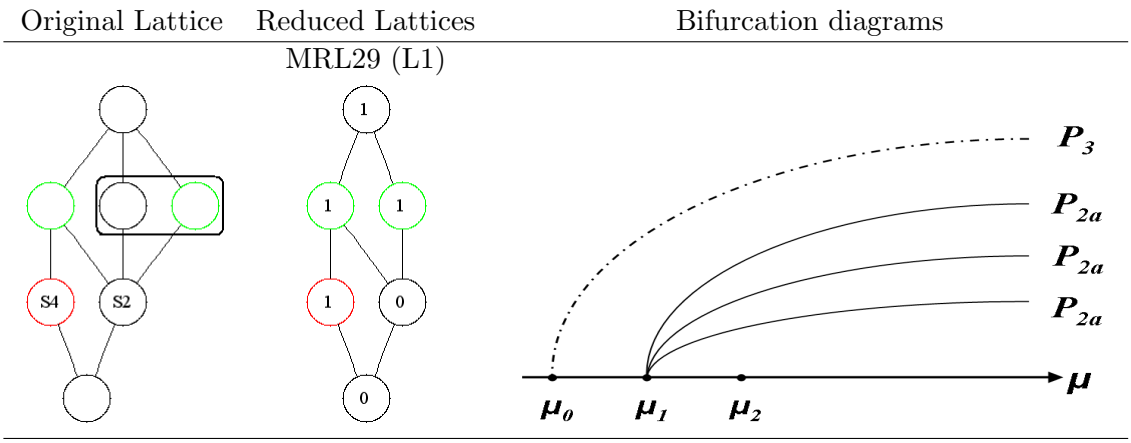

Figure 8.28: Existence of bifurcating branches for 4-cell valency 2 regular homogeneous networks with a pair of double eigenvalues and one eigenvector in $\triangle$ (split over two pages).

Case II: $(\lambda_0, \lambda_0, \lambda_1, \lambda_1)$ **with** $g(\lambda_1) = 1$

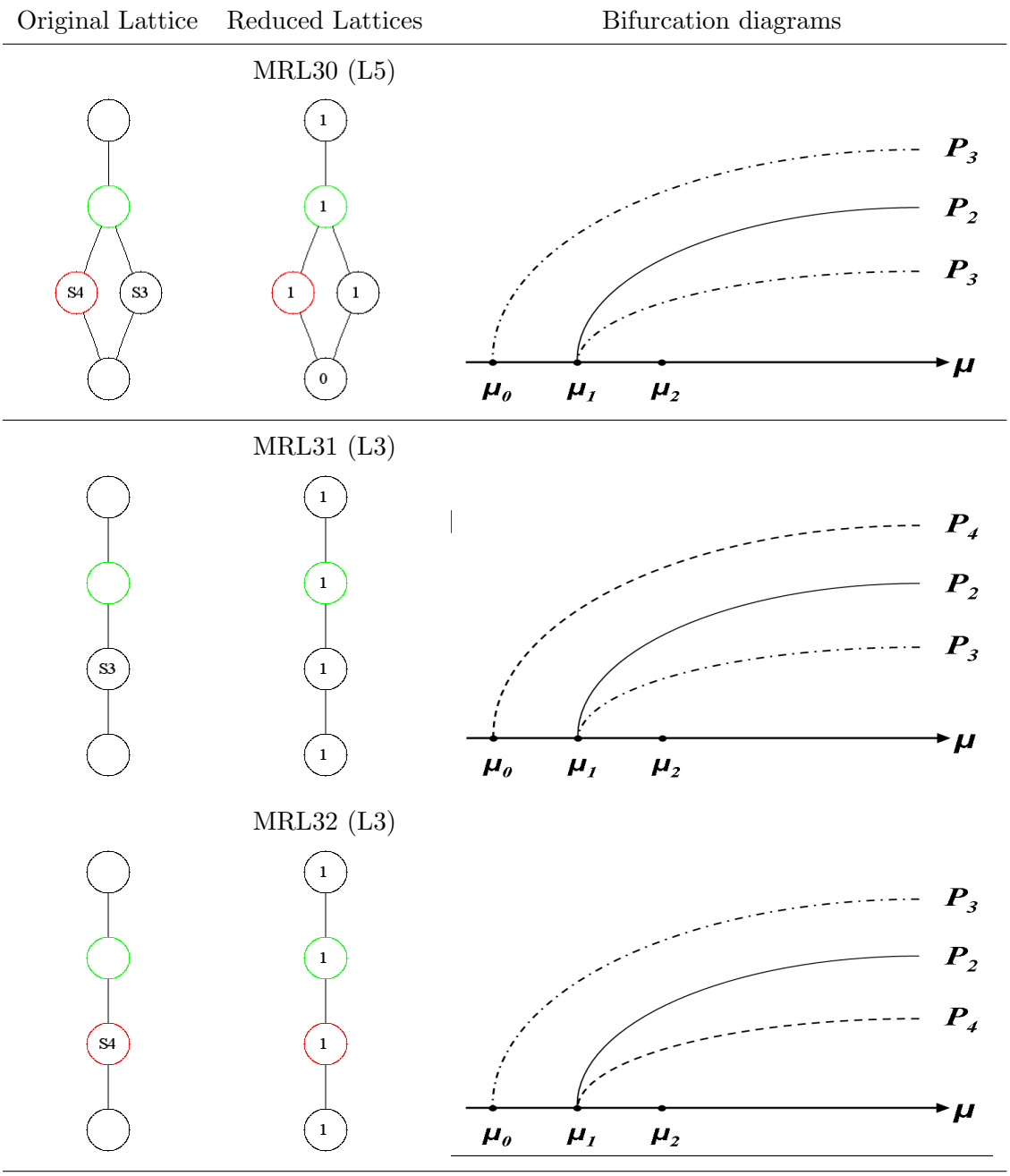

8.7.4 Double Eigenvalues and one eigenvector in $\triangle$

Let $(\lambda_0, \lambda_0, \lambda_1, \lambda_2)$ be the eigenvalues, where one eigenvector associated with the double eigenvalue λ_0 is in $\triangle$ The green node in each lattice corresponds to the balanced equivalence relation generated from the eigenvector structure whose corresponding eigenvalue is either λ_1 or λ_2. The bifurcation point associated with this "green" single eigenvalue is plotted as μ_1 or μ_2 on the horizontal axis.

Red nodes correspond to balanced equivalence relations generated from eigenvector struc-

tures of the double eigenvalue λ_0. The bifurcation point associated with this "red" double eigenvalue is plotted as μ_0 on the horizontal axis, where it is not shown but there exists a synchrony-preserving bifurcating branch.

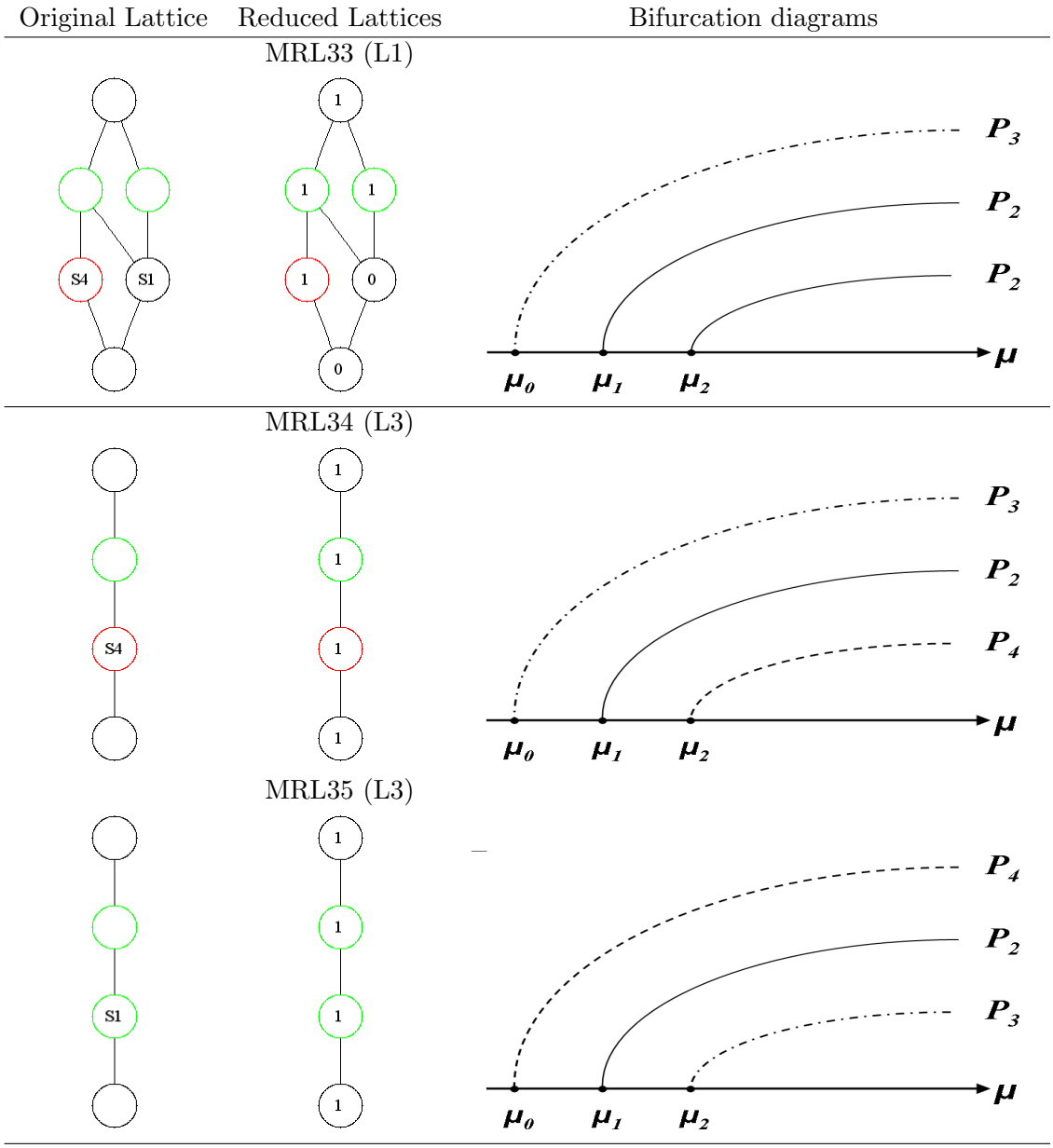

Figure 8.29: Existence of bifurcating branches for 4-cell valency 2 regular homogeneous networks with double eigenvalues and one eigenvector in $\triangle$.

8.7.5 Triple Eigenvalues with Geometric Multiplicity 3

Let $(\lambda_0, \lambda_1, \lambda_1, \lambda_1)$ be a set of eigenvalues of the adjacency matrix of a given four-cell regular homogeneous network $\mathcal{G}$. λ_0 is equal to the valency of the network and λ_1 is a repeated eigenvalue (the algebraic multiplicity is three) with the geometric multiplicity three.

Red nodes correspond to balanced equivalence relations generated from eigenvector structures of the triple eigenvalue λ_1. The bifurcation point associated with this "red" triple eigenvalue is plotted as μ_1 on the horizontal axis.

There are only three four-cell valency 2 regular homogeneous networks, where the associated adjacency matrices has a triple eigenvalue with three linearly independent vectors; namely #1, #408 and #311. The dynamical behaviours of #1 and #408 are known to be equivalent.

These original lattices are reduced as described in Subsection 8.6.3, but the groupings are not illustrated due to the complexity of the figures.

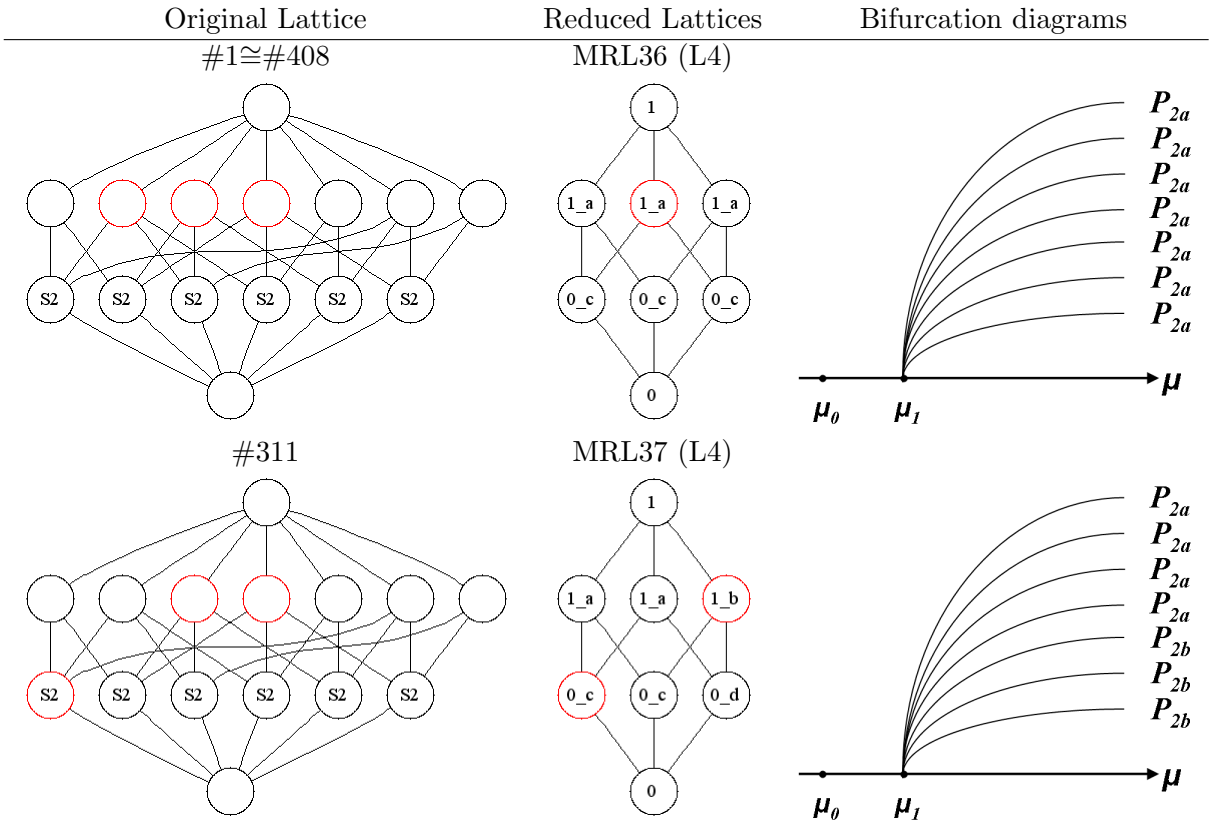

Figure 8.30: Existence of bifurcating branches for 4-cell valency 2 regular homogeneous networks with triple eigenvalues and three eigenvectors.

8.7.6 Triple Eigenvalues with Geometric Multiplicity 2

Let $(\lambda_0, \lambda_1, \lambda_1, \lambda_1)$ be a set of eigenvalues of the adjacency matrix of a given four-cell regular homogeneous network $\mathcal{G}$. λ_1 has the algebraic multiplicity is three with the geometric multiplicity two.

Red nodes correspond to balanced equivalence relations generated from eigenvector structures of the triple eigenvalue λ_1. The bifurcation point associated with this "red" triple eigenvalue is plotted as μ_1 on the horizontal axis.

There are six four-cell valency 2 regular homogeneous networks which have exceptional existence of synchrony-breaking bifurcating branches. The minimal reduced lattice of network #344 does not match to any of 14 lattice structures of simple eigenvalue four-cell networks. The minimal reduced lattices of networks #6, #13, #270, #410 and #343 is the same as $L1$, however, xppaut simulation and mathematica shows additional solution branches outside the balanced polydiagonals. Hence we have non-zero $\eta(p)$ for the bottom elements.

Networks #64 and #137 are the only networks which have the minimal reduced lattice MRL41. Numerical analysis shows that there are two branches in the trivial polydiagonal P_4 from μ_1, which have been included in the figure.

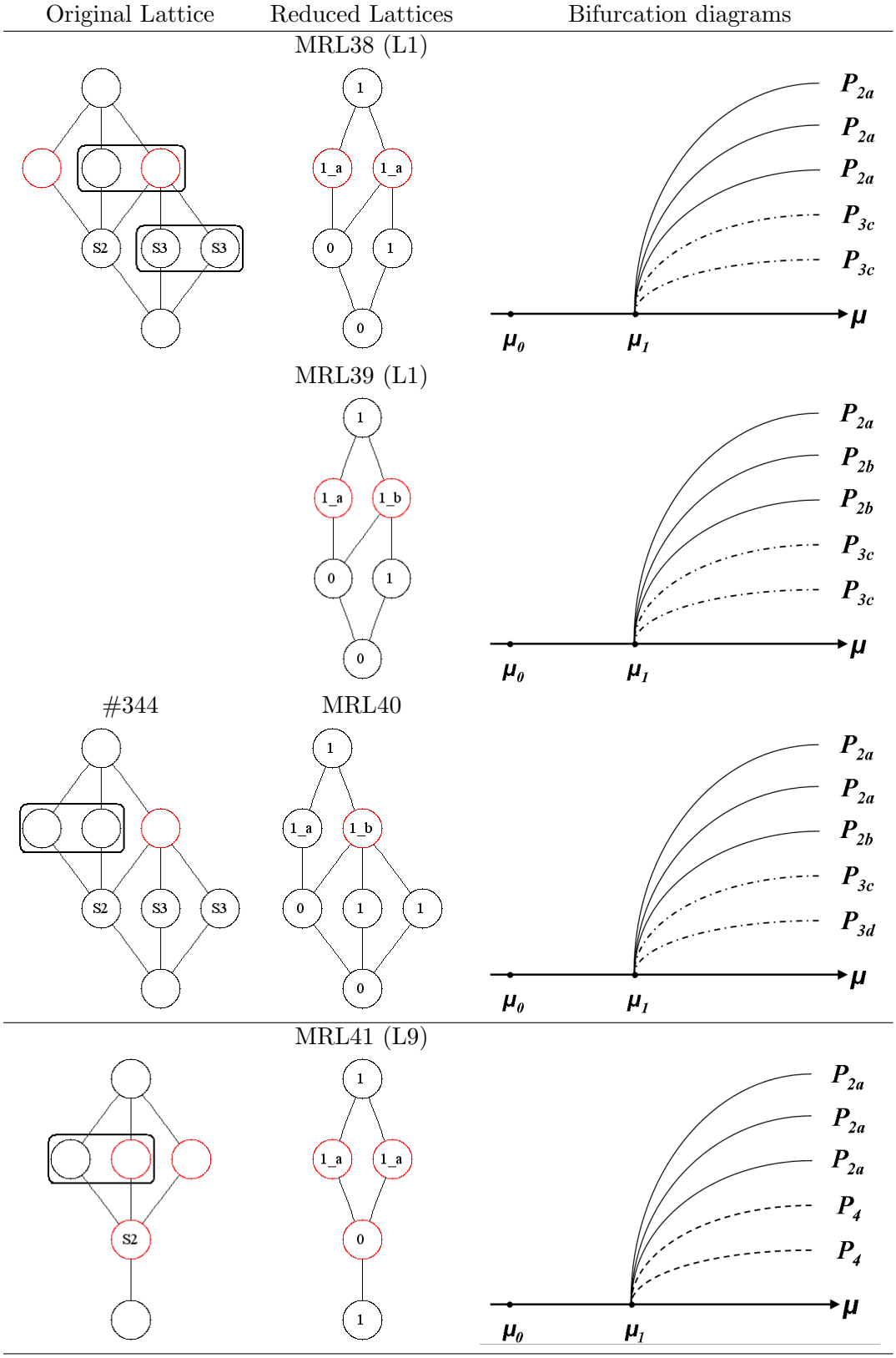

Figure 8.31: Existence of bifurcating branches for 4-cell valency 2 regular homogeneous networks with triple eigenvalues and two eigenvectors (split over two pages).

MRL42 (L3)

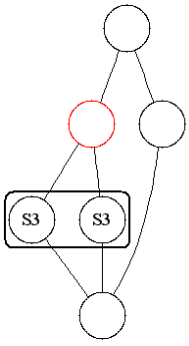

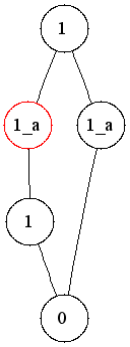

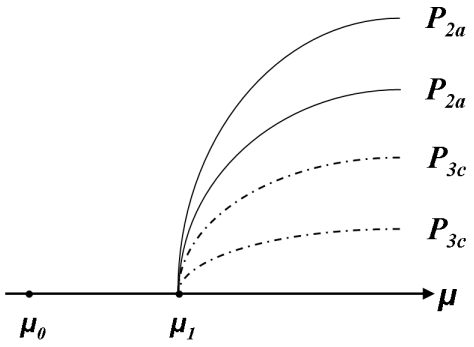

MRL43 (L5)

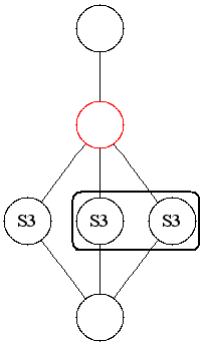

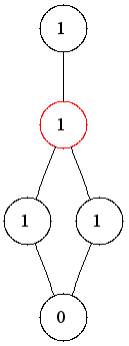

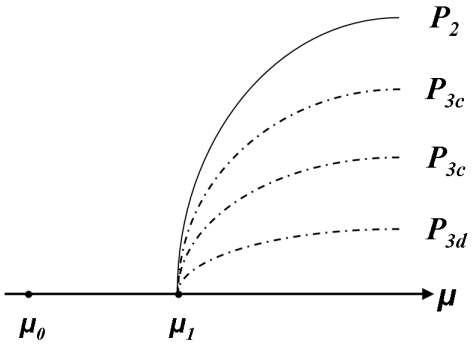

#6, #13, #270, #410 MRL44

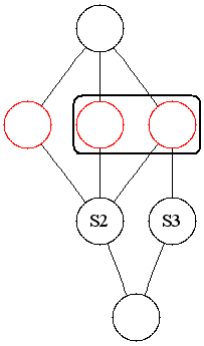

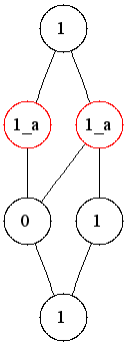

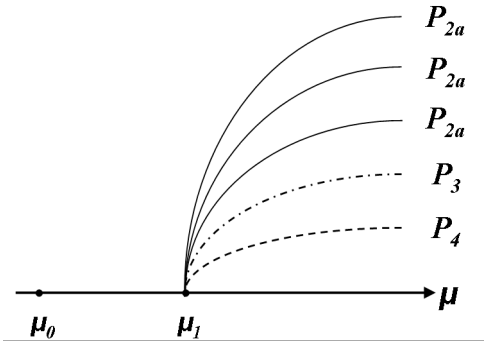

#343 MRL45

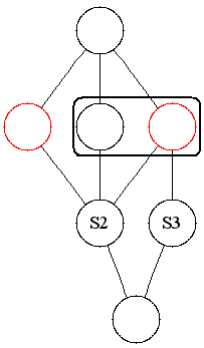

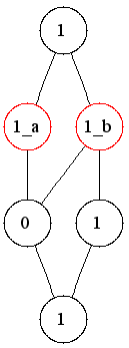

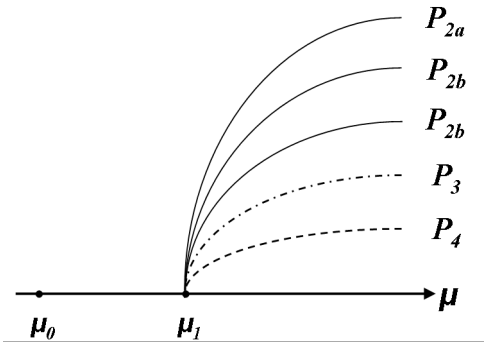

8.7.7 Triple Eigenvalues with Geometric Multiplicity 1

Red nodes correspond to balanced equivalence relations generated from eigenvector structures of the triple eigenvalue λ_1 with the geometric multiplicity one. The bifurcation point associated with this "red" triple eigenvalue is plotted as μ_1 on the horizontal axis.

Note that the reduced lattice is the same as the original lattice as there is only one linearly independent eigenvector corresponding to the triple eigenvalue λ_1.

From numerical analysis, it seems there exist two branches in the trivial polydiagonal P_4. Therefore, two bifurcating branches in P_4 from the bifurcation point μ_1 are drawn.

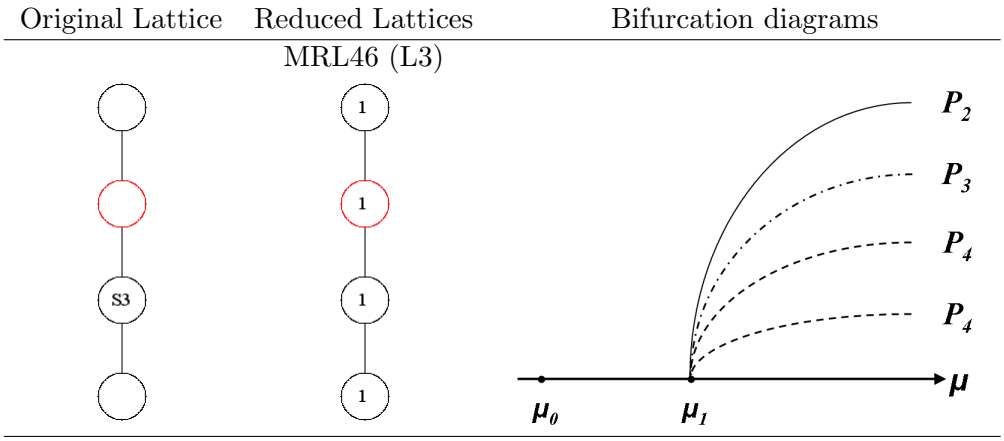

Figure 8.32: Existence of bifurcating branches for 4-cell valency 2 regular homogeneous networks with triple eigenvalues and one eigenvector.

8.8 Conclusions

If the dimension of an eigenspace is more than one, the spanning eigenvectors can generate more balanced equivalence relations than the algebraic multiplicity of the corresponding eigenvalue. Hence there is no one-to-one relationships between balanced equivalence relations and eigenvectors. Furthermore, often the topologies of the quotient networks defined by the corresponding balanced polydiagonals are identical (this constrains identical dynamical behaviour). This causes multiple bifurcating branches from a single bifurcating branch, and the solution branches behave in a similar manner.

To remove additional lattice elements, which are generated by the multiple dimensionality of an eigenspace, we considered a reduction of lattice by minimally merging topologically identical quotient network lattice elements together. Once the reduction is completed, then $\eta(p)$ is assigned to each lattice element, and the remaining analysis follows as for the simple eigenvalue networks.

The number of multiple bifurcating branches, which was ignored in the reduction of the lattice, can be obtained from the original lattice.

All non-simple eigenvalue three and four-cell regular homogeneous networks of valency 2 were classified, and schematic diagrams which show the existence of bifurcating branches, the dimension of balanced polydiagonals, where bifurcating branches lie, and the grouping of bifurcation types using algebraic symbols are listed. There are eleven four-cell valency 2 regular homogeneous networks, which have exceptional lattice structures. Five four-cell networks #29, #51,#293, #303 and #76 have double eigenvalues and two eigenvectors. The rest of six four-cell networks #343, #6, #13, #270, #410 and #344 have triple eigenvalues and two eigenvectors. The existence of bifurcating branches of these networks were analysed using xppaut and mathematica.

An eigenvector with the geometric multiplicity $g(\lambda)$ may generate more than $g(\lambda)$ balanced equivalence relations. However, in the implementation of the computer algorithm, at most $g(\lambda)$ balanced equivalence relations are identified as being generated by the eigenvector and coloured accordingly (red in the diagrams in Section 8.7, medium grey in Appendix A). Although non-trivial to implement, the program could potentially label all the possible balanced equivalence relations from a given eigenvalue, which would make the figure colouring less misleading.

Chapter 9

Conclusions and Future Work

9.1 Conclusions

Group-theoretic enumeration formulas for regular homogeneous networks of valency r by Aldosray and Stewart (2005) were extended for more generalised networks which allow different valencies for each cell in Chapter 2. Furthermore, we considered another type of generalised network, which allows different cell types, represented by different colours. The relevant group action on coloured networks is defined in (2.10) as a product of two different kinds of permutation: one is for an adjacency matrix, and the other is for cell colouring. Lemma 2.8 proved this defines a group action. The cardinalities of fixed-point sets were calculated as a product of the number of fixed adjacency matrices and the number of fixed colour vectors. The above enumeration is computationally inexpensive (when $n \leq 6$, the number of colours is up to four, and the valency $r \leq 6$).

To analyse network dynamics, we next considered a visualisation of regular homogeneous networks in Chapter 3. This visualisation is computationally more expensive (keeping the number of cells to at most five, and the valency $r \leq 4$ is tractable). From all possible adjacency matrices, those corresponding to isomorphic connected networks were selected, and furthermore strongly connected networks were determined. These adjacency matrices were used for visualising networks.

Next, in Chapter 4, we showed how to compute all possible balanced equivalence relations for regular homogeneous networks. Proposition 4.1 proved that finding a balanced equivalence relation $\bowtie$ of a given network $\mathcal{G}$ is equivalent to determining an invariant polydiagonal subspace of the corresponding adjacency matrix A of $\mathcal{G}$. Furthermore, in Theorem 4.4, we proved that a polydiagonal subspace $\triangle_{\bowtie}$ is invariant if and only if it satisfies the relation:

$$P_{\bowtie} A P_{\bowtie} = A P_{\bowtie}$$

where $P_{\bowtie}$ is the projection mapping along polysynchronous direction $\triangle_{\bowtie}$.

In Lemma 4.1 followed by Proposition 4.3, we proved that an adjacency matrix has a block structure if a polysynchronous subspace $\triangle_{\bowtie}$ is invariant under A, and this led to a computer algorithm to search all possible balanced equivalence relations just from the adjacency matrices. In this computer algorithm, firstly we consider all possible equivalence relations on the set of cells. All corresponding columns of the adjacency matrix in the same conjugacy class are summed up, and the corresponding rows are compared. If the equivalence relation is balanced, then these rows are identical. This result follows from Lemma 4.1 and Proposition 4.3. For each balanced equivalence relation, the corresponding quotient network was also displayed (quotient networks are not shown in the Appendix). Stewart (2007) proved that all balanced equivalence relations form a lattice using a refinement relation in a general context. Using the refinement relation, we generated explicit forms of the lattices of balanced equivalence relations of all three and four-cell network of valency 2 (listed in Appendix A).

In Chapter 5, we reviewed basic local bifurcation theory, followed by Liapunov-Schmidt reduction. We included a result from Golubitsky and Stewart (2008) which proves that nondegeneracy conditions can be computed as an inner product of the corresponding eigenvectors of the adjacency matrix of a network. We described why generic codimension-one local synchrony-breaking steady-state bifurcations of regular homogeneous networks are usually transcritical or pitchfork bifurcations, but can be more degenerate in rare cases (Golubitsky and Stewart, 2008). Finally we showed that symmetric coupling constrains the form of the Taylor expansion of admissible vector fields.

In Chapter 6, we analysed the generic bifurcation type of two-cell regular homogeneous networks of valency 2. There are five such networks and their nondegeneracy conditions for the existence for generic bifurcations (transcritical or pitchfork) were computed using Liapunov-Schmidt reduction or the Implicit Function Theorem using the Taylor expansion form from Chapter 5. The results in this chapter were used in Example 7.5 in Chapter 7 and in Chapter 8.

Stewart (2007) showed that there exists a bijection between a lattice of balanced equivalence relations, denoted by $\Lambda_{\mathcal{G}}$, and a lattice of balanced polydiagonals, denoted by $V_{\mathcal{G}}^P$. In the first part of Chapter 7, we further proved that there exists a third form of lattice, denoted by $U_{\mathcal{G}}^P$, constructed from the eigenvalues of the quotient networks. The lattice $U_{\mathcal{G}}^P$ is important for the determination of the existence of synchrony-breaking branches, and in which balanced polydiagonal these branches lie.

For the remainder of Chapter 7, we only considered the case of regular homogeneous networks whose adjacency matrices have simple eigenvalues. Theorem 7.2 proved that there exist important lattice nodes which are defined by the eigenvector structures of the adjacency matrix

of the network. These lattice nodes are called lattice generators. Furthermore, in Lemma 7.10, we proved that the three forms of lattices, $\Lambda_{\mathcal{G}}$, $V_{\mathcal{G}}^P$ and $U_{\mathcal{G}}^P$ are order-isomorphic for simple eigenvalue networks. This Lemma 7.10 led to Theorem 7.3, which showed that the full lattice of a simple eigenvalue network was generated using these lattice generators.

Next, a number $\eta(p)$ was assigned for each lattice element in $U_{\mathcal{G}}^P$ as described in Definition 7.11. These numbers $\eta(p)$ have to satisfy a condition stated in Proposition 7.3 and their properties allowed the construction of all possible lattice structures. We showed there are 3 possible lattice structures and 14 possible lattice structures, for three-cell and four-cell regular homogeneous networks (of any valency), respectively.

In particular, we now summarise the results for three and four cell regular homogeneous networks of valency 2. There are 21 networks with simple real eigenvalues and 6 networks with simple complex eigenvalues for three-cell regular homogeneous networks of valency 2. In these three-cell regular networks, all 3 possible lattice structures are observed. Hence all 27 simple (real or complex) eigenvalue three-cell regular homogeneous networks of valency 2 were classified into 3 types of lattice. Similarly, there are 98 networks with simple real eigenvalues and 130 networks simple complex eigenvalues for four-cell regular homogeneous networks of valency 2. There are 14 possible lattice structures for four-cell simple eigenvalue networks, however, two of these lattices are not observed for four-cell networks of valency 2. The thirteenth lattice was found for valency 3, while the fourteenth lattice has not yet been found considering up to valency 5. Therefore, this result shows that all 228 simple (real or complex) eigenvalue four-cell regular homogeneous networks of valency 2 were classified into 12 lattice structures. Note that these networks include ODE-equivalent networks, as defined in Dias and Stewart (2005).

A lattice node in $U_{\mathcal{G}}^P$ with non-zero $\eta(p)$ indicates the existence of synchrony-breaking bifurcating branches in the corresponding polysynchronous subspace, proved in Lemma 7.12. A special case of this lemma is the existence of synchrony-breaking bifurcating branches corresponding to balanced two-colourings, stated in Lemma 7.13. This result follows from Lemma 7.7, which proved that equivalence relations generated from eigenvectors with only two distinct entries are always balanced, and Lemma 7.12. Theorem 2.1. in Wang and Golubitsky (2005) shows the equivalent result to Lemma 7.13 for planar lattice dynamical systems. Using an order-isomorphism from $U_{\mathcal{G}}^P$ to $V_{\mathcal{G}}^P$, the rank of any non-zero $\eta(p)$ represents the dimension of the corresponding polysynchronous subspace. Therefore, using the number $\eta(p)$ and its position in the lattice, schematic diagrams for the existence of bifurcating branches were drawn for three-cell and four-cell regular homogeneous networks with simple real eigenvalues. The distinct bifurcation diagrams (for the existence of branches, not the types of bifurcation) were further

classified into 9 different types for four-cell regular homogeneous networks. Types of bifurcation for each branch can be computed by Liapunov-Schmidt reduction using the corresponding quotient network.

Finally in Chapter 8, we applied this lattice classification method to non-simple eigenvalue networks. Although all quotient networks of simple eigenvalue networks are topologically distinct (Corollary 7.2), some quotient networks are topologically identical for many non-simple eigenvalue networks, shown in Proposition 8.3. This happens when the dimension of an eigenspace is more than one and it makes the lattice size of non-simple eigenvalue networks bigger than the lattice size of simple eigenvalue networks.

Our main purpose for using lattice structures is to detect which balanced polydiagonals belong to eigenspaces, and which determine bifurcating branch directions for local bifurcations. In simple eigenvalue networks, this method works well since there is one-to-one relationship between balanced polydiagonals and eigenspaces. However, for non-simple eigenvalue networks, this approach is not so straightforward because there are other lattice elements which arise from the multiple dimensionality of eigenspaces.

To detect one-to-one relationships between balanced polydiagonals and the corresponding eigenspaces (for example, at most two balanced polydiagonals from a two dimensional eigenspace), we defined a reduced lattice as described in Definition 8.1, where topologically identical quotient networks are minimally merged.

Once we had obtained a reduced lattice from the original lattice, $\eta(p)$ were assigned for each lattice element in a similar manner to simple eigenvalue networks. The number of multiple bifurcating branches from a single bifurcation point (corresponding to a repeated eigenvalue) was observed from the original lattice. Diagrams which show the existence of bifurcating branches (unique or non-unique) were listed for all three and four-cell regular homogeneous networks of valency 2 with non-simple real eigenvalues.

9.2 Discussion and Future Work

There is a theorem which states:

Theorem 9.1. *A square adjacency matrix is irreducible if and only if its directed graph is strongly connected.*

Proof. See Brualdi (2006). □

It seems that similar enumeration formulas could be applied to the enumeration of strongly connected networks.

Leite and Golubitsky (2006) found that there are exactly five three-cell regular homogeneous networks with eigenvalue type $S3$ (double eigenvalues with one eigenvector). They analysed these networks and found that three networks which they denoted 3, 27 and 28 (#12 (equivalently #37), #6 and #14 in our Table 3.2) have nontrivial bifurcating solutions whose rates of growth are different in distinct cells, while in networks 6 and 11 (#28 and #18 in our Table 3.2) the growth rate of solutions in a given bifurcating branch is equal for all cells. In our analysis, networks 6 and 11 are found to be strongly connected networks. It is worth analysing if strongly connected networks influence the growth rate in cells.

Aguiar *et al.* (2008) use an algorithm to search all possible adjacency matrices which have a given quotient network. This is the opposite direction from our algorithm which generates all possible quotient networks from a given network. If we are interested in a particular quotient network as in Aguiar *et al.* (2007), their approach is computationally inexpensive and searches target networks efficiently.

The number of n-cell regular homogeneous networks increases as valency increases, however, the structures of lattices of balanced equivalence relations of the networks are independent of valency. Golubitsky and Stewart (2008) found an exceptional four-cell homogeneous regular network of valency 736, where the generic bifurcation behaviour is different from other networks. Generic bifurcation type is determined by nondegeneracy conditions using Liapunov-Schmidt reduction, which deals with nonlinear terms. By contrast, balanced equivalence relations are determined from a linear admissible vector field. While existence of local bifurcation branches and their directions is not affected by higher order terms of the admissible vector field, the generic type of bifurcations might be influenced by nonlinear terms.

Observe that the number of distinct lattice structures (14 for simple eigenvalue four-cell networks and 3 for simple eigenvalue three-cell networks) is much less than the number of networks. Furthermore, the number of distinct bifurcation diagrams of four-cell regular homogeneous networks with simple eigenvalues is even smaller than 14, at just 9. This observation leads to the classification of existence of bifurcation branches. Since the diagrams of the existence of bifurcating branches do not consider the position (order on the bifurcation parameter axis) of critical eigenvalues, the equivalence of the existence of bifurcating branches would be topological. If we add the information about the types of bifurcating branches, this classification would be more complex and the number of categories would increase.

In our computer algorithm, balanced equivalence relations generated from eigenvector structures are coloured differently to be distinguished from other balanced equivalence relations. For one dimensional eigenvectors (associated with a simple eigenvalue) most linear al-

gebra implementations will return a unit vector for the eigenvector which is well defined other than the sign. However, for multidimensional eigenspaces the precise numerical values of the spanning eigenvectors which the computer algorithm selects will depend on the implementation details. This means that for example given a double eigenvalue, where the eigenspace is a plane (e.g. $(x, y, z) = (a, b, 0)$), the eigenvectors could be any two vectors spanning this plane. The eigenspace may contain multiple possible polydiagonals (in this example $(a, a, 0)$, $(a, 0, 0)$ and $(0, b, 0)$) but it is non-trivial to compute these from any two eigenvectors. If we can overcome this difficulty, colouring scheme of the lattices of non-simple eigenvalue networks would look simpler.

There are some exceptional four-cell regular homogeneous networks of valency 2, where the reduced lattice does not match any simple eigenvalue lattice structure. These are networks #29, #51, #293, #303 and #76 with double eigenvalues and two eigenvectors, and networks #343, #6, #13, #270, #410 and #344 with triple eigenvalues and two eigenvectors. We speculate that these exceptional networks may have special adjacency matrix structures.

If two networks $\mathcal{G}$ and $\widetilde{\mathcal{G}}$ are ODE-equivalent (Dias and Stewart, 2005), then they have the same lattice of balanced equivalence relations Λ. There exist many networks which have the same lattice of balanced equivalence relations, however, they do not satisfy the definition of ODE-equivalence. Lattice classifications show that their bifurcation existence diagrams are equivalent. We speculate that there exists a category broader than ODE-equivalence to classify network bifurcation behaviour.

In this thesis, we considered synchrony-breaking steady-state bifurcations. A similar analysis can be extended to synchrony-breaking Hopf bifurcations.

In applications, we are particularly interested in stable solutions. In this thesis we only considered the existence of bifurcating branches, however, the relationships between the network structure and the stability of these branches can be analysed.

9.3 Towards Applications

We aimed to classify qualitative dynamical behaviours solely from the network architecture (topology), not from specific function forms of a system. This kind of approach is inverted compared to conventional methods which use specific function forms and reduce qualitative dynamical behaviours, or use all available data as much possible and extract the essence of a given complex system. However, in complex networks, it is quite hard to determine specific function forms, but easier to find linkage information. Mochizuki (2007) used this approach to determine the number of possible steady state solutions (which correspond to the number of different

cell types) in gene regulatory networks for early development in a sea urchin species. Similarly, Albert and Othmer (2003) analysed whether gene expression patterns of the Drosophila segment polarity was determined by the topology of the network, but not from the detailed form of the rate laws described by a system of ODEs.

Another aspect of our analysis is the size of networks. We analysed and classified bifurcation behaviours of much smaller networks than the complex networks which we can find in real world. However, this does not imply that analysing small networks is far from practical applications.

Recently, it has been discovered that there are several small size subnetworks, which frequently occur within complex networks throughout many branches of science such as WWW, gene regulatory networks, food webs, electric circuit, etc. These small networks are called **network motifs** and are considered to be building blocks of complex networks (Milo *et al.*, 2005), which carry important functionality needed in a complex network.

Kashtan *et al.* (2004) found that larger network motifs have topological similarities to smaller network motifs. They defined *motif generalisations*, which are families of motifs of different sizes which share a common network architecture and analysed their dynamical behaviours.

Ishihara *et al.* (2005) also analysed a similar generalization of one network motif, the feed-forward loop. They considered several combinations of feed-forward loops and suggested their cross talk would play important roles in morphogenesis.

Golubitsky and Lauterbach (2008) introduces the notion of a product network, where the nodes (cells) of one network are replaced by copies of another network. This might give a formalism for a generalisation of small networks (network motifs) to build larger networks.

One of immediate generalisation of regular homogeneous networks would be to allow different cell types in a network. These networks were enumerated in Chapter 2. In such networks, the entries of adjacency matrices can no longer be represented as a single positive integer, but could require algebraic symbols or one adjacency matrix per connection type. However, the computation of all possible balanced equivalence relations would follow in a similar manner. Equality of numbers would be replaced by the equality of algebraic symbols. This work is ongoing.

Appendix A

Listing of Homogeneous Coupled Cell Network Lattices

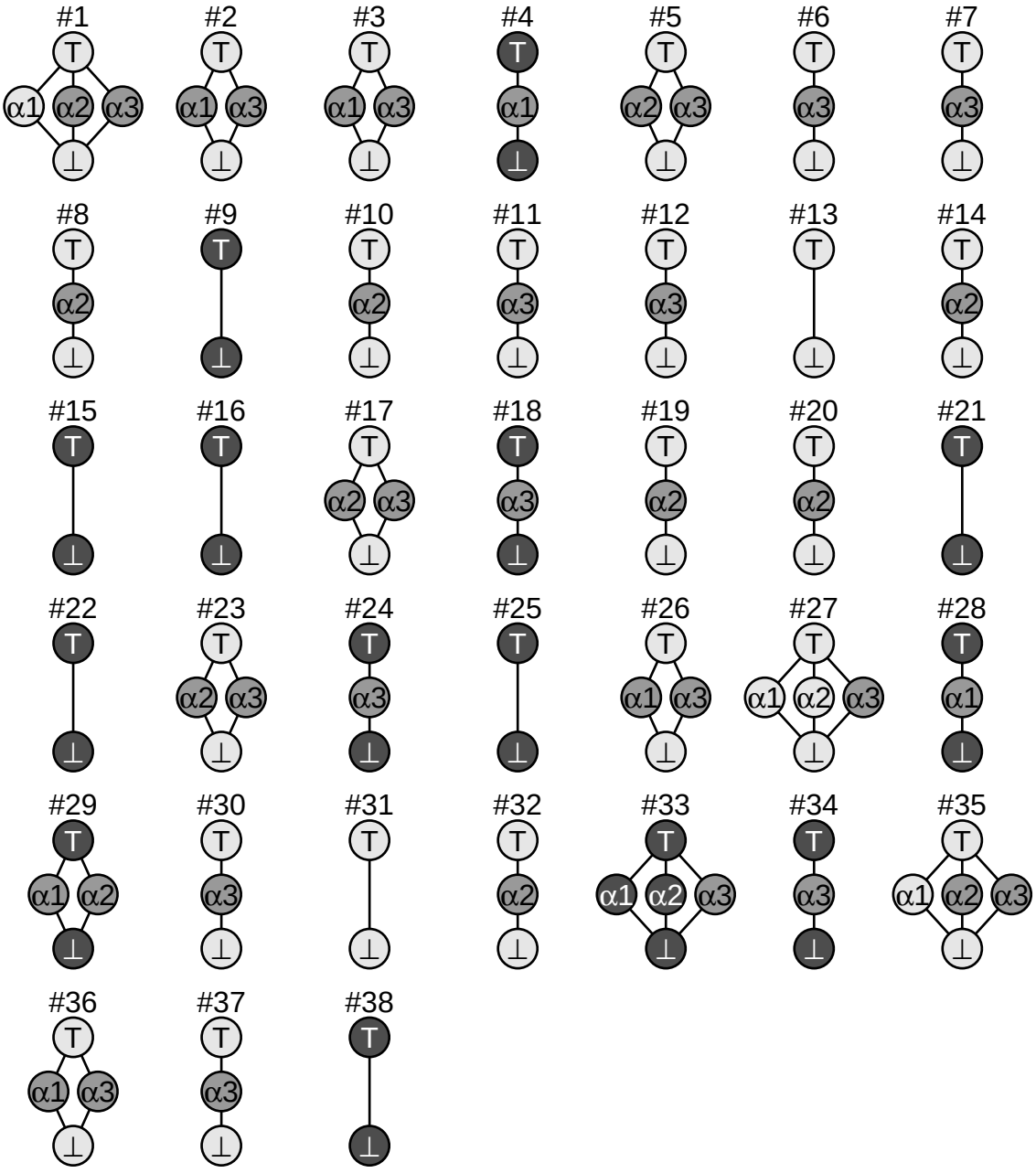

Figure A.1: All lattices of balanced equivalence relations for the 38 connected networks with three cells and valency two ($n = 3$, $r = 2$, see Figure 3.2). The lattices for the 14 strongly connected networks are shown with dark grey nodes, the rest have pale grey nodes. Nodes in the medium grey are associated with equivalence relations generated by eigenvectors. $\top$ denotes the top lattice element, $\{\{1,2,3\}\}$, $\bot$ the bottom lattice element, $\{\{1\},\{2\},\{3\}\}$, while $\alpha 1, \ldots, \alpha 3$ denote $\{\{1,2\},\{3\}\}$, $\{\{1,3\},\{2\}\}$ and $\{\{1\},\{2,3\}\}$ respectively.

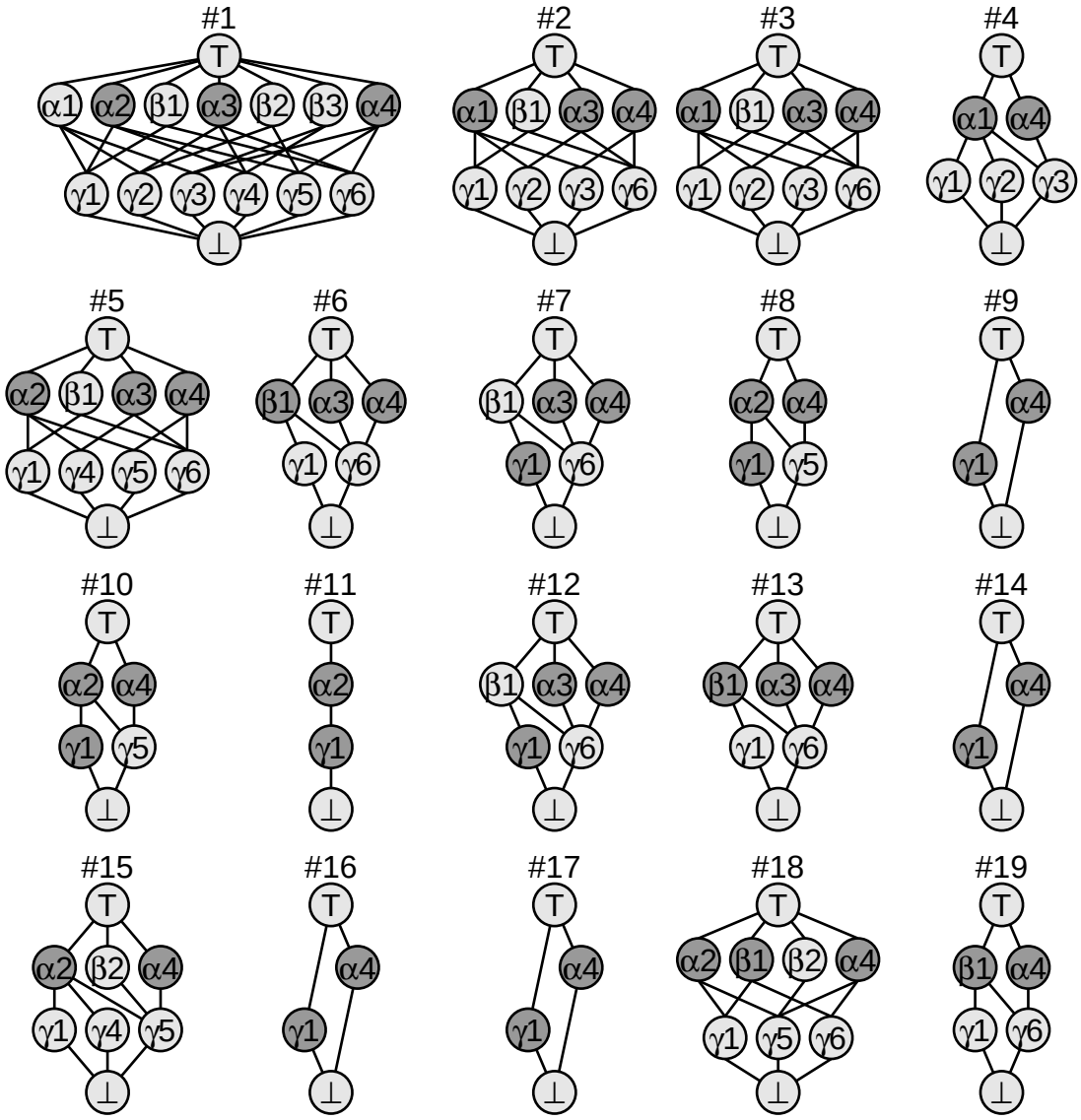

Figure A.2: All lattices of balanced equivalence relations for the 416 connected networks with four cells and valency two ($n = 4$, $r = 2$, see Figure 3.3), split over fifteen pages. The lattices for the 108 strongly connected networks are shown with dark grey nodes, the rest have pale grey nodes. Nodes in the medium grey are associated with equivalence relations generated by eigenvectors. $\top$ denotes the top lattice element, $\{\{1,2,3,4\}\}$, $\bot$ the bottom lattice element, $\{\{1\},\{2\},\{3\},\{4\}\}$, $\alpha 1,\ldots,\alpha 4$ denote $\{\{1,2,3\},\{4\}\}$, $\{\{1,2,4\},\{3\}\}$, $\{\{1,3,4\},\{2\}\}$ and $\{\{1\},\{2,3,4\}\}$ (triplet and singleton), $\beta 1,\ldots\beta 3$ denote $\{\{1,2\},\{3,4\}\}$, $\{\{1,3\},\{2,4\}\}$ and $\{\{1,4\},\{2,3\}\}$ (two pairs), and finally $\gamma 1,\ldots,\gamma 6$ denote $\{\{1,2\},\{3\},\{4\}\}$, $\{\{1,3\},\{2\},\{4\}\}$, $\{\{1\},\{2,3\},\{4\}\}$, $\{\{1,4\},\{2\},\{3\}\}$, $\{\{1\},\{2,4\},\{3\}\}$, and $\{\{1\},\{2\},\{3,4\}\}$ (pair and two singletons) respectively.

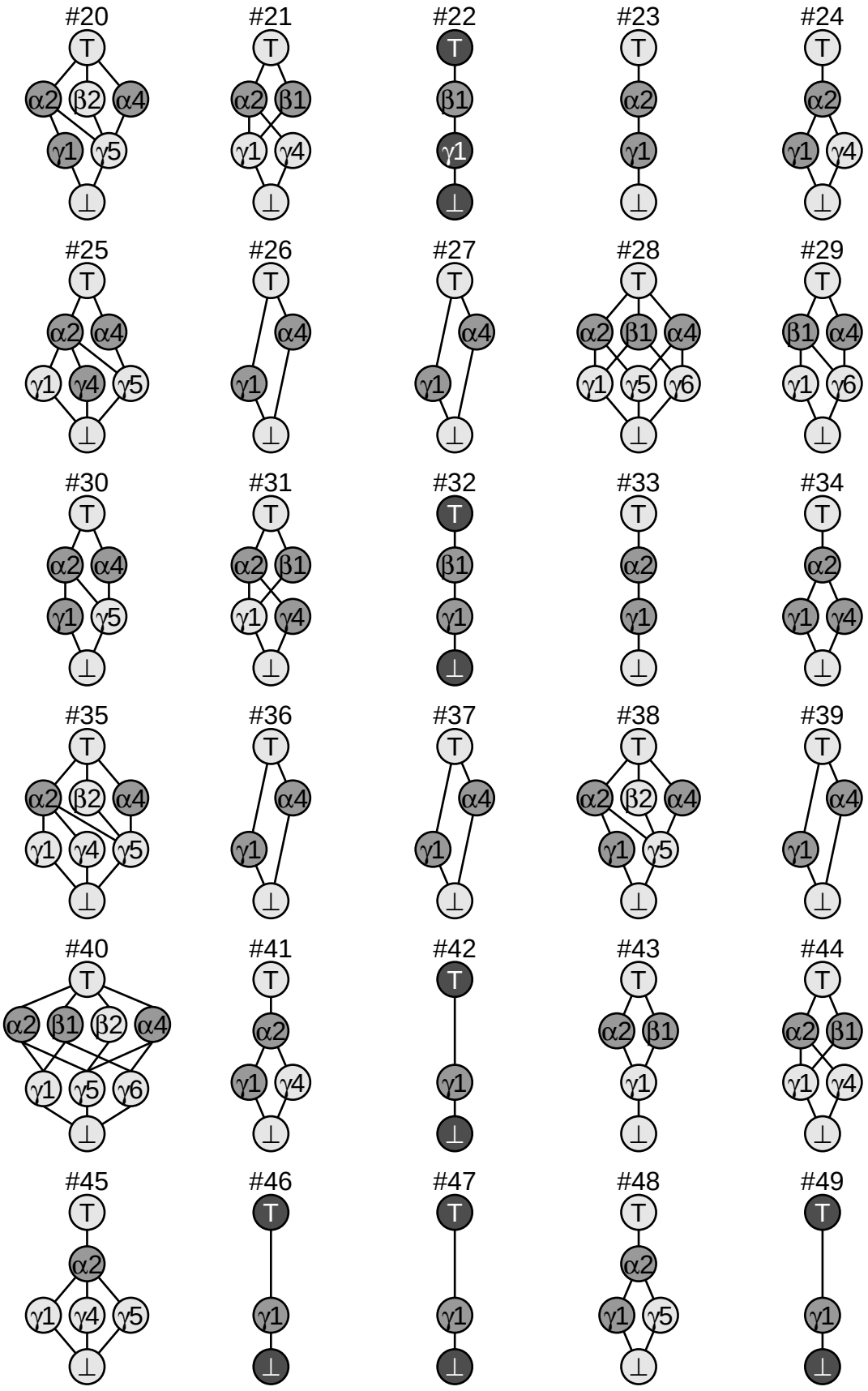
#20
⊤
α2
β2
α4
γ1
γ5
⊥
#21
⊤
α2
β1
γ1
γ4
⊥
#22
⊤
β1
γ1
⊥
#23
⊤
α2
γ1
⊥
#24
⊤
α2
γ1
γ4
⊥
#25
⊤
α2
α4
γ1
γ4
γ5
⊥
#26
⊤
α4
γ1
⊥
#27
⊤
α4
γ1
⊥
#28
⊤
α2
β1
α4
γ1
γ5
γ6
⊥
#29
⊤
β1
α4
γ1
γ6
⊥
#30
⊤
α2
α4
γ1
γ5
⊥
#31
⊤
α2
β1
γ1
γ4
⊥
#32
⊤
β1
γ1
⊥
#33
⊤
α2
γ1
⊥
#34
⊤
α2
γ1
γ4
⊥
#35
⊤
α2
β2
α4
γ1
γ4
γ5
⊥
#36
⊤
α4
γ1
⊥
#37
⊤
α4
γ1
⊥
#38
⊤
α2
β2
α4
γ1
γ5
⊥
#39
⊤
α4
γ1
⊥
#40
⊤
α2
β1
β2
α4
γ1
γ5
γ6
⊥
#41
⊤
α2
γ1
γ4
⊥
#42
⊤
γ1
⊥
#43
⊤
α2
β1
γ1
⊥
#44
⊤
α2
β1
γ1
γ4
⊥
#45
⊤
α2
γ1
γ4
γ5
⊥
#46
⊤
γ1
⊥
#47
⊤
γ1
⊥
#48
⊤
α2
γ1
γ5
⊥
#49
⊤
γ1
⊥

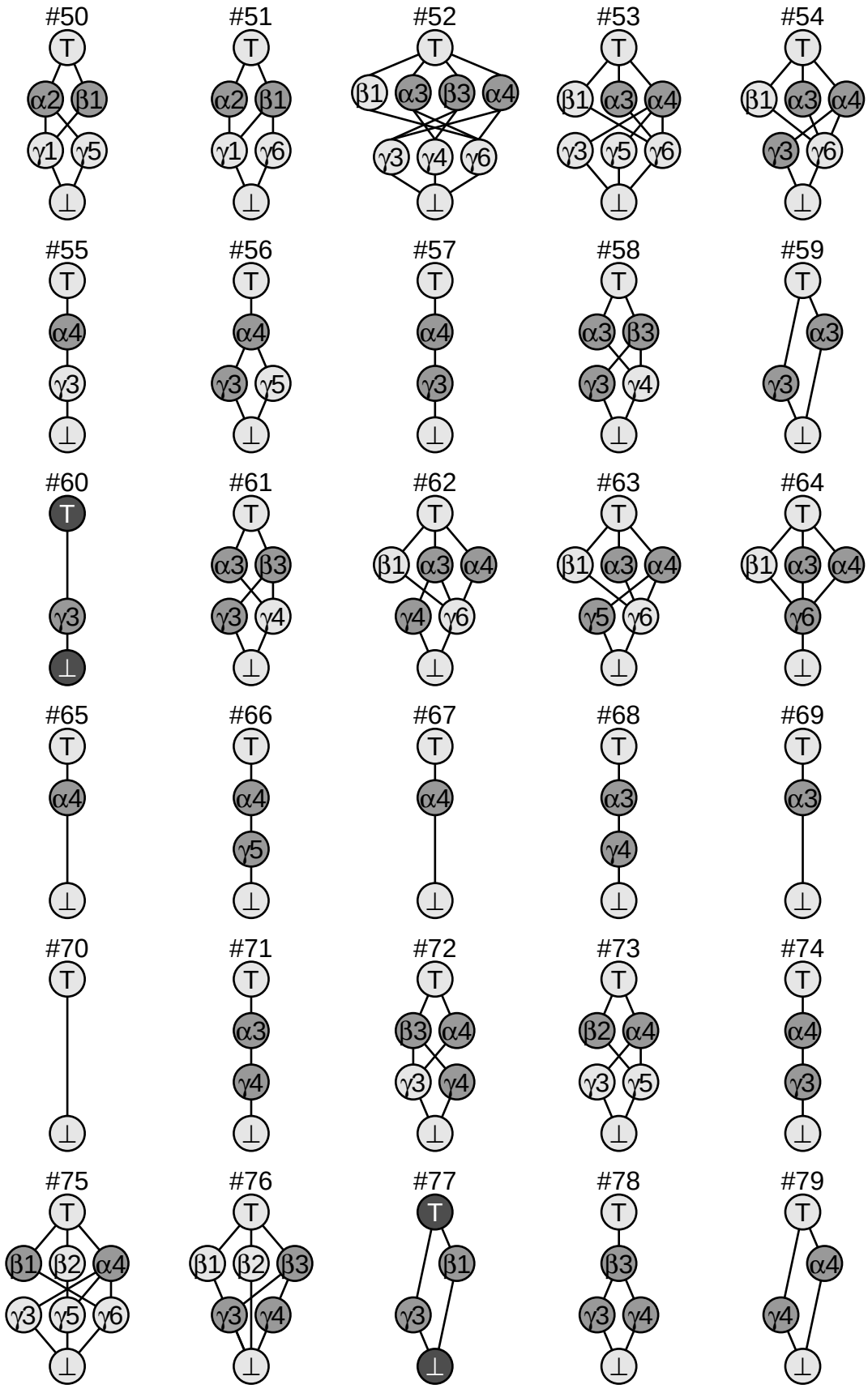
#50
⊤
α2
β1
γ1
γ5
⊥
#51
⊤
α2
β1
γ1
γ6
⊥
#52
⊤
β1
α3
β3
α4
γ3
γ4
γ6
⊥
#53
⊤
β1
α3
α4
γ3
γ5
γ6
⊥
#54
⊤
β1
α3
α4
γ3
γ6
⊥
#55
⊤
α4
γ3
⊥
#56
⊤
α4
γ3
γ5
⊥
#57
⊤
α4
γ3
⊥
#58
⊤
α3
β3
γ3
γ4
⊥
#59
⊤
α3
γ3
⊥
#60
⊤
γ3
⊥
#61
⊤
α3
β3
γ3
γ4
⊥
#62
⊤
β1
α3
α4
γ4
γ6
⊥
#63
⊤
β1
α3
α4
γ5
γ6
⊥
#64
⊤
β1
α3
α4
γ6
⊥
#65
⊤
α4
⊥
#66
⊤
α4
γ5
⊥
#67
⊤
α4
⊥
#68
⊤
α3
γ4
⊥
#69
⊤
α3
⊥
#70
⊤
⊥
#71
⊤
α3
γ4
⊥
#72
⊤
β3
α4
γ3
γ4
⊥
#73
⊤
β2
α4
γ3
γ5
⊥
#74
⊤
α4
γ3
⊥
#75
⊤
β1
β2
α4
γ3
γ5
γ6
⊥
#76
⊤
β1
β2
β3
γ3
γ4
⊥
#77
⊤
β1
γ3
⊥
#78
⊤
β3
γ3
γ4
⊥
#79
⊤
α4
γ4
⊥

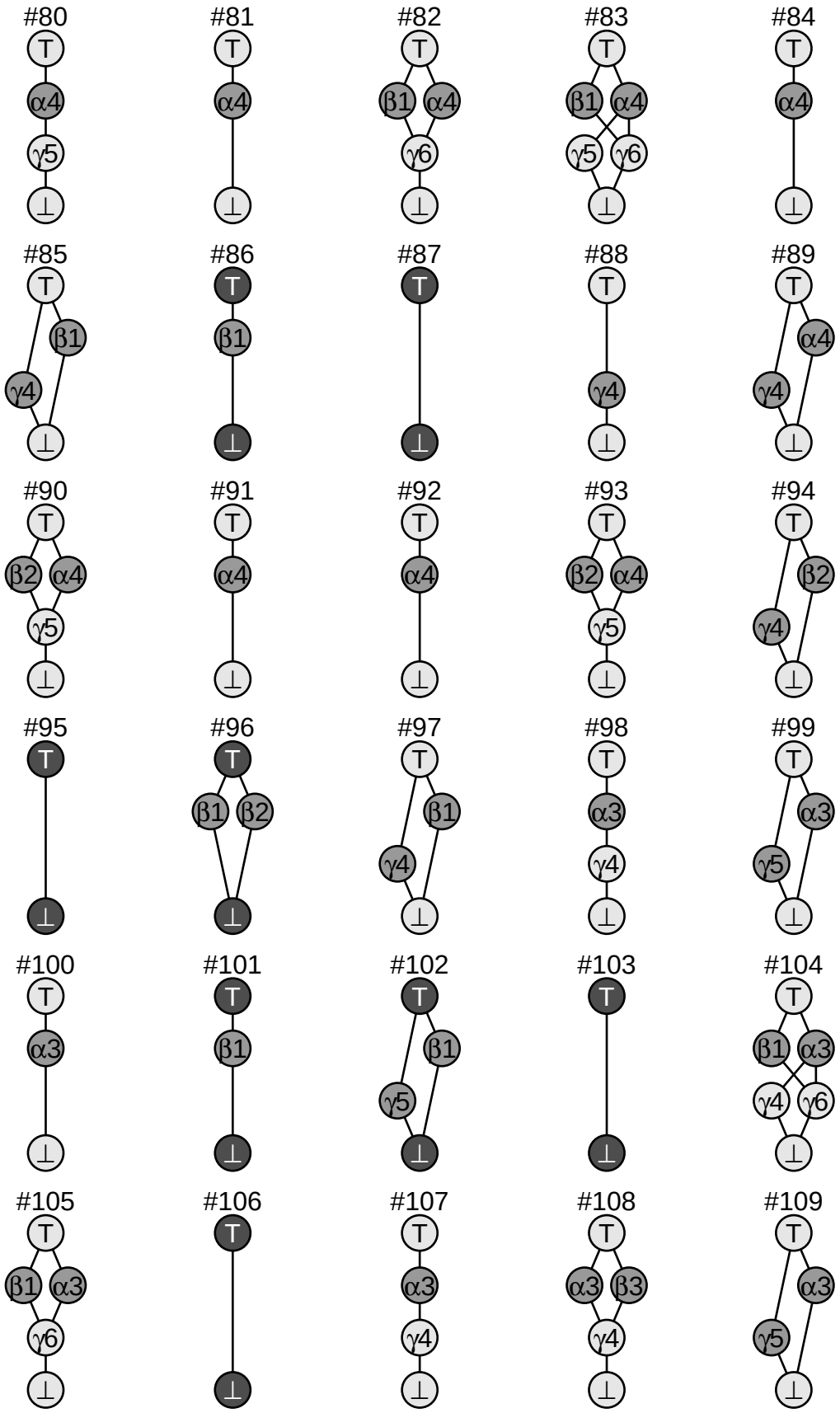
#80
T
α4
γ5
⊥
#81
T
α4
⊥
#82
T
β1
α4
γ6
⊥
#83
T
β1
α4
γ5
γ6
⊥
#84
T
α4
⊥
#85
T
β1
γ4
⊥
#86
T
β1
⊥
#87
T
⊥
#88
T
γ4
⊥
#89
T
α4
γ4
⊥
#90
T
β2
α4
γ5
⊥
#91
T
α4
⊥
#92
T
α4
⊥
#93
T
β2
α4
γ5
⊥
#94
T
β2
γ4
⊥
#95
T
⊥
#96
T
β1
β2
⊥
#97
T
β1
γ4
⊥
#98
T
α3
γ4
⊥
#99
T
α3
γ5
⊥
#100
T
α3
⊥
#101
T
β1
⊥
#102
T
β1
γ5
⊥
#103
T
⊥
#104
T
β1
α3
γ4
γ6
⊥
#105
T
β1
α3
γ6
⊥
#106
T
⊥
#107
T
α3
γ4
⊥
#108
T
α3
β3
γ4
⊥
#109
T
α3
γ5
⊥

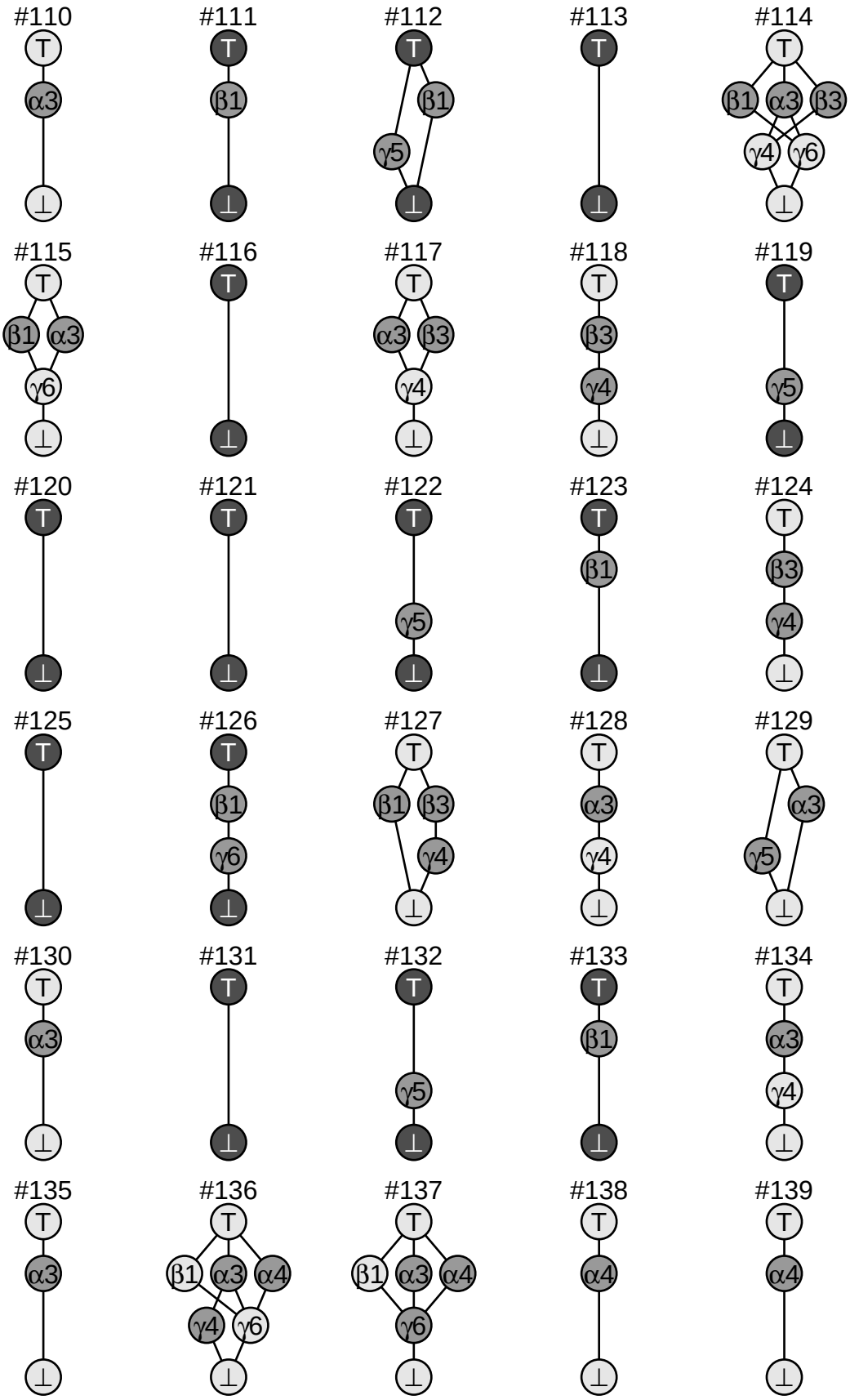
#110
⊤
α3
⊥
#111
⊤
β1
⊥
#112
⊤
β1
γ5
⊥
#113
⊤
⊥
#114
⊤
β1
α3
β3
γ4
γ6
⊥
#115
⊤
β1
α3
γ6
⊥
#116
⊤
⊥
#117
⊤
α3
β3
γ4
⊥
#118
⊤
β3
γ4
⊥
#119
⊤
γ5
⊥
#120
⊤
⊥
#121
⊤
⊥
#122
⊤
γ5
⊥
#123
⊤
β1
⊥
#124
⊤
β3
γ4
⊥
#125
⊤
⊥
#126
⊤
β1
γ6
⊥
#127
⊤
β1
β3
γ4
⊥
#128
⊤
α3
γ4
⊥
#129
⊤
α3
γ5
⊥
#130
⊤
α3
⊥
#131
⊤
⊥
#132
⊤
γ5
⊥
#133
⊤
β1
⊥
#134
⊤
α3
γ4
⊥
#135
⊤
α3
⊥
#136
⊤
β1
α3
α4
γ4
γ6
⊥
#137
⊤
β1
α3
α4
γ6
⊥
#138
⊤
α4
⊥
#139
⊤
α4
⊥

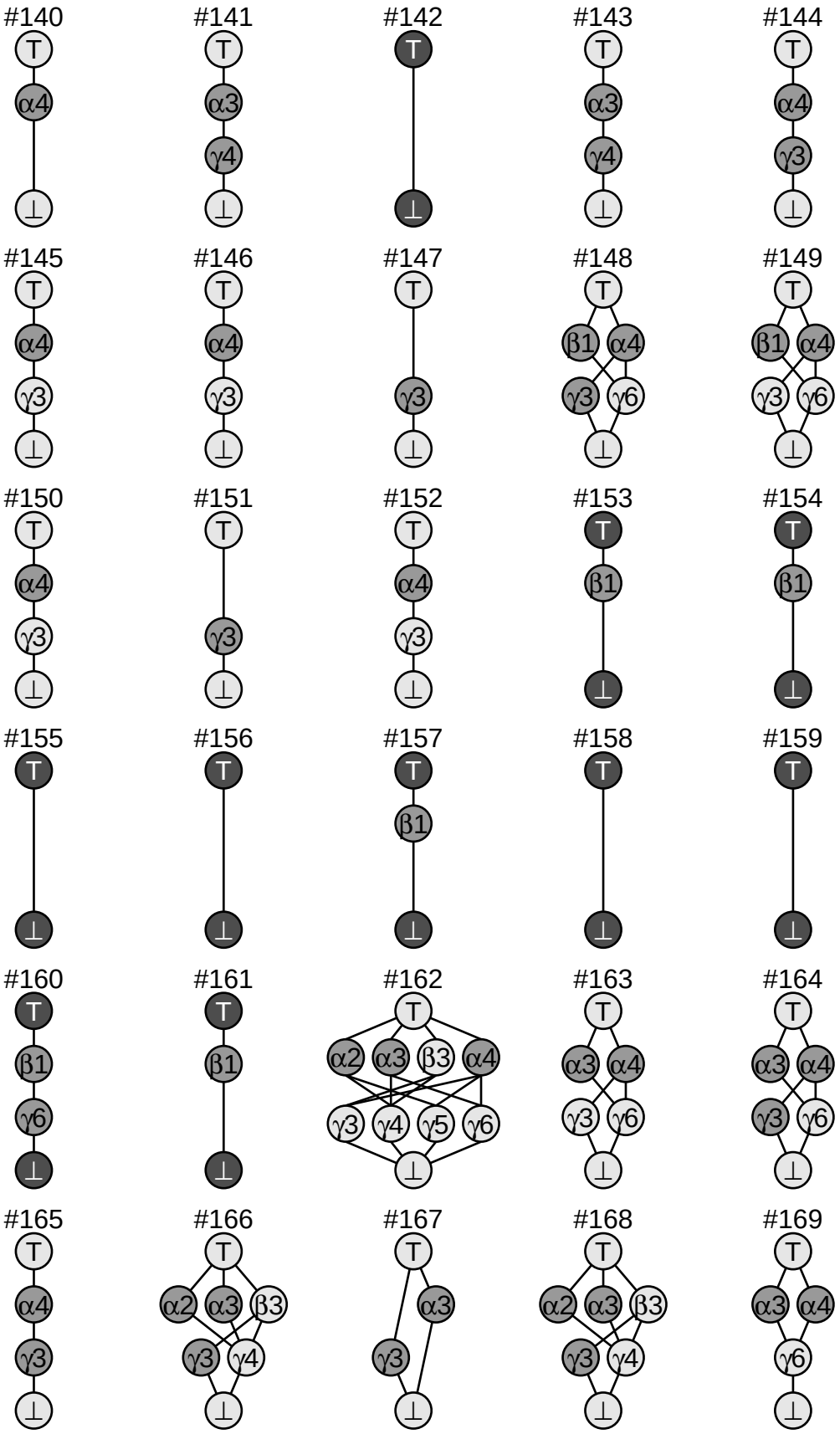
#140
⊤
α4
⊥
#141
⊤
α3
γ4
⊥
#142
⊤
⊥
#143
⊤
α3
γ4
⊥
#144
⊤
α4
γ3
⊥
#145
⊤
α4
γ3
⊥
#146
⊤
α4
γ3
⊥
#147
⊤
γ3
⊥
#148
⊤
β1
α4
γ3
γ6
⊥
#149
⊤
β1
α4
γ3
γ6
⊥
#150
⊤
α4
γ3
⊥
#151
⊤
γ3
⊥
#152
⊤
α4
γ3
⊥
#153
⊤
β1
⊥
#154
⊤
β1
⊥
#155
⊤
⊥
#156
⊤
⊥
#157
⊤
β1
⊥
#158
⊤
⊥
#159
⊤
⊥
#160
⊤
β1
γ6
⊥
#161
⊤
β1
⊥
#162
⊤
α2
α3
β3
α4
γ3
γ4
γ5
γ6
⊥
#163
⊤
α3
α4
γ3
γ6
⊥
#164
⊤
α3
α4
γ3
γ6
⊥
#165
⊤
α4
γ3
⊥
#166
⊤
α2
α3
β3
γ3
γ4
⊥
#167
⊤
α3
γ3
⊥
#168
⊤
α2
α3
β3
γ3
γ4
⊥
#169
⊤
α3
α4
γ6
⊥

#170

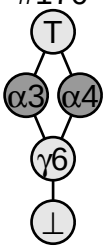

#171

#172

#173

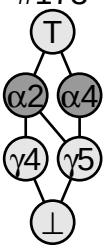

#174

#175

#176

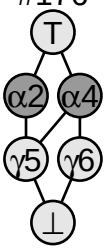

#177

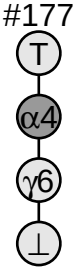

#178

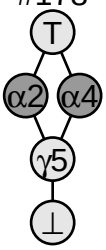

#179

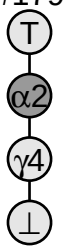

#180

#181

#182

#183

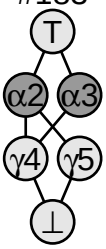

#184

#185

#186

#187

#188

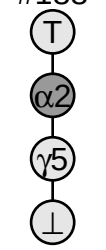

#189

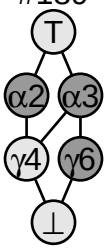

#190

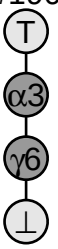

#191

#192

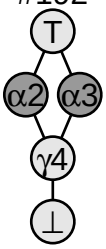

#193

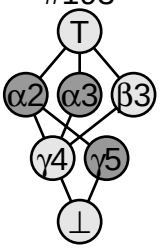

#194

#195

#196

#197

#198

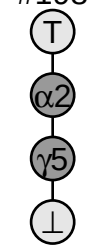

#199

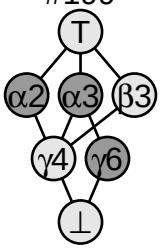

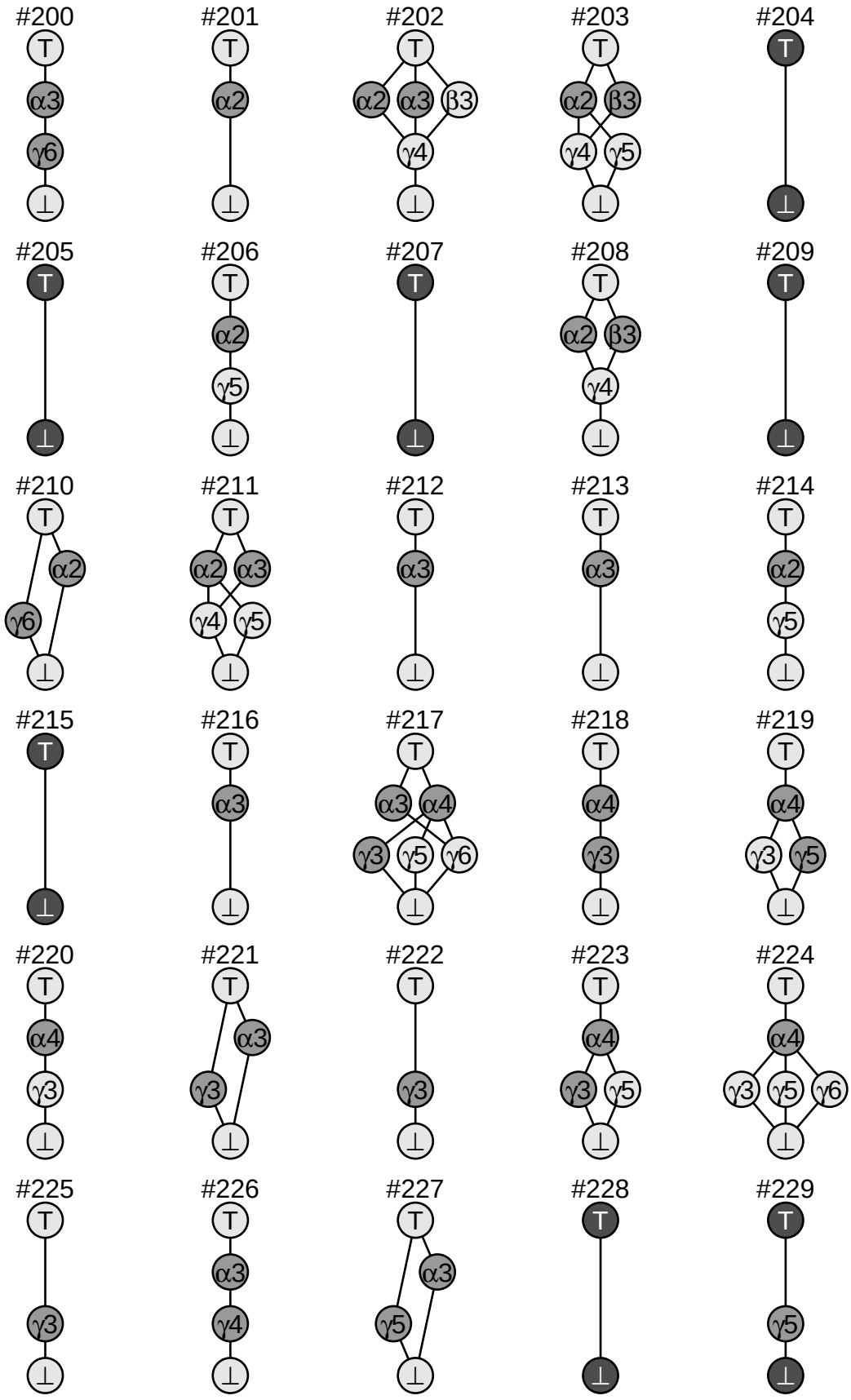
#200
⊤
α3
γ6
⊥
#201
⊤
α2
⊥
#202
⊤
α2
α3
β3
γ4
⊥
#203
⊤
α2
β3
γ4
γ5
⊥
#204
⊤
⊥
#205
⊤
⊥
#206
⊤
α2
γ5
⊥
#207
⊤
⊥
#208
⊤
α2
β3
γ4
⊥
#209
⊤
⊥
#210
⊤
α2
γ6
⊥
#211
⊤
α2
α3
γ4
γ5
⊥
#212
⊤
α3
⊥
#213
⊤
α3
⊥
#214
⊤
α2
γ5
⊥
#215
⊤
⊥
#216
⊤
α3
⊥
#217
⊤
α3
α4
γ3
γ5
γ6
⊥
#218
⊤
α4
γ3
⊥
#219
⊤
α4
γ3
γ5
⊥
#220
⊤
α4
γ3
⊥
#221
⊤
α3
γ3
⊥
#222
⊤
γ3
⊥
#223
⊤
α4
γ3
γ5
⊥
#224
⊤
α4
γ3
γ5
γ6
⊥
#225
⊤
γ3
⊥
#226
⊤
α3
γ4
⊥
#227
⊤
α3
γ5
⊥
#228
⊤
⊥
#229
⊤
γ5
⊥

#230

#231

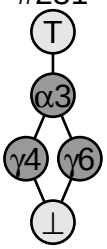

#232

#233

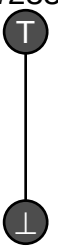

#234

#235

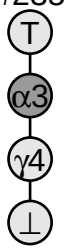

#236

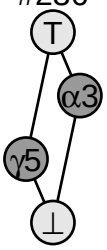

#237

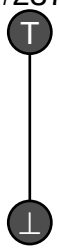

#238

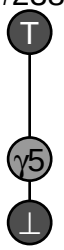

#239

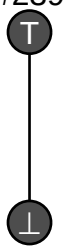

#240

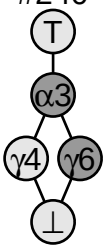

#241

#242

#243

#244

#245

#246

#247

#248

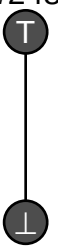

#249

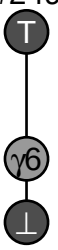

#250

#251

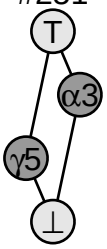

#252

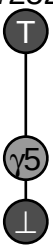

#253

#254

#255

#256

#257

#258

#259

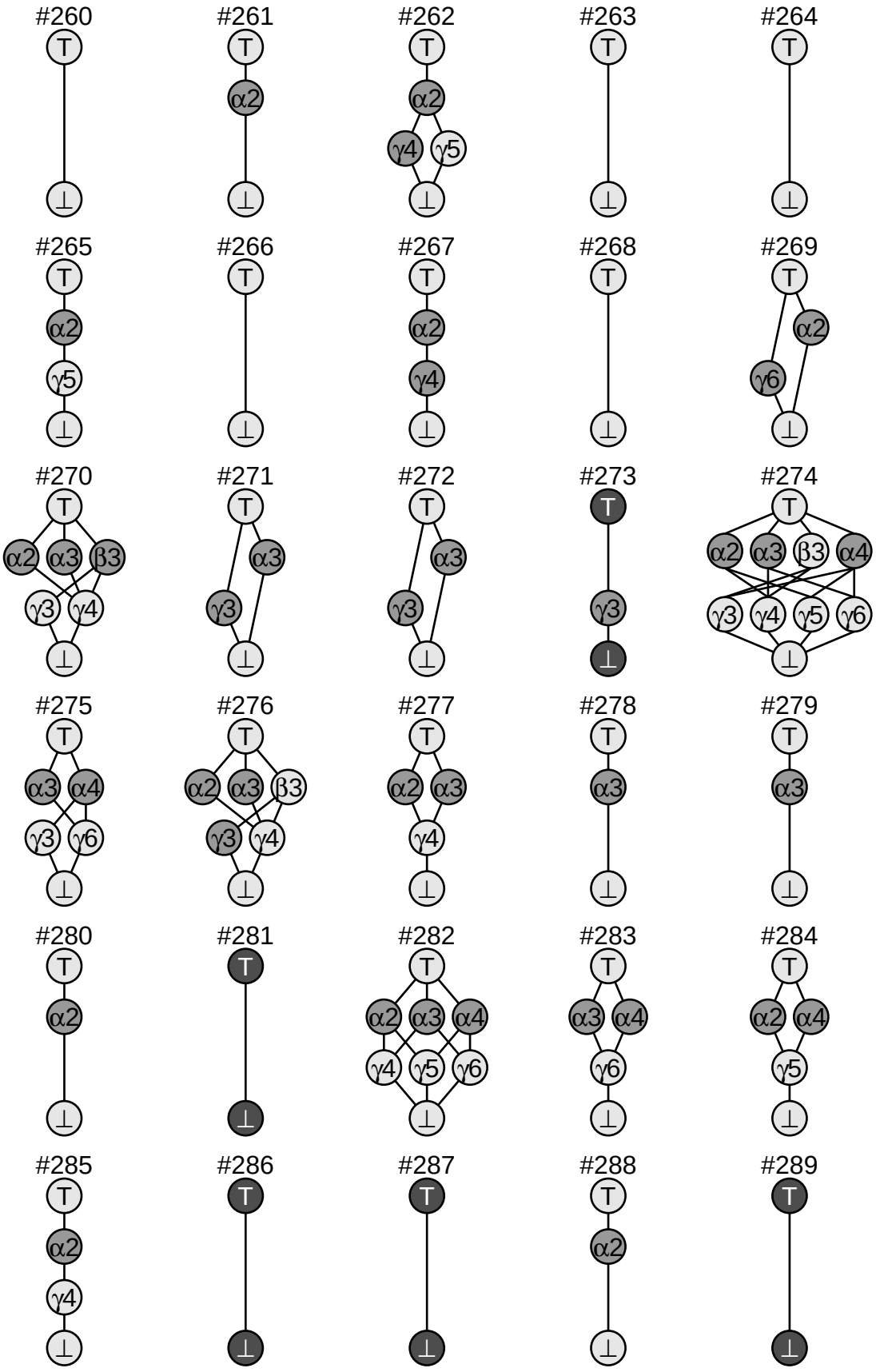
#260
#261
#262
#263
#264
#265
#266
#267
#268
#269
#270
#271
#272
#273
#274
#275
#276
#277
#278
#279
#280
#281
#282
#283
#284
#285
#286
#287
#288
#289

#290

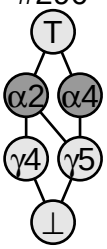

#291

#292

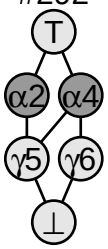

#293

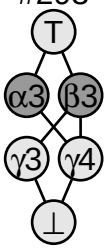

#294

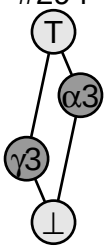

#295

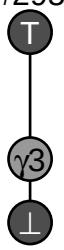

#296

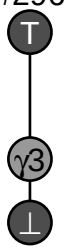

#297

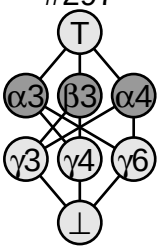

#298

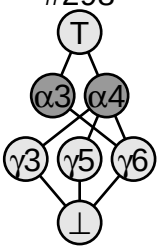

#299

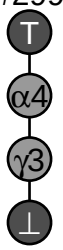

#300

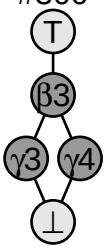

#301

#302

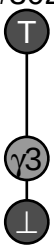

#303

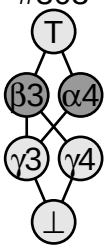

#304

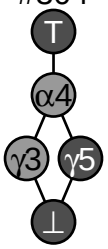

#305

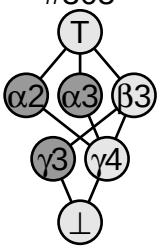

#306

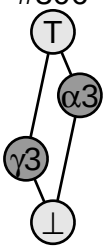

#307

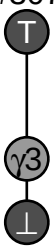

#308

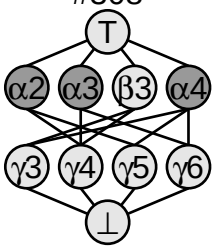

#309

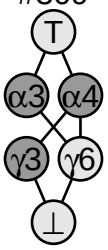

#310

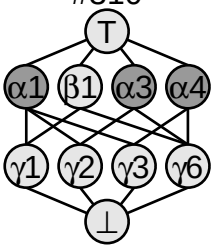

#311

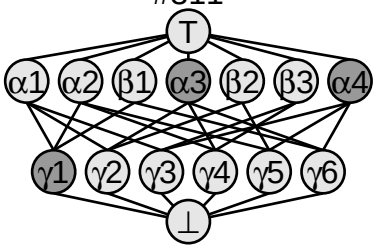

#312

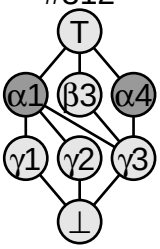

#313

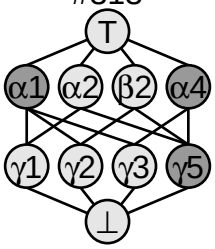

#314

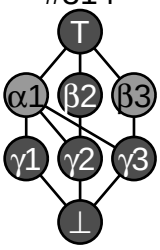

#315

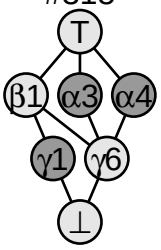

#316

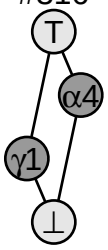

#317

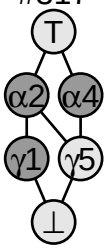

#318

#319

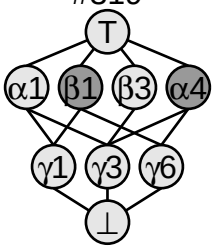

#320

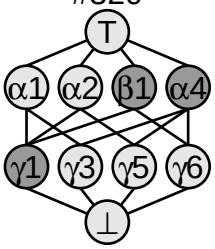

#321

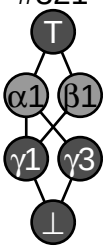

#322

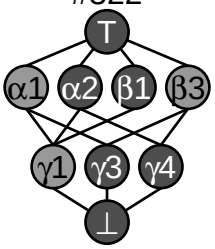

#323

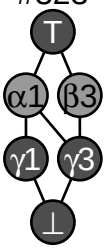

#324

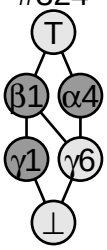

#325

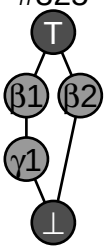

#326

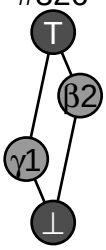

#327

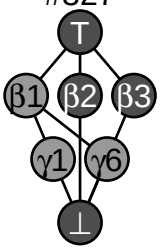

#328

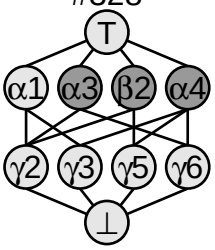

#329

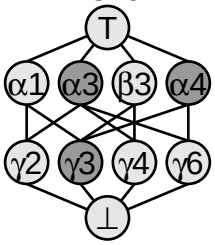

#330

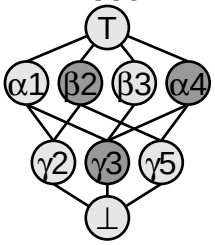

#331

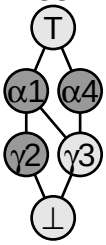

#332

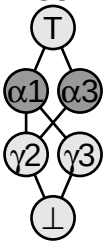

#333

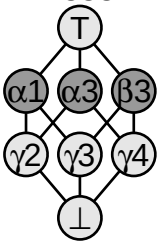

#334

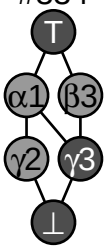

#335

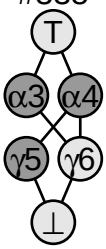

#336

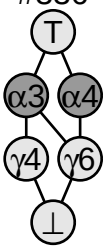

#337

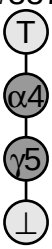

#338

#339

#340

#341

#342

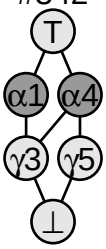

#343

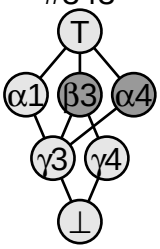

#344

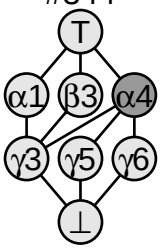

#345

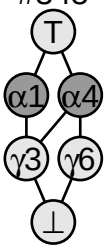

#346

#347

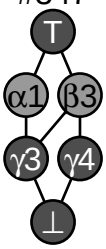

#348

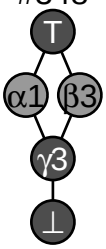

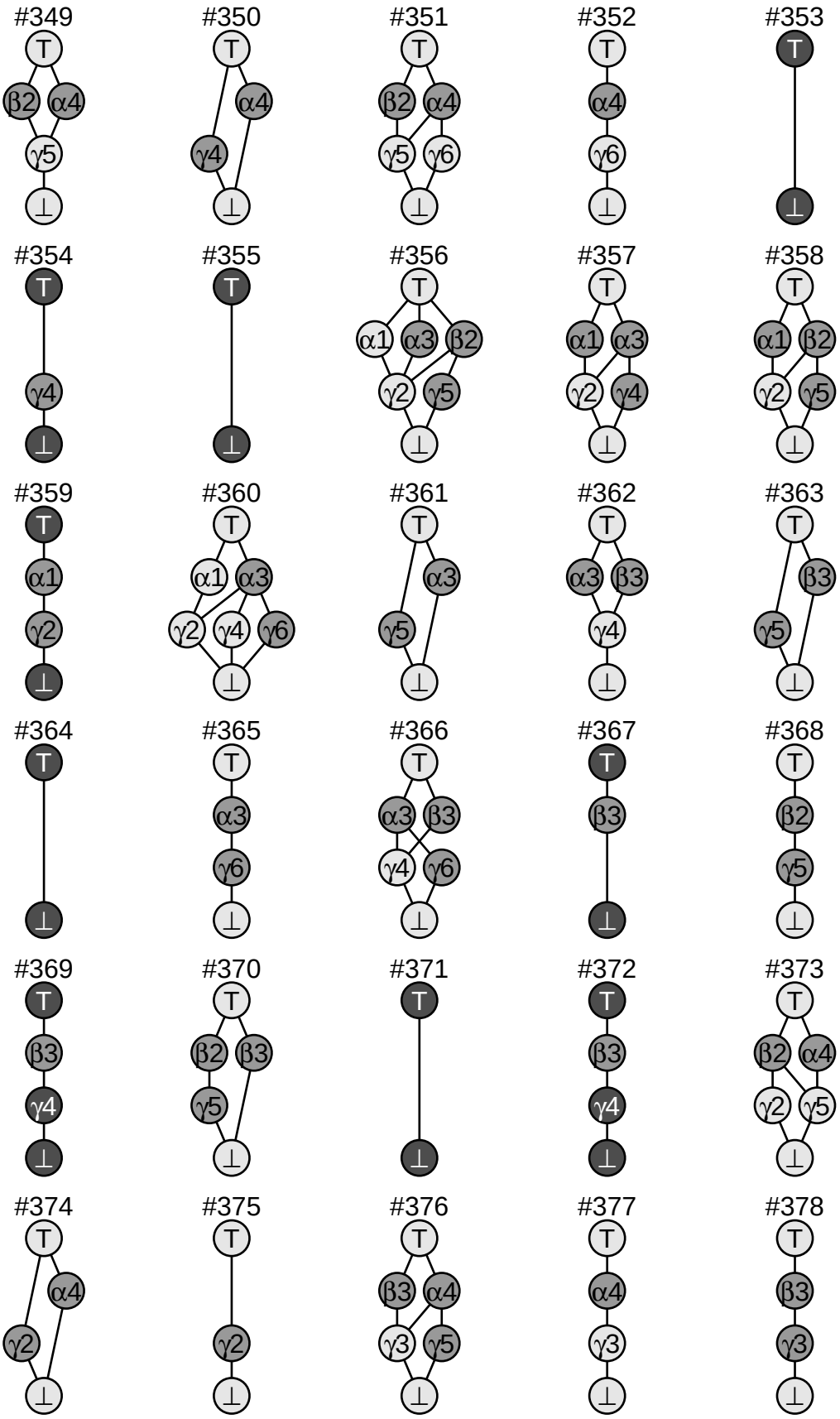
#349
⊤
β2
α4
γ5
⊥
#350
⊤
α4
γ4
⊥
#351
⊤
β2
α4
γ5
γ6
⊥
#352
⊤
α4
γ6
⊥
#353
⊤
⊥
#354
⊤
γ4
⊥
#355
⊤
⊥
#356
⊤
α1
α3
β2
γ2
γ5
⊥
#357
⊤
α1
α3
γ2
γ4
⊥
#358
⊤
α1
β2
γ2
γ5
⊥
#359
⊤
α1
γ2
⊥
#360
⊤
α1
α3
γ2
γ4
γ6
⊥
#361
⊤
α3
γ5
⊥
#362
⊤
α3
β3
γ4
⊥
#363
⊤
β3
γ5
⊥
#364
⊤
⊥
#365
⊤
α3
γ6
⊥
#366
⊤
α3
β3
γ4
γ6
⊥
#367
⊤
β3
⊥
#368
⊤
β2
γ5
⊥
#369
⊤
β3
γ4
⊥
#370
⊤
β2
β3
γ5
⊥
#371
⊤
⊥
#372
⊤
β3
γ4
⊥
#373
⊤
β2
α4
γ2
γ5
⊥
#374
⊤
α4
γ2
⊥
#375
⊤
γ2
⊥
#376
⊤
β3
α4
γ3
γ5
⊥
#377
⊤
α4
γ3
⊥
#378
⊤
β3
γ3
⊥

#379

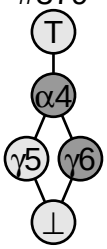

#380

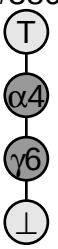

#381

#382

#383

#384

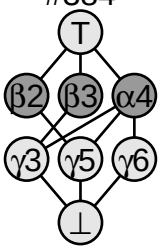

#385

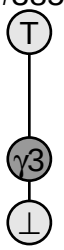

#386

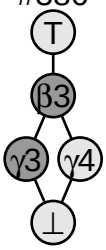

#387

#388

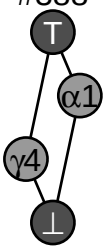

#389

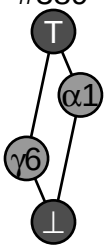

#390

#391

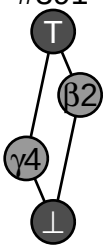

#392

#393

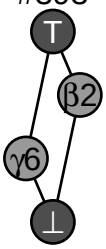

#394

#395

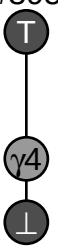

#396

#397

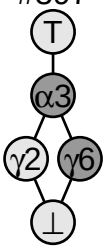

#398

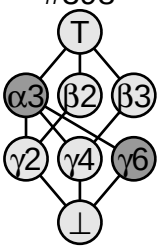

#399

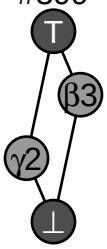

#400

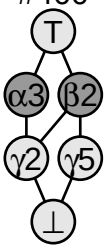

#401

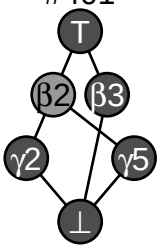

#402

#403

#404

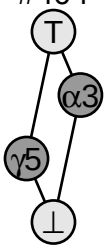

#405

#406

#407

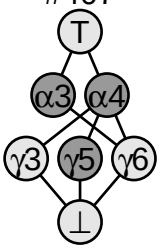

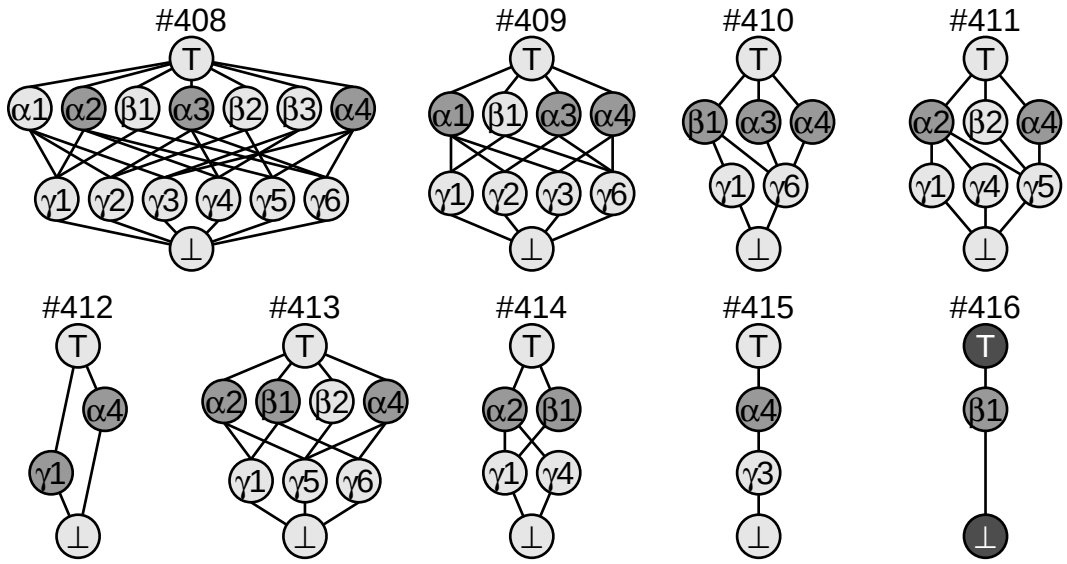
#408
⊤
α1 α2 β1 α3 β2 β3 α4
γ1 γ2 γ3 γ4 γ5 γ6
⊥
#409
⊤
α1 β1 α3 α4
γ1 γ2 γ3 γ6
⊥
#410
⊤
β1 α3 α4
γ1 γ6
⊥
#411
⊤
α2 β2 α4
γ1 γ4 γ5
⊥
#412
⊤
α4
γ1
⊥
#413
⊤
α2 β1 β2 α4
γ1 γ5 γ6
⊥
#414
⊤
α2 β1
γ1 γ4
⊥
#415
⊤
α4
γ3
⊥
#416
⊤
β1
⊥

Appendix B

Tables of Quotient Networks for Four-cell valency two Networks

All two-cell and three-cell quotient networks of a given four-cell valency 2 regular homogeneous network are listed. We categorised networks in a same class if they have the same set of quotient networks (for both two-cell and three-cell quotients). In this classification, ODE-equivalent networks of two-cell and three-cell networks are used. We list ODE-equivalent networks in the following:

ODE-equivalent two-cell networks	ODE-equivalent three-cell networks
#1 ≅#4	#1 ≅#35
#3 ≅#5	#3 ≅#36
	#12 ≅#37
	#25 ≅#38

For simple eigenvalues, lattices L1 to L12 are observed, as defined in Figure 7.7. For non-simple eigenvalues the minimal reduced lattices are given (MRL1 to MRL46 as defined in the figures in Section 8.7) together with the equivalent simple eigenvalue lattice number where appropriate.

B.1 Simple Real Eigenvalues

All quotient networks with simple real eigenvalues are listed below, sorted according to their lattice in the order shown in Figure 7.7. For example there are 18 such networks with lattice L1, but these cover only 15 classes of behaviour.

For example, the first row in the table shows network #148 which has lattice structure L1 with 2 two-cell quotient networks and 2 three-cell quotient networks. These quotient networks are listed in the same order (left to right) as in Figure 7.7, or equivalently Figure 7.12 which also shows the bifurcation behaviour. From this lattice structure L1, we expect to have three synchrony-breaking branches in total from three distinct bifurcation points. The types of these three bifurcating branches are determined by two-cell quotient networks #1 and #2, and three-cell quotient network #11, but not by three-cell quotient network #2 (see Figure 7.12).

Class	Network	Lattice	2-cell Quotients		3-cell Quotients	
1	#148(S1)	L1	#1	#2	#11(S1)	#2(S1)
2	#331(S1)	L1	#1	#2	#34(S1)	#17(S1)
3	#324(S1)	L1	#1	#2	#34(S1)	#2(S1)
4	#61(S1)	L1	#1	#4	#10(S1)	#26(S1)
5	#10(S1)	L1	#1	#4	#10(S1)	#5(S1)
〃	#30(S1)	L1	#1	#4	#10(S1)	#5(S1)
6	#317(S1)	L1	#1	#4	#32(S1)	#26(S1)
7	#58(S1)	L1	#1	#4	#8(S1)	#26(S1)
8	#72(S1)	L1	#1	#4	#32(S1)	#5(S1)
9	#164(S1)	L1	#1	#4	#7(S1)	#5(S1)
10	#8(S1)	L1	#1	#4	#8(S1)	#5(S1)
〃	#189(S1)	L1	#1	#4	#8(S1)	#5(S1)
11	#31(S1)	L1	#2	#4	#20(S1)	#23(S1)
12	#309(S1)	L1	#2	#4	#24(S1)	#23(S1)
13	#334(S1)	L1	#2	#5	#34(S1)	#29(S1)
14	#358(S1)	L1	#4	#5	#32(S1)	#36(S1)
15	#357(S1)	L1	#4	#5	#8(S1)	#36(S1)
〃	#366(S1)	L1	#4	#5	#8(S1)	#36(S1)
16	#14(S1)	L2	#1		#13(S1)	
〃	#89(S1)	L2	#1		#13(S1)	
〃	#269(S1)	L2	#1		#13(S1)	
17	#79(S1)	L2	#1		#31(S1)	
〃	#316(S1)	L2	#1		#31(S1)	
〃	#374(S1)	L2	#1		#31(S1)	
18	#9(S1)	L2	#1		#9(S1)	
〃	#59(S1)	L2	#1		#9(S1)	
〃	#210(S1)	L2	#1		#9(S1)	
19	#94(S1)	L2	#2		#13(S1)	
20	#85(S1)	L2	#2		#31(S1)	
21	#77(S1)	L2	#2		#9(S1)	
22	#97(S1)	L2	#3		#13(S1)	
23	#221(S1)	L2	#4		#13(S1)	
24	#361(S1)	L2	#4		#31(S1)	
〃	#404(S1)	L2	#4		#31(S1)	
25	#167(S1)	L2	#4		#9(S1)	
26	#363(S1)	L2	#5		#31(S1)	
27	#326(S1)	L2	#5		#9(S1)	
28	#66(S1)	L3	#1		#11(S1)	
〃	#141(S1)	L3	#1		#11(S1)	
〃	#143(S1)	L3	#1		#11(S1)	
〃	#380(S1)	L3	#1		#11(S1)	
29	#165(S1)	L3	#1		#7(S1)	
30	#11(S1)	L3	#4		#10(S1)	
〃	#33(S1)	L3	#4		#10(S1)	
31	#198(S1)	L3	#4		#20(S1)	
〃	#234(S1)	L3	#4		#20(S1)	
32	#118(S1)	L3	#4		#32(S1)	
33	#200(S1)	L3	#4		#8(S1)	
〃	#241(S1)	L3	#4		#8(S1)	

Class	Network	Lattice	2-cell Quotients			3-cell Quotients		
34	#297(S1)	L4	#1	#2	#4	#17(S1)	#23(S1)	#26(S1)
35	#282(S1)	L4	#1	#2	#4	#17(S1)	#23(S1)	#5(S1)
36	#28(S1)	L4	#1	#2	#4	#2(S1)	#23(S1)	#5(S1)
37	#333(S1)	L4	#2	#4	#5	#23(S1)	#29(S1)	#36(S1)
38	#34(S1)	L5	#4			#10(S1)	#20(S1)	
39	#78(S1)	L5	#4			#10(S1)	#32(S1)	
40	#300(S1)	L5	#4			#20(S1)	#32(S1)	
41	#231(S1)	L5	#4			#20(S1)	#8(S1)	
42	#147(S1)	L6				#13(S1)		
〃	#151(S1)	L6				#13(S1)		
〃	#222(S1)	L6				#13(S1)		
〃	#225(S1)	L6				#13(S1)		
〃	#318(S1)	L6				#13(S1)		
43	#88(S1)	L6				#31(S1)		
〃	#243(S1)	L6				#31(S1)		
〃	#247(S1)	L6				#31(S1)		
〃	#375(S1)	L6				#31(S1)		
〃	#382(S1)	L6				#31(S1)		
〃	#385(S1)	L6				#31(S1)		
44	#60(S1)	L6				#9(S1)		
〃	#249(S1)	L6				#9(S1)		
45	#65(S1)	L7	#1					
〃	#67(S1)	L7	#1					
〃	#69(S1)	L7	#1					
〃	#84(S1)	L7	#1					
〃	#92(S1)	L7	#1					
〃	#171(S1)	L7	#1					
〃	#191(S1)	L7	#1					
〃	#258(S1)	L7	#1					
〃	#338(S1)	L7	#1					
46	#172(S1)	L7	#4					
〃	#181(S1)	L7	#4					
〃	#201(S1)	L7	#4					
〃	#261(S1)	L7	#4					
〃	#339(S1)	L7	#4					
47	#367(S1)	L7	#5					
48	#70(S1)	L8						
〃	#87(S1)	L8						
〃	#341(S1)	L8						
49	#82(S1)	L9	#1	#2		#2(S1)		
50	#117(S1)	L9	#1	#4		#26(S1)		
〃	#208(S1)	L9	#1	#4		#26(S1)		
51	#178(S1)	L9	#1	#4		#5(S1)		
〃	#192(S1)	L9	#1	#4		#5(S1)		
52	#96(S1)	L10	#2	#3				
53	#114(S1)	L11	#1	#2	#4	#2(S1)	#26(S1)	
54	#325(S1)	L12	#2	#5		#34(S1)		
55	#127(S1)	L12	#3	#4		#32(S1)		
56	#370(S1)	L12	#4	#5		#32(S1)		

B.2 Simple Complex Eigenvalues

The following networks have a pair of complex conjugate eigenvalues. For these networks, synchrony-breaking Hopf bifurcations occur, instead of steady-state bifurcations. Again, for each network we list the lattice type (defined in Figure 7.7), and the two-cell and three-cell quotient networks, which are used to classify theses networks into classes.

Class	Network	Lattice	2-cell Quotients	3-cell Quotients
1	#16	L2	#1	#15
〃	#99	L2	#1	#15
〃	#271	L2	#1	#15
2	#17	L2	#1	#16
〃	#39	L2	#1	#16
〃	#272	L2	#1	#16
3	#26	L2	#1	#21
〃	#109	L2	#1	#21
〃	#294	L2	#1	#21
4	#27	L2	#1	#22
〃	#36	L2	#1	#22
〃	#129	L2	#1	#22
5	#37	L2	#1	#25
6	#350	L2	#1	#38
7	#389	L2	#2	#15
〃	#102	L2	#2	#15
8	#112	L2	#2	#21
9	#227	L2	#4	#15
10	#236	L2	#4	#21
〃	#306	L2	#4	#21
11	#251	L2	#4	#22
12	#412	L2	#4	#38
13	#388	L2	#5	#15
〃	#393	L2	#5	#15
14	#391	L2	#5	#21
15	#399	L2	#5	#38

Class	Network	Lattice	2-cell Quotients	3-cell Quotients
16	#42	L6		#16
〃	#49	L6		#16
〃	#273	L6		#16
17	#47	L6		#25
18	#46	L6		#22
〃	#132	L6		#22
〃	#252	L6		#22
〃	#296	L6		#22
〃	#302	L6		#22
〃	#307	L6		#22
19	#119	L6		#15
〃	#122	L6		#15
〃	#229	L6		#15
〃	#244	L6		#15
〃	#246	L6		#15
〃	#392	L6		#15
20	#238	L6		#21
〃	#295	L6		#21
〃	#301	L6		#21
〃	#395	L6		#21
〃	#405	L6		#21
21	#354	L6		#38

Class	Network	Lattice	2-cell Quotients	3-cell Quotients
22	#81	L7	#1	
〃	#91	L7	#1	
〃	#100	L7	#1	
〃	#110	L7	#1	
〃	#130	L7	#1	
〃	#135	L7	#1	
〃	#138	L7	#1	
〃	#139	L7	#1	
〃	#140	L7	#1	
〃	#174	L7	#1	
〃	#175	L7	#1	
〃	#278	L7	#1	
〃	#279	L7	#1	
〃	#288	L7	#1	
23	#101	L7	#2	
〃	#111	L7	#2	
〃	#153	L7	#2	
〃	#154	L7	#2	
〃	#157	L7	#2	
〃	#291	L7	#2	
24	#123	L7	#3	
〃	#133	L7	#3	
〃	#161	L7	#3	
25	#184	L7	#4	
〃	#185	L7	#4	
〃	#194	L7	#4	
〃	#195	L7	#4	
〃	#212	L7	#4	
〃	#213	L7	#4	
〃	#280	L7	#4	
〃	#216	L7	#4	
〃	#253	L7	#4	
〃	#387	L7	#4	
26	#396	L7	#5	
〃	#416	L7	#5	

Class	Network	Lattice	2-cell Quotients	3-cell Quotients
27	#95	L8		
〃	#103	L8		
〃	#106	L8		
〃	#113	L8		
〃	#116	L8		
〃	#120	L8		
〃	#121	L8		
〃	#125	L8		
〃	#131	L8		
〃	#155	L8		
〃	#156	L8		
〃	#158	L8		
〃	#159	L8		
〃	#180	L8		
〃	#187	L8		
〃	#197	L8		
〃	#204	L8		
〃	#205	L8		
〃	#207	L8		
〃	#209	L8		
〃	#215	L8		
〃	#228	L8		
〃	#230	L8		
〃	#233	L8		
〃	#237	L8		
〃	#239	L8		
〃	#242	L8		
〃	#245	L8		
〃	#248	L8		
〃	#256	L8		
〃	#260	L8		
〃	#263	L8		
〃	#264	L8		
〃	#266	L8		
〃	#268	L8		
〃	#281	L8		
〃	#286	L8		
〃	#287	L8		
〃	#289	L8		
〃	#353	L8		
〃	#355	L8		
〃	#364	L8		
〃	#371	L8		
〃	#381	L8		
〃	#383	L8		
〃	#390	L8		
〃	#403	L8		

B.3 Non-simple Double Eigenvalues

For all four cell valency two networks with non-simple double eigenvalues, we list their minimal reduced lattice (MRL1 to MRL35 as defined in Section 8.7) and their two-cell and three-cell quotient networks.

For example, the first network listed is four-cell network #2. This has minimal reduced lattice MRL1, which has the same structure as L4 for simple eigenvalue networks (see Figure 8.26). There are 3 two-cell quotient networks and 3 three-cell quotient networks in the minimal reduced lattice. From this minimal reduced lattice, we expect to have three synchrony-breaking bifurcating branches in two-dimensional balanced polydiagonals (P_2). The types of these bifurcating branches are determined by 2 topologically distinct two-cell quotient networks, #1 and #2. To determine how many bifurcating branches there exist for the original lattice (this network), we observe how many corresponding lattice nodes there are to the lattice nodes in the minimal reduced lattice. There is only one lattice node correspond to two-cell quotient network #2 (as this quotient network is generated from a simple eigenvalue). On the other hand, there are three lattice nodes in the original lattice which correspond to two-cell quotient network #1 (related to non-simple eigenvalue). Hence, in total, we expect there exist four synchrony-breaking bifurcating branches. One branch occurs at the bifurcation point corresponding to the distinct eigenvalue and the type of bifurcation is determined by two-cell network #2. The other three branches occur at the same bifurcation point corresponding to the double eigenvalue and their bifurcation types are generically the same as these are determined by the same two-cell quotient networks.

Note that some quotient networks have complex conjugate eigenvalues in the following table.

Class	Network	Lattice	2-cell Quotients			3-cell Quotients		
1	#2	MRL1 (L4)	#2	#1	#1	#2(S1)	#2(S1)	#1(S2)
2	#3	MRL1 (L4)	#3	#1	#1	#3(S1)	#3(S1)	#1(S2)
〃	#409	MRL1 (L4)	#5	#4	#4	#36(S1)	#36(S1)	#35(S2)
3	#5	MRL1 (L4)	#4	#1	#1	#5(S1)	#5(S1)	#1(S2)
〃	#162	MRL1 (L4)	#1	#4	#4	#5(S1)	#5(S1)	#35(S2)
4	#274	MRL1 (L4)	#2	#1	#1	#17(S1)	#17(S1)	#1(S2)
5	#308	MRL1 (L4)	#2	#4	#4	#23(S1)	#23(S1)	#35(S2)
6	#310	MRL1 (L4)	#4	#1	#1	#23(S1)	#23(S1)	#1(S2)
7	#313	MRL2 (L4)	#2	#5	#1	#29(S1)	#17(S1)	#27(S2)
8	#329	MRL2 (L4)	#4	#5	#1	#36(S1)	#5(S1)	#27(S2)
9	#320	MRL3 (L4)	#1	#2	#2	#17(S1)	#2(S1)	#33(S2)
10	#319	MRL4 (L4)	#2	#5	#1	#29(S1)	#2(S1)	#27(S2)
11	#18	MRL5 (L4)	#2	#1	#1	#17(S1)	#2(S1)	#1(S2)
12	#52	MRL5 (L4)	#4	#1	#1	#26(S1)	#5(S1)	#1(S2)
13	#40	MRL6 (L4)	#3	#1	#1	#3(S1)	#3(S1)	#1(S2)
〃	#413	MRL6 (L4)	#5	#4	#4	#36(S1)	#36(S1)	#35(S2)
14	#322	MRL7 (L4)	#5	#2	#2	#29(S1)	#29(S1)	#33(S2)
15	#330	MRL8 (L4)	#4	#5	#1	#36(S1)	#26(S1)	#27(S2)
16	#4	MRL9 (L1)	#3	#1		#4(S1)	#3(S1)	
17	#298	MRL9 (L1)	#2	#1		#24(S1)	#17(S1)	
18	#25	MRL10 (L1)	#4	#1		#20(S1)	#5(S1)	
19	#217	MRL10 (L1)	#1	#4		#11(S1)	#5(S1)	
20	#407	MRL10 (L1)	#2	#4		#34(S1)	#23(S1)	
21	#360	MRL11 (L1)	#4	#2		#8(S1)	#23(S1)	
22	#29	MRL12	#2	#1		#24(S1)	#2(S1)	
23	#51	MRL12	#3	#1		#4(S1)	#3(S1)	
24	#293	MRL12	#4	#1		#20(S1)	#26(S1)	
25	#303	MRL12	#2	#4		#32(S1)	#23(S1)	
26	#75	MRL13 (L1)	#1	#2		#7(S1)	#2(S1)	
27	#134	MRL13 (L1)	#2	#5		#24(S1)	#29(S1)	
28	#384	MRL14 (L1)	#1	#4		#11(S1)	#26(S1)	
29	#398	MRL15 (L1)	#4	#5		#20(S1)	#36(S1)	
30	#202	MRL16 (L9)	#4	#4		#35(S2)		
31	#7	MRL17 (L1)	#1	#1		#7(S1)	#1(S2)	
32	#12	MRL17 (L1)	#1	#1		#11(S1)	#1(S2)	
33	#166	MRL17 (L1)	#4	#4		#8(S1)	#35(S2)	
34	#168	MRL17 (L1)	#4	#4		#10(S1)	#35(S2)	
35	#305	MRL17 (L1)	#4	#4		#20(S1)	#35(S2)	
36	#276	MRL17 (L1)	#1	#1		#19(S1)	#1(S2)	

Class	Network	Lattice	2-cell Quotients		3-cell Quotients	
37	#20	MRL18 (L1)	#1	#1	#19(S1)	#1(S2)
38	#38	MRL18 (L1)	#1	#1	#7(S1)	#1(S2)
〃	#54	MRL18 (L1)	#1	#1	#7(S1)	#1(S2)
39	#63	MRL18 (L1)	#1	#1	#11(S1)	#1(S2)
〃	#136	MRL18 (L1)	#1	#1	#11(S1)	#1(S2)
40	#193	MRL18 (L1)	#4	#4	#20(S1)	#35(S2)
41	#199	MRL18 (L1)	#4	#4	#8(S1)	#35(S2)
42	#356	MRL18 (L1)	#4	#4	#32(S1)	#35(S2)
43	#76	MRL19	#4	#2	#8(S1)	#32(S1)
44	#327	MRL20 (L12)	#3	#5	#4(S1)	
45	#19	MRL21 (L1)	#2	#1	#2(S3)	#18(S1)
46	#21	MRL21 (L1)	#1	#2	#14(S3)	#17(S1)
〃	#290	MRL21 (L1)	#1	#2	#14(S3)	#17(S1)
47	#44	MRL21 (L1)	#1	#3	#12(S3)	#3(S1)
〃	#414	MRL21 (L1)	#4	#5	#37(S3)	#36(S1)
48	#50	MRL21 (L1)	#1	#3	#14(S3)	#3(S1)
49	#73	MRL21 (L1)	#1	#2	#6(S3)	#2(S1)
〃	#83	MRL21 (L1)	#1	#2	#6(S3)	#2(S1)
50	#104	MRL21 (L1)	#1	#2	#14(S3)	#2(S1)
51	#149	MRL21 (L1)	#1	#2	#12(S3)	#2(S1)
52	#163	MRL21 (L1)	#1	#4	#6(S3)	#5(S1)
〃	#176	MRL21 (L1)	#1	#4	#6(S3)	#5(S1)
53	#173	MRL21 (L1)	#4	#1	#37(S3)	#5(S1)
〃	#211	MRL21 (L1)	#1	#4	#12(S3)	#5(S1)
〃	#336	MRL21 (L1)	#4	#1	#37(S3)	#5(S1)
54	#183	MRL21 (L1)	#1	#4	#14(S3)	#5(S1)
55	#203	MRL21 (L1)	#1	#4	#14(S3)	#26(S1)
〃	#342	MRL21 (L1)	#1	#4	#14(S3)	#26(S1)
56	#275	MRL21 (L1)	#2	#1	#18(S3)	#17(S1)
〃	#292	MRL21 (L1)	#2	#1	#18(S3)	#17(S1)
57	#321	MRL21 (L1)	#5	#2	#28(S3)	#29(S1)
〃	#347	MRL21 (L1)	#5	#2	#28(S3)	#29(S1)
58	#323	MRL21 (L1)	#2	#5	#18(S3)	#29(S1)
59	#332	MRL21 (L1)	#5	#4	#28(S3)	#36(S1)
〃	#400	MRL21 (L1)	#5	#4	#28(S3)	#36(S1)
60	#345	MRL21 (L1)	#1	#2	#6(S3)	#17(S1)
61	#351	MRL21 (L1)	#1	#4	#6(S3)	#26(S1)
62	#373	MRL21 (L1)	#4	#1	#37(S3)	#26(S1)
63	#22	MRL22 (L3)	#4		#18(S3)	
64	#107	MRL22 (L3)	#1		#14(S3)	
〃	#134	MRL22 (L3)	#1		#14(S3)	
〃	#188	MRL22 (L3)	#1		#14(S3)	
〃	#255	MRL22 (L3)	#1		#14(S3)	
〃	#265	MRL22 (L3)	#1		#14(S3)	
65	#150	MRL22 (L3)	#1		#12(S3)	
〃	#152	MRL22 (L3)	#1		#12(S3)	
〃	#220	MRL22 (L3)	#1		#12(S3)	
66	#179	MRL22 (L3)	#4		#12(S3)	
〃	#182	MRL22 (L3)	#4		#12(S3)	
〃	#235	MRL22 (L3)	#4		#12(S3)	
〃	#340	MRL22 (L3)	#4		#37(S3)	
67	#372	MRL22 (L3)	#5		#28(S3)	
〃	#406	MRL22 (L3)	#5		#28(S3)	

Class	Network	Lattice	2-cell Quotients	3-cell Quotients	
68	#23	MRL23 (L3)	#1	#19(S1)	
69	#57	MRL23 (L3)	#1	#7(S1)	
70	#144	MRL23 (L3)	#1	#5(S1)	
71	#259	MRL23 (L3)	#4	#20(S1)	
72	#359	MRL23 (L3)	#2	#34(S1)	
73	#365	MRL23 (L3)	#4	#8(S1)	
74	#368	MRL23 (L3)	#4	#32(S1)	
75	#32	MRL24 (L3)	#2	#24(S1)	
76	#74	MRL24 (L3)	#1	#7(S1)	
77	#124	MRL24 (L3)	#4	#32(S1)	
78	#126	MRL24 (L3)	#3	#4(S1)	
〃	#160	MRL24 (L3)	#3	#4(S1)	
79	#190	MRL24 (L3)	#4	#8(S1)	
〃	#232	MRL24 (L3)	#4	#8(S1)	
80	#196	MRL24 (L3)	#4	#20(S1)	
〃	#226	MRL24 (L3)	#4	#20(S1)	
〃	#250	MRL24 (L3)	#4	#20(S1)	
81	#218	MRL24 (L3)	#1	#11(S1)	
82	#299	MRL24 (L3)	#2	#24(S1)	
83	#24	MRL25 (L5)	#1	#19(S1)	#14(S3)
84	#41	MRL25 (L5)	#1	#7(S1)	#12(S3)
85	#48	MRL25 (L5)	#1	#7(S1)	#14(S3)
86	#56	MRL25 (L5)	#1	#7(S1)	#6(S3)
87	#223	MRL25 (L5)	#1	#11(S1)	#6(S3)
88	#240	MRL25 (L5)	#4	#8(S1)	#37(S3)
89	#304	MRL25 (L5)	#2	#24(S1)	#18(S3)
90	#379	MRL25 (L5)	#1	#11(S1)	#14(S3)
91	#386	MRL25 (L5)	#4	#32(S1)	#37(S3)
92	#397	MRL25 (L5)	#4	#20(S1)	#37(S3)
93	#219	MRL25 (L5)	#1	#11(S1)	#12(S3)
94	#43	MRL26 (L9)	#1 #3	#3(S1)	
〃	#362	MRL26 (L9)	#5 #4	#36(S1)	
95	#90	MRL26 (L9)	#1 #2	#2(S1)	
〃	#93	MRL26 (L9)	#2 #1	#2(S1)	
〃	#105	MRL26 (L9)	#2 #1	#2(S1)	
〃	#115	MRL26 (L9)	#1 #2	#2(S1)	
96	#108	MRL26 (L9)	#1 #4	#26(S1)	
〃	#349	MRL26 (L9)	#4 #1	#26(S1)	
97	#169	MRL26 (L9)	#4 #1	#5(S1)	
〃	#170	MRL26 (L9)	#1 #4	#5(S1)	
〃	#277	MRL26 (L9)	#1 #4	#5(S1)	
98	#283	MRL26 (L9)	#1 #2	#17(S1)	
99	#284	MRL26 (L9)	#2 #4	#23(S1)	
100	#348	MRL26 (L9)	#5 #2	#29(S1)	
101	#86	MRL27 (L7)	#2		
102	#142	MRL28 (L8)			

(A pair of) Double Eigenvalues with One Eigenvector in $\triangle$

Class	Network	Lattice	2-cell Quotients	3-cell Quotients
1	#62	MRL29 (L1)	#1 #1	#30(S4) #1(S2)
〃	#315	MRL29 (L1)	#1 #1	#30(S4) #1(S2)
2	#262	MRL30 (L5)	#1	#30(S4) #14(S3)
3	#254	MRL31 (L3)	#1	#12(S3)
4	#377	MRL31 (L3)	#1	#14(S3)
5	#337	MRL32 (L3)	#1	#30(S4)
6	#376	MRL33 (L1)	#1 #4	#30(S4) #26(S1)
7	#68	MRL34 (L3)	#1	#30(S4)
〃	#71	MRL34 (L3)	#1	#30(S4)
〃	#267	MRL34 (L3)	#1	#30(S4)
8	#378	MRL35 (L3)	#4	#32(S1)
9	#402	MRL35 (L3)	#4	#20(S1)

B.4 Non-simple Triple Eigenvalues

For all four-cell valency two networks with non-simple triple eigenvalues, we list their minimal reduced lattice (MRL36 to MRL46 as defined in Section 8.7) and their two-cell and three-cell quotient networks.

Class	Network	Lattice	2-cell Quotients			3-cell Quotients		
1	#1	MRL36 (L4)	#1	#1	#1	#1(S2)	#1(S2)	#1(S2)
〃	#408	MRL36 (L4)	#4	#4	#4	#35(S2)	#35(S2)	#35(S2)
2	#311	MRL37 (L4)	#1	#1	#5	#27(S2)	#27(S2)	#1(S2)
3	#15	MRL38 (L1)	#1	#1		#1(S2)	#14(S3)	
4	#35	MRL38 (L1)	#1	#1		#1(S2)	#12(S3)	
〃	#411	MRL38 (L1)	#4	#4		#35(S2)	#37(S3)	
5	#53	MRL38 (L1)	#1	#1		#1(S2)	#6(S3)	
6	#312	MRL39 (L1)	#1	#5		#27(S2)	#28(S3)	
7	#344	MRL40	#5	#1		#27(S2)	#6(S3)	#14(S3)
8	#64	MRL41 (L9)	#1	#1		#1(S2)		
〃	#137	MRL41 (L9)	#1	#1		#1(S2)		
9	#401	MRL42 (L3)	#5			#28(S3)		
10	#45	MRL43 (L5)	#1			#12(S3)	#14(S3)	
11	#224	MRL43 (L5)	#1			#12(S3)	#6(S3)	
12	#6	MRL44	#1	#1		#1(S2)	#6(S3)	
13	#13	MRL44	#1	#1		#1(S2)	#12(S3)	
〃	#410	MRL44	#4	#4		#35(S2)	#37(S3)	
14	#270	MRL44	#1	#1		#1(S2)	#14(S3)	
15	#343	MRL45	#1	#5		#27(S2)	#28(S3)	
16	#55	MRL46 (L3)	#1			#6(S3)		
〃	#80	MRL46 (L3)	#1			#6(S3)		
〃	#177	MRL46 (L3)	#1			#6(S3)		
〃	#352	MRL46 (L3)	#1			#6(S3)		
17	#145	MRL46 (L3)	#1			#12(S3)		
〃	#146	MRL46 (L3)	#1			#12(S3)		
〃	#214	MRL46 (L3)	#1			#12(S3)		
〃	#415	MRL46 (L3)	#4			#37(S3)		
18	#98	MRL46 (L3)	#1			#14(S3)		
〃	#128	MRL46 (L3)	#1			#14(S3)		
〃	#186	MRL46 (L3)	#1			#14(S3)		
〃	#206	MRL46 (L3)	#1			#14(S3)		
〃	#257	MRL46 (L3)	#1			#14(S3)		
〃	#285	MRL46 (L3)	#1			#14(S3)		
19	#346	MRL46 (L3)	#5			#28(S3)		
〃	#369	MRL46 (L3)	#5			#28(S3)		
〃	#394	MRL46 (L3)	#5			#28(S3)		

Bibliography

Aguiar, M. A. D., Dias, A. P., Golubitsky, M., and Leite, M. C. A. (2007). Homogeneous coupled cell networks with S_3-symmetric quotient. *Discrete and Continuous Dynam. Sys. Supplement*, pages 1–9.

Aguiar, M. A. D., Dias, A. P., Golubitsky, M., and Leite, M. C. A. (2008). Bifurcation from quotient coupled cell networks. *Phisica D, Submitted*.

Aittokallio, T. and Schwikowski, B. (2006). Graph-based methods for analysing networks in cell biology. *Briefings in Bioinformatics.*, **7**, 243–255.

Albert, R. and Barabási, A. L. (2002). Statistical mechanics of complex networks. *Rev. Mod. Phys.*, **74**, 47–97.

Albert, R. and Othmer, H. G. (2003). The topology of the regulatory interactions predicts the expression pattern of the drosophila segment polarity genes. *J. Theor. Biol.*, **223**, 1–18.

Aldosray, F. and Stewart, I. (2005). Enumeration of homogeneous coupled cell networks. *Int. J. Bifurcation Chaos*, **15**, 2361–2372.

Bernard, K. and Hill, D. R. (2005). *Introductory Linear Algebra (Eighth Edition)*. Pearson Prentice Hall, San Diego.

Biggs, N. L. (1989). *Discrete Mathematics (Revised Edition)*. Oxford University Press, Oxford.

Brualdi, R. (2006). *Combinatorial matrix classes*. Cambridge University Press, Cambridge.

Davey, B. A. and Priestley, H. A. (1990). *Introduction to Lattices and Order*. Cambridge University Press, Cambridge.

Dias, A. and Stewart, I. (2005). Linear equivalence and ode-equivalence for coupled cell networks. *Nonlinearity*, **18**, 1003–1020.

Golubitsky, M. and Lauterbach, R. (2008). Bifurcations from synchrony in homogeneous networks: linear theory. *SIAM J. Appl. Dynam. Sys., Submitted*.

Golubitsky, M. and Schaeffer, D. G. (1990). *Singularities and Groups in Bifurcation Theory, Volume I*. Springer-Verlag, New York.

Golubitsky, M. and Stewart., I. (2002). *The Symmetry Perspective From Equilibrium to Chaos in Phase Space and Physical Space*. Birkhäuser.

Golubitsky, M. and Stewart, I. (2006). Nonlinear dynamics of networks: the groupoid formalism. *Bull. Amer. Math. Soc.*, **43**, 305–364.

Golubitsky, M. and Stewart, I. (2008). Synchrony-breaking bifurcations at simple eigenvalues for regular networks. *To appear*.

Golubitsky, M., Stewart, I. N., and Schaeffer, D. G. (1998). *Singularities and Groups in Bifurcation Theory, Volume II*. Springer-Verlag, New York.

Golubitsky, M., Stewart, I., and Török, A. (2005). Patterns of synchrony in coupled cell networks with multiple arrows. *SIAM J. Appl. Dynam. Sys*, **4**, 78–100.

Hohn, F. (1973). *Elementary Matrix Algebra (Third Edition)*. Collier-Macmillan.

Ishihara, S., Fujimoto, K., and Shibata, T. (2005). Cross talking of network motifs in gene regulation that generate temporal pulses and spatial stripes. *Genes to Cells.*, **10**, 1025–1038.

Kashtan, N., Itzkovitz, S., Milo, R., and Alon, U. (2004). Topological generalization of network motifs. *Phys. Rev. E.*, **70**, 031909 1–12.

Koshy, T. (2003). *Discrete Mathematics with Applications*. Elsevier Academic Press, San Diego.

Lancaster, P. and Tismenetsky, M. (1985). *The Theory of Matrices Second Edition with Applications*. Academic Press,San Diego.

Leite, M. and Golubitsky, M. (2006). Homogeneous three-cell networks. *Nonlinearity*, **19**, 2313–2363.

Lotka, A. J. (1920). Analytical note on certain rhythmic relations in organic systems. *Proc. Natl. Acad. Sci.*, **6**, 410–415.

Lotka, A. J. (1925). *Elements of Physical Biology.* Williams and Wilkins Co., Baltimore.

Milo, R., Shen-Orr, S., Itzkovitz, S., Kashtan, N., Chklovskii, D., and Alon, U. (2005). Network motifs: Simple building blocks of complex networks. *Science.*, **298**, 824–827.

Mincheva, M. and Roussel, M. (2007). Graph-theoretic methods for the analysis of chemical and biochemical networks. I. multistability and oscillations in ordinary differential equation models. *J. Math. Biol.*, **55**, 61–86.

Mochizuki, A. (2007). Structure of regulatory networks and diversity of gene expression patterns. *J. Theor. Biol.*, **250**, 307–321.

Newman, M. E. J. (2006). The structure of scientific collaboration networks. *Bull. Amer. Math. Soc.*, **43**, 305–364.

Schröder, B. S. W. (1990). *Ordered Sets An Introduction*. Birkhäuser.

Slomson, A. (1991). *Introduction to Combinatorics*. Chapman and Hall, London.

Stewart, I. (2004). Networking opportunity. *Nature.*, **427**, 601–604.

Stewart, I. (2007). The lattice of balanced equivalence relations of a coupled cell network. *Math. Proc. Camb. Phil. Soc.*, **143**, 165–183.

Stewart, I., Golubitsky, M., and Pivato, M. (2003). Symmetry groupoids and patterns of synchrony in coupled cell networks. *SIAM J. Appl. Dynam. Sys*, **2**, 609–646.

Strogatz, S. H. (2001). Exploring complex networks. *Nature.*, **410**, 268–276.

Takigawa-Imamura, H. and Mochizuki, A. (2006). Predicting regulation of the phosphorylation cycle of KaiC clock protein using mathematical analysis. *J. Biol. Rhythms*, **21**(405).

Volterra, V. (1926). Variazioni e fluttuazioni del numero d'individui in specie animal conviventi. *Mem. R. Accad. Naz. dei Lincei.*, **2**.

Wang, Y. and Golubitsky, M. (2005). Two-colour patterns of synchrony in lattice dynamical systems. *Nonlinearity*, **18**, 631–657.

Watts, D. J. and Strogatz, S. H. (1998). Collective dynamics of 'small-world' networks. *Nature.*, **393**, 440–442.

Wiggins, S. (1990). *Introduction to Applied Nonlinear Dynamical Systems and Chaos*. Springer-Verlag, New York.